Written submission from Bruce Power

In the Matter of

Request for authorization to return Bruce Nuclear Generating Station (NGS) A Unit 3 to service, following its current planned outage

Public Hearing - Hearing in writing based on written submissions

October 2021

Mémoire de Bruce Power

À l'égard de

Demande concernant l'autorisation de la remise en service de la tranche 3 de la centrale nucléaire de Bruce-A à la fin de son arrêt prévu actuel

Audience Publique - Audience fondée sur des mémoires

Octobre 2021

September 17, 2021

BP-CORR-00531-02033

Mr. M. Leblanc   Dr. A. Viktorov
Commission Secretary   Director General
Canadian Nuclear Safety Commission   Canadian Nuclear Safety Commission
P.O. Box 1046   P.O. Box 1046
280 Slater Street   280 Slater Street
Ottawa, Ontario   Ottawa, Ontario
K1P 5S9   K1P 5S9

Dear Mr. Leblanc and Dr. Viktorov:

<u>Bruce A Unit 3: Return to Service Additional Information</u>

The purpose of this letter is to provide the additional information related to the elevated
hydrogen equivalent concentrations ([H]eq), in a well-defined area of some pressure
tubes, which is supplemental to Bruce Power's request for Commission authorization to
return Unit 3 to service (Reference 1), as committed in Reference 2 and to request
Commission approval to return Unit 3 to service following the current planned outage.

Context

Through extensive inspections, analysis utilizing evidence from results and testing,
Bruce Power can confirm the following key principles that remain core to our submission
and are further verified and reinforced through this submission of additional information:

1. Overall Hydrogen uptake is not increasing in the pressure tubes beyond the
   predicted rate. It is redistribution due to a progression of total hydrogen concentration
   to the top of the tube in a limited region of interest that can conservatively be
   bounded. In the balance of the tube, hydrogen concentrations are below the
   licensing limits.

2. The apparent cause evaluation completed by Bruce Power identified, through two
   independent sources, that the observed redistribution of hydrogen equivalent
   concentration is due to the temperature gradient, with the top of the pressure tube
   cooler than the bottom. Bruce Power is working with industry to finalize the root
   cause of the elevated concentration. While this additional verification is underway,
   Bruce Power is proposing a conservative region of interest.

3. There are no flaws in the conservatively identified region of interest demonstrated
   through hundreds of previous inspections, re-verifications and expanded activities in
   Unit 3. Statistical analysis, collectively and on a unitized basis for Unit 3,
   demonstrates an extremely low probability of the presence of dispositionable flaws in
   this region.

Bruce Power Maury Burton, Chief Regulatory Officer
P.O. Box 1540 B10 2nd Floor E, Tiverton ON N0G 2T0
Telephone 519-361-5291
maury.burton@brucepower.com

4. Due to the pressure tube and bundle configuration on the Bruce units, no flaws are expected to ever occur in this region of interest.

5. Additional operational measures are being put in place to build operational safety margin during heat-up and cool-down in particular as well as during cold Primary Heat Transport (PHT) conditions where there is low but finite potential for over-pressure conditions to occur. This is focused on further increasing defense in depth during the less than 3% of operating hours on a reactor where this is applicable.

6. All operating units have been inspected over the last 18-months, and planned outages are sequentially scheduled to validate conclusions over the next 18 months. This is a safe, planned manner to effectively carry-out this work.

Additional Information

In Reference 2, Bruce Power committed to the provision of additional information in support of the request for Commission authorization for the return to service of Unit 3 (Reference 1), including:

1) The complete set of verified inspection results from the current Unit 3 planned outage (A2131) scrape campaign (i.e. the results from the 3 independent scrape windows), which is provided in Attachment A;

2) A justification as to the use of the existing Delayed Hydride Crack (DHC) initiation model for elevated hydrogen equivalent concentration applications, which is provided in Enclosure 1;

3) A margin engineering evaluation of the Circumferential Wet Scrape Tool (CWEST) scrape flaws near the outlet rolled joint burnish mark in the Unit 3 pressure tubes, which is provided in Section 4 of Enclosure 2;

4) A statistical analysis as to the probability of the existence of an undetected, significant flaw within the region of interest, which is provided as Enclosure 3;

5) A test plan for DHC initiation tests in elevated hydrogen equivalent concentration conditions, which is also provided within Enclosure 1; and,

6) A risk informed approach to fracture protection for the region of interest, which is provided as Enclosure 3.

Unit 3 Inspection and Unit 6 Surveillance Results

The inspections carried-out on Unit 3 represent the most extensive campaign conducted on a CANDU reactor for hydrogen concentrations and flaws. This extensive campaign, which has provided substantial evidence, provides confidence that the hydrogen isotope and flaw distributions in the outlet rolled joint regions of both Unit 3 and other units at Bruce Power are well understood.

Mr. M. Leblanc and Dr. A. Viktorov   September 17, 2021

A compilation of the verified measurement results from the three scrape windows undertaken during the current Unit 3 outage (A2131) and the verified measurements for the punch samples obtained from the Unit 6 surveillance tubes, B6S13 (inlet and outlet rolled joints) and B6N07 (outlet rolled joint), are provided in Attachment A. These measurement results confirm the region of interest can be defined as:

- Axially – From the burnish mark to 75 mm inboard of the burnish mark, and
- Circumferentially – 60 degrees on either side of 12 o'clock for a total of 120 degrees.

Enclosures 4 and 5 provide Bruce Power's assessment of the region of interest and a technical justification as to its extent. Enclosure 4 gives an overview of the physical understanding of the mechanism by which [H]eq is redistributed to the region of interest. This is fully consistent with the existing understanding of H isotope behaviour in pressure tubes. Enclosure 5 shows the circumferential distribution of [H]eq as determined from the A2131 scrapes and punch samples from the B6S13 outlet rolled joint at several axial positions. The high [H]eq data are comfortably bounded by the proposed extents of 120 degrees centred at 12 o'clock and 75 mm inboard of the burnish mark.

Note that Bruce Power has conservatively expanded the axial extent of the region of interest from 50mm (based on measured [H]eq values through extensive inspections on Unit 3 pressure tubes during the current outage and the Unit 6 surveillance tubes) to 75mm inboard of the outlet burnish mark.

Bruce Power's inspection program is designed to look for evidence of changes in the pressure tubes so that further analysis and corrective actions can be taken to ensure safety. As opposed to random selection, pressure tubes are specifically selected for inspection and surveillance to meet the requirements of CSA N285.4. This approach is consistent with the requirements of the licensing basis, and ensures results gathered are representative and bounding of all unit conditions.

DHC Initiation Model and Test Plans

Section 2 of Enclosure 1 provides Bruce Power's justification as to the application of crack initiation models to elevated [H]eq regions in pressure tubes. The Enclosure provides a review of the basis of the process-zone model for predicting DHC initiation at flaws and investigates whether the material DHC properties, which are key inputs to the crack initiation models, are adversely affected by very high levels of [H]eq. Based on the available data and the theoretical understanding, Bruce Power concluded that the DHC properties are not affected by elevated levels of [H]eq.

A test plan to confirm the expectation that there is no effect of elevated [H]eq on crack initiation due to DHC, hydrided region overload and fatigue is provided in Section 3 of Enclosure 1. The test plan includes both the upcoming tests in the short-term and proposed tests over the longer term. The planned short-term tests are focused on DHC initiation at notches in unirradiated material. All the other tests are longer-term tests and will be subject to refinement based upon the results from the short-term tests.
Bruce Power, in concert with industry, will adjust the proposed longer-term tests once the results of the short-term tests are reviewed.

Scrape Witness Marks

Section 4 of Enclosure 1 also provides a margin engineering evaluation of CWEST scrape witness marks in the outlet rolled joint burnish mark regions of the Unit 3 pressure tubes with elevated levels of [H]eq (i.e. 220 ppm). The evaluation was performed to 246,000 EFPH. The geometry of a scrape witness mark is deliberately benign, avoiding tight radius features that would concentrate stress, to minimizes stress concentration at the edge of the flaw and this evaluation demonstrates that there are substantial margins to crack initiation due to DHC, hydride region overloads (HROL) and fatigue for the axial component, and on the lower-bound KIH for the circumferential component. This is expected as the methodology and tooling used in this sampling technique is well understood through significant experience on a large population of channels.

Statistical Analysis

In Enclosure 2, a unitized statistical analysis is performed to demonstrate the very low probability of the existence of a reportable flaw and a dispositionable flaw in the region of interest, given there has never been a flaw detected in the region of interest, based on available inspection results obtained to-date.

The conclusion reached for Unit 3 (and all Bruce Power units) is that the probability is < 0.5% for a dispositionable flaw and, as a result, the risk of having a significant flaw in the region of interest, that could challenge pressure tubes fitness for service, is also low.

As noted during the Commission Hearing on September 10, 2021, unlike the pressure tube and fuel channel configuration at Pickering, the Bruce Power units, like Darlington, have a fueling system design that minimizes the likelihood of interaction of the fuel bundles with the top of the tube, so flaws should not occur. This has been verified and re-verified through hundreds of inspections.

Fracture Protection in the Region of Interest

Enclosure 3 provides a risk-informed deterministic evaluation of fracture protection for the region of interest in outlet rolled joints in Unit 3. The risk-informed deterministic evaluation of fracture protection was performed for postulated levels of [H]eq of up to 250 ppm. Measured fracture toughness from small test specimens comprised of irradiated Zircaloy-2 and Zircaloy-4 material with high levels of [H]eq were used in the context of surrogate materials to gain insights into the fracture toughness of zirconium pressure tubes at high levels of [H]eq. The fracture toughness values for Zircaloy-2 and Zircaloy-4 are, in general, lower than the fracture toughness values for pressure tube material at a given [H]eq level. The conclusion was that, in the event of the unanticipated existence of an axial through-wall flaw in the region of interest, flaw stability can still be demonstrated. Strong fracture protection consistent with fitness for service requirements is maintained. In addition, a burst test (BT-50) was recently performed at 65ºC and the preliminary fracture toughness value was 41.5 MPa√m with [H]eq of 178 ppm. This result supports the validity of the analysis for higher [H]eq concentrations.

Conservatism in the Region of Interest

While Bruce Power is confident that the extent of the conservatively expanded region of interest can be further limited based upon, both, the results of the inspections to date and preliminary modelling analysis, there is a recognition that CNSC staff are continuing to review the provided information, and further refinements to the area of interest may be undertaken as CNSC staff confidence increases.

Results from the modelling analysis completed to date by Bruce Power are favourable and correlate to the results measured in Unit 3 and the Unit 6 surveillance tube. Based on discussions, this work will be provided to CNSC staff for review and further consideration. The forthcoming analysis will provide additional insight as to the rate of change of hydrogen equivalent concentration within the region of interest and may be useful in specifying or predicting a threshold as to when pressure tubes become subject to elevated levels of hydrogen.

As noted, Bruce Power has taken an evidence-based, conservative approach to defining the region of interest that will be well-bounded from both results and the short operating interval of Unit 3 prior to its Major Component Replacement.

In the meantime, Bruce Power has upcoming opportunities, starting with the Unit 7 planned outage scheduled to begin in November, to seek to further reinforce evidence of the elevated hydrogen equivalent concentrations, and to confirm expectations, with respect to the extent of the region of interest, with physical measurements taken from other units. Bruce Power expects that the results from forthcoming outages will confirm Bruce Power's understanding and ability to identify bounding behaviour within the reactor core. While the region of interest is being validated, should results differ from Bruce Power's expectations, the conservatively bounded region of interest ensures there will be an opportunity to take action in response to an unanticipated finding. This is not expected to occur given the conservative approach taken to defining this region with evidence and considerable margin.

In addition to a conservatively established region of interest based on evidence from inspections, as noted, the framework of the risk-informed approach for fracture protection (Enclosure 3) is applicable to any location of the tube with elevated hydrogen equivalent concentrations. As concluded in Enclosure 3, flaw stability is demonstrated for up to 250 ppm [H]eq in an unlikely event of a through-wall flaw in the location of high [H]eq. Therefore, the risk of a pressure tube rupture resulting from a through-wall flaw in Bruce Unit 3 prior to the commencement of the Major Component Replacement, scheduled to begin in 18 months, is very low. Safety and Pressure Tube integrity is strongly demonstrated.

Mr. M. Leblanc and Dr. A. Viktorov   September 17, 2021

If you require further information or have any questions regarding this submission, please contact Ms. Lisa Clarke, Director, Regulatory Affairs, at (519) 361-2673 extension 16144, or lisa.clarke@brucepower.com.

Yours truly,

Lisa Clarke
Digitally signed by
Lisa Clarke
Date: 2021.09.17
15:23:41 -04'00'

Maury Burton
Chief Regulatory Officer
Bruce Power

cc: CNSC Bruce Site Office
        Mr. L. Sigouin, CNSC Ottawa

Attach.

Enclosures:

1.   B-31100 LOF NSAS, Revision 000, "Re: Justification for Application of Crack Initiation Models to High Hydrogen Equivalent Concentration Regions in Pressure Tubes".

2.   B-REP-31110-00004, Revision 000, "Estimation of Encountering Reportable & Dispositionable Pressure Tube Flaws in Various Regions of Interest in Bruce Power Units 3-8".

3.   NK21-REP-31100-00219, B2038/RP/009, R00, "Risk-Informed Deterministic Evaluation of Fracture Protection for the Region of Interest in Outlet Rolled Joints in Bruce Unit 3".

4.   B-03644.4 LOF NSAS, Revision 000, "Concentrating Hydrogen Isotopes at the Top of Tube at the Outlet End Rolled Joint Region".

5.   NK21-03644.4 LOF NSAS, Revision 000, "Re: Hydrogen Equivalent Concentration Measurements Taken Near the Outlet Burnish Mark in the Bruce Unit 3 2021 Outage (A2131)".

References:

1.   Letter, M. Burton to M. Leblanc, "Designated Officer Order to Bruce Power – Unit 3 Planned Outage Restart Authorization", August 13, 2021, BP-CORR-00531-01935.

2.   Letter, M. Burton to M. Leblanc and A. Viktorov, "Bruce A and Bruce B: Return to Service Supplemental Information", September 9, 2021, BP-CORR-00531-02004.

Attachment A

Summary of [D] and [H] Inlet and Outlet RJ Measurements for the Unit 3 2021 Outage and Unit 6 surveillance tubes: B6S13 and B6N07

Table 1- Summary of [D] and [H] measurements for A2131 Outlet RJ (all windows)

Ch. No.	Ch. ID (FEO /BEO)	Nominal Location (o'clock from ORJ end)	Location (from Outlet end (mm) **(Note 1)**	$[D]_{meas}$ (ppm)	$[H]_{meas}$ (ppm)	$[H]i_{nitial}$ (offcut) ppm
1	F16 (FEO)	O1 (+20)	9	1340	111	12.6
		O1 (-20)	9	930	80	
		O3 (+20)	42	880	79	
		O4 (+20) BM-10	54	670	67	
		O4 (-20) BM-10	54	310	29	
		O4 (-90) BM-10	55	115	15	
		O4H- (+50) BM-10	56	123	16	
		O4H+ (-66) BM-10	56	115	13	
		O4B- (+20) BM+20	90	180	23	
		O4BT (-8) BM+20	**89**	**300**	**34**	
		O4B+ (-38) BM+20	89	119	18	
		O4A (+20) BM+43	112	240	31	
		O4A (-90) BM+43	113	96	16	
		O5 (+20)	128	190	29	
		O6 (+20)	370	71	22	
		O6 (-20)	345	69	20	
2	L11 (FEO)	O1 (+20)	9	790	60	9.3
		O1 (-20)	9	132	13	
		O3 (+20)	42	470	37	
		O3 (-20)	40	121	13	
		O4 (+20) BM-10	54	350	29	
		O4 (-20) BM-10	54	115	14	
		O4 (-90) BM-10	55	96	12	
		O4H- (+50) BM-10	57	108	11	
		O4H+ (-66) BM-10	57	98	11	
		O4B- (+20) BM+20	90	136	14	
		O4BT (-8) BM+20	**90**	**137**	**15**	
		O4B+ (-38) BM+20	89	101	17	

Ch. No.	Ch. ID (FEO /BEO)	Nominal Location (o'clock from ORJ end)	Location (from Outlet end (mm) **(Note 1)**	$[D]_{meas}$ (ppm)	$[H]_{meas}$ (ppm)	$[H]i_{nitial}$ (offcut) ppm
		O4A (-20) BM+43	113	99	12	
		O4A (-90) BM+43	114	88	11	
		O5 (+20)	128	115	15	
		O6 (+20)	370	67	14	
3	G15 (FEO)	O1 (+8)	10	1016	103	11.3
		O3 (+8)	43	739	75	
		O4 (+8) BM-10	56	531	63	
		O4 (+60) BM-10	56	119	23	
		O4 (-20) BM-10	56	152	22	
		O4 (-90) BM-10	57	104	18	
		O4H+(-66) BM-10	58	102	19	
		O4B-(+22) BM+20	91	183	31	
		O4BT(-8) BM+20	92	**227**	**34**	
		O4B+(-38) (BM+20)	92	107	23	
		O4A (+8) BM+43	114	178	30	
		O6 (+8)	371	70	18	
4	K10 (FEO)	O1 (+8)	9	853	74	7.4
		O3 (+8)	41	496	50	
		O4 (+8) BM-10	55	330	35	
		O4 (+60) BM-10	55	126	30	
		O4 (-90) BM-10	56	95	23	
		O4H+ (-66) BM-10	57	102	16	
		O4B- (+22) BM+20	89	144	27	
		O4BT (-8) BM+20	89	**152**	**26**	
		O4B+ (-38) BM+20	90	103	19	
		O4A (+8) BM+43	113	120	26	
		O4A (-90) BM+43	113	80	16	
		O6 (+8)	370	60	29	
5	Q16 (FEO)	O1 (+8)	9	730	96	10.9
		O3 (+8)	42	441	61	
		O4 (+8) BM-10	55	314	51	
		O4 (+60)	55	93	21	

Ch. No.	Ch. ID (FEO /BEO)	Nominal Location (o'clock from ORJ end)	Location (from Outlet end (mm) **(Note 1)**	$[D]_{meas}$ (ppm)	$[H]_{meas}$ (ppm)	$[H]i_{nitial}$ (offcut) ppm
		BM-10				
		O4 (-20) BM-10	55	152	29	
		O4 (-90) BM-10	56	87	26	
		O4H+(-66) BM-10	56	95	21	
		O4B-(+22) BM+20	89	111	40	
		O4BT(-8) BM+20	90	**168**	**33**	
		O4B+(-38) BM+20	89	104	34	
		O4A (+8) BM+43	113	130	32	
		O6 (+8)	370	68	26	
6	H06 (FEO)	O1T (-8)	9	310	66	15
		O3T (-8)	42	210	49	
		O4T (-8) (BM-10)	57	171	42	
		O4BT(-8) (BM+20)	89	**122**	**40***	
		O4BH+(-66) (BM+20)	88	76	21	
		O4AT(-8) (BM+43)	112	104	41*	
		O6T(-8)	394	59	27	
7	X09 (FEO)	O1T (-8)	11	475	73	14.9
		O3T (-8)	44	238	42	
		O4T (-8) (BM-10)	58	186	40	
		O4BT(-8) (BM+20)	**90**	**118**	**24**	
		O4BH+(-66) (BM+20)	89	93	27	
		O4AT(-8) (BM+43)	113	107	24	
		O6T(-8)	396	53	26	
8	O20 (FEO)	O1T(-8)	10	921.0	96.0	12.3
		O4T(-8) (BM-10)	56	451.0	53.0	
		O4BT(-8) (BM+20)	89	**218.0**	**35.0**	
		O6T(-8)	395	64.0	26.0	
9	Q12 (FEO)	O1T(-8)	11	850	99	10.3
		O3T(-8)	42	620	75	
		O4T(-8) (BM-10)	57	400	52	
		O4BT(-8) (BM+20)	90	**185**	**30**	
		O4BH+(-66) (BM+20)	89	89	18	

Ch. No.	Ch. ID (FEO /BEO)	Nominal Location (o'clock from ORJ end)	Location (from Outlet end (mm) **(Note 1)**	$[D]_{meas}$ (ppm)	$[H]_{meas}$ (ppm)	$[H]i_{nitial}$ (offcut) ppm
		O4AT(-8) (BM+43)	112	142	29*	
		O6T(-8)	395	67	23*	
10	N04 (BEO)	O2T (-8)	27	337	58	14.7
		O4T (-8)	58	205	40	
		O4H+(-66) (BM-10)	57	87	22	
		O4H-(+50) (BM-10)	57	92	28	
		O4BT (-8) (BM+20)	**91**	**120**	**29**	
		O4B- (+22) (BM+20)	91	104	32	
		O4AT (-8) (BM+43)	114	100	28	
11	O15 (BEO)	O1T (-8)	12	303	56	8.7
		O3T (-8)	43	185	35	
		O4T (-8) (BM-10)	58	151	31	
		O4H+(-66) (BM-10)	57	79	21	
		O4H-(+50) (BM-10)	57	83	21	
		O4BT (-8) (BM+20)	89	107	25	
		O4AT (-8) (BM+43)	113	94	24	
12	O17 (BEO)	O1T (-8)	11	122	28	9.0
		O3T (-8)	43	110	23	
		O4T (-8) (BM-10)	57	103	26	
		O4H+(-66) (BM-10)	56	83	22	
		O4H-(+50) (BM-10)	57	86	35	
		O4BT (-8) (BM+20)	89	94	23	
		O4AT (-8) (BM+43)	114	89	20	
13	O13 (BEO)	O1T (-8)	11	443	72	12.5
		O3T (-8)	43	298	45	
		O4T (-8) (BM-10)	57	216	50	
		O4H+(-66) (BM-10)	56	98	33	
		O4H-(+50) (BM-10)	56	96	32	
		O4BT (-8) (BM+20)	89	126	29	
		O4AT (-8) (BM+43)	112	108	26	
14	P14	O1T (-8)	10	191	34	9.0

Ch. No.	Ch. ID (FEO /BEO)	Nominal Location (o'clock from ORJ end)	Location (from Outlet end (mm) **(Note 1)**	$[D]_{meas}$ (ppm)	$[H]_{meas}$ (ppm)	$[H]i_{nitial}$ (offcut) ppm
	(BEO)	O3T (-8)	42	125	24	
		O4T (-8) (BM-10)	56	108	24	
		O4H+(-66) (BM-10)	55	79	20	
		O4H-(+50) (BM-10)	56	80	21	
		O4BT (-8) (BM+20)	88	91	20	
		O4AT (-8) (BM+43)	111	86	22	
15	Q13 (BEO)	O1T (-8)	12	582	87	11.7
		O3T (-8)	43	467	73	
		O4T (-8) (BM-10)	59	341	61	
		O4H+(-66) (BM-10)	57	89	21	
		O4H-(+50) (BM-10)	58	91	21	
		O4BT (-8) (BM+20)	91	183	35	
		O4AT (-8) (BM+43)	114	139	29	
16	L12 (BEO)	O1T (-8)	10	156	27	6.7
		O3T (-8)	42	111	20	
		O4T (-8) (BM-10)	57	99	23	
		O4H+(-66) (BM-10)	56	86	21	
		O4H-(+50) (BM-10)	57	79	17	
		O4BT (-8) (BM+20)	90	87	18	
		O4AT (-8) (BM+43)	113	83	19	
17	F05 (BEO)	O1T (-8)	11	75	25	11.7
		O3T (-8)	43	82	25	
		O4T (-8) (BM-10)	57	82	23	
		O4H+(-66) (BM-10)	57	72	25	
		O4H-(+50) (BM-10)	57	74	21	
		O4BT (-8) (BM+20)	90	76	21	
		O4AT (-8) (BM+43)	114	69	27	
18	L22 (BEO)	O1T (-8)	12	42	24	9.3
		O3T (-8)	43	41	14	
		O4T (-8) (BM-10)	58	42	21	
		O4H+(-66)	57	41	18	

Ch. No.	Ch. ID (FEO /BEO)	Nominal Location (o'clock from ORJ end)	Location (from Outlet end (mm) **(Note 1)**	$[D]_{meas}$ (ppm)	$[H]_{meas}$ (ppm)	$[H]i_{nitial}$ (offcut) ppm
		(BM-10)				
		O4H-(+50) (BM-10)	58	43	19	
		O4BT (-8) (BM+20)	91	42	21	
		O4AT(-8) (BM+43)	114	43	18	
19	R10 (BEO)	O1T(+8)	8	199	26	5.5
		O2T(+8)	23	161	26	
		O3T(+8)	40	122	20	
		O4AT(+8) (BM+43)	112	93	16	
		O6T(+8)	367	56	16	
20	S13 (BEO)	O1T(-8)	11	314	38	6.0
		O3T(-8)	44	163	21	
		O4T(-8) (BM-10)	57	133	19	
		O4H+(-66) (BM-10)	58	97	16	
		O4H-(+50) (BM-10)	56	97	15	
		O4BT(-8) (BM+20)	90	105	17	
		O4AT(-8) (BM+43)	112	98	17	
21	C11 (FEO)	O1 (+20)	5	790	97	11
		O1 (-20)	5	125	20	
		O3 (+20)	36	400	52	
		O3 (-20)	36	112	18	
		O4 (+20) (BM-10)	50	280	39	
		O4 (-20) (BM-10)	50	105	21	
		O4 (-90) (BM-10)	50	89	16	
		O4A (-20) (BM+43)	109	95	19	
		O4A (-90) (BM+43)	109	82	14	
		O5 (+20)	123	104	22	
		O6 (+20)	364	65	19	
22	D16 (FEO)	O3 (-90)	37	78	13	13.1
		O4 (+20) (BM-10)	51	138	22	
		O4 (-20) (BM-10)	51	99	17	
		O4 (-90) (BM-10)	51	79	14	
		O4A (+20) (BM+43)	110	95	18	
		O4A (-90) (BM+43)	110	75	14	
23	B12	O1 (+8)	11	69	18	9.7

Ch. No.	Ch. ID (FEO /BEO)	Nominal Location (o'clock from ORJ end)	Location (from Outlet end (mm) **(Note 1)**	$[D]_{meas}$ (ppm)	$[H]_{meas}$ (ppm)	$[H]i_{nitial}$ (offcut) ppm
	(FEO)	O3 (+8)	42	70	14	
		O4 (+8) (BM-10)	56	71	19	
		O4 (+60) (BM-10)	56	65	16	
		O4 (-90) (BM-10)	56	61	16	
		O4A (+8) (BM+43)	115	69	18	
		O4A (-90) (BM+43)	115	60	19	
24	M02 (FEO)	O1 (+8)	11	240	24	10.3
		O3 (+8)	42	154	18	
		O4 (+8) (BM-10)	57	132	13	
		O4 (+60) (BM-10)	57	117	14	
		O4 (-90) (BM-10)	57	105	12	
		O4A (+8) (BM+43)	115	109	15	
		O4A (-90) (BM+43)	115	96	16	
25	T03 (FEO)	O1 (+8)	12	270	28	11.0
		O3 (+8)	43	138	18	
		O4 (+8) (BM-10)	57	125	17	
		O4 (+60) (BM-10)	57	100	16	
		O4 (-90) (BM-10)	57	84	15	
		O4A (+8) (BM+43)	116	95	17	
		O4A (-90) (BM+43)	116	81	15	
26	U20 (FEO)	O1 (+8)	11	490	39	10.4
		O3 (+8)	42	230	22	
		O4 (+8) (BM-10)	57	162	18	
		O4 (+60) (BM-10)	57	121	15	
		O4 (-90) (BM-10)	57	106	14	
		O4A (+8) (BM+43)	115	114	18	
		O4A (-90) (BM+43)	115	99	17	
27	C15 (FEO)	O1 (+36)	11	643	84	10.8
		O3 (+36)	42	314	51	
		O4 (+8) (BM-10)	57	200	37	
		O4 (+60)	57	105	26	

Ch. No.	Ch. ID (FEO /BEO)	Nominal Location (o'clock from ORJ end)	Location (from Outlet end (mm) (Note 1)	$[D]_{meas}$ (ppm)	$[H]_{meas}$ (ppm)	$[H]i_{nitial}$ (offcut) ppm
		(BM-10)				
		O4 (-90) (BM-10)	57	93	20	
		O4A (+8) (BM+43)	115	111	26	
		O4A (-90) (BM+43)	115	83	20	
		O6 (+8)	369	66	30	
28	E05 (FEO)	O1 (+8)	11	134	14	8.6
		O3 (+8)	42	111	17	
		O4 (+8) (BM-10)	57	109	12	
		O4 (+60) (BM-10)	57	100	13	
		O4 (-90) (BM-10)	57	90	11	
		O4A (+8) (BM+43)	115	97	14	
		O4A (-90) (BM+43)	115	82	12	
		O6 (+8)	370	60	14	
29	F04 (FEO)	O1 (+8)	11	680	62	8.3
		O3 (+8)	42	380	37	
		O4 (+8) (BM-10)	57	250	30	
		O4 (+34) (BM-10)	57	250	27	
		O4 (+60) (BM-10)	57	-	-	
		O4 (-90) (BM-10)	57	122	16	
		O4A (+8) (BM+43)	115	124	18	
		O4A (-90) (BM+43)	115	95	13	
		O6 (+8)	370	65	14	
30	K16 (FEO)	O4 (+8) (BM-10)	56	300	29	8.7
		O4 (+60) (BM-10)	56	130	14	
		O4 (-90) (BM-10)	56	117	11	
		O4A (+8) (BM+43)	114	121	15	
		O4A (+60) (BM+43)	114	102	14	
		O4A (-90) (BM+43)	114	95	12	
		O6 (+8)	369	60	14	
31	V17 (FEO)	O1 (+8)	10	86	13	7.2
		O3 (+8)	41	89	14	
		O4 (+8)	56	89	14	

Ch. No.	Ch. ID (FEO /BEO)	Nominal Location (o'clock from ORJ end)	Location (from Outlet end (mm) **(Note 1)**	[D]$_{meas}$ (ppm)	[H]$_{meas}$ (ppm)	[H]i$_{nitial}$ (offcut) ppm
		(BM-10)				
		O4 (+60) (BM-10)	56	85	12	
		O4 (-90) (BM-10)	56	78	13	
		O4A (+8) (BM+43)	114	83	13	
		O4A (-90) (BM+43)	114	74	15	
		O6 (+8)	369	58	13	
32	D07 (BEO)	O1 (+8)	4	84	19	9.2
		O3 (+8)	35	86	20	
		O4 (+8) (BM-10)	50	85	20	
		O4 (+60) (BM-10)	50	80	19	
		O4 (-90) (BM-10)	50	74	17	
		O4A (+8) (BM+43)	108	77	21	
		O4A (-90) (BM+43)	108	67	16	
		O6 (+8)	363	47	19	
33	E20 (BEO)	O1 (+8)	8	69	19	10.3
		O3 (+8)	39	71	20	
		O4 (+8) (BM-10)	54	71	23	
		O4 (+60) (BM-10)	54	67	22	
		O4 (-90) (BM-10)	54	61	16	
		O4A (+8) (BM+43)	112	65	19	
		O4A (-90) (BM+43)	112	56	16	
		O6 (+8)	367	46	18	
34	G10 (BEO)	O1 (+8)	5	370	44	11.0
		O3 (+8)	36	200	28	
		O4 (+8) (BM-10)	51	139	20	
		O4 (+60) (BM-10)	51	83	13	
		O4 (-90) (BM-10)	51	71	13	
		O4A (+8) (BM+43)	109	89	18	
		O4A (-90) (BM+43)	109	68	16	
		O6 (+8)	364	57	14	
35	G14 (BEO)	O1 (+8)	5	400	66	11.3
		O3 (+8)	36	260	42	
		O4 (+8)	52	180	31	

Ch. No.	Ch. ID (FEO /BEO)	Nominal Location (o'clock from ORJ end)	Location (from Outlet end (mm) **(Note 1)**	$[D]_{meas}$ (ppm)	$[H]_{meas}$ (ppm)	$[H]i_{nitial}$ (offcut) ppm
		(BM-10)				
		O4 (+60) (BM-10)	52	84	17	
		O4 (-90) (BM-10)	52	73	14	
		O4A (+8) (BM+43)	109	92	21	
		O4A (-90) (BM+43)	109	67	14	
36	J14 (BEO)	O1 (+8)	5	190	20	9.3
		O3 (+8)	36	126	19	
		O4 (+8) (BM-10)	52	107	<13	
		O4 (+60) (BM-10)	52	91	11	
		O4 (-90) (BM-10)	52	78	13	
		O4A (+8) (BM+43)	109	88	16	
		O4A (-90) (BM+43)	109	71	14	
37	K15 (BEO)	O1 (+8)	5	109	29	8.0
		O3 (+8)	36	98	21	
		O4 (+8) (BM-10)	52	89	32	
		O4 (+60) (BM-10)	52	85	29	
		O4 (-90) (BM-10)	52	78	17	
		O4A (+8) (BM+43)	109	71	14	
		O4A (-90) (BM+43)	109	66	24	
38	M13 (BEO)	O1 (+20)	6	363	57	7.3
		O3 (+20)	37	230	35	
		O4 (+8) (BM-10)	53	197	38	
		O4 (+60) (BM-10)	53	103	29	
		O4 (-90) (BM-10)	53	94	27	
		O4A (+8) (BM+43)	110	104	25	
		O4A (-90) (BM+43)	110	83	29	
		O6 (+20)	365	57	26	
39	Q23 (BEO)	O1 (+8)	5	73	34	9.0
		O3 (+8)	36	75	23	
		O4 (+8) (BM-10)	51	75	20	
		O4 (+60) (BM-10)	51	72	19	

Ch. No.	Ch. ID (FEO /BEO)	Nominal Location (o'clock from ORJ end)	Location (from Outlet end (mm) (Note 1)	$[D]_{meas}$ (ppm)	$[H]_{meas}$ (ppm)	$[H]i_{nitial}$ (offcut) ppm
		O4 (-90) (BM-10)	51	67	18	
		O4A (+8) (BM+43)	109	71	19	
		O4A (-90) (BM+43)	109	63	17	
40	U11 (BEO)	O1 (+8)	13	46	21	8.8
		O3 (+8)	44	46	21	
		O4A (+8) (BM+43)	117	46	22	
		O4A (+60) (BM+43)	117	41	23	
		O4A (-90) (BM+43)	117	37	19	
		O6 (+8)	372	37	29	
41	V18 (BEO)	O1 (+8)	5	76	26	10.3
		O3 (+8)	36	79	21	
		O4 (+8) (BM-10)	51	78	20	
		O4 (+60) (BM-10)	51	76	25	
		O4 (-90) (BM-10)	51	70	21	
		O4A (+8) (BM+43)	109	72	30	
		O4A (-90) (BM+43)	109	64	18	
42	M16 (FEO)	O1 (+20)	13	126	18	8.7
		O3 (+20)	44	116	15	
		O5 (+20)	131	93	16	
		O6 (+20)	372	63	16	

Notes:
1   The axial locations are based on UT from 3rd window (PTs # 1-to 20 inspected during 3rd window), otherwise are estimated based on scrape locations relative to E-face provided in the CWEST inspection bulletins and the channel specific EF to End of PT distance.
* organic contamination noted during analyses which affect the [H] measurements, hence the [H]eq based on measured [H].

Table 2- Summary of [D] and [H] measurements for A2131 Inlet RJ (all windows)

Ch. No.	Ch. ID (FEI /BEI)	Nominal Location (o'clock from ORJ end)	Location (from Outlet end (mm) **(Note 1)**	$[D]_{meas}$ (ppm)	$[H]_{meas}$ (ppm)	$[H]i_{nitial}$ (offcut) ppm
1	F16 (BEI)	I4T(+8) (BM-10)	59	53	16	12.6
		I4H-(-50) (BM-10)	59	54	17	
		I4H+(+66) (BM-10)	59	53	15	
2	G15 (BEI)	I1T(+8)	8	130.0	46.0	11.3
		I4T(+8) (BM-10)	55	54.0	25.0	
		I4AT(+8) (BM+43)	110	41.0	18.0	
		I6T(+8)	395	14.0	28.0	
3	K10 (BEI)	I1T(+8)	9	169.0	32.0	7.4
		I4T(+8) (BM-10)	55	65.0	23.0	
		I4AT(+8) (BM+43)	111	48.0	15.0	
		I6T(+8)	394	15.0	16.0	
4	L11 (BEI)	I4T(+8) (BM-10)	55	63	13	9.3
		I4H-(-50) (BM-10)	55	63	15	
		I4H+(+66) (BM-10)	55	63	11	
5	O10 (BEI)	I2T(+8)	25	177.0	50.0	12.7
		I4H-(-50) (BM-10)	56	69.0	21.0	
		I4T(+8) (BM-10)	56	69.0	23.0	
		I4H+(+66) (BM-10)	56	66.0	25.0	
		I4A-(-22) (BM+43)	112	46.0	18.0	
		I4AT(+8) (BM+43)	112	46.0	49.0	
		I4A+(+38) (BM+43)	113	45.0	20.0	
		I6T(+8)	396	13.0	20.0	
6	O20 (BEI)	I2T(+8)	26	139.0	33.0	12.3
		I4T(+8) (BM-10)	57	57.0	18.0	
		I4AT(+8) (BM+43)	113	44.0	18.0	
		I6T(+8)	396	12.0	23.0	
7	Q16 (BEI)	I2T(+8)	27	89.0	26.0	10.9
		I4T(+8) (BM-10)	58	56.0	20.0	
		I4AT(+8) (BM+43)	114	45.0	28.0	

		I6T(+8)	397	16.0	72.0*	
		I2T(+8)	27	89.0	26.0	
		I4T(+8) (BM-10)	58	56.0	20.0	
		I4AT(+8) (BM+43)	114	45.0	28.0	
8	E20 (FEI)	I1 (+20)	11	78.0	14	10.3
		I3 (+20)	42	-	-	
		I5 (+20)	129	51.0	15	
		I6 (+20)	370	22.0	15	
9	R22 (FEI)	I1 (+20)	12	145.0	20	7
		I3 (+20)	43	-	-	
		I5 (+20)	130	64.0	14	
		I6 (+20)	371	23.0	13	

Notes:

1   The axial locations are based on UT from 3rd window (PTs # 1-to 7 inspected during 3rd window), otherwise are estimated based on scrape locations relative to E-face provided in the CWEST inspection bulletins and the channel specific EF to End of PT distance.

* organic contamination noted during analyses which affect the [H] measurements, hence the [H]eq based on measured [H].

Table 3- Summary of [D] and [H] measurements for Removed Tube B6S13 Outlet RJ

Axial Location (mm)	Circumferential Location (clock)*	[H] (mg/kg)	[D] (mg/kg)
8	12	55	520
13	12	55	530
28	12	57	520
44	12	51	450
59	12	44	360
	1	34	280
	2	14	106
	3	13	94
	4	12	94
	5	12	95
	6	12	96
	7	13	96
	8	13	96
	9	13	93
	10	13	99
	11	18	137
69 (burnish mark)	12	46	330
	1	32	260
	2	14	103
	3	13	94
	4	12	92
	5	12	93
	6	12	93

Axial Location (mm)	Circumferential Location (clock)*	[H] (mg/kg)	[D] (mg/kg)
	7	14	94
	8	13	94
	9	13	95
	10	14	97
	11	19	141
79	12	42	340
	1	27	220
	2	14	105
	3	12	91
	4	12	90
	5	12	90
	6	12	91
	7	11.8	92
	8	12.0	93
	9	13.1	100
	10	17	132
	11	25	210
89/90 (burnish mark + 20 mm)	12	22	152
	1	19	142
	2	13	96
	3	11.8	89
	4	12	87
	5	12	88
	6	12.5	88
	7	11	88
	8	12	88
	9	12.2	87
	10	12	90
	11	13	99
145	12	17	109
	2	13.9	86
	3	12.3	78
	4	12.3	76
	5	11.8	77
	6	11.9	78
	7	11.8	77
	8	11.9	77
	9	11.8	76
	10	12	79
	11	14	87

* clock position as viewed from the outlet end of the tube

Table 4- Summary of [D] and [H] measurements for Removed Tube B6S13 Inlet RJ

Axial Location (mm)	Circumferential Location (clock)	[H] (mg/kg)	[D] (mg/kg)
8	12	21	220
13	12	25	250
28	12	24	230
45	12	19	162
63	12	14	105
79	12	18	131
90 (burnish mark + 20)	12	11	59
150	12	11	45

Table 5- Summary of [D] and [H] measurements for Removed Tube B6N07 Outlet RJ

Axial Location (mm)	Circumferential Location (clock)*	[H] (mg/kg)	[D] (mg/kg)
71	12	15	118
71	1	12.4	94
71	3	10.1	79
71	6	10.1	78
71	9	10.5	80
71	11	13.4	98
90	12	14	101
90	1	11.7	89
90	3	10.0	75
90	6	10.2	74
90	9	10.0	76
90	11	12.5	93

* clock position as viewed from the outlet end of the tube

Enclosure 1

B-31100 LOF NSAS, Revision R00

Re: Justification for Application of Crack Initiation Models to High Hydrogen Equivalent Concentration Regions in Pressure Tubes

Supplier Document Acceptance Form

Bruce Power™

KINECTRICS

RE: JUSTIFICATION FOR APPLICATION OF CRACK INITIATION MODELS TO HIGH HYDROGEN EQUIVALENT CONCENTRATION REGIONS IN PRESSURE TUBES

B-31100 LOF NSAS

REV. 000

☒ Accepted ☐ Accepted As Noted – Revision Required
☐ Rejected ☐ Accepted As Noted – No Revision Required
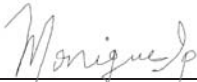
FOR USE AT BRUCE POWER

ACCEPTED: **MONIQUE IP**

(Print Name) (Signature)

TITLE: **SENIOR TECHNICAL OFFICER**

(Print Title)

DATE: **17SEP2021**

(DDMMMYYYY)

ACCEPTANCE OF THIS DOCUMENT DOES NOT RELIEVE THE

CONTRACTOR OF RESPONSIBILITY FOR ANY ERRORS OR OMISSIONS.

September 16, 2021

Jason Goldberg

Nuclear Safety Analysis and Support

Bruce Power

123 Front St. W., 4th Floor

Toronto, ON M5J 2M2

Re: Justification for Application of Crack Initiation Models to High Hydrogen Equivalent Concentration Regions in Pressure Tubes

1.   INTRODUCTION

High levels of hydrogen equivalent concentration (H_{eq}) have been detected in the outlet rolled joints of Bruce Unit 3 during the 2021 outage (A2131). Bruce Unit 3 has operated to 231,964 Equivalent Full Power Hours (EFPH), or 271,330 Hot Hours (HH), at the current time. The axial and circumferential extents of the higher than expected levels of H_{eq} have been found to be concentrated in a localized region extending from the outlet end of the pressure tube for a distance approximately 50 mm inboard of the outlet rolled joint burnish mark with a central tendency about the top of the pressure tube. In Attachment A of the Canadian Nuclear Safety Commission (CNSC) correspondence to Bruce Power on Aug 5, 2021 [1], CNSC requested additional information regarding the recent elevated H_{eq} from scrape campaigns. The CNSC request as outlined under Item 9 of Attachment A is:

"Bruce Power is requested to submit a detailed plan for research activities to verify the assumptions that crack initiation models are not impacted by elevated [Heq]. Current crack initiation models are only supported by data from material with [Heq] up to 110 ppm."

In a subsequent email communication from CNSC to Bruce Power [2], CNSC made the following request:

"Based on the presentation that Bruce Power provided at the August 12th meeting on the A2131 scrape campaign results to date, CNSC staff request that the following additional information is included in the Unit 3 restart submission:

Confirmation that crack initiation models remain valid for the elevated Heq values measured inboard of the burnish mark in some of the Unit 3 pressure tubes at the location of the scrapes."

A justification for the application of the current crack initiation models for evaluation of flaws in pressure tube regions with elevated levels of H_{eq} above 110 ppm is provided in Section 2 of this letter. Detailed test plans to obtain experimental data to support the understanding that the crack initiation models for Delayed Hydride Cracking (DHC), hydrided region overloads (HROL) and fatigue are not impacted by elevated levels of H_{eq} above 110 ppm are provided in Section 3 of this letter.

During the current outage, deuterium was sampled at standard and non-standard locations inboard and outboard of the outlet rolled joint burnish mark using the Circumferential West Scrape Tool (CWEST) to better characterize the H_{eq} distributions in the regions of interest. The inboard locations sampled were at 20 mm, 43 mm and nominally 303 mm from the outlet rolled joint burnish mark [3]. The highest measured H_{eq} at the 20 mm location inboard of the outlet burnish mark was 184 ppm [4]. Based on the measured H_{eq}, the maximum value predicted at the 20 mm location inboard of the outlet rolled joint burnish mark at the end of the evaluation period of 246,000 EFPH, which is the date of the Major Component Replacement (MCR), is 200 ppm. In addition, it is recommended in Reference [4] to also use an H_{eq} of 220 ppm as a sensitivity case to address uncertainties in assumptions and inputs used in the calculations for future projections of H_{eq}. Since a review of inspection data from all Bruce reactors has confirmed the extremely low probability of forming a dispositionable service-induced flaw in this small, localized region of elevated H_{eq}, the primary focus is demonstration of no crack initiation from scrape flaws. A margin assessment for demonstration of protection against crack initiation from scrape flaws in the outlet rolled joints of Bruce Unit 3 pressure tubes using a postulated level of H_{eq} of 220 ppm is provided in Section 4. A summary is provided in Section 5.

2. JUSTIFICATION OF APPLICATION OF CRACK INITIATION MODELS TO HIGH HYDROGEN EQUIVALENT CONCENTRATION REGIONS IN PRESSURE TUBES

2.1 Bulk Levels of Hydrogen Equivalent Concentrations Greater than *TSSD* at the Peak Temperature

From Attachment A of Reference [5], the amount of H_{eq} in solution available for hydride accumulation at a flaw is limited by the peak operating temperature. Over the operating temperature range from 250 through 310°C, the maximum H_{eq} concentration in solution will range from 37 through 84 ppm by conservatively assuming the Khatamian *TSSD* equation. Levels of H_{eq} above the *TSSD* concentration at the peak operating temperature will remain as bulk hydrides and would not affect flaw-tip hydride accumulation. This is supported by the results in Reference [6] that demonstrated that the threshold stresses for DHC initiation from flaws are not affected by the hydrogen concentrations under outlet end temperature thermal cycles at H_{eq} levels up to 110 ppm. Levels of H_{eq} in excess of the *TSSD* concentration at 310°C would remain as bulk hydrides, which should have no effect on the DHC initiation and growth processes that encompass diffusion of hydrogen, and formation and fracture of reoriented hydrides at the flaw tip.

The independence of the process-zone model for predicting DHC initiation from levels of H_{eq} greater than *TSSD* at the peak temperature is described below in the context of the basic principles of the model.

2.2 Process-Zone Model for Predicting DHC Initiation at Flaws

2.2.1 Review of Fundamentals of Process-Zone Model

Hydrided regions formed at the tip of a blunt notch in a cantilever beam test specimen from an unirradiated pressure tube are shown in Figure 2-1. A hydrided region that emanates from a flaw tip, together with the particular sub-region that is fracturing, can be viewed as a single entity [7]. This single entity is represented by an infinitesimally thin two-dimensional strip, or process zone, with a length, s, emanating from a flaw tip. Within this process zone the tensile stress is idealized to have a uniform value p_H as illustrated in Figure 2-1. The relative displacement across the process zone at the flaw surface is equal to v_T as illustrated in Figure 2-1. The process-zone displacement v_T is a measure of the expansion of the thickness of the hydrided region. As the amount of precipitated hydride increases, and because of the expansion [8] associated with the hydride precipitation, the stress p_H decreases while v_T increases. It is assumed that loss of cohesion at the trailing edge of the process zone at the flaw-tip surface, which corresponds to DHC initiation, occurs when v_T attains a critical value v_c. Furthermore, there exists a limiting threshold level of p_H below which the hydrided region is unable to fracture, and this threshold level is denoted as p_c. The p_c is taken to correspond to the threshold stress for DHC initiation at a planar surface assuming the formation of an "infinitely long" hydride. For DHC initiation to occur, two conditions must be satisfied [7].

$$v_T \geq v_c \tag{2-1}$$

and

$$p_H \quad \geq \quad p_c \tag{2-2}$$

where

p_c =   threshold stress for DHC initiation at a planar surface
p_H =   process-zone restraining stress
v_c =   critical process-zone displacement for DHC initiation
v_T =   process-zone displacement due to the applied stress

A schematic illustration of whether DHC will initiate is shown in Figure 2-2. This figure is for flaw-tip hydride ratcheting conditions where growth of the hydrided region occurs with each thermal cycle. The hydrided region will grow in size with each Heatup/Cooldown cycle up to a limit and p_H will progressively decrease. In particular, the threshold peak stress, σ_{TH}, is defined as the lowest level of initial peak flaw-tip stress prior to hydride formation, at which DHC initiation can possibly occur, as indicated schematically in Figure 2-2. Furthermore, if the hydrided region stress p_H falls below p_c prior to v_T having reached v_c, DHC initiation should not occur despite further development of the hydrided region. This corresponds to the lower curve in Figure 2-2.

As described above, p_c is the threshold stress below which a hydrided region cannot fracture, and can be equated with the threshold stress in the case where a hydrided region of effectively "infinite length" emanates from a planar surface. With regard to v_c, it is recognized that when the Dugdale-Bilby-Cottrell-Swinden representation [9][10], is applied to a long crack at threshold conditions such that $p_H = p_c$, then

$$v_c \quad = \quad \frac{K_{IH}^{\;2}}{E' \, p_c} \tag{2-3}$$

where

$$E' \quad = \quad \frac{E}{1 - v^2} \tag{2-4}$$

and

E =   Young's modulus of the Zr-Nb pressure tube material
K_{IH} =   threshold stress intensity factor for DHC initiation at a crack
v =   Poisson's ratio of the Zr-Nb pressure tube material

One method for measuring K_{IH} is to use a pre-cracked cantilever beam test specimen, as illustrated schematically in Figure 2-3. The method for measuring p_c is to use a nominally smooth cantilever beam test specimen as illustrated schematically in Figure 2-3. A series of specimens are subjected to a range of applied stress levels to determine the stress for the onset of

DHC, which is taken as p_c. With knowledge of K_{IH} and p_c, which gives v_c from Eq. (2-3), it is possible in principle to predict DHC initiation at any flaw. An implicit assumption in using the process-zone methodology is that p_c and v_c are flaw geometry independent. Validation of this assumption was achieved through comparison of process-zone model predictions with results of DHC initiation experiments on unirradiated and irradiated test specimens with a wide range of notch geometries.

The length, s, of the process zone is calculated by simulating two crack loading problems as illustrated in Figure 2-4.

(i) a fictitious crack of length, s, subjected to the applied stress distribution $\sigma(x)$ due to the flaw
(ii) a fictitious crack of length, s, subjected to a uniform cohesive, restraining stress p_H

The end of the process zone away from the flaw tip is modelled as a fictitious crack tip at which the stresses must be finite. This means that the sum of the two stress intensity factors, K_I, from the two loads (i) and (ii) must be zero. For the stress distribution ahead of the flaw tip due to the applied loads and as calculated in the absence of the process zone, $\sigma(x)$, and the process-zone uniform stress, p_H, the length, s, of the process-zone is calculated using

$$K_I\big(s, \sigma(x)\big) + K_I\big(s, p_H\big) = 0 \qquad (2\text{-}5)$$

where

$K_I(s, \sigma(x))$ = stress intensity factor of the fictitious crack of length, s, due to the applied stress $\sigma(x)$

$K_I(s, p_H)$ = stress intensity factor of the fictitious crack of length, s, due to the restraining stress, p_H

The process-zone displacement, v_T, is the sum of the displacements at $x = 0$ of the fictitious crack of length, s, due to the applied stress $\sigma(x)$ and the restraining stress p_H.

$$v_T = v_T\big(0, s, \sigma(x)\big) + v_T\big(0, s, p_H\big) \qquad (2\text{-}6)$$

where

$v_T(0, s, \sigma(x))$ = crack-opening displacement at $x = 0$ of the fictitious crack of length, s, due to the applied stress $\sigma(x)$

$v_T(0, s, p_H))$ = crack-opening displacement at $x = 0$ of the fictitious crack of length, s, due to the restraining stress p_H

The engineering process-zone models for evaluation of DHC initiation in Annex A of the CSA Standard N285.8 [11] are based on the above basic principles.

2.2.2 Applicability of Process-Zone Model to High Hydrogen Equivalent Concentrations

In the criteria for DHC initiation that are given by Eqs. (2-1) and (2-2), there is no explicit dependency on the level of H_{eq}. This means that there is no upper limit on H_{eq} for Eq. (2-1) and (2-2) to still be valid. The level of H_{eq} refers to both the concentration of H_{eq} in solution as well as the bulk concentration of H_{eq} including hydrides.

The calculation of the length, s, of the process-zone is based on the assumption that there is an "infinite" amount of H_{eq} available to precipitate in the hydrided region to satisfy Eq. (2-5). There is no explicit dependency of Eq. (2-5) on the level of H_{eq}. This means that there is no upper limit on H_{eq} for Eq. (2-5) to still be valid. The process-zone model is based on the assumption that the hydrided region is formed under hydride ratcheting conditions with a sufficient number of thermal cycles to achieve a fully developed hydrided region.

Similar to the calculation of the length of the process-zone, the calculation of the process-zone displacement, v_T, is based on the assumption that there is an "infinite" amount of H_{eq} available to precipitate in the hydrided region to result in the displacements of Eq. (2-6). There is no explicit dependency of Eq. (2-6) on the level of H_{eq}. This means that there is no upper limit on H_{eq} for Eq. (2-6) to still be valid.

Based on the above, consideration of the validity of the process-zone model for high levels of H_{eq} is reduced to consideration of whether the material DHC properties p_c and K_{IH} are adversely affected by very high levels of H_{eq}. This is discussed below.

2.2.3 Applicability of DHC Threshold Property p_c to High Hydrogen Equivalent Concentrations

As stated above, p_c is taken to correspond to the threshold stress for DHC initiation at a planar surface assuming the formation of an "infinitely long" radial hydride. The value of p_c that is measured in an experiment is equal to the nominal applied stress. The actual stress in the radial hydrided region is the nominal applied tensile stress minus the compressive stress component due to the volumetric expansion strain of precipitated hydride. The most conservative measurement of p_c is for the situation where the compressive stress component due to the hydride volumetric expansion strain is zero, since there is no reduction in the stress in the radial hydrided region due to the volumetric expansion strain to mitigate cracking. Solutions for the compressive stress component due to the volumetric expansion strain of precipitated hydride are provided in Reference [12]. From Reference [12], the compressive stress component due to the volumetric expansion strain approaches zero as the radial hydrided region thickness divided by length aspect ratio approaches zero. In the limit of an "infinitely long" hydrided region, the compressive stress component is zero. An objective of the tests to measure p_c is to achieve radial hydrided regions of sufficient length to result in a compressive stress component due to the volumetric expansion strain that is essentially zero. This results in the most conservative measurement of p_c.

Values of p_c are measured by performing DHC initiation tests on specimens with nominally smooth surfaces, with specific thermo-mechanical cycles designed to form long radial hydrided regions emanating from the surface of the specimens. For the p_c tests that have been performed, the resultant radial hydrided regions are relatively long with very low thickness divided by length aspect ratios. For example, the lower-bound value of p_c of 450 MPa in the CSA Standard N285.8 is based on DHC initiation tests performed on cantilever beam bending specimens with small, blunt scratches that were removed from the ex-service pressure tube P3L09 [13]. The nominal bulk H_{eq} in the specimens was 70 ppm. The test specimens were thermally cycled under load. There were a number of radial hydrided regions in the specimens with depths in the range of 0.5 through 1.0 mm [13]. The corresponding radial hydrided region thickness divided by length aspect ratios are of the order of 0.01. From the solutions in Reference [12], the compressive stress component due to the volumetric expansion strain for this aspect ratio is essentially zero. This means that p_c was measured with no mitigation due to a compressive stress component, and is therefore the most conservative measurement. For the case of a significant number of thermal cycles under hydride ratcheting conditions, as was the case in Reference [13], the lengths of the radial hydrided regions are considered to not be dependent on the concentration of H_{eq} in solution nor on the bulk concentration of H_{eq}. Even if the radial hydrided regions were longer, the actual value of p_c would still be essentially equal to the nominal applied stress, and there would be no decrease in the measured p_c.

2.2.4 Applicability of DHC Threshold Property K_{IH} to High Hydrogen Equivalent Concentrations

As stated above, K_{IH} is the threshold isothermal stress intensity factor for the onset of DHC from a crack [11]. K_{IH} tests on pressure tube material are performed using a decreasing-load procedure at different temperatures. The choice of test temperature and thermal cycle for the K_{IH} tests are designed to have sufficient hydrogen in solution to optimize the diffusion controlled DHC process. This is done by cooling to the test temperature from a peak temperature that is at least 50°C higher. Any hydrogen in excess of the *TSSD* concentration at the peak temperature would remain as bulk hydrides, and is expected to have no effect on the precipitation and fracture of the crack-tip reoriented hydrides.

A multi-variable statistical analysis was performed in Reference [14] using the K_{IH} database on ex-service pressure tubes released in 2007 [15] to determine the parameters affecting K_{IH}. The database consisted of 212 data points from 27 pressure tubes with specimens taken at different locations along the tubes. The range of the hydrogen equivalent concentration of the specimens was 5 to 77 ppm. The statistical analysis showed that the mean K_{IH} was 6.62 MPa√m with a standard deviation of 0.93 MPa√m. The analysis concluded that K_{IH} was not affected by the bulk H_{eq}. This conclusion is supported by separate experimental studies that are described below.

K_{IH} values were obtained from an ex-service pressure tube with an H_{eq} of 153 ppm [16]. The measured values were not lower than the mean K_{IH} value of the pressure tubes in the database described in Reference [14]. This is consistent with the conclusion from the statistical analysis [14] that K_{IH} is not affected by the bulk H_{eq}.

Reference [6] summarizes the results of K_{IH} measurements on unirradiated and irradiated pressure tube specimens containing different levels of H_{eq}, as shown in Table 2-1. These test results show that K_{IH} in unirradiated and irradiated pressure tube materials are not lowered by the higher bulk hydrogen concentration.

2.2.5 Future Validation of Process-Zone Model Against DHC Initiation Experiments with High Hydrogen Equivalent Concentrations

As described in Section 3, short-term DHC initiation tests will be performed on notched specimens with an H_{eq} of nominally 220 ppm. The results will be compared with those from test specimens from the same pressure tube with a lower level of H_{eq}. A process-zone evaluation procedure in Annex A of the CSA Standard N285.8 will be used to predict the results of the DHC initiation tests with an H_{eq} of nominally 220 ppm. The process-zone prediction results will be reported with the test results.

As also described in Section 3, longer-term DHC initiation tests are proposed to be performed on notched specimens with high levels of H_{eq}. A process-zone evaluation procedure in Annex A of the CSA Standard N285.8 would also be used to predict the results of these DHC initiation tests.

2.3 Applicability of Hydrided Region Overload Models to High Hydrogen Equivalent Concentrations

For crack initiation due to a hydrided region overload with high levels of H_{eq}, the amount of H_{eq} in solution that is available for hydride accumulation at the flaw is limited by the peak operating temperature, and the accumulation of flaw-tip hydrides and their overload resistance under hydride ratcheting conditions are not affected by further increases in the bulk H_{eq} concentration. A model to predict crack initiation due to a hydrided region overload that was developed in Reference [17] is based on test data with levels of H_{eq} up to 110 ppm with notch-tip hydrides formed at a peak temperature of 300°C or lower. No statistically significant effect of H_{eq} on the overload resistance was observed. The work demonstrated the applicability of the hydrided region overload resistance model to high levels of H_{eq}. Hydrided region overload tests with high levels of H_{eq} are proposed as described in Section 3.

2.4 Fatigue Crack Initiation Models

2.4.1 Applicability of Fatigue Crack Initiation Models to High Hydrogen Equivalent Concentrations

The fatigue crack initiation models were developed based on test data from specimens subjected to pre-conditioning thermal cycles with a peak temperature of 300°C or lower to form notch-tip hydrides prior to the fatigue tests. The potential influence of H_{eq} on fatigue crack initiation behaviour was investigated in Reference [18]. The test data that was analyzed had two levels of H_{eq} of 60 and 100 ppm. The work concluded that the effect of H_{eq} on the number of load cycles to fatigue crack initiation is statistically insignificant for H_{eq} in the range of 60 to 100 ppm. This finding is consistent with the understanding that the concentration of H_{eq} in solution that is

available for hydride accumulation at the flaw tip is limited by the peak temperature and not the H_{eq}.

2.4.2 Future Validation of Fatigue Crack Initiation Models Against Fatigue Experiments with High Hydrogen Equivalent Concentrations

As described in Section 3, fatigue crack initiation tests are proposed on notched specimens with high levels of H_{eq}. The fatigue test results would be compared with those from test specimens from the same pressure tube with a lower level of H_{eq}. The fatigue crack initiation models would be compared with the results from the fatigue crack initiation tests with high levels of H_{eq} to validate the models for these levels of H_{eq}.

Table 2-1: K_{IH} Values for Different Bulk Hydrogen Concentrations [6]

Tube No.	Material	H_{eq} (ppm)	No. of Samples Tested	Peak Temperature Prior to Cooldown (°C)	Test Temperature (°C)	K_{IH} (MPa√m)
M328-40	Unirradiated	30 100	13 3	285 350	180 200	9.0 ± 1 10.4
R766	Unirradiated	67 100	2 1	310 310	250 250	8.5 9
B6G12	Pre-irradiated	43 66	10 7	280 300	200 200	6.0 ± 0.4 6.2 ± 0.5
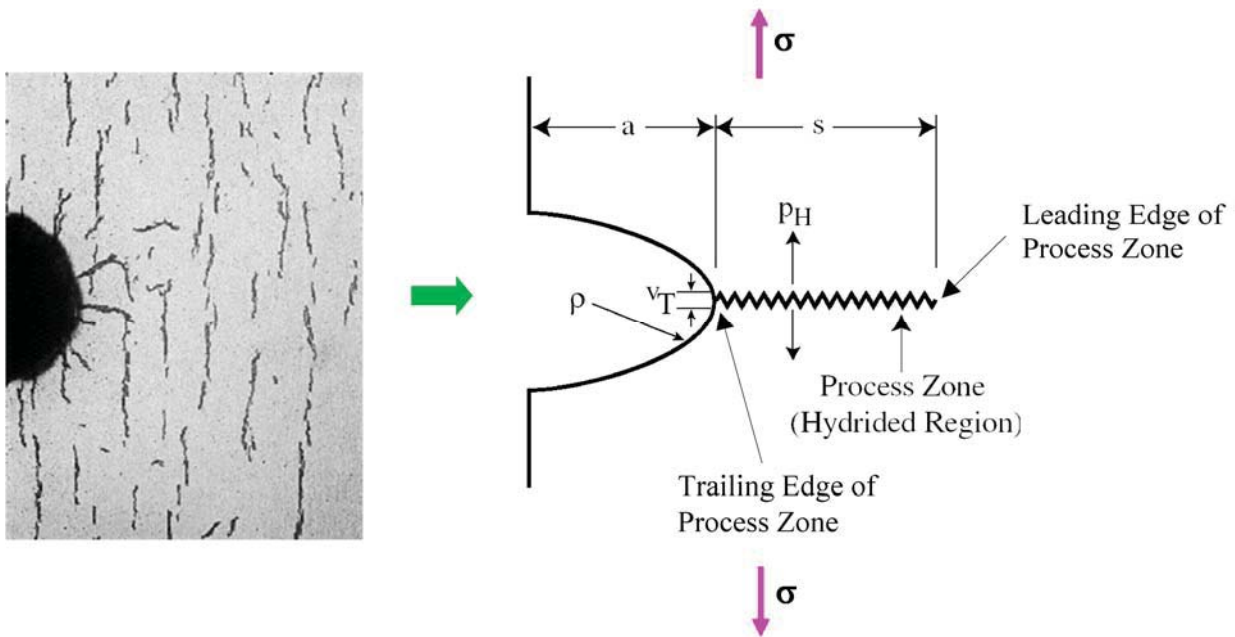
Figure 2-1: Hydrided Regions at a Notch Tip and Corresponding Process Zone (notch root radius is 0.10 mm)
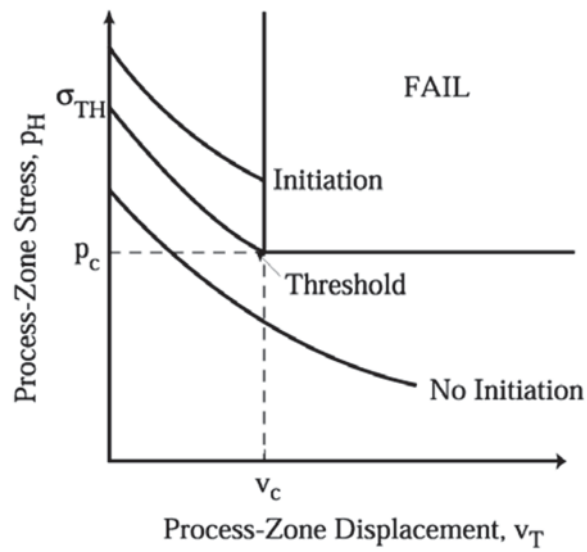
Figure 2-2: Various p_H Versus v_T Behaviour as a Hydrided Region Develops at a Flaw Tip
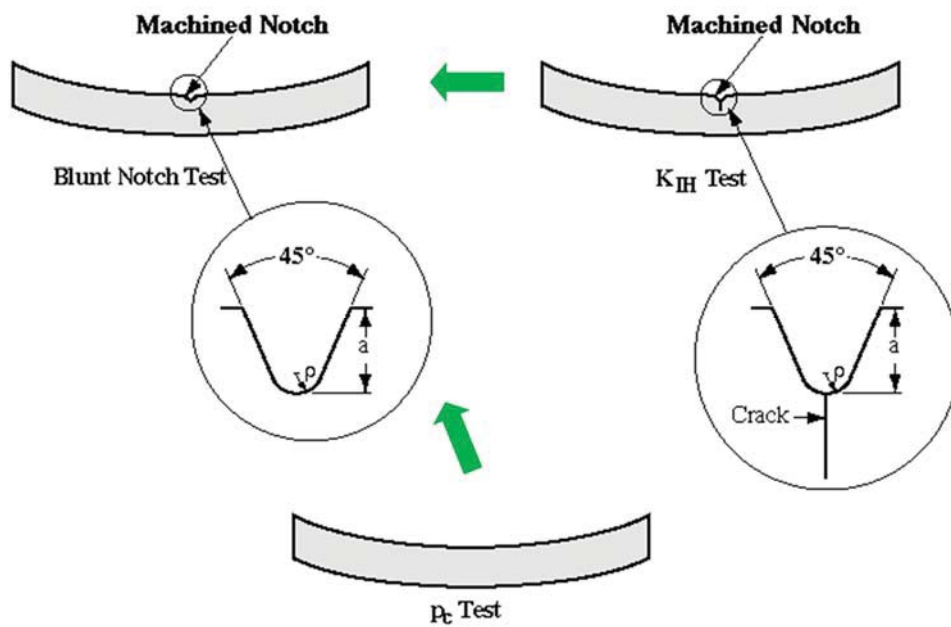
Figure 2-3: Test Specimens used to Measure K_{IH}, p_c, and Threshold Peak Stress for DHC Initiation
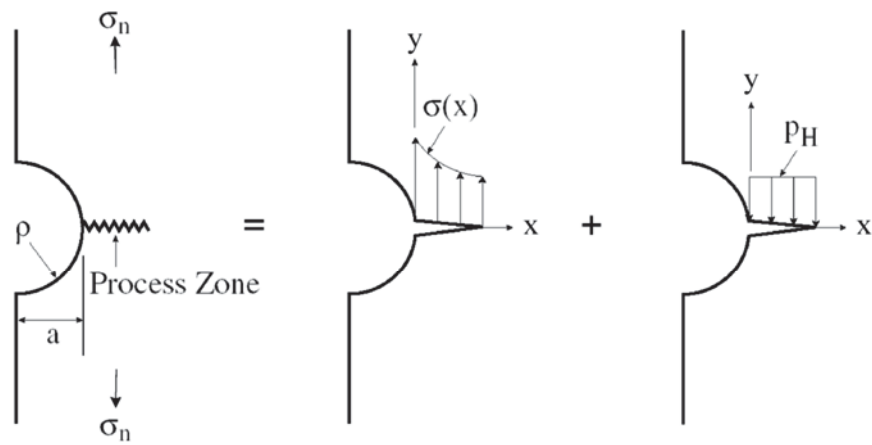
**Figure 2-4: Illustration of Method of Superposition
Used in the Process-Zone Model**

3. **TEST PLAN TO EVALUATE THE EFFECT OF HIGH HYDROGEN EQUIVALENT CONCENTRATION ON CRACK INITIATION DUE TO DELAYED HYDRIDE CRACKING, HYDRIDED REGION OVERLOAD AND FATIGUE**

This section describes the detailed test plans to provide experimental data and understanding to verify the expectation that crack initiation models are not impacted by elevated H_{eq}. The test plans intend to address the four different crack initiation mechanisms listed below:

- Delayed Hydride Cracking (DHC) initiation from a crack (K_{IH}),
- DHC initiation from blunt notches (K_{TH}),
- Overload crack initiation from blunt notches, and
- Fatigue crack initiation from blunt notches.

3.1 Proposed DHC Initiation Tests from a Crack (K_{IH})

K_{IH} measurements on both irradiated and unirradiated pressure tube materials are typically obtained from hydrided pressure tube materials with H_{eq} less than 100 ppm. Table 3-1 outlines the proposed tests to examine the effect of elevated H_{eq} on K_{IH}. It is proposed to perform K_{IH} tests on two unirradiated pressure tubes and one irradiated pressure tube. For testing on unirradiated pressure tubes, the hydrogen concentrations selected for testing are nominally 60 ppm and 220 ppm. The H_{eq} of 60 ppm represents the typical H_{eq} used for K_{IH} experiments. An H_{eq} of 220 ppm is considered a reasonable value to bound the recent elevated hydrogen equivalent concentration measurements from Bruce Unit 3. For testing on the irradiated pressure tube, the lower level of the H_{eq} is selected to be 60 ppm. The higher H_{eq} level (>200 ppm) will be defined based on the H_{eq} level that can be achieved in irradiated material from the appropriate hydriding procedure that is currently under development to ensure there is no significant recovery of the irradiation damage which can potentially affect the DHC initiation process. The 19 mm C-shape specimens containing machined blunt V-notches with a nominal depth of 1.0 mm and a nominal root radius of 0.015 mm are selected for the proposed K_{IH} tests, where K_{IH} will be measured from cracks that will be formed at the blunt notch tips. The test temperature is tentatively selected to be 200°C, which is a typical test temperature used for irradiated and unirradiated K_{IH} measurements. Nominally five to six specimens are proposed for testing at each test condition. Comparison of the measured K_{IH} values at these two levels of H_{eq} will be used to examine the effect of H_{eq} on K_{IH}.

The second last column of Table 3-1 provides the target completion dates.

3.2 Proposed DHC Initiation Tests from Blunt Notches

DHC initiation tests on blunt notches are proposed to be performed under constant load and hydride ratcheting thermal cycles. In a DHC initiation test, multiple groups of specimens are loaded to different load levels, quantified by the applied effective stress intensity factor, K_{EFF}, to measure the threshold level of the K_{EFF} for DHC initiation, referred to as K_{TH}. The K_{EFF} is as calculated for a crack with the same planar dimensions as the blunt notch. In References [6] and [19], threshold DHC initiation tests were performed on notched cantilever beam (CB) specimens with root radii of 0.015 mm and 0.1 mm, prepared from unirradiated pressure tube M328-40

hydrided to 110 ppm H_{eq}. The results demonstrated that the measured K_{TH} values were not affected by the elevated H_{eq} up to 110 ppm under fuel channel outlet temperature cycles, compared to that of the specimens with 57 ppm H_{eq} [6]. These tests were part of the technical basis to justify the applicability of the process-zone methodology for DHC initiation evaluation for high H_{eq}.

The proposed DHC initiation tests to justify the applicability of the process-zone based DHC initiation evaluation methodology at elevated H_{eq} beyond 110 ppm are separated into two stages: Short-Term tests and Long-Term tests. Details are provided in Sections 3.2.1 and 3.2.2.

3.2.1 Planned Short-Term DHC Initiation Tests from Blunt Notches

DHC initiation tests are generally long-duration tests and time-consuming to obtain the test results. The planned Short-Term DHC initiation tests are included to provide experimental data in a short time frame to demonstrate that the DHC initiation threshold is not affected by a high level of H_{eq}. Table 3-2 presents the planned Short-Term DHC initiation tests.

The experiments will be performed on unirradiated pressure tube BB049. This tube is selected for testing because the measured DHC initiation threshold at 60 ppm H_{eq} is available from previous work [20] for comparison with the currently planned tests at a higher H_{eq}. In Reference [20], constant load DHC initiation tests were performed on 38 mm CB specimens containing machined 45° V-notches with a notch depth of 0.75 mm and a root radius of 0.015 mm under hydride ratcheting thermal cycles that included one initial creep cycle (300°C/24h + 185°C/3h hold during cooldown) followed by multiple (greater than 19) hydride ratcheting cycles (270°C/1h + 185°C/3h hold during cooldown). Two groups of six (6) specimens were tested. There were no failures in the first group that was tested at K_{EFF} of 8 MPa√m, and all six (6) specimens failed in the second group tested at K_{EFF} of 9 MPa√m. The measured K_{TH} was therefore between 8 and 9 MPa√m.

The planned Short-Term DHC initiation tests are presented in the last row of Table 3-2. A section removed from the unirradiated pressure tube BB049 will be electrolytically hydrided and homogenized to nominally 220 ppm H_{eq}. As in the previous tests in Reference [20], 38 mm CB specimens containing 45° V-notches with a notch depth of 0.75 mm and a root radius of 0.015 mm will be machined from the hydrided tube section for testing. Two groups of six (6) specimens are planned for testing using the same test facility as was used for the tests at 60 ppm H_{eq} [20]. The first group will be tested at K_{EFF} of 8 MPa√m under hydride ratcheting thermal cycles which include one initial creep cycle (300°C/24h + 185°C/3h hold during cooldown) followed by multiple (greater than 19) hydride ratcheting cycles (300°C/1h + 185°C/3h hold during cooldown). The creep cycle is identical to that used previously [20], and the 300°C peak temperature of the hydride ratcheting cycle is selected to represent the outlet operating temperature. If there are no failures in the first group at K_{EFF} of 8 MPa√m, it can be concluded that the measured K_{TH} will be greater than 8 MPa√m, and this is not lower than the measured K_{TH} of 8~9 MPa√m at 60 ppm H_{eq} [20]. The results will therefore demonstrate that the measured K_{TH} is not adversely affected up to the elevated H_{eq} of 220 ppm. In this case, there is no need to test the second group of specimens. If there are failures at K_{EFF} of 8 MPa√m, the second group of specimens will be tested at K_{EFF} of 7 MPa√m.

The measured K_{TH} values will also be used to validate the predicted threshold values from the process-zone based DHC initiation model [11], as described in Section 2 of this document.

3.2.2 Proposed Long-Term DHC Initiation Tests from Blunt Notches

Tables 3-3 and 3-4 present the proposed Long-Term DHC initiation tests on blunt notches to perform systematic experimental studies to justify the applicability of the process-zone based DHC initiation model for evaluation of flaws at H_{eq} higher than 220 ppm (referred to as "> 220 ppm" in this document).

The test conditions of the first set of the proposed tests in Table 3-3 are identical to the 220 ppm tests outlined in the Short-Term DHC initiation tests in Table 3-2 with the exception that the target nominal H_{eq} will be higher than 220 ppm. The purpose is to examine the impact of $H_{eq} >$ 220 ppm on the measured K_{TH} from notches with a root radius of 0.015 mm under hydride ratcheting thermal cycles that are representative of the outlet operating conditions.

The second set of the proposed tests in Table 3-3 will be performed on specimens prepared from the unirradiated pressure tube BB049 with a 0.75 mm notch depth, 0.015 mm notch root radius and a nominal H_{eq} of 60 ppm. Prior to hydriding, the tube section will be subjected to a heat-treatment to simulate the diffusion anneal temperature and hold time that are required to achieve the nominal > 220 ppm H_{eq}. The results from the second set of tests will be compared with the measured K_{TH} from the 60 ppm tests in the Short-Term tests in Table 3-2 to examine the potential impact of the hydriding procedure to achieve the $H_{eq} >$ 220 ppm on the microstructure of the material (such as decomposition of beta phase and reduction of dislocation density) and the measured DHC initiation threshold.

The third and fourth sets of the proposed tests in Table 3-3 will be performed on specimens prepared from the unirradiated pressure tube BB049 with a 0.75 mm notch depth, 0.1 mm notch root radius and two different nominal H_{eq}: 60 ppm and > 220 ppm. The purpose is to examine the impact of $H_{eq} >$ 220 ppm on the measured K_{TH} from notches with a root radius of 0.1 mm.

The proposed tests in Table 3-4 will be performed on specimens prepared from an irradiated pressure tube containing an elevated H_{eq}. Instead of the 38 mm CB specimens used for testing of unirradiated pressure tube material, 19 mm CB or C-shape specimens will be used for testing of irradiated pressure tube material to minimize material consumption and potential radiation dose uptake by workers. The selected root radius for testing is 0.015 mm. Similar to the proposed K_{IH} tests in Table 3-1, the H_{eq} will be finalized based on the H_{eq} level that can be achieved in irradiated material from the appropriate hydriding procedure that is currently under development to ensure there is no significant recovery of the irradiation damage which can potentially affect the DHC initiation process.

The measured K_{TH} values will also be used to validate the predicted threshold values from the process-zone based DHC initiation model [11].

3.3 Proposed Hydrided Region Overload Crack Initiation Tests from Blunt Notches

Tables 3-5 to 3-7 present the proposed hydrided region overload crack initiation tests on blunt notches to perform systematic experimental studies to justify the applicability of the hydrided region overload crack initiation model for evaluation of flaws at H_{eq} of 220 ppm and higher.

The second and third sets of the proposed tests in Table 3-5 will be performed on specimens prepared from the unirradiated pressure tube BB049 at two different H_{eq} levels: 220 ppm, and > 220 ppm. The experiments will be performed on 19 mm CB or C-shape specimens containing machined V-notches with a depth of 1.0 mm and a root radius of 0.015 mm. At each H_{eq} level, two groups of specimens, with nominally four (4) specimens in each group, will be prepared for testing. These two groups of specimens will be subjected to the specified hydride formation thermal cycles to form notch-tip hydrides at two different K_{EFF} levels, namely K_f: of 5.5 or 7.0 MPa√m. Overload tests will be performed at room temperature to measure the overload fracture K_{EFF}, referred to as K'. The ratio of K'/K_f is used to quantify the overload fracture resistance. It should be noted that the first set of experiments in Table 3-5 at 60 ppm H_{eq} are existing data from the same test specimens and conditions that are available for comparison. The purpose of the three sets of tests outlined in this table is to examine the effect of H_{eq} on the overload fracture resistance of the specimens from an unirradiated pressure tube with a root radius of 0.015 mm with notch-tip hydrides formed under ratcheting cycles at different K_f levels.

The fourth set of the proposed tests in Table 3-5 will be performed on specimens prepared from the unirradiated pressure tube BB049 at 60 ppm H_{eq} with a notch depth of 1.0 mm and a notch root radius of 0.015 mm. Similar to the second set of the DHC initiation tests shown in Table 3-3, prior to hydriding, the tube section will be subjected to a heat-treatment to simulate the peak temperature and hold time that are required to achieve the nominal > 220 ppm H_{eq}. The results from the fourth set of tests will be compared with the measured overload fracture resistance from the 60 ppm tests without heat treatment (the first set of tests in Table 3-5) to examine the potential impact of the hydriding procedure to achieve > 220 ppm H_{eq} on the microstructure of the material and the measured overload resistance.

The proposed tests in Table 3-6 will be performed on specimens prepared from the unirradiated pressure tube BB049 at two different H_{eq} levels: 60 ppm and > 220 ppm. The experiments will be performed on 19 mm C-shape specimens containing machined V-notches with a depth of 1.0 mm and a root radius of 0.05 mm. At each H_{eq} level, one group of specimens, with nominally four (4) specimens in the group, will be prepared for testing. The specimens will be subjected to the specified hydride formation cycles to form notch-tip hydrides at K_f of 8.0 MPa√m. Overload tests will be performed at room temperature. The experiments outlined in this table will be used to evaluate the effect of root radius on overload fracture resistance at different H_{eq}.

The proposed tests in Table 3-7 will be performed on specimens prepared from an irradiated pressure tube containing two H_{eq} levels: 60 ppm and an elevated level of H_{eq}. Similar to the proposed K_{IH} and DHC initiation tests, the elevated level of H_{eq} will be finalized based on the H_{eq} level that can be achieved in irradiated material from the appropriate hydriding procedure that is currently under development to ensure there is no significant recovery of the irradiation

damage. The experiments will be performed on 19 mm C-shape specimens containing machined V-notches with a depth of 1.0 mm and a root radius of 0.015 mm. At each H_{eq} level, one group of specimens, with nominally four (4) specimens in the group, will be prepared for testing. The specimens will be subjected to the specified hydride formation cycles to form notch-tip hydrides at K_f of 5.5 MPa√m. Overload tests will be performed at room temperature. The experiments outlined in this table will be used to examine the effect of H_{eq} on overload fracture resistance at different H_{eq} in irradiated material.

3.4   Proposed Fatigue Crack Initiation Tests from Blunt Notches

Table 3-8 presents the proposed fatigue crack initiation tests in an air environment on blunt notches to perform systematic experimental studies to justify the applicability of the fatigue crack initiation models for evaluation of flaws at H_{eq} higher than 220 ppm . The purpose of the experiments outlined in Table 3-8 is to examine the effect of H_{eq} on the measured number of cycles to fatigue crack initiation in an air environment under various testing conditions that cover different H_{eq}, different root radii, different alternating stress levels, and at a test temperature that is representative of the fuel channel outlet operating temperature.

The first set of the proposed tests in Table 3-8 will be performed on specimens prepared from the unirradiated pressure tube BB049 with two H_{eq} levels: 60 ppm and > 220 ppm. The test specimens will be identical to those used in previous fatigue crack initiation experiments [21], referred to as 7 mm gauge length dogbone specimens. The specimens contain machined V-notches with a depth of 0.8 mm and a root radius of 0.015 mm or 0.1 mm. For the specimens with the same root radius, two alternating stress levels are selected for testing. Fatigue tests will be performed at 300°C at 0.5 s load rise time.

The second set of the proposed tests in Table 3-8 will be performed on specimens prepared from the second unirradiated pressure tube G1770 with two H_{eq} levels: 60 ppm and > 220 ppm to address the effect of material variability. The test conditions are identical to those listed for the proposed tests on BB049.

Table 3-9 presents the proposed fatigue crack initiation tests in a simulated reactor coolant environment on blunt notches to perform systematic experimental studies to justify the applicability of the fatigue crack initiation model for evaluation of flaws at H_{eq} > 220 ppm. The test conditions outlined in this table are identical to those of the tests outlined in Table 3-8 with the exception of the test environment. The results from Table 3-9 will be used to examine the effect of H_{eq} on fatigue crack initiation behavior in a simulated reactor coolant environment. The results from Table 3-9 will also be compared with those from Table 3-8 to examine the effect of a water environment on fatigue crack initiation behavior at different H_{eq}.

Table 3-1: Proposed Long-Term K_{IH} Tests to Examine the Effect of Elevated H_{eq}

Material	Nominal H_{eq} (ppm)	Specimen Geometry	Nominal Notch Geometry	Nominal Test Temperature (°C)	Target Completion Date	Comments
Unirradiated, Tube#1	60	19 mm C-Shape	45° V-notch: 1.0 mm depth, 0.015 mm root radius	200	Q1, 2023	Proposed tests on 1st unirradiated tube to examine H_{eq} effect
Unirradiated, Tube#1	220	19 mm C-Shape	45° V-notch: 1.0 mm depth, 0.015 mm root radius	200	Q1, 2023	Proposed tests on 1st unirradiated tube to examine H_{eq} effect
Unirradiated, Tube#2	60	19 mm C-Shape	45° V-notch: 1.0 mm depth, 0.015 mm root radius	200	Q3, 2023	Proposed tests on 2nd unirradiated tube to address material variability
Unirradiated, Tube#2	220	19 mm C-Shape	45° V-notch: 1.0 mm depth, 0.015 mm root radius	200	Q2, 2023	Proposed tests on 2nd unirradiated tube to address material variability
Irradiated, one tube	60	19 mm C-Shape	45° V-notch: 1.0 mm depth, 0.015 mm root radius	200	Q1, 2024	Proposed tests on irradiated tube
Irradiated, one tube	Elevated $H_{eq} >$ 200 ppm, to be defined	19 mm C-Shape	45° V-notch: 1.0 mm depth, 0.015 mm root radius	200	Q1, 2024	Proposed tests on irradiated tube

Table 3-2: Planned Short-Term DHC Initiation Tests on Effect of Elevated H_{eq}

Material	Nominal H_{eq} (ppm)	Specimen Geometry	Nominal Notch Geometry	Applied K_{EFF} (MPa√m)	Thermal Cycles	Measured K_{TH} (MPa√m)	Target Completion Date	Comments
Unirradiated BB049	60	38 mm CB	45° V-notch: 0.75 mm depth, 0.015 mm root radius	8: 0/6 failure 9: 6/6 failure	1 creep cycle (300°C/24h + 185°C/3h hold during cooldown) plus multiple ratcheting cycles (270°C/1h + 185°C/3h hold during cooldown)	8~9	Completed (Existing data)	Existing test data from COG-JP-4363-V088 [20], available for comparison
Unirradiated BB049	220	38 mm CB	45° V-notch: 0.75 mm depth, 0.015 mm root radius	8: 6 specimens[1] 7: 6 specimens[2]	1 creep cycle (300°C/24h + 185°C/3h hold during cooldown) plus multiple ratcheting cycles (300°C/1h + 185°C/3h hold during cooldown)	To be determined	Q4 2021	To compare the measured K_{TH} at 220 ppm with the previously measured K_{TH} at 60 ppm to demonstrate K_{TH} is not reduced at higher H_{eq}.

Notes:
[1]: The experiments at K_{EFF} = 8 MPa√m will be performed as a 1st priority to demonstrate K_{TH} is not affected.
[2]: The experiments at K_{EFF} = 7 MPa√m will be performed if there are failures at K_{EFF} = 8 MPa√m.

Table 3-3: Proposed Long-Term DHC Initiation Tests on Effect of Elevated H_{eq}: Higher H_{eq} and Effect of Root Radius

Material	Nominal H_{eq} (ppm)	Specimen Geometry	Nominal Notch Geometry	Applied K_{EFF} (MPa√m)	Thermal Cycles	Target Completion Date	Comments
Unirradiated BB049	> 220 ppm (to be defined)	38 mm CB	45° V-notch: 0.75 mm depth, 0.015 mm root radius	Multiple levels	1 creep cycle (300°C/24h + 185°C/3h hold during cooldown) plus multiple ratcheting cycles (300°C/1h + 185°C/3h hold during cooldown)	Q2 2023	To compare with the measured K_{TH} at 220 ppm H_{eq} under Short-Term tests.
Unirradiated BB049	60 ppm	38 mm CB	45° V-notch: 0.75 mm depth, 0.015 mm root radius	Multiple levels	1 creep cycle (300°C/24h + 185°C/3h hold during cooldown) plus multiple ratcheting cycles (270°C/1h + 185°C/3h hold during cooldown)	Q4 2022	Prior to hydriding, tube section will be subjected to heat-treatment simulating > 220 ppm hydriding procedure. To compare with the measured K_{TH} at 60 ppm H_{eq} under Short-Term tests.
Unirradiated BB049	60 ppm	38 mm CB	45° V-notch: 0.75 mm depth, 0.1 mm root radius	Multiple levels	1 creep cycle (300°C/24h + 185°C/3h hold during cooldown) plus multiple ratcheting cycles (270°C/1h + 185°C/3h hold during cooldown)	Q3 2023	Proposed tests on specimens with larger root radius
Unirradiated BB049	> 220 ppm (to be defined)	38 mm CB	45° V-notch: 0.75 mm depth, 0.1 mm root radius	Multiple levels	1 creep cycle (300°C/24h + 185°C/3h hold during cooldown) plus multiple ratcheting cycles (300°C/1h + 185°C/3h hold during cooldown)	Q4 2023	Proposed tests on specimens with larger root radius

Table 3-4: Proposed Long-Term DHC Initiation Tests on Effect of Elevated H_{eq}: Tests on Irradiated Material

Material	Nominal H_{eq} (ppm)	Specimen Geometry	Nominal Notch Geometry	Applied K_{EFF} (MPa√m)	Thermal Cycles	Target Completion Date	Comments
Irradiated, one tube	Elevated H_{eq} > 200 ppm, to be defined	19 mm CB or C-shape	45° V-notch: 0.75 mm depth, 0.015 mm root radius	Multiple levels	1 creep cycle (300°C/300h + 185°C/3h hold during cooldown) plus multiple ratcheting cycles (300°C/1h + 185°C/3h hold during cooldown)	Q2 2024	Proposed tests on irradiated tube (hydriding procedure to be determined)

Table 3-5: Proposed Hydrided Region Overload Crack Initiation Tests on Effect of Elevated H_{eq}

Material	Nominal H_{eq} (ppm)	Specimen Geometry	Nominal Notch Geometry	Applied K_{EFF} during Hydride Formation (MPa√m) and Number of Specimens in Test Group	Thermal Cycles	Overload Test Temperature	Target Completion Date	Comments
Unirradiated BB049	60 ppm	19 mm C-Shape	45° V-notch: 1.0 mm depth, 0.015 mm root radius	5.5: 4 specimens 7.0: 4 specimens	1 creep cycle (300°C/24h + 185°C/3h hold during cooldown) plus 9 ratcheting cycles (270°C/1h + 185°C/3h hold during cooldown)	Room temperature	Completed. (Existing data)	Existing test data from Reference [22], available for comparison
Unirradiated BB049	220 ppm	19 mm C-Shape	45° V-notch: 1.0 mm depth, 0.015 mm root radius	5.5: 4 specimens 7.0: 4 specimens	1 creep cycle (300°C/24h + 185°C/3h hold during cooldown) plus 9 ratcheting cycles (300°C/1h + 185°C/3h hold during cooldown)	Room temperature	Q1 2023	To compare with the previously measured overload fracture resistance at 60 ppm to demonstrate overload resistance is not reduced at higher H_{eq}
Unirradiated BB049	> 220 ppm	19 mm C-Shape	45° V-notch: 1.0 mm depth, 0.015 mm root radius	5.5: 4 specimens 7.0: 4 specimens	1 creep cycle (300°C/24h + 185°C/3h hold during cooldown) plus 9 ratcheting cycles (300°C/1h + 185°C/3h hold during cooldown)	Room temperature	Q1 2024	To compare with the previously measured overload fracture resistance at 60 and 220 ppm to demonstrate overload resistance is not reduced at higher H_{eq}
Unirradiated BB049	60 ppm	19 mm C-Shape	45° V-notch: 1.0 mm depth, 0.015 mm root radius	5.5: 4 specimens 7.0: 4 specimens	1 creep cycle (300°C/24h + 185°C/3h hold during cooldown) plus 9 ratcheting cycles (270°C/1h + 185°C/3h hold during cooldown)	Room temperature	Q4 2022	Prior to hydriding, tube section will be subjected to heat-treatment simulating > 220 ppm hydriding procedure. To compare with the overload fracture resistance at 60 ppm H_{eq} without heat treatment.

Table 3-6: Proposed Hydrided Region Overload Crack Initiation Tests on Effect of Effect of Elevated H_{eq}: Effect of Root Radius

Material	Nominal H_{eq} (ppm)	Specimen Geometry	Nominal Notch Geometry	Applied K_{EFF} during Hydride Formation (MPa√m) and Number of Specimens in Test Group	Thermal Cycles	Overload Test Temperature	Target Completion Date	Comments
Unirradiated BB049	60 ppm	19 mm C-Shape	45° V-notch: 1.0 mm depth, 0.05 mm root radius	8.0: 4 specimens	1 creep cycle (300°C/24h + 185°C/3h hold during cooldown) plus 9 ratcheting cycles (270°C/1h + 185°C/3h hold during cooldown)	Room temperature	Q1 2023	Establish overload fracture resistance at 60 ppm H_{eq}
Unirradiated BB049	> 220 ppm	19 mm C-Shape	45° V-notch: 1.0 mm depth, 0.05 mm root radius	8.0: 4 specimens	1 creep cycle (300°C/24h + 185°C/3h hold during cooldown) plus 9 ratcheting cycles (300°C/1h + 185°C/3h hold during cooldown)	Room temperature	Q1 2024	To compare with the overload fracture resistance at 60 ppm to demonstrate overload resistance is not reduced at higher H_{eq}.

Table 3-7: Proposed Hydrided Region Overload Crack Initiation Tests on Effect of Elevated H_{eq}: Irradiated Tube

Material	Nominal H_{eq} (ppm)	Specimen Geometry	Nominal Notch Geometry	Applied K_{EFF} during Hydride Formation (MPa√m) and Number of Specimens in Test Group	Thermal Cycles	Overload Test Temperature	Target Completion Date	Comments
Irradiated tube	60	19 mm C-Shape	45° V-notch: 1.0 mm depth, 0.015 mm root radius	5.5: 4 specimens	1 creep cycle (300°C/300h + 185°C/3h hold during cooldown) plus 9 ratcheting cycles (270°C/1h + 185°C/3h hold during cooldown)	Room temperature	Q2 2024	Proposed tests on irradiated tube
Irradiated tube	Elevated H_{eq} > 200 ppm, to be defined	19 mm C-Shape	45° V-notch: 1.0 mm depth, 0.015 mm root radius	5.5: 4 specimens	1 creep cycle (300°C/300h + 185°C/3h hold during cooldown) plus 9 ratcheting cycles (300°C/1h + 185°C/3h hold during cooldown)	Room temperature	Q2 2024	Proposed tests on irradiated tube

Table 3-8: Proposed Fatigue Crack Initiation Tests in Air Environment on Effect of Elevated H_{eq}

Material	Nominal H_{eq} (ppm)	Specimen Geometry	Nominal Notch Geometry	Alternating Elastic von-Mises Peak Stress (MPa)	Fatigue Test Temperature (°C)	Load Rise Time (s)	Target Completion Date	Comments
Unirradiated, BB049	60 ppm and > 220 ppm	7mm gauge length dogbone specimen	45° V-notch: 0.8 mm depth, 0.015 mm root radius and 0.1 mm root radius	0.015 mm radius: two stress levels 0.1 mm root radius: two stress levels	300	0.5	Q1 2023	Tests on 1st tube to examine effect of H_{eq}
Unirradiated, G1770	60 ppm and > 220 ppm	7mm gauge length dogbone specimen	45° V-notch: 1.0 mm depth, 0.015 mm root radius and 0.1 mm root radius	0.015 mm radius: two stress levels 0.1 mm root radius: two stress levels	300	0.5	Q1 2024	Tests on 2nd tube to address effect of material variability

Table 3-9: Proposed Fatigue Crack Initiation Tests in Simulated Reactor Coolant Environment on Effect of Elevated H_{eq}

Material	Nominal H_{eq} (ppm)	Specimen Geometry	Nominal Notch Geometry	Alternating Elastic von-Mises Peak Stress (MPa)	Fatigue Test Temperature (°C)	Load Rise Time (s)	Target Completion Date	Comments
Unirradiated, BB049	60 ppm and > 220 ppm	7mm gauge length dogbone specimen	45° V-notch: 0.8 mm depth, 0.015 mm root radius and 0.1 mm root radius	0.015 mm radius: two stress levels 0.1 mm root radius: two stress levels	300	0.5	Q3 2023	Tests on 1st tube to examine effect of H_{eq}
Unirradiated, G1770	60 ppm and > 220 ppm	7mm gauge length dogbone specimen	45° V-notch: 1.0 mm depth, 0.015 mm root radius and 0.1 mm root radius	0.015 mm radius: two stress levels 0.1 mm root radius: two stress levels	300	0.5	Q4 2024	Tests on 2nd tube to address effect of material variability

4. MARGIN ASSESSMENT FOR SCRAPE FLAWS IN THE OUTLET ROLLED JOINTS OF BRUCE UNIT 3 PRESSURE TUBES WITH HIGH HYDROGEN EQUIVALENT CONCENTRATIONS

A review of inspection data from all Bruce reactors has confirmed the extremely low probability of forming a dispositionable service-induced flaw in the small, localized region of interest of elevated H_{eq}. Therefore, the primary interest is demonstration of no crack initiation from scrape flaws in this region. An assessment of the acceptability of the circumferential deuterium sampling scrape flaws inboard of the outlet rolled joint burnish mark in Bruce Unit 3 pressure tubes taken during the A2131 outage has been done as described in Reference [23]. The assessment was done using PTFAP V5-1 [24][25], which implements the requirements of Clause 5 of the CSA Standard N285.8-15 [11]. The assessment has been performed to an end of evaluation period of 246,000 EFPH.

A review of the margins to crack initiation due to DHC, hydrided region overloads and fatigue for these scrape flaws in the high H_{eq} regions inboard of the outlet burnish mark in Bruce Unit 3 pressure tubes is provided in this section.

4.1 Overview of Assessment of CWEST Scrape Flaws Near the Outlet Rolled Joint Burnish Mark in Bruce Unit 3 Pressure Tubes

4.1.1 Methodology

Each CWEST scrape flaw was resolved into axial and circumferential components. The axial component of each scrape flaw was treated as volumetric and assessed for crack initiation due to fatigue, DHC under sustained loading conditions, and hydrided region overloads, as well as for minimum safety factors against plastic collapse. The circumferential component of each CWEST scrape flaw was treated as planar and assessed for flaw growth due to fatigue and DHC, as well as for minimum safety factors against plastic collapse and fracture initiation.

As described in Section 1, in the outlet rolled joint region, scrape sampling was done at three locations [3] to better characterize the H_{eq} in different pressure tubes:
- 20 mm inboard of outlet burnish mark
- 43 mm inboard of outlet burnish mark
- nominally 303 mm inboard of the outlet burnish mark

The scrape flaws at 20 mm inboard of the outlet burnish mark are subjected to rolled joint residual stresses. For Bruce Unit 3, the rolled joint type is normal clearance, non-over extended and stress relieved. The rolled joint residual stress relaxes with time due to thermal creep. The residual stress at the scrape location varies for each pressure tube, as it is dependent on the channel-specific operating conditions. Since the scrape at 20 mm inboard of the outlet rolled joint burnish mark is subjected to residual stresses, and therefore, a larger total stress compared to the two other scrape locations, the scrape at the 20 mm location is bounding in terms of margins against crack initiation due to DHC and hydrided region overloads. A bounding assessment was therefore performed in [23] for a flaw with the outboard edge residing at the 20 mm location from the outlet rolled joint burnish mark and extending inboard. The bounding

assessment was performed for all channels scraped during the A2131 outage in the outlet rolled joint region and planned to be operated in the fuelled condition.

Three channels are planned to be operated in a defuelled state in Bruce Unit 3 post-restart. These three channels have been scraped, and the recommended bounding H_{eq} at a distance of 20 mm inboard of the outlet rolled joint burnish mark at the end of the evaluation period is 100 ppm [4]. The crack initiation models used in flaw evaluations are based on test data from material with up to 110 ppm H_{eq}. Therefore, the margin review in this document was performed for scrape flaws in fuelled channels only.

4.1.2 Inputs

Pressure Tube Dimensions: Conservative pressure tube dimensions calculated at the end of the evaluation period of 246,000 EFPH in PTFAP based on design dimensions and regression analysis were used.

Flaw Locations: The assessment was performed for scrapes with the outboard edge of the scrape at the 20 mm location inboard of the outlet rolled joint burnish mark.

The flaw rotary start is 350° with respect to the inspection end and measured clockwise from the top of the pressure tube.

Flaw Geometry: The CWEST scrape is a circumferential flaw, with an axial length of 10 mm, circumferential length of 16° and a maximum depth of 0.384 mm. The flaw geometry of the axial component is assessed as a bearing pad fretting flaw geometry with an axial length of 10 mm and a depth of 0.384 mm. The actual root radius of the axial flaw component is 1.0 mm, but to be within the validity limit of the stress concentration factor equation, a root radius of 0.384 mm is used. The circumferential flaw component is conservatively assessed as planar. A bounding circumferential length of 20° was used in the assessment.

Flaw Formation Time: The flaw formation time and inspection time were both set to 231,964 EFPH, the operating time to the A2131 outage.

Operating and Loading Conditions: The operating pressures and temperatures specific to the flaw location were calculated in PTFAP. The rolled joint residual stresses at the scrape flaws were calculated in PTFAP at the current time of 231,964 EFPH, and these residual stresses were used in the flaw evaluations.

Hydrogen Equivalent Concentration: An H_{eq} of 220 ppm at the end of evaluation period of 246,000 EFPH was used in the assessment of the scrapes at the 20 mm location inboard of the outlet rolled joint burnish mark as recommended in [4].

4.1.3 Results

The DHC, hydrided region overload and fatigue crack initiation evaluation results for the axial flaw component are summarized in Table 4-1. The detailed assessment results, including the results for the plastic collapse assessment, are provided in Reference [23]. The axial flaw

components satisfy the requirements of CSA N285.8-15 [11] until the end of the evaluation period as shown in Reference [23].

The DHC and fatigue crack growth evaluation results for the circumferential flaw component are summarized in Table 4-2. The detailed assessment results, including the results for the fracture initiation and plastic collapse assessment, are provided in Reference [23]. The circumferential flaw components satisfy the requirements of CSA N285.8-15 until the end of the evaluation period as shown in Reference [23].

4.2 Review of Margins for Scrape Flaws in the Outlet Rolled Joints of Bruce Unit 3 Pressure Tubes with High Hydrogen Equivalent Concentrations

Axial Flaw Components

From Table 4-1, crack initiation due to DHC, hydrided region overloads and fatigue is not predicted to occur up to the end of evaluation period of 246,000 EFPH. The table also provides the factors on the DHC initiation threshold, which was calculated as the ratio of the threshold peak stress for DHC initiation and the flaw-tip peak stress at hydride precipitation during Cooldown. The factor on the DHC initiation threshold ranges from 1.43 to 1.50, with the minimum being 1.43 for the scrape in pressure tube B3N04. The highest H_{eq} at the 20 mm location inboard of the outlet rolled joint burnish mark during the A2131 scrape campaign was measured in pressure tube B3F16. The factor on the DHC initiation threshold is 1.46 for pressure tube B3F16.

The ratio of the critical stress for crack initiation due to a hydrided region overload to the applied maximum stress during a hydrided region overload is also provided in Table 4-1. The ratio ranges from 1.59 to 2.02, with the minimum being 1.59 for pressure tube B3V17. The ratio for pressure tube B3F16 is 2.00.

Also, from Table 4-1, the cumulative fatigue usage factor for the scrape flaws is 0.004.

The results show that there are substantial margins to crack initiation due to DHC, hydrided region overloads and fatigue. There are a number of reasons for the substantial margins as follows. The CWEST scrape flaw is an engineered flaw. The geometry is designed to have a low stress concentration to ensure that the scrape flaw has large margins against crack initiation. The scrape flaw has a maximum depth of 0.384 mm and the axial component of the flaw has a root radius of nominally 1 mm, which results in a very low stress concentration. To be within the validity limit of the stress concentration factor equation applicable to the bearing pad fretting flaw geometry that was used in the assessment, the root radius was conservatively set equal to the flaw depth of 0.384 mm. Even with the assumed smaller root radius, the scrape flaw has a low stress concentration that contributes to the large margins against crack initiation. In addition, the evaluated scrape flaws are at the fuel channel outlet with the associated lower internal pressure compared with the inlet. As described in above in Section 4.1.1, the scrape flaw is subjected to rolled joint residual stresses. However, the rolled joint residual stresses at the fuel channel outlet in late life are relatively low, as the stresses relax over time due to creep. This also contributes to the large margins against crack initiation due to DHC and hydrided region overloads. Since the scrape flaws were formed during the current outage, the number of stress

cycles to MCR in the fatigue evaluation are relatively low, and this results in a very low fatigue usage factor.

The assessment of the outlet rolled joint scrapes was done for an H_{eq} of 220 ppm at the end of evaluation period of 246,000 EFPH. As discussed in Section 3.1, the amount of H_{eq} in solution available for hydride accumulation at a flaw is limited by the peak operating temperature. Over the operating temperature range from 290 through 300°C in the outlet rolled joint region, the maximum H_{eq} concentration in solution will range from 65 through 74 ppm by conservatively assuming the Khatamian *TSSD* equation. Levels of H_{eq} above the *TSSD* concentration at the peak operating temperature will remain as bulk hydrides and will not affect flaw-tip hydride accumulation. Similarly, as described in Section 2.3, for crack initiation due to a hydrided region overload with high levels of H_{eq}, the amount of H_{eq} in solution that is available for hydride accumulation at the flaw is limited by the peak operating temperature, and the accumulation of flaw-tip hydrides and their overload resistance under hydride ratcheting conditions are not affected by the H_{eq} concentration. Further, as discussed in Section 2.4, the effect of H_{eq} on the number of load cycles to fatigue crack initiation is statistically insignificant for H_{eq} in the range of 60 to 100 ppm. Future tests to validate the application of the DHC, hydrided region overload and fatigue crack initiation evaluation models to high H_{eq} levels are proposed, as described in Section 3.

The substantial margins to crack initiation due to DHC, hydrided region overloads and fatigue, as seen in Table 4-1, would cover any unanticipated sensitivity to higher levels of H_{eq}. In addition, the root radius of the axial flaw component of the CWEST scrape is 1 mm. To be within the validity limit of the stress concentration factor equation applicable to the bearing pad fretting flaw geometry that was used in the assessment, the root radius was set equal to the flaw depth of 0.384 mm. This is conservative.

Circumferential Flaw Components

Table 4-2 provides the results of the assessment of the circumferential component of the scrapes with the outboard edge of the scrape at the 20 mm location inboard of the outlet rolled joint burnish mark of all tubes scraped during the A2131 outage that are planned to be operated in the fuelled condition. Crack growth due to DHC is predicted to not occur up to the end of the evaluation period considering the post-fatigue crack growth flaw dimensions. The ratio of the lower-bound threshold stress intensity factor for DHC initiation from a crack, K_{IH} to the applied stress intensity factor, K_I is also provided in the table. The minimum ratio is 1.74.

The results show that there is limited fatigue crack growth and substantial margins to crack initiation due to DHC. The scrape flaw has a maximum depth of only 0.384 mm. Due to the texture of the material, the threshold K_{IH} for the circumferential flaw component is large and shows a high resistance to DHC initiation. As described above for the axial flaw component, the evaluated scrape flaws are at the fuel channel outlet with the associated lower internal pressure, and lower rolled joint residual stresses. Since the scrape flaws were formed during the current outage, the number of stress cycles to MCR in the fatigue evaluation are relatively low, and this results in a very low fatigue crack growth.

As discussed in Section 2.2.4, K_{IH} is not expected to be affected by the bulk H_{eq}. Long-term tests to obtain K_{IH} data on specimens with high H_{eq} levels up to 220 ppm are proposed as discussed in Section 3. The margin on the lower-bound K_{IH} from the assessment of scrape flaws is considered sufficient to cover any unanticipated sensitivity to higher levels of H_{eq}.

Table 4-1: Summary of DHC, Hydrided Region Overload and Fatigue Crack Initiation Results for Axial Flaw Component of Scrape Flaws at the 20 mm Location from Outlet Rolled Joint Burnish Mark in all Channels Scraped During A2131 Outage and Planned to be Operated in the Fuelled Condition

Channel Identification	H_{eq} at Flaw Location at End of Evaluation Period of 246,000 EFPH (ppm)	Stress Concentration Factor, k_t	Normal Operating Temperature (°C)	Applied Peak Flaw-Tip Stress for DHC Initiation Evaluation (MPa)	Threshold Peak Stress for DHC Initiation (MPa)	Ratio of Threshold Peak Stress for DHC Initiation to Applied Peak Flaw-Tip Stress	Ratio of Critical Overload Stress / Applied Overload Stress	Fatigue Cumulative Usage Factor
B3F16	220	2.59	295.8	422.6	618.2	1.46	2.00	0.004
B3C11	220	2.59	300.1	411	618.2	1.50	1.60	0.004
B3L11	220	2.59	296.1	421.8	618.2	1.47	2.00	0.004
B3D16	220	2.59	293.3	429.8	618.2	1.44	1.97	0.004
B3D07	220	2.59	299.9	411.8	618.2	1.50	1.60	0.004
B3E20	220	2.59	299.5	413	618.2	1.50	1.60	0.004
B3G10	220	2.59	296.2	421.9	618.2	1.47	2.00	0.004
B3G14	220	2.59	296	422.6	618.2	1.46	2.00	0.004
B3K15	220	2.59	295.6	423.6	618.2	1.46	1.99	0.004
B3M13	220	2.59	295.2	424.8	618.2	1.46	1.99	0.004
B3Q23	220	2.59	297.1	419.6	618.2	1.47	2.01	0.004
B3V18	220	2.59	298.6	415.5	618.2	1.49	1.60	0.004
B3B12	220	2.59	299.1	413.7	618.2	1.49	1.60	0.004
B3C15	220	2.59	299.6	412.4	618.2	1.50	1.60	0.004
B3E05	220	2.59	299.5	412.7	618.2	1.50	1.60	0.004
B3F04	220	2.59	298.8	414.4	618.2	1.49	1.60	0.004

Channel Identification	H_{eq} at Flaw Location at End of Evaluation Period of 246,000 EFPH (ppm)	Stress Concentration Factor, k_t	Normal Operating Temperature (°C)	Applied Peak Flaw-Tip Stress for DHC Initiation Evaluation (MPa)	Threshold Peak Stress for DHC Initiation (MPa)	Ratio of Threshold Peak Stress for DHC Initiation to Applied Peak Flaw-Tip Stress	Ratio of Critical Overload Stress / Applied Overload Stress	Fatigue Cumulative Usage Factor
B3G15	220	2.59	296	422.1	618.2	1.46	2.00	0.004
B3K16	220	2.59	294.9	425.2	618.2	1.45	1.99	0.004
B3M02	220	2.59	298	416.7	618.2	1.48	2.02	0.004
B3Q16	220	2.59	294.6	426	618.2	1.45	1.98	0.004
B3T03	220	2.59	294.7	425.7	618.2	1.45	1.98	0.004
B3U20	220	2.59	298.5	415.3	618.2	1.49	1.60	0.004
B3V17	220	2.59	298.4	415.6	618.2	1.49	1.59	0.004
B3H06	220	2.59	293.3	429.7	618.2	1.44	1.97	0.004
B3O20	220	2.59	294.7	425.7	618.2	1.45	1.98	0.004
B3Q12	220	2.59	294.7	425.7	618.2	1.45	1.98	0.004
B3X09	220	2.59	296	422.2	618.2	1.46	2.00	0.004
B3F05	220	2.59	299.9	411.8	618.2	1.50	1.60	0.004
B3L12	220	2.59	295	425.2	618.2	1.45	1.99	0.004
B3L22	220	2.59	299.5	413	618.2	1.50	1.60	0.004
B3N04	220	2.59	292.5	432.4	618.2	1.43	1.96	0.004
B3O13	220	2.59	295.2	424.7	618.2	1.46	1.99	0.004
B3O15	220	2.59	296.1	422.1	618.2	1.46	2.00	0.004
B3O17	220	2.59	295.9	422.7	618.2	1.46	2.00	0.004
B3P14	220	2.59	295.7	423.3	618.2	1.46	2.00	0.004
B3Q13	220	2.59	294.9	425.5	618.2	1.45	1.99	0.004

Channel Identification	H_{eq} at Flaw Location at End of Evaluation Period of 246,000 EFPH (ppm)	Stress Concentration Factor, k_t	Normal Operating Temperature (°C)	Applied Peak Flaw-Tip Stress for DHC Initiation Evaluation (MPa)	Threshold Peak Stress for DHC Initiation (MPa)	Ratio of Threshold Peak Stress for DHC Initiation to Applied Peak Flaw-Tip Stress	Ratio of Critical Overload Stress / Applied Overload Stress	Fatigue Cumulative Usage Factor
B3S13	220	2.59	293.9	428.4	618.2	1.44	1.97	0.004
B3R10	220	2.59	294.3	427.3	618.2	1.45	1.98	0.004

Table 4-2: Summary of DHC and Fatigue Crack Growth Evaluation Results for Circumferential Flaw Component of Scrape Flaws at the 20 mm Location from Outlet Rolled Joint Burnish Mark in all Channels Scraped During A2131 Outage and Planned to be Operated in the Fuelled Condition

Channel Identification	H_{eq} at Flaw Location at End of Evaluation Period of 246,000 EFPH (ppm)	Flaw Depth (mm)	Flaw Length (mm)	Post-Fatigue Growth Flaw Depth (mm)	Post-Fatigue Growth Flaw Length (mm)	Applied Stress Intensity Factor, K_I (MPa√m)	Lower-Bound Threshold Stress Intensity Factor, K_{IH} (MPa√m)	Ratio of Lower-Bound K_{IH} to Applied K_I	Allowable Heatup/Cooldown Cycles
B3F16	220	0.384	19.5	0.425	19.54	8.46	15	1.77	51
B3C11	220	0.384	19.5	0.425	19.54	8.27	15	1.81	51
B3L11	220	0.384	19.5	0.425	19.54	8.45	15	1.78	51
B3D16	220	0.384	19.5	0.425	19.54	8.58	15	1.75	51
B3D07	220	0.384	19.5	0.425	19.54	8.28	15	1.81	51
B3E20	220	0.384	19.5	0.425	19.54	8.3	15	1.81	51
B3G10	220	0.384	19.5	0.425	19.54	8.45	15	1.78	51
B3G14	220	0.384	19.5	0.425	19.54	8.46	15	1.77	51
B3K15	220	0.384	19.5	0.425	19.54	8.48	15	1.77	51
B3M13	220	0.384	19.5	0.425	19.54	8.49	15	1.77	51
B3Q23	220	0.384	19.5	0.425	19.54	8.41	15	1.78	51
B3V18	220	0.384	19.5	0.425	19.54	8.34	15	1.80	51
B3B12	220	0.384	19.5	0.425	19.54	8.31	15	1.81	51
B3C15	220	0.384	19.5	0.425	19.54	8.29	15	1.81	51
B3E05	220	0.384	19.5	0.425	19.54	8.3	15	1.81	51
B3F04	220	0.384	19.5	0.425	19.54	8.33	15	1.80	51
B3G15	220	0.384	19.5	0.425	19.54	8.45	15	1.78	51
B3K16	220	0.384	19.5	0.425	19.54	8.51	15	1.76	51

Channel Identification	H_{eq} at Flaw Location at End of Evaluation Period of 246,000 EFPH (ppm)	Flaw Depth (mm)	Flaw Length (mm)	Post-Fatigue Growth Flaw Depth (mm)	Post-Fatigue Growth Flaw Length (mm)	Applied Stress Intensity Factor, K_I (MPa√m)	Lower-Bound Threshold Stress Intensity Factor, K_{IH} (MPa√m)	Ratio of Lower-Bound K_{IH} to Applied K_I	Allowable Heatup/Cooldown Cycles
B3M02	220	0.384	19.5	0.425	19.54	8.36	15	1.79	51
B3Q16	220	0.384	19.5	0.425	19.54	8.52	15	1.76	51
B3T03	220	0.384	19.5	0.425	19.54	8.52	15	1.76	51
B3U20	220	0.384	19.5	0.425	19.54	8.34	15	1.80	51
B3V17	220	0.384	19.5	0.425	19.54	8.35	15	1.80	51
B3H06	220	0.384	19.5	0.425	19.54	8.58	15	1.75	51
B3O20	220	0.384	19.5	0.425	19.54	8.52	15	1.76	51
B3Q12	220	0.384	19.5	0.425	19.54	8.52	15	1.76	51
B3X09	220	0.384	19.5	0.425	19.54	8.46	15	1.77	51
B3F05	220	0.384	19.5	0.425	19.54	8.28	15	1.81	51
B3L12	220	0.384	19.5	0.425	19.54	8.5	15	1.76	51
B3L22	220	0.384	19.5	0.425	19.54	8.3	15	1.81	51
B3N04	220	0.384	19.5	0.425	19.54	8.62	15	1.74	51
B3O13	220	0.384	19.5	0.425	19.54	8.49	15	1.77	51
B3O15	220	0.384	19.5	0.425	19.54	8.45	15	1.78	51
B3O17	220	0.384	19.5	0.425	19.54	8.46	15	1.77	51
B3P14	220	0.384	19.5	0.425	19.54	8.47	15	1.77	51
B3Q13	220	0.384	19.5	0.425	19.54	8.51	15	1.76	51
B3S13	220	0.384	19.5	0.425	19.54	8.56	15	1.75	51
B3R10	220	0.384	19.5	0.425	19.54	8.54	15	1.76	51

5.   SUMMARY

High levels of H_{eq} have been detected in the outlet rolled joints of Bruce Unit 3. The higher than expected levels of H_{eq} have been found to be concentrated in a localized region extending from the outlet end of the pressure tube for approximately 50 mm inboard of the outlet burnish mark with a central tendency about the top of the pressure tube. The crack initiation models currently being used for pressure tube flaw assessments are based on data from pressure tube material with up to 110 ppm H_{eq}. The CNSC has requested information to confirm that the crack initiation models are valid for evaluation of flaws in the pressure tube regions with elevated H_{eq} levels. Detailed plans for research activities to support the understanding that the crack initiation models are not impacted by elevated H_{eq} have also been requested.

(a) Justification for the application of the current crack initiation models for evaluation of flaws in pressure tube regions with elevated levels of H_{eq} above 110 ppm is provided in this letter. The justification is based on the fact that with high levels of H_{eq}, the amount of H_{eq} in solution that is available for hydride accumulation at the flaw is limited by the peak operating temperature, and the accumulation of flaw-tip hydrides and their resistance to crack initiation mechanisms under hydride ratcheting conditions are not affected by the H_{eq} concentration. The same consideration is also applicable for the overload and fatigue crack initiation database for model development in which the formation of the notch-tip hydrides is governed by the peak temperature of the hydride formation thermal cycles and not by the bulk H_{eq}. Also, the process-zone methodology to evaluate DHC initiation under hydride ratcheting conditions has no upper H_{eq} limit and the input parameters K_{IH} and p_c are considered to be not affected by bulk H_{eq} concentration.

(b) Detailed test plans to obtain experimental data to support the understanding that the crack initiation models for DHC, hydrided region overloads and fatigue are not impacted by an increase in the H_{eq} above 110 ppm are provided in this letter. The test plans include short-term tests to determine whether the threshold effective stress intensity factor for crack initiation due to DHC from blunt notches is reduced by an H_{eq} level of 220 ppm. A longer-term test plan is also proposed that addresses DHC initiation from a crack (K_{IH}) and blunt notches (K_{TH}), overload crack initiation from blunt notches, and fatigue crack initiation from blunt notches. Both unirradiated and irradiated material with varying levels of H_{eq} are proposed to be tested in the long-term plan.

(c) A margin assessment for demonstration of protection against crack initiation from scrape flaws in the outlet rolled joint region 20 mm inboard of the burnish mark of Bruce Unit 3 pressure tubes with elevated levels of H_{eq} is provided. The scrape flaws at the 20 mm location inboard of the outlet rolled joint burnish mark satisfy the requirements of CSA N285.8-15 until the end of the evaluation period as shown in Reference [23]. There are substantial margins to crack initiation due to DHC, hydrided region overloads and fatigue for the axial component, and on the lower-bound K_{IH} for the circumferential component, which would cover any unanticipated sensitivity to higher levels of H_{eq}.

6.   REFERENCES

[1]   CNSC Correspondence, L. Sigouin to M. Burton, "Bruce A and B: CNSC Review of Bruce Power's Response to Action Item 2021-07-23406 regarding Elevated Hydrogen Equivalent Concentration Measurements", August 5, 2021, e-Doc 6611665 File 4.01.02, BP-CORR-00531-01930.

[2]   CNSC Email, A. Robert to A. Glover et al., "FW: B3 Scrape Campaign Results", August 13, 2021.

[3]   Letter to L. Micuda, "Re: Recommended Outage Inspection Scope for the A2131 Additional Revisit Window," Kinectrics File No. B2038/SOW/0001 R00, July 29, 2021

[4]   Letter from C. Nam and K. Harrison to D. Scarth, "Re: Postulated Bounding [H]eq Levels for Bruce Unit 3 Fracture Protection Evaluation," Kinectrics File No. B2038/LET/0009 R00, August 24, 2021.

[5]   Bruce Power Letter, M. Burton to L. Sigouin, "Bruce A and B: Methodology to Disposition Hydrogen Equivalent Concentration Exceeding TSSd in Body of Tube Region of Pressure Tubes," BP-CORR-00531-00384, September 15, 2020.

[6]   Shek, G.K., "Response to CNSC Review Team's Comments on Report COG-03-1043 Addressing Effect of End-of-Life Hydrogen on Flaw Evaluation Procedure for Delayed Hydride Crack Initiation", COG-05-1075, January 2006.

[7]   Scarth, D.A. and Smith, E., "Technical Basis for DHC Initiation Evaluation Procedures for Volumetric Flaws in Draft CSA Standard N285.8," COG Report No. COG-00-84, November 2001.

[8]   Carpenter, G.J.C., *Journal of Nuclear Materials*, Vol. 48, p. 264, 1973.

[9]   Dugdale, D.S., "Yielding of Steel Sheets Containing Slits," *Journal of Mechanics and Physics of Solids*, Vol. 8, pp. 100-104, 1960.

[10]   Bilby, B.A., Cottrell, A.H. and Swinden, K.H., "The Spread of Plastic Yield from a Notch," *Proceedings, Royal Society of London*, Vol. A-272, pp. 304-314, 1963.

[11]   Technical Requirements for In-Service Evaluation of Zirconium Alloy Pressure Tubes in CANDU Reactors," Canadian Standards Association, CSA Standard N285.8-15, with Update No. 1.

[12]   Shi, S.-Q. and Puls, M.P., "Criteria for Fracture Initiation at Hydrides in Zirconium Alloys I. Sharp Crack Tip," *Journal of Nuclear Materials*, Vol. 208, pp. 232-242, 1994.

[13]   Rodgers, D.K., "Crack Initiation at Fuelling Scratches in Irradiated P3L09 Pressure Tube Material," Atomic Energy of Canada Ltd., CRL, Report No. COG-90-180, December 1990.

[14]   Gutkin, L., "Statistical Assessment of KIH Database for Irradiated Zr-2.5Nb," COG Report No. COG-06-1101, February 2007.

[15]   Resta Levi, M., "Revision of KIH Database on Irradiated Material," COG Report No. COG-05-1017, June 2006.

[16] Resta Levi, M. and Puls, M.P., "DHC Behaviour of Irradiated Zr-2.5Nb Pressure Tubes up to 365°C," *18th International Conference on Structural Mechanics in Reactor Technology* (SMIRT 18-G10_3), Beijing, China, August 7-12, 2005.

[17] Gutkin, L. and Scarth, D.A., "Statistical Model for Evaluation of Flaws for Crack Initiation Due to Hydrided Region Overload," COG Report No. COG-08-1041, January 2009.

[18] Liu, C. and Scarth, D.A., "Version 2 Statistical-Based Fatigue Crack Initiation Model for Axial Flaws In Zr Nb Pressure Tubes," Draft COG report No. COG-19-1006, 2021.

[19] Shek, G.K. and Seahra, H., "Threshold Stress for DHC Initiation from Blunt Flaws in Pressure Tubes with End-of-Life Hydrogen Concentration", COG-03-1043, July 2004.

[20] Shek, G.K., "Delayed Hydride Cracking Initiation from Angled Blunt Flaws in Unirradiated Pressure Tube Material", COG-JP-4363-V088, May 2011.

[21] Cui, J., "Fatigue Crack Initiation Tests on Unirradiated Pressure Tube G1770 in Air Environment", COG-JP-4491-V173, June 2020.

[22] Cui, J., "Release of Version R6 of the Fuel Channel Overload Crack Initiation Database", COG OP-19-1003, April 2020.

[23] Klarner, L., "Postulated Flaw Assessment of CWEST Scrapes in Bruce Unit 3 2021 Outage (A2131)," Kinectrics File No. B2038/RE/0086 R00, September 16, 2021.

[24] Mok, D.H.B., "Software Theory and User Manual for Computer Code PTFAP Version 5-0," Kinectrics File No. PS275/MA/001 R00, June 08, 2018.

[25] Mok, D.H.B., "Letter to R. Ahmad, A. Glover, "Release of Computer Code PTFAP Version 5-1", Kinectrics File No. PS275/025/000001 R00, August 30, 2018.

Prepared
by: _____ Sept 16, 2021
Doug Scarth
Technical Director – Fracture
Programs,
Materials and Major Components

Prepared
by: _____ Sept 16, 2021
Gordon Shek
Principal Engineer,
Materials and Major Components

Prepared
by: _____
Jun Cui
2021.09.16
16:31:18 -04'00'
Jun Cui,
Service Line Lead – Experimental
Design and Application,
Materials and Major Components

Prepared
by: _____ Sept 16, 2021
Preeti Doddihal
Senior Scientist,
Materials and Major Components
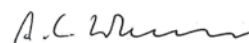
Verified
by: _____ Sept 16, 2021
Steven Xu,
Principal Engineer,
Materials and Major Components
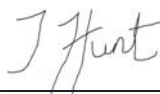
Reviewed
by: _____
Andrew C. Wallace
2021.09.16
16:59:08 -04'00'
Andy Wallace,
Technical Director,
Materials and Major Components

Approved
by: _____ Sept. 16, 2021
Tanya Hunt,
Service Line Director (Acting),
Fuel Channel Integrity &
Methods,
Materials & Major Components

Enclosure 2

B-REP-31110-00004, Revision 000

Estimation of Encountering Reportable & Dispositionable Pressure Tube Flaws in Various Regions of Interest in Bruce Power Units 3-8

Bruce *Power*™

KINECTRICS

ESTIMATION OF ENCOUNTERING REPORTABLE & DISPOSITIONABLE
PRESSURE TUBE FLAWS IN VARIOUS REGIONS OF INTEREST IN BRUCE
POWER UNITS 3-8

B-REP-31110-00004

REV. 000

☒ Accepted	☐ Accepted As Noted – Revision Required
☐ Rejected	☐ Accepted As Noted – No Revision Required

FOR USE AT BRUCE POWER

ACCEPTED: **MONIQUE IP**   *Monique Ip*

(Print Name)   (Signature)

TITLE: **SENIOR TECHNICAL OFFICER**

(Print Title)

DATE: **17SEP2021**

(DDMMMYYYY)

ACCEPTANCE OF THIS DOCUMENT DOES NOT RELIEVE THE

CONTRACTOR OF RESPONSIBILITY FOR ANY ERRORS OR OMISSIONS.

Estimation of Encountering Reportable & Dispositionable Pressure Tube Flaws in Various Regions of Interest in Bruce Power Units 3-8

B2266/RP/001 R00

September 16, 2021

Prepared by:
for   Dirk Leemans, P.Eng.
Contractor
Component Integrity and Inspection
Engineering.

Verified
(reviewed)
by:
Gregory Allen, P.Eng.
Section Manager (Acting)
Fuel Channel Integrity Support.

Verified (Lead)
by:
Suresh Datla
Senior Analyst
Component Integrity and Inspection
Engineering.

Approved by:
Jaff Robertson, P.Eng
Service Line Director
Fuel Channel Integrity & Operations

Revision Summary

Rev	Date	Author	Comments
R00	Sept 2021	D. Leemans	Initial issue.

Uncontrolled if copied or printed from Kinectrics Intranet

TABLE OF CONTENTS

B2266/RP/001 R00   Kinectrics   Page 3 of 13
Uncontrolled if copied or printed from Kinectrics Intranet
Form 114 R35   Associated Procedures: AWI-4-26

LIST OF TABLES

1.0   INTRODUCTION

As part of the evaluation of the fitness for service of Bruce Unit 3, concerns were expressed about the probability of encountering flaws of significance (flaws requiring disposition) in specific regions of interest of the pressure tubes for the population of channels which were not yet inspected full length. The region in question is centered around the top of the pressure tube over a limited axial extent inboard of the Outlet Burnish Mark (OBM), corresponding to measurements of elevated hydrogen isotope concentration. This report provides estimates of the probability of encountering flaws in the reactor in these regions and submits that these probabilities are reassuringly low.

The following sections describe the methodology and results of the current work and compare these probability estimates with other approaches to estimate the flaw probability in the regions of interest.

2.0   IDENTIFYING THE REGIONS OF INTEREST

Two regions of interests with different circumferential extents have been identified within the pressure tube:

1. Region 1 which extends inboard from the outlet burnish mark (OBM) for 75 mm and whose circumferential extent is 60 degrees (from -30 degrees to + 30 degrees with the top of the pressure tube being zero degrees);
2. Region 2 which extends inboard from the OBM for 75 mm and whose circumferential extent is 120 degrees (from -60 degrees to + 60 degrees with the top of the pressure tube being zero degrees).

While determining the most appropriate definition of the region of interest is beyond the scope of this work, measurements of deuterium concentration obtained in the A2131 outage support Region 2 per [1].

3.0

OVERALL APPROACH TO ESTIMATING THE PROBABILITY OF ENCOUNTERING A DISPOSITIONABLE FLAW IN THE REGIONS OF INTEREST OF THE UNINSPECTED PRESSURE TUBES IN BRUCE REACTORS

The probability of encountering a dispositionable flaw in a region of interest in a channel is related to four constituent elements[1]:

i.   The probability of encountering k reportable flaws in the outlet fuel bundle region of a channel;

ii.   The conditional probability given a reportable flaw is present, its axial position (mid flaw position) is within 75 mm inboard of the OBM;

---

[1] For each of these probabilities the possibility of having more than one flaw in the channel being present is taken into account.

iii.   The conditional probability given a reportable flaw is present close to the OBM, its circumferential location is such that it falls within the region of interest.

iv.   The product of the three probabilities itemized above provides the probability of a reportable flaw being in the region of interest. Using the conditional probability that given the presence of a reportable flaw that there is actually a dispositionable flaw present allows the evaluation of the presence of a dispositionable flaw in the channel.

4.0   THE MAJOR DATABASE ON REPORTABLE FLAWS IN BRUCE REACTOR UNITS

The primary input to this analysis was a database containing the size and location of all unique flaws obtained during the inspections of the area up to the first fuel bundle with respect to the outlet burnish mark in all Bruce Units 3-8 reactors. It is this database that allows the reliable estimates of many of the conditional probabilities mentioned above. This database and its construction are detailed in [2].

The decision was made to include only flaws up to the axial extent of the first fuel bundle in the outlet end. Increasing the axial extent would increase the number of flaws per tube but would decrease the conditional probability of having the flaw in the axial region of interest. It was judged that the product of these two probabilities would be virtually unaffected by increasing the axial extent of the database. Reducing the axial extent would reduce the sample size and therefore imperil the estimation of the underlying probabilities.

5.0   DETAILED DESCRIPTION OF THE ESTIMATION OF THE PROBABILITY OF ENCOUNTERING DISPOSITIONABLE FLAWS IN THE REGIONS OF INTEREST IN THE UNINSPECTED PRESSURE TUBE POPULATION IN BRUCE POWER REACTORS

5.1   Description of the Probability of Having K Reportable Flaws up to the End of the First Bundle

This probability is assumed to follow a Poisson distribution

$$\Pr(X = k) = \frac{\lambda^k e^{-\lambda}}{k!}$$

where k is the number of flaws occurring within a channel and λ is the mean incidence rate. In the database there are 557 reportable flaws up to the end of the first bundle in the inspection of 448 unique channels and therefore the estimated λ is 1.243304. Figure 1 shows the dependence of probability on the number of flaws in the channel.

The following assumptions underpin these statements:

i.   Flaws occur independently;

ii.   The incidence rate is independent of reactor;

iii.   The incidence rate is independent of the location of the pressure tube in the reactor (e.g., Zone);

iv.   The incidence rate is independent of operating time.

    v.   No distinction is made between different flaw types.

5.2 Description of the Probability of Having I Reportable Flaws Close to the Outlet Burnish Mark

The conditional probability of having the flaw within 75 mm of the OBM given that a flaw is present is estimated to be 0.011606. This is based on the estimation of the cumulative distribution of the axial position at 75 mm[2].

The probability of having I (≤ K) flaws close to the OBM given that there are K flaws in the pressure tube is binomially distributed.

$$\Pr(X = I|K) = \frac{k!}{I!\,(k - I)!}(1 - p)^{k-I}p^{I}$$

These binomial probabilities for I are then multiplied with the Poisson probability of k flaws and then summed over all k values (up to 10 were used)[3] which gives the probability of having I flaws close to the OBM.

$$Prob(Y = I) = \sum_{k=I}^{10} \Pr(X = I|K)p(K)$$

Figure 2 shows how this probability drops off quickly with increasing values of I.

5.3 Description of the Probability of Having J Reportable Flaws Close to the Outlet Burnish Mark and at the Top of the Pressure Tube

The conditional probability of having a flaw circumferentially at the top of the pressure tube given that a flaw close to the OBM is present assumes that this probability is independent of axial position and therefore the whole database can be used to fit a distribution to the circumferential location. A large number of candidate continuous distribution functions were evaluated including gamma, extreme value, Weibull, Laplace, and lognormal. However, a very good fit was obtained with a simple normal distribution[4].

The parameters of this normal distribution are a mean of 176.41 degrees and a standard deviation of 39.03 degrees. Figure 3 and Figure 4 show the adequacy of the fit.

For the two areas of interest (-30/+30. -60/+60) the conditional probability of having the flaw on top of the pressure tube given that a flaw is present close to the OBM is respectively 0.013% and 0.22%.

---

[2] Given the discontinuous nature of the distribution of the axial position (the majority of flaws are clustered around the residency locations of the fuel bundle bearing pads) no effort was made to fit this distribution to a known probability density distribution. The cumulative probability was estimated by linear interpolation between the two points neighboring 75 mm.

[3] The cutoff of 10 flaws is arbitrary but by this value the probabilities have become vanishingly small.

[4] A three-parameter lognormal distribution does also an adequate job in fitting the circumferential location distribution.

B2266/RP/001 R00   Kinectrics   Page 7 of 13
Uncontrolled if copied or printed from Kinectrics Intranet
Form 114 R35   Associated Procedures: AWI-4-26

As above the probability of having J (≤ I) flaws at the top given that there are I reportable flaws close to the OBM is binomially distributed. Figure 5 shows the probability of having J reportable flaws in the larger area of interest (circumferentially the top 120 degrees of the pressure tube).

$$Prob(Y = J) = \sum_{I=I}^{10} \Pr (X = J|I)p(I)$$

5.4   Description of the Probability of Having H Dispositionable Flaws Close to the OBM and at the Top of the Pressure Tube

The conditional probability of having a dispositionable flaw circumferentially at the top of the pressure tube and close to the OBM given that a reportable flaw is present circumferentially at the top of the pressure tube and close to the OBM is based on the observation that from the 557 reportable flaws in the database 187 were found to be dispositionable (p= 0.335727).

The probability of having H (≤ J) dispositionable flaws at the top of the pressure tube close to the OBM given that there are J reportable flaws at the top of the pressure tube close to the OBM is binomially distributed.

$$Prob(Y = H) = \sum_{J=I}^{10} \Pr (X = H|J)p(J)$$

6.0   RESULTS

6.1   Probability Estimates for Encountering Flaws in the Regions of Interest per Channel

As noted from the outset it is assumed that there is no dependence on reactor and these estimates are applicable to the present situation. The probability of encountering at least one dispositionable flaw in the region of interest per channel is given by

$$Prob(dispositionable) = \sum_{H=I}^{10} \Pr (Y = H)$$

The results are tabulated in Table 1. As expected, these probabilities depend strongly on the circumferential extent of the region of interest. The larger the circumferential extent the larger the probability of encountering a flaw in the region of interest. Also, the probability of encountering a dispositionable flaw is about one third of the probability of encountering a reportable flaw.

6.2 Probability Estimates for Encountering Flaws in the Regions of Interest in the Uninspected Population of Pressure Tubes for Bruce Power Reactors.

The probability of encountering at least one reportable flaw in the regions of interest in the population of uninspected pressure tubes for Bruce Power reactors is tabulated in Table 2 while similar probabilities for dispositionable flaws are given in Table 3.

$$Prob(dispositionable\ in\ uninspected) = 1 - (1 - Prob(dispositionable))^n$$

where n is the number of uninspected channels.

7.0 DISCUSSION

The results of this estimation of the probability of encountering flaws close to the OBM and at the top of the pressure tube indicate the following:

a. Systematically the highest estimates of the probability of encountering flaws in the regions of interest is for Region 2 and for reportable flaws.

b. The inspections carried out in A2131 (which were not considered when deriving the probabilities) did not reveal the presence of flaws in the regions of interest. This is consistent with the probability estimates provided in this report, which indicate that such an observation would have been very unlikely.

8.0 CONCLUSIONS

Based on calculations using the approach as detailed above, the following is concluded regarding the estimated probabilities of the occurrence of flaws in the region of interest (Region 2 as defined in Section 2.0):

- The estimated probability of at least 1 dispositionable flaw being present in Region 2 in a single uninspected channel is 1.07E-05 for Bruce Units 3 to 8.

- The largest estimated probability of at least 1 dispositionable flaw being present in Region 2 in the population of uninspected channels in each reactor core is 4.44E-03; this corresponds to Bruce Unit 6, which is currently shut down for MCR and has the largest number of uninspected pressure tubes.

9.0 REFERENCES

1. H. Zhou, Letter to L. Micuda, "Hydrogen Equivalent Concentration Measurements Taken Near the Outlet Burnish Mark in the Bruce Unit 3 2021 Outage (A2131)," Kinectrics File: B2038/LET/0013 R00, September 13, 2021.
2. J. Robertson, "B3-B8 Database of Pressure Tube Flaws Just Inboard of the Outlet Burnish Mark," Kinectrics File: B2266/RP/0002 R00, September 15, 2021.

Table 1: Probability per Channel of Encountering at Least One Flaw in the Regions of Interest

	60 degrees	120 degrees
Reportable	1.86918E-06	3.17434E-05
Dispositionable	6.27535E-07	1.06572E-05

Table 2: Probability of Encountering at Least One Reportable Flaw in the Regions of Interest in the Uninspected Population of Pressure Tubes

	Unique Channels	# Uninspected	Region 1	Region 2
Unit	Full Length Inspected	Channels	60 degrees	120 degrees
3	78	402	7.51E-04	1.27E-02
4	82	398	7.44E-04	1.26E-02
5	77	403	7.53E-04	1.27E-02
6	62	418	7.81E-04	1.32E-02
7	70	410	7.66E-04	1.29E-02
8	79	401	7.49E-04	1.26E-02

Table 3: Probability of Encountering at Least One Dispositionable Flaw in the Regions of Interest in the Uninspected Population of Pressure Tubes

	Unique Channels	# Uninspected	Region 1	Region 2
Unit	Full Length Inspected	Channels	60 degrees	120 degrees
3	78	402	2.52E-04	4.28E-03
4	82	398	2.50E-04	4.23E-03
5	77	403	2.53E-04	4.29E-03
6	62	418	2.62E-04	4.44E-03
7	70	410	2.57E-04	4.36E-03
8	79	401	2.52E-04	4.26E-03

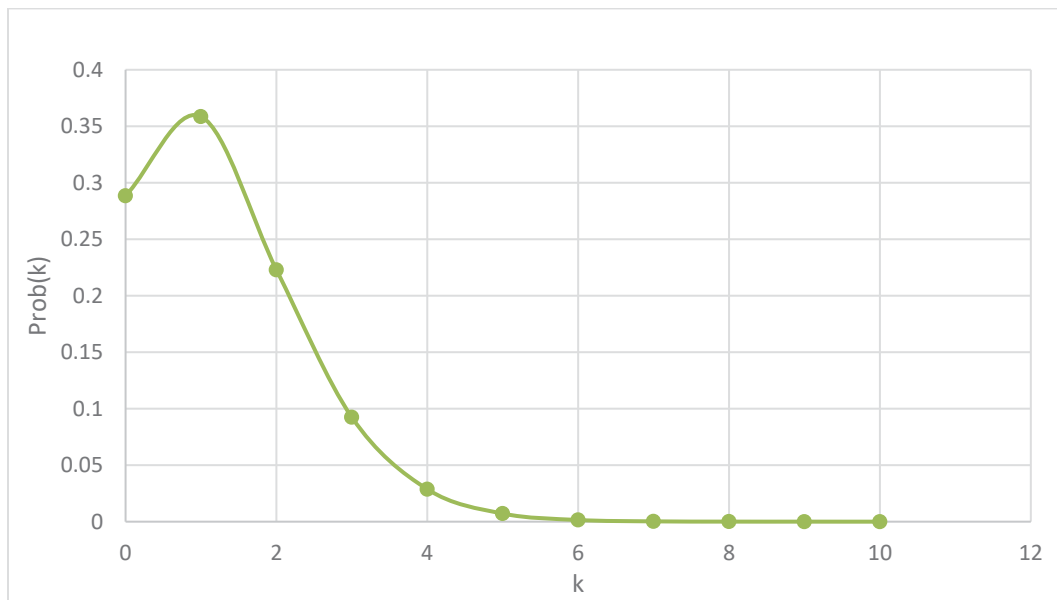*Uncontrolled if copied or printed from Kinectrics Intranet*

Figure 1: Probability of Encountering k Reportable Flaws in a Single Channel
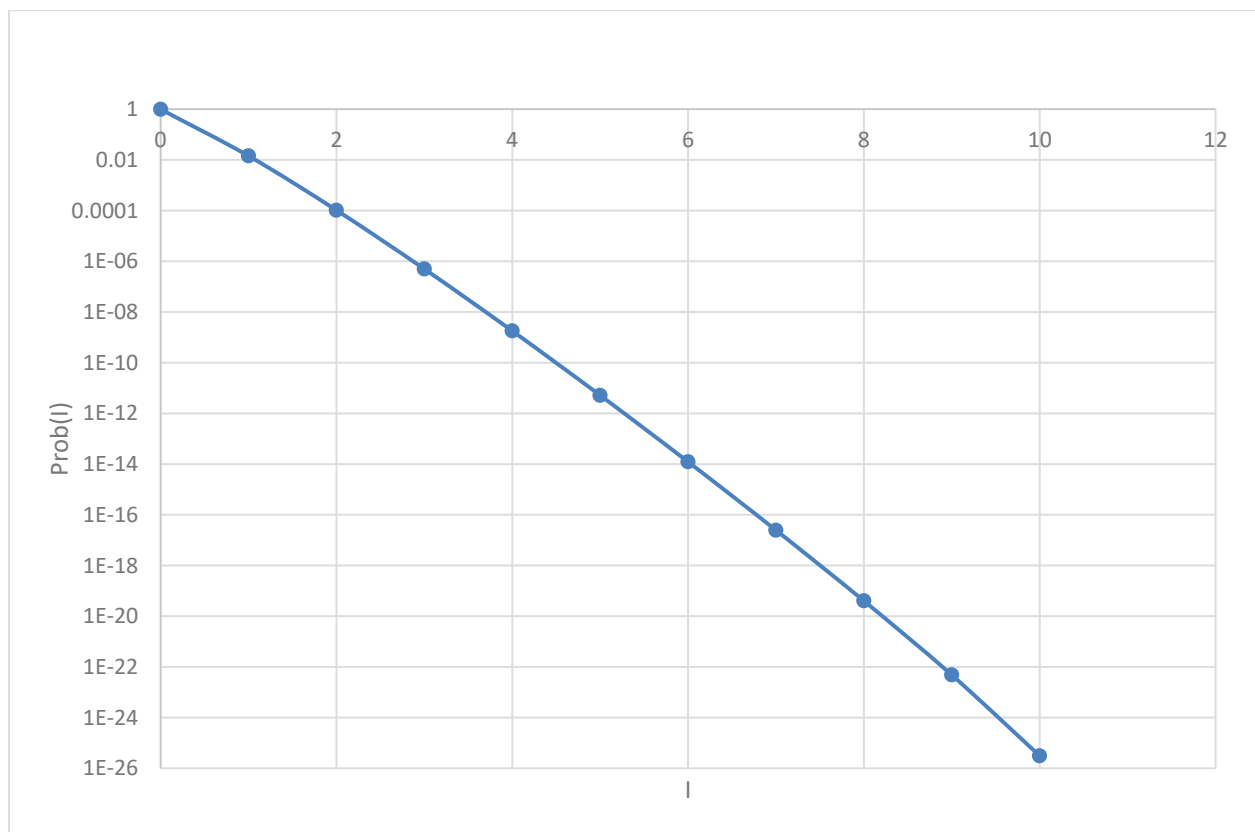
Figure 2: Probability of l Reportable Flaws Close to the OBM in a Single Channel

Uncontrolled if copied or printed from Kinectrics Intranet
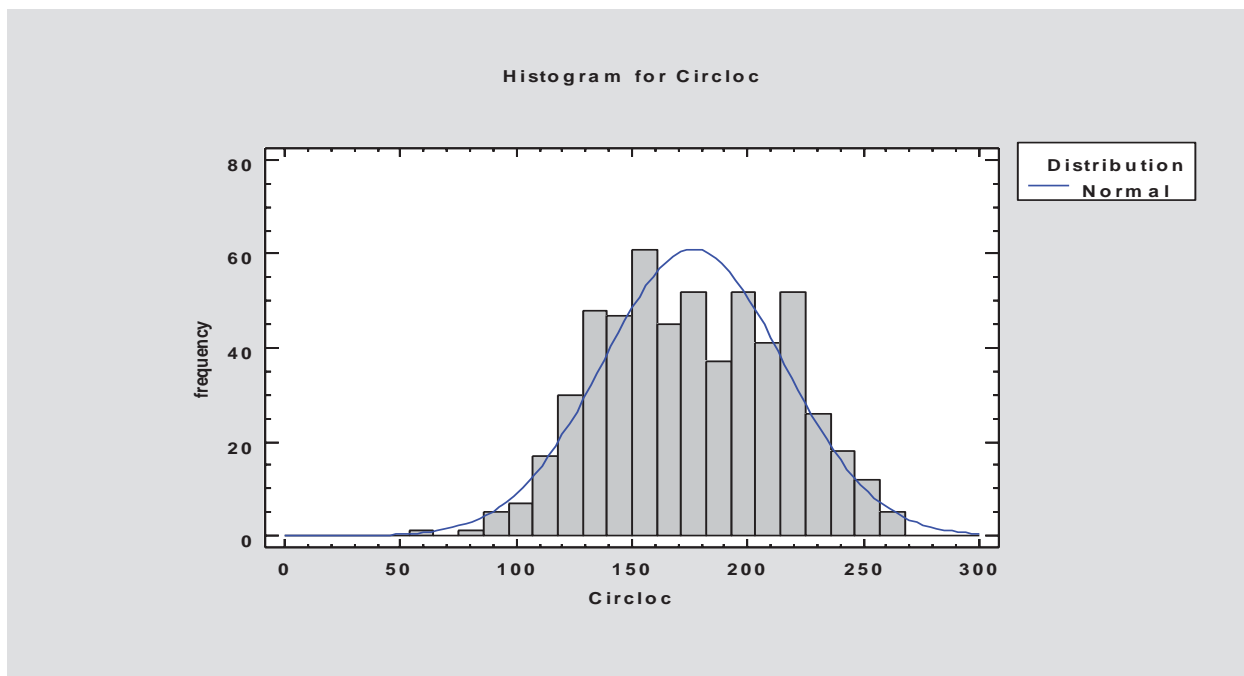
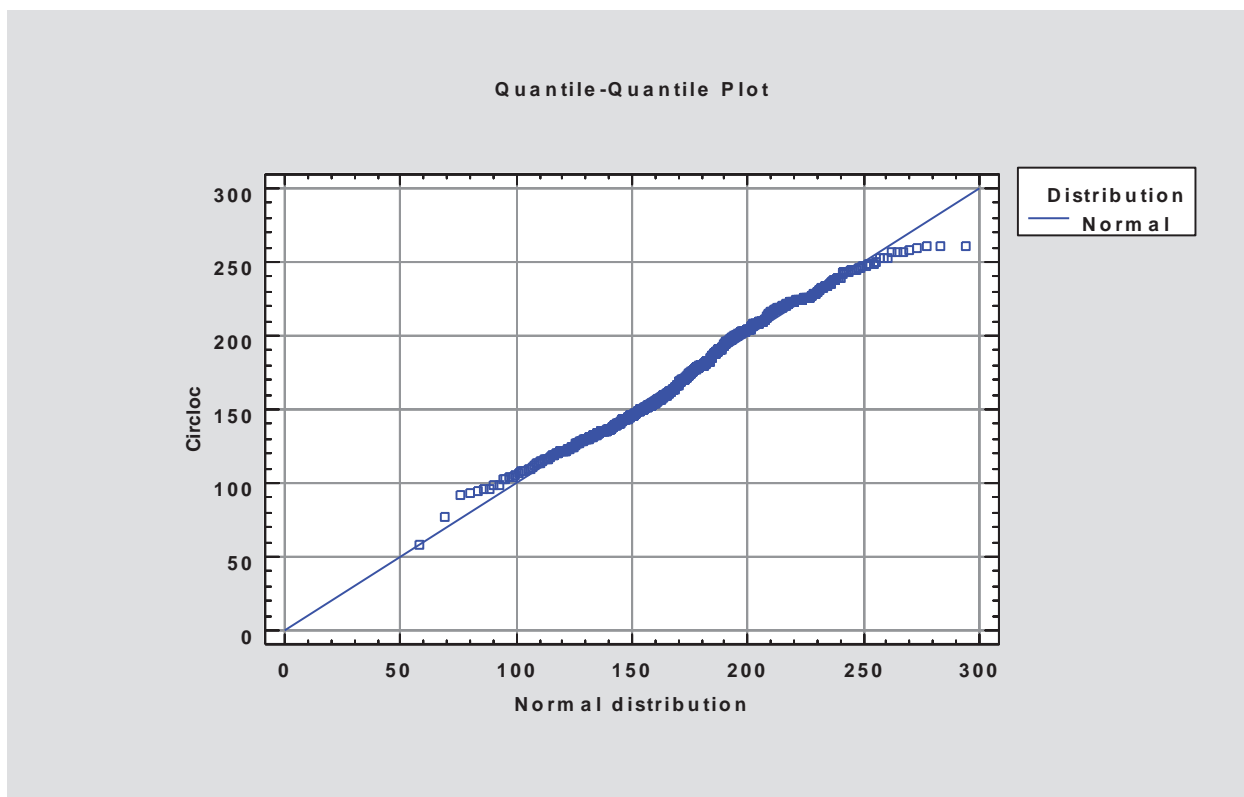**Figure 3: Histogram for the Distribution of the Circumferential Location**

Figure 4: Quantile-Quantile Plot of Observed Distribution and Proposed Distribution
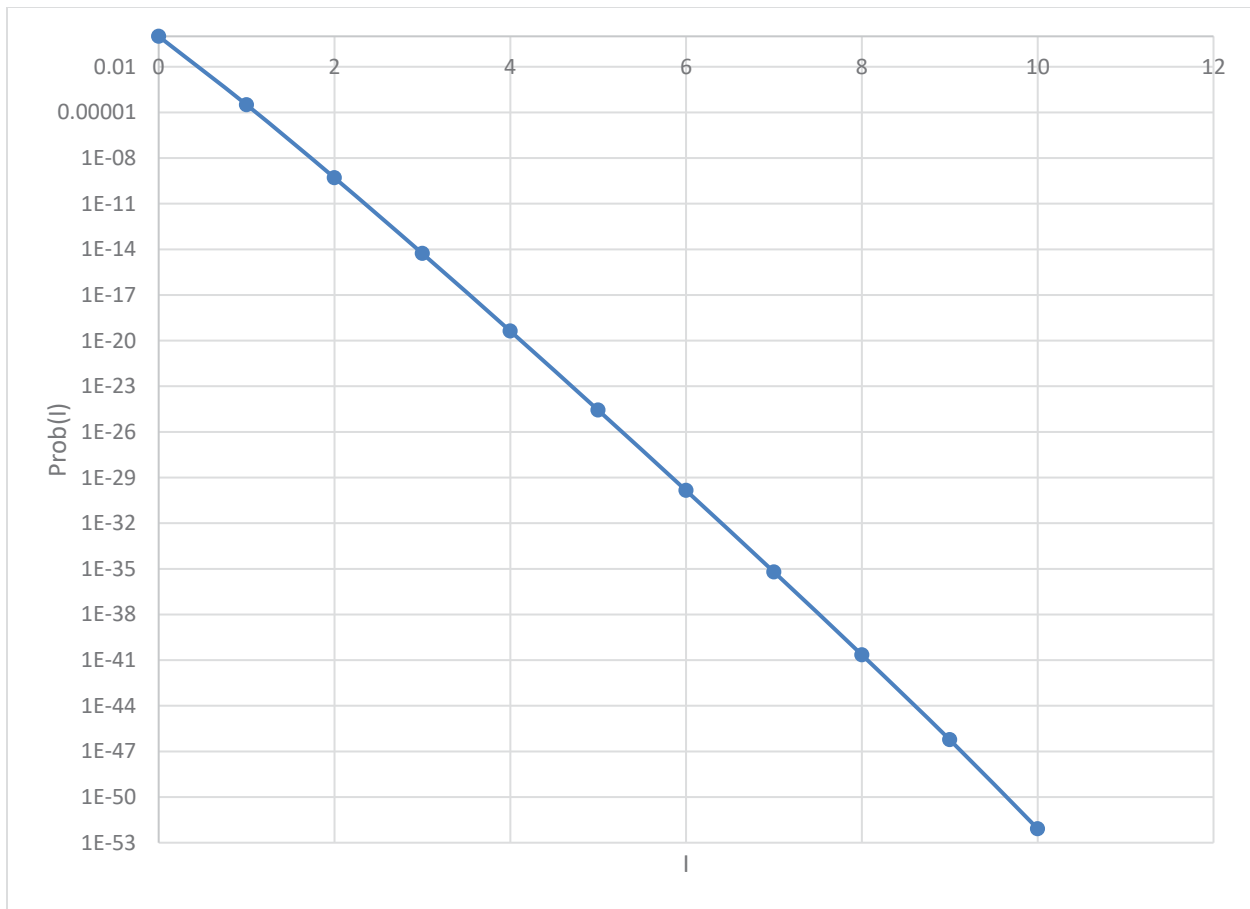
Figure 5: Probability of J Reportable Flaws in the Top 120 Degrees for the Region of Interest.

Enclosure 3

NK21-REP-31100-00129, Revision 000

Risk-Informed Deterministic Evaluation of Fracture Protection for the Region of Interest in Outlet Rolled Joints in Bruce Unit 3

KINECTRICS NSS INC.

RISK-INFORMED DETERMINISTIC EVALUATION OF FRACTURE PROTECTION FOR THE REGION OF INTEREST IN OUTLET

NK21-REP-31100-00129

REV. 0

☒ Accepted   ☐ Accepted As Noted – Revision Required

☐ Rejected   ☐ Accepted As Noted – No Revision Required

FOR USE AT BRUCE POWER

ACCEPTED: **DAVID CHO**

(Print Name)   (Signature)

TITLE: **TECHNICAL ADVISOR**

(Print Title)

DATE: **17SEP2021**

(DDMMMYYYY)

ACCEPTANCE OF THIS DOCUMENT DOES NOT RELIEVE THE CONTRACTOR OF RESPONSIBILITY FOR ANY ERRORS OR OMISSIONS.

BRUCE A UNIT 3 (A2131) FUEL CHANNEL OUTAGE SUPPORT AND DISPOSITION OUTAGE SUPPORT

RISK-INFORMED DETERMINISTIC EVALUATION OF FRACTURE PROTECTION FOR THE REGION OF INTEREST IN OUTLET ROLLED JOINTS IN BRUCE UNIT 3

Kinectrics Report No. B2038/RP/0009 R00
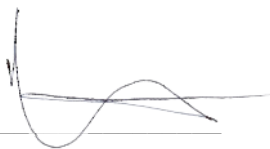
Prepared for
Bruce Power

Issue Date

2021-Sep-15

RISK-INFORMED DETERMINISTIC EVALUATION OF FRACTURE PROTECTION FOR THE REGION OF INTEREST IN OUTLET ROLLED JOINTS IN BRUCE UNIT 3

**Kinectrics Report No.
B2038/RP/0009 R00**

Prepared by	Verified by	Reviewed by	Approved by
D.A. Scarth	C. Liu	A.C. Wallace	J. Robertson
Technical Director – Fracture Programs MMC	Senior Scientist MMC	Technical Director MMC	Service Line Director MMC
Date prepared September 15, 2021	Date verified September 15, 2021	Date reviewed September 15, 2021	Date approved September 15 2021

RISK-INFORMED DETERMINISTIC EVALUATION OF FRACTURE PROTECTION FOR THE REGION OF INTEREST IN OUTLET ROLLED JOINTS IN BRUCE UNIT 3

Kinectrics Report No. B2038/RP/0009 R00

Revision History

Rev 00	Description			
	Revision 00 was issued to Bruce Power.			
	Issue Date	Prepared by	Verified by	Reviewed by	Approved by
	2021-September-15	D.A. Scarth	C. Liu	A.C. Wallace	J. Robertson

DISCLAIMER

Kinectrics prepared this report as a work of authorship sponsored by their Client. This report has been prepared solely for the benefit of the Client and may not be used or relied upon in whole or in part by any other person or entity without Client permission or without Kinectrics' permission if required by the Contract between Client and Kinectrics Inc. Neither Kinectrics, their client nor any person acting on behalf of them: (a) makes any warranty or representation whatsoever, express or implied, or assumes any legal liability of responsibility for any third party's use, or the results of such use, with respect to (i) the use of any information, apparatus, method, process, or similar item disclosed in this report including the merchantability or fitness for any particular purpose of any information contained in this report or the respective works or services supplied or performed or (ii) that such use does not infringe on or interfere with privately owned rights, including any party's intellectual property; or (b) assumes responsibility for any damages or other liability whatsoever (including any consequential damages resulting from a third party's selection or use of this report or any information, apparatus, method, process, or similar item disclosed.

![Kinectrics logo] **KINECTRICS**

RISK-INFORMED DETERMINISTIC EVALUATION OF FRACTURE PROTECTION FOR THE REGION OF INTEREST IN OUTLET ROLLED JOINTS IN BRUCE UNIT 3

Kinectrics Report No. B2038/RP/0009 R00

Executive Summary

High levels of hydrogen equivalent concentration (H_{eq}) have been detected in the front-end outlet rolled joints of Bruce Unit 3. The axial and radial extents of the higher than expected levels of H_{eq} inboard of the outlet rolled joint burnish mark have been found to be confined to a localized region with a central tendency about the top of the pressure tube. This localized region inboard of the outlet rolled joint burnish mark with a central tendency about the top of the pressure tube that has higher than expected levels of H_{eq} is defined in this report as the region of interest. A risk-informed deterministic evaluation of fracture protection based on a postulated axial through-wall flaw in the front-end outlet rolled joints in fuelled channels in Bruce Unit 3 has been performed for the region of interest for the predicted high levels of H_{eq}, as well as for postulated levels of H_{eq} that are higher than predicted levels, as described in this report. The scope of the risk-informed deterministic evaluation of fracture protection is limited to the region of interest. Based on the results from rising pressure burst tests and fracture toughness modelling, for the same set of conditions such as H_{eq}, the back end of a pressure tube is known to have a higher fracture toughness than the front end. For the same set of conditions such as H_{eq}, the results of the risk-informed deterministic evaluation of fracture protection for the region of interest in the front-end outlet rolled joints in this report can be used as a conservative bound on the results from a risk-informed deterministic evaluation of fracture protection of the region of interest in the back-end outlet rolled joints in Bruce Unit 3. Although the results of the evaluation in this report are specific to the region of interest in the front-end outlet rolled joints in Bruce Unit 3, the framework of the risk-informed deterministic evaluation of fracture protection is applicable to a region of interest in any Bruce reactor.

The risk-informed deterministic evaluation of fracture protection was performed for the region of interest for postulated levels of H_{eq} of up to 250 ppm. The highest level of H_{eq} in a rising pressure burst test specimen from the front end of the pressure tube is 178 ppm and corresponds to the burst test BT-50 specimen B6N07-2. Measured fracture toughness from small test specimens comprised of irradiated Zircaloy-2 and Zircaloy-4 materials with a range of levels of H_{eq} that in some cases exceed 250 ppm were obtained from the literature and used in the context of surrogate materials to gain insights into the fracture toughness of zirconium alloys at these high levels of H_{eq}. A conservative value of fracture toughness from the set of fracture toughness values for irradiated Zircaloy-2 and Zircaloy-4 materials was used to develop an adjustment factor that is less than 1.0 and is intended to account for uncertainty in the application of the Revision 2 engineering fracture toughness model to these postulated high levels of H_{eq} in the region of interest. The values of fracture toughness that were used in the evaluation were predicted by the Revision 2 engineering fracture toughness model and then reduced by multiplying by the adjustment factor.

A risk-informed deterministic evaluation of fracture protection for the Service Level A reactor Heatup and Cooldown transients was performed for the region of interest based on revised Heatup and Cooldown pressure-temperature operating limits for Bruce Unit 3 that are intended to increase fracture protection margins. The safety factors on internal pressure for the revised pressure-temperature operating limits for reactor Heatup and Cooldown were calculated using

Proprietary and Confidential

RISK-INFORMED DETERMINISTIC EVALUATION OF FRACTURE PROTECTION FOR THE REGION OF INTEREST IN OUTLET ROLLED JOINTS IN BRUCE UNIT 3

Kinectrics Report No.
B2038/RP/0009 R00

postulated axial through-wall flaw lengths of 18 and 20 mm, and postulated levels of H_{eq} of 200 through 250 ppm. For a postulated axial through-wall flaw length of 18 mm and postulated levels of H_{eq} of 200 through 250 ppm, the safety factors on internal pressure for reactor Heatup and Cooldown are greater than 1.20. The lowest safety factor is 1.12, and is for a postulated axial through-wall flaw length of 20 mm and an H_{eq} of 250 ppm.

A risk-informed deterministic evaluation of fracture protection was also performed for the region of interest based on revised pressure-temperature limits for a Service Level C overpressure excursion that were used in the development of a revised procedure for the DCC Feedpump trip to mitigate a Cold Over-Pressurization Transient and increase fracture protection margins. The safety factors on internal pressure were calculated for the Service Level C overpressure excursion using postulated axial through-wall flaw lengths of 18 and 20 mm, and postulated levels of H_{eq} of 200 through 250 ppm. For the postulated axial through-wall flaw length of 18 mm and postulated levels of H_{eq} of 200 through 250 ppm, and for the postulated axial through-wall flaw length of 20 mm and levels of H_{eq} of 200 through 240 ppm, the safety factors on internal pressure are greater than 1.0. The lowest safety factor is 0.99, and is for a postulated axial through-wall flaw length of 20 mm and an H_{eq} of 250 ppm. These safety factors essentially meet the required safety factor of 1.0 in the acceptance criteria for fracture protection during a Service Level C event in the CSA Standard N285.8.

The risk-informed deterministic evaluation of fracture protection for the region of interest in front-end outlet rolled joints in Bruce Unit 3 involves a number of conservatisms. A review of volumetric inspection results has confirmed that the small region of a pressure tube that is postulated to have a higher than expected level of H_{eq} in a localized region just inboard of the outlet burnish mark with a central tendency about the top of the pressure tube is very unlikely to contain flaws that are of a severity that would be a site for crack initiation and growth. The postulated through-wall flaw is assumed to be not leaking and not detected. The lower temperature portions of the fracture toughness curves that are most limiting in fracture protection evaluations of front-end outlet rolled joints in Bruce Unit 3 do not take into account the benefit of the higher irradiation temperatures at the outlets that result in an increase in the fracture toughness.

In the event of the unanticipated existence of an axial through-wall flaw in the region of interest in a front-end outlet rolled joint in Bruce Unit 3, and given the conservatisms in the deterministic evaluation of fracture protection, these results demonstrate there would be a low risk of instability of a flaw with a length up to 20 mm in the region of interest during reactor Heatup or Cooldown, or during an overpressure excursion.

RISK-INFORMED DETERMINISTIC EVALUATION OF FRACTURE PROTECTION FOR THE REGION OF INTEREST IN OUTLET ROLLED JOINTS IN BRUCE UNIT 3

Kinectrics Report No. B2038/RP/0009 R00

Table of Contents

Page No.

RISK-INFORMED DETERMINISTIC EVALUATION OF FRACTURE PROTECTION FOR THE REGION OF INTEREST IN OUTLET ROLLED JOINTS IN BRUCE UNIT 3

Kinectrics Report No. B2038/RP/0009 R00

RISK-INFORMED DETERMINISTIC EVALUATION OF FRACTURE PROTECTION FOR THE REGION OF INTEREST IN OUTLET ROLLED JOINTS IN BRUCE UNIT 3

Kinectrics Report No.
B2038/RP/0009 R00

RISK-INFORMED DETERMINISTIC EVALUATION OF FRACTURE PROTECTION FOR THE REGION OF INTEREST IN OUTLET ROLLED JOINTS IN BRUCE UNIT 3

Kinectrics Report No.
B2038/RP/0009 R00

List of Tables

RISK-INFORMED DETERMINISTIC EVALUATION OF FRACTURE PROTECTION FOR THE REGION OF INTEREST IN OUTLET ROLLED JOINTS IN BRUCE UNIT 3

Kinectrics Report No.
B2038/RP/0009 R00

List of Figures

Page No.

RISK-INFORMED DETERMINISTIC EVALUATION OF FRACTURE PROTECTION FOR THE REGION OF INTEREST IN OUTLET ROLLED JOINTS IN BRUCE UNIT 3

Kinectrics Report No.
B2038/RP/0009 R00

RISK-INFORMED DETERMINISTIC EVALUATION OF FRACTURE PROTECTION FOR THE REGION OF INTEREST IN OUTLET ROLLED JOINTS IN BRUCE UNIT 3

Kinectrics Report No.
B2038/RP/0009 R00

RISK-INFORMED DETERMINISTIC EVALUATION OF FRACTURE PROTECTION FOR THE REGION OF INTEREST IN OUTLET ROLLED JOINTS IN BRUCE UNIT 3

Kinectrics Report No.
B2038/RP/0009 R00

List of Acronyms and Symbols

Acronyms

CCTS	=	Curved Compact Tension Specimen
C-L	=	fracture toughness test specimen orientation that corresponds to an axial through-wall crack in the pressure tube under an applied hoop stress
CSA	=	Canadian Standards Association
EFPH	=	Equivalent Full Power Hours
MCR	=	Major Component Replacement
RD	=	fracture toughness test specimen orientation where the applied load is in the plate width direction perpendicular to the plate rolling direction and crack growth is in the plate rolling direction
ROH	=	Reactor Outlet Header
T-W	=	fracture toughness test specimen orientation where the applied load is in the plate thickness direction and crack growth is in the plate width direction perpendicular to the rolling direction
W-T	=	fracture toughness test specimen orientation where the applied load is in the plate width direction perpendicular to the rolling direction and crack growth is in plate thickness direction

Symbols

c	=	half-length of the postulated axial through-wall flaw, m
Cl	=	chlorine concentration, ppm
d_{FL}	=	distance between the axial location of the postulated axial through-wall flaw at the outlet rolled joint burnish mark and the inlet end of the pressure tube, = 6.243 m
D_{fr}	=	distance from the front end of the pressure tube, m
F_{sp}	=	correction factor to account for the potential effect of reinforcement of the sealing patch on the results from rising pressure burst tests, = 1.04
HCC	=	Hydride Continuity Coefficient, dimensionless
H_{eq}	=	hydrogen equivalent concentration, ppm
K_c	=	fracture toughness for axial through-wall flaw instability, MPa√m
$K_{c,adj}$	=	adjusted fracture toughness to account for uncertainty in the application of the Revision 2 engineering fracture toughness model to high levels of H_{eq} of up to 250 ppm, MPa√m
$K_{c,ref}$	=	fracture toughness from the Revision 2 engineering fracture toughness model at a reference set of conditions, MPa√m
$L_p(Pr)$	=	crack length at initial wall penetration for a specific cumulative probability, Pr, mm
K_{exp}	=	reference value of measured fracture toughness, MPa√m
L_{pm}	=	mean value of the crack length at initial wall penetration, mm
L_{PT}	=	length of the pressure tube, = 6.312 m

Proprietary and Confidential

RISK-INFORMED DETERMINISTIC EVALUATION OF FRACTURE PROTECTION FOR THE REGION OF INTEREST IN OUTLET ROLLED JOINTS IN BRUCE UNIT 3

Kinectrics Report No.
B2038/RP/0009 R00

$L_p(Pr)$	=	crack length at initial wall penetration for a specific cumulative probability, Pr, mm
M_b	=	bulging factor for an axial through-wall flaw, dimensionless
$N(L_{Pm}, sd_{Lp})$	=	normal distribution of crack length at initial wall penetration with a mean, L_{pm}, and standard deviation, sd_{Lp}, mm
p_{cr}	=	critical internal pressure at instability of a postulated axial through-wall flaw, MPa
p_{FL}	=	internal pressure at the location of the postulated axial through-wall flaw, MPa
$(p_{Flcr})_{ROH}$	=	critical internal pressure at the ROH at instability of a postulated axial through-wall flaw, MPa
Pr	=	cumulative probability of the crack length at initial penetration being less than L_p, dimensionless
Δp_{ROH}	=	pressure differential between the axial location of the postulated axial through-wall flaw at the outlet rolled joint burnish mark and the ROH, MPa
Δp_{ROH}^{in}	=	pressure differential between the thermalhydraulic inlet of the fuel channel and the ROH, MPa
Δp_{ROH}^{out}	=	pressure differential between the thermalhydraulic outlet of the fuel channel and the ROH, MPa
R_i	=	pressure tube inner radius, m
R_m	=	pressure tube mean radius, m
sd_{Lp}	=	standard deviation of crack length at initial wall penetration, mm
SF	=	safety factor on internal pressure, dimensionless
T	=	temperature, °C
T_{irr}	=	irradiation temperature, °C
$U(\zeta, 29)$	=	ζ-quantile of Student's t-distribution with 29 degrees of freedom, dimensionless
$U(\zeta, 34)$	=	ζ-quantile of Student's t-distribution with 34 degrees of freedom, dimensionless
w	=	pressure tube wall thickness, m
β_H	=	adjustment factor on fracture toughness to account for uncertainty in the application of the Revision 2 engineering fracture toughness model to high levels of H_{eq} of up to 250 ppm, dimensionless
ε_{Kc1}	=	error term for fracture toughness for levels of H_{eq} of 30 ppm or less and for temperatures less than or equal to 150°C from Clause D.13.2.2.2 of the CSA Standard N285.8, dimensionless
ε_{Kc2}	=	error term for fracture toughness for levels of H_{eq} of 30 ppm or less and for temperatures greater than 150°C from Clause D.13.2.2.2 of the CSA Standard N285.8, dimensionless
σ_f	=	flow stress of the material, MPa
σ_u	=	lower-bound transverse ultimate tensile strength, MPa
σ_{ys}	=	lower-bound transverse yield strength, MPa
ζ	=	single-tailed statistical confidence level, dimensionless

RISK-INFORMED DETERMINISTIC EVALUATION OF FRACTURE PROTECTION FOR THE REGION OF INTEREST IN OUTLET ROLLED JOINTS IN BRUCE UNIT 3

Kinectrics Report No. B2038/RP/0009 R00

1.   INTRODUCTION

High levels of hydrogen equivalent concentration (H_{eq}) have been detected in the front-end outlet rolled joints of Bruce Unit 3 [1]. The axial and radial extents of the higher than expected levels of H_{eq} inboard of the outlet rolled joint burnish mark have been found to be confined to a localized region with a central tendency about the top of the pressure tube. This localized region inboard of the outlet rolled joint burnish mark with a central tendency about the top of the pressure tube that has higher than expected levels of H_{eq} is defined in this report as the region of interest. A risk-informed deterministic evaluation of fracture protection based on a postulated axial through-wall flaw in the front-end outlet rolled joints in fuelled channels in Bruce Unit 3 has been performed for the region of interest for the predicted high levels of H_{eq}, as well as for postulated levels of H_{eq} that are higher than predicted levels. The scope of the risk-informed deterministic evaluation of fracture protection is limited to the region of interest. Based on the results from rising pressure burst tests and fracture toughness modelling, for the same set of conditions such as H_{eq}, the back end of a pressure tube is known to have a higher fracture toughness than the front end. This is due to a more favourable bulk hydride morphology at the back end. For the same set of conditions such as H_{eq}, the results of the risk-informed deterministic evaluation of fracture protection for the region of interest in the front-end outlet rolled joints in this report can be used as a conservative bound on the results from a risk-informed deterministic evaluation of fracture protection of the region of interest in the back-end outlet rolled joints in Bruce Unit 3. Although the results of the evaluation in this report are specific to the region of interest in the front-end outlet rolled joints in Bruce Unit 3, the framework of the risk-informed deterministic evaluation of fracture protection is applicable to a region of interest in any Bruce reactor.

The risk-informed deterministic evaluation of fracture protection was performed for the region of interest for the postulated levels of H_{eq} of up to 250 ppm. The highest level of H_{eq} in a rising pressure burst test specimen from the front end of the pressure tube is 178 ppm and corresponds to the burst test BT-50 specimen B6N07-2. Measured fracture toughness from small test specimens comprised of irradiated Zircaloy-2 and Zircaloy-4 materials with a range of levels of H_{eq} that in some cases exceed 250 ppm were obtained from the literature and used in the context of surrogate materials to gain insights into the fracture toughness of zirconium alloys at these high levels of H_{eq}. A conservative value of fracture toughness from the set of fracture toughness values for irradiated Zircaloy-2 and Zircaloy-4 materials was used to develop an adjustment factor that is less than 1.0 and is intended to account for uncertainty in the application of the Revision 2 engineering fracture toughness model [2] to these postulated high levels of H_{eq} in the region of interest. The values of fracture toughness that were used in the evaluation were predicted by the Revision 2 engineering fracture toughness model and then reduced by multiplying by the adjustment factor.

A risk-informed deterministic evaluation of fracture protection for the Service Level A reactor Heatup and Cooldown transients was performed for the region of interest based on revised Heatup and Cooldown pressure-temperature operating limits for Bruce Unit 3 that are intended to increase fracture protection margins [3]. The safety factors on internal pressure for the revised pressure-temperature operating limits for reactor Heatup and Cooldown were calculated. A risk-

Proprietary and Confidential

RISK-INFORMED DETERMINISTIC EVALUATION OF FRACTURE PROTECTION FOR THE REGION OF INTEREST IN OUTLET ROLLED JOINTS IN BRUCE UNIT 3

Kinectrics Report No.
B2038/RP/0009 R00

informed deterministic evaluation of fracture protection was also performed for the region of interest based on revised pressure-temperature limits for a Service Level C overpressure excursion that were used in the development of a revised procedure for the DCC Feedpump trip to mitigate a Cold Over-Pressurization Transient and increase fracture protection margins [3]. The safety factors on internal pressure were calculated for the Service Level C overpressure excursion.

This risk-informed deterministic evaluation of fracture protection for the region of interest was performed over an evaluation period of operation of Bruce Unit 3 up to the Major Component Replacement (MCR) that is estimated to be bounded by 246,000 Equivalent Full Power Hours (EFPH). This work was performed for Bruce Power.

RISK-INFORMED DETERMINISTIC EVALUATION OF FRACTURE PROTECTION FOR THE REGION OF INTEREST IN OUTLET ROLLED JOINTS IN BRUCE UNIT 3

Kinectrics Report No. B2038/RP/0009 R00

2.   OVERVIEW OF EVALUATION

(a) Application of the Revision 2 engineering fracture toughness model [2] to the region of interest that is the localized region inboard of the outlet rolled joint burnish mark with a central tendency about the top of the pressure tube that has higher than expected levels of H_{eq} is discussed in Section 3 of this report. The region of interest has high levels of H_{eq} beyond the current validity limits and scope of the model for the front-end outlet of the pressure tube.

(b) Measured fracture toughness from small test specimens comprised of irradiated Zircaloy-2 and Zircaloy-4 materials with a range of levels of H_{eq} that in some cases exceed 250 ppm were obtained from the literature and used in the context of surrogate materials to gain insights into the fracture toughness of zirconium alloys at these high levels of H_{eq}. Fracture toughness tests and levels of fracture toughness of irradiated Zr-2.5Nb pressure tube material, Zircaloy-2 materials, and Zircaloy-4 materials, with medium to high levels of H_{eq}, are described in Section 4. The fracture toughness of irradiated Zircaloy-2 and Zircaloy-4 materials are compared in Section 4 with fracture toughness from small specimens from hydrided irradiated burst test specimens from Zr-2.5Nb pressure tubes.

(c) A conservative value of fracture toughness from the set of fracture toughness values for irradiated Zircaloy-2 and Zircaloy-4 materials was used to develop an adjustment factor that is less than 1.0 and is intended to account for uncertainty in the application of the Revision 2 engineering fracture toughness model to postulated high levels of H_{eq} of up to 250 ppm in the region of interest. The values of fracture toughness that were used in the evaluation were predicted by the Revision 2 engineering fracture toughness model and then reduced by multiplying by the adjustment factor. The development of the adjustment factor is described in Section 5.

(d) The deterministic fracture protection evaluation procedure for reactor Heatup and Cooldown is described in Section 6. This includes the methods of calculation of the lower-bound fracture toughness, the critical internal pressure at instability of a postulated axial through-wall flaw, and the safety factor on internal pressure.

(e) The deterministic fracture protection evaluation procedure for the overpressure excursion is described in Section 7. This includes the methods of calculation of the lower prediction bound on fracture toughness, and the safety factor on internal pressure.

(f) Inputs for the risk-informed deterministic evaluation of fracture protection are described in Section 8. These include the postulated axial through-wall flaw location and length, pressure tube dimensions, hydrogen equivalent concentration and chlorine concentration, the pressure differential between the location of a postulated axial through-wall flaw at the outlet rolled joint burnish mark and the Reactor Outlet Header (ROH), and revised pressure-temperature limits for reactor Heatup and Cooldown and the overpressure excursion.

RISK-INFORMED DETERMINISTIC EVALUATION OF FRACTURE PROTECTION FOR THE REGION OF INTEREST IN OUTLET ROLLED JOINTS IN BRUCE UNIT 3

Kinectrics Report No. B2038/RP/0009 R00

(g) The safety factor on internal pressure is the ratio of the calculated critical internal pressure at flaw instability divided by the actual internal pressure at the location of the postulated axial through-wall flaw. The safety factors on internal pressure for the revised pressure-temperature operating limits for reactor Heatup and Cooldown for Bruce Unit 3 were calculated for the region of interest as described in Section 9.

(h) The safety factors on internal pressure for the revised pressure-temperature limits for the overpressure excursion for Bruce Unit 3 were calculated for the region of interest as described in Section 10.

(i) Conservatisms in the risk-informed deterministic evaluation of fracture protection are described in Section 11.

RISK-INFORMED DETERMINISTIC EVALUATION OF FRACTURE PROTECTION FOR THE REGION OF INTEREST IN OUTLET ROLLED JOINTS IN BRUCE UNIT 3

Kinectrics Report No. B2038/RP/0009 R00

3. APPLICATION OF REVISION 2 ENGINEERING FRACTURE TOUGHNESS MODEL FOR HIGH LEVELS OF HYDROGEN EQUIVALENT CONCENTRATION BEYOND THE CURRENT MODEL SCOPE

The development of the Revision 2 engineering fracture toughness model for Zr-2.5Nb pressure tubes for the lower-shelf and transition temperature regimes first involved development of a Revision 2 analytical cohesive-zone model to predict the fracture toughness in the lower-shelf and transition temperature regimes as described in the report COG-JP-4583-V012-R01 [4]. This analytical model was then used in the report COG-JP-4583-V094 [2] to develop the Revision 2 engineering fracture toughness model. The Revision 2 engineering fracture toughness model predicts fracture toughness as a function of the distance from the front end of the pressure tube, hydrogen equivalent concentration (H_{eq}), chlorine concentration, temperature under evaluation, and irradiation temperature.

Application of the Revision 2 engineering fracture toughness model to high levels of H_{eq} beyond the current validity limits and scope of the model for the front-end outlet of the pressure tube is discussed below. Application of the Revision 2 engineering fracture toughness model to these high levels of H_{eq} is limited to the region of interest that is the localized region inboard of the outlet rolled joint burnish mark with a central tendency about the top of the pressure tube that has higher than expected levels of H_{eq}.

3.1 Levels of Hydrogen Equivalent Concentration Relative to Current Scope of Revision 2 Engineering Fracture Toughness Model

From Section 10.2 of Reference [2], for distances within 1.5 m from the front end of the pressure tube and based on levels of H_{eq} in the rising pressure burst test results, the recommended upper validity limit on H_{eq} in the Revision 2 engineering fracture toughness model is 100 ppm. This upper validity limit is intended for generic applications of the Revision 2 engineering fracture toughness model. Justification of a higher validity limit on H_{eq} of 120 ppm for distances within 1.5 m from the front end outlets in Bruce Unit 3 is provided in Reference [5].

From Reference [2], the Revision 2 analytical cohesive-zone fracture toughness model [4] was used to predict values of fracture toughness that were then used to develop the Revision 2 engineering fracture toughness model. The levels of H_{eq} that were used in the Revision 2 analytical cohesive-zone model calculations ranged up to 160 ppm. Application to levels of H_{eq} up to 160 ppm is considered to not be an extrapolation beyond the technical basis of the Revision 2 engineering fracture toughness model.

For the purpose of the risk-informed deterministic evaluation of fracture protection for the region of interest, the calculations in the current report were performed using postulated levels of H_{eq} of 200 through 250 ppm. The focus of the calculations was at the inboard tip of the postulated 18 or 20 mm long axial through-wall flaw that extends a distance of 18 or 20 mm inboard of the burnish mark, respectively. Application of the model beyond an H_{eq} of 160 ppm and up to 250 ppm is an extrapolation and was necessary to meet the scope of the risk-informed deterministic evaluation of fracture protection. As described in Section 5 of this report, a

RISK-INFORMED DETERMINISTIC EVALUATION OF FRACTURE PROTECTION FOR THE REGION OF INTEREST IN OUTLET ROLLED JOINTS IN BRUCE UNIT 3

Kinectrics Report No.
B2038/RP/0009 R00

conservative value of fracture toughness from the set of fracture toughness values for irradiated Zircaloy-2 and Zircaloy-4 materials was used to develop an adjustment factor that is less than 1.0 and is intended to account for uncertainty in the application of the Revision 2 engineering fracture toughness model to the postulated high levels of H_{eq} of up to 250 ppm in the region of interest. The values of fracture toughness that were used in the evaluation were predicted by the Revision 2 engineering fracture toughness model and then reduced by multiplying by the adjustment factor.

As stated above, the fracture toughness from the Revision 2 engineering fracture toughness model depends on the distance from the front end of the pressure tube [2]. The predicted fracture toughness decreases with a decrease in the distance from the front end. Calculation of the fracture toughness using the distance from the outlet rolled joint burnish mark to the front end of 0.069 m instead of the distance from the inboard tip of the postulated 20 mm long axial through-wall flaw to the front end of 0.089 m results in an insignificant decrease in the fracture toughness of 0.1% over the temperature range of interest. For simplicity, the fracture toughness was calculated using the distance from the outlet rolled joint burnish mark to the front end as a bounding distance for both postulated flaw lengths. This will cover any small variation in the location of the inboard tip of the postulated flaw due to a small variation in the location of the outlet rolled joint burnish mark.

The 97.5% lower prediction bounds on fracture toughness from the Revision 2 engineering fracture toughness model for a distance of 0.069 m from the front end of the pressure tube, irradiation temperature of 290°C, levels of H_{eq} of 50 through 250 ppm, and a chlorine concentration of 5.5 ppm, were calculated using the procedure in Section 9 of Reference [2]. The variation with temperature of the calculated 97.5% lower prediction bounds on fracture toughness is shown in Figure 3-1. As expected, the predicted fracture toughness decreases with an increase in H_{eq}. The rate at which the 97.5% lower prediction bounds on fracture toughness decrease relative to an increase in H_{eq} is lower at higher levels of H_{eq}.

3.2 Comparison of Revision 2 Engineering Fracture Toughness Model Against Result from Rising Pressure Burst Test BT-50 with a Hydrogen Equivalent Concentration of 178 ppm

Rising pressure burst test BT-50 was performed on specimen B6N07-2 [6,7] that was removed from the front end of the pressure tube that was the inlet. The axial through-wall flaw in the burst test specimen was located a distance of 0.79 m from the inlet end of the pressure tube. The specimen was hydrided to an H_{eq} of 178 ppm. The chlorine concentration of pressure tube B6N07 is not known. The burst test was performed at a temperature of 65°C. The preliminary fracture toughness, K_c, was calculated to be 41.5 MPa√m based on an assumed starting flaw length of 55 mm and an estimated flow stress of 1,034 MPa [6]. The specimen burst near the onset of crack growth and after only 0.78 mm of crack extension. The crack growth behaviour of this specimen is representative of the lower-shelf fracture regime [6].

The 97.5% lower prediction bound and best estimate fracture toughness from the Revision 2 engineering fracture toughness model were calculated as a function of temperature for the

RISK-INFORMED DETERMINISTIC EVALUATION OF FRACTURE PROTECTION FOR THE REGION OF INTEREST IN OUTLET ROLLED JOINTS IN BRUCE UNIT 3

Kinectrics Report No. B2038/RP/0009 R00

conditions of the rising pressure burst test BT-50 specimen B6N07-2 using the procedure in Section 9 of Reference [2]. A distance of 0.79 m from the front end of the pressure tube, and an H_{eq} of 178 ppm, were used. Two levels of chlorine concentration of 1.0 and 5.0 ppm that cover the expected range were used. From Reference [8], the irradiation temperature was taken to be 260°C.

The 97.5% lower prediction bound and best estimate fracture toughness from the Revision 2 engineering fracture toughness model for the conditions of rising pressure burst test BT-50, for the two levels of chlorine concentration of 1.0 and 5.0 ppm, and at the burst test temperature of 65°C, are given in Table 3-1. The preliminary measured fracture toughness, K_c, of 41.5 MPa√m is also given in Table 3-1 for comparison with the predicted fracture toughness. The predicted fracture toughness at 65°C is very insensitive to the chlorine concentration. The best estimate predictions of fracture toughness are slightly conservative relative to the burst test result. The 97.5% lower prediction bounds on fracture toughness are very conservative relative to the burst test result.

The variation with temperature of the calculated 97.5% lower prediction bounds on fracture toughness, and the best estimate fracture toughness, for the two levels of chlorine concentration of 1.0 and 5.0 ppm, are shown in Figure 3-2. The preliminary fracture toughness, K_c, of 41.5 MPa√m is also plotted in Figure 3-2 for comparison with the predicted fracture toughness. At lower temperatures the predicted fracture toughness is very insensitive to the chlorine concentration. Similar to Table 3-1, the best estimate predictions of fracture toughness are slightly conservative relative to the burst test result, and the 97.5% lower prediction bounds on fracture toughness are very conservative relative to the burst test result.

The conservative values of the 97.5% lower prediction bound and best estimate fracture toughness relative to the result from rising pressure burst test BT-50 with an H_{eq} of 178 ppm supports the application of the Revision 2 engineering fracture toughness model to higher levels of H_{eq}.

3.3 Unquantified Conservatism in Application of Fracture Toughness Curves from Revision 2 Engineering Fracture Toughness Model to Fuel Channel Outlets at Lower Temperatures

A multi-variable statistical analysis of fracture toughness measured from small Curved Compact Tension Specimens (CCTS) from as-removed and hydrided irradiated pressure tube sections is described in Reference [9]. The purpose of the statistical analysis was to identify important explanatory variables that affect fracture toughness. The statistical analysis demonstrated that an increase in the irradiation temperature resulted in an increase in the fracture toughness of both the as-removed and hydrided irradiated pressure tube material [9].

The sub-model for prediction of the transition temperature to the upper-shelf fracture regime that is a part of the Revision 2 engineering fracture toughness model includes irradiation temperature as a predictor [2]. For the application of the Revision 2 engineering fracture toughness model to front-end outlet rolled joints in Bruce Unit 3, the lower temperature portions of the fracture

RISK-INFORMED DETERMINISTIC EVALUATION OF FRACTURE PROTECTION FOR THE REGION OF INTEREST IN OUTLET ROLLED JOINTS IN BRUCE UNIT 3

Kinectrics Report No.
B2038/RP/0009 R00

toughness curves are most limiting in fracture protection evaluations. The lower temperature portions of the fracture toughness curves are essentially independent of the transition temperature to the upper-shelf fracture regime. The lower temperature portions of the fracture toughness curves are based on the analytical cohesive-zone fracture toughness model [4] that is a part of the technical basis for the Revision 2 engineering fracture toughness model and does not include irradiation temperature as a predictor. The lower temperature portions of the fracture toughness curves that are most limiting therefore do not take into account the benefit of the higher irradiation temperatures at the outlets that result in an increase in the fracture toughness, which represents an unquantified conservatism.

3.4 Future Work to Address Levels of Hydrogen Equivalent Concentration Beyond the Current Scope of the Revision 2 Engineering Fracture Toughness Model

A justification of the application of the Revision 2 engineering fracture toughness model for levels of H_{eq} of 160 ppm or higher is planned to be developed. It is recommended that rising pressure burst tests be performed on specimens that are hydrided to levels of H_{eq} that would support the application of the Revision 2 engineering fracture toughness model at the higher levels of H_{eq} used in the evaluations. All of the burst tests that have been performed to date on hydrided irradiated specimens at 250°C have exhibited upper-shelf fracture behaviour, and the fracture toughness is considered to not be affected by the existence of hydrides.

RISK-INFORMED DETERMINISTIC EVALUATION OF FRACTURE PROTECTION FOR THE REGION OF INTEREST IN OUTLET ROLLED JOINTS IN BRUCE UNIT 3

Kinectrics Report No. B2038/RP/0009 R00

TABLE 3-1
97.5% LOWER PREDICTION BOUND AND BEST ESTIMATE FRACTURE TOUGHNESS FROM THE REVISION 2 ENGINEERING FRACTURE TOUGHNESS MODEL FOR THE CONDITIONS OF RISING PRESSURE BURST TEST BT-50 FRONT-END INLET SPECIMEN B6N07-2 WITH AN H_{eq} OF 178 ppm

Chlorine Concentration used in Prediction of Fracture Toughness (ppm)	97.5% Lower Prediction Bound on Fracture Toughness, K_c, at 65°C (MPa√m)	Best Estimate Fracture Toughness, K_c, at 65°C (MPa√m)	Preliminary Measured Fracture Toughness, K_c, from Burst Test BT-50 at 65°C (MPa√m)
1.0	29.3	39.1	41.5
5.0	29.0	38.7	

RISK-INFORMED DETERMINISTIC EVALUATION OF FRACTURE PROTECTION FOR THE REGION OF INTEREST IN OUTLET ROLLED JOINTS IN BRUCE UNIT 3

Kinectrics Report No. B2038/RP/0009 R00

Figure 3-1: Variation with Temperature of 97.5% Lower Prediction Bound on Fracture Toughness Predicted Using Revision 2 Engineering Model for a Distance of 0.069 m from the Front End of the Pressure Tube, Irradiation Temperature of 290°C and Chlorine Concentration of 5.5 ppm

RISK-INFORMED DETERMINISTIC EVALUATION OF FRACTURE PROTECTION FOR THE REGION OF INTEREST IN OUTLET ROLLED JOINTS IN BRUCE UNIT 3

Kinectrics Report No. B2038/RP/0009 R00
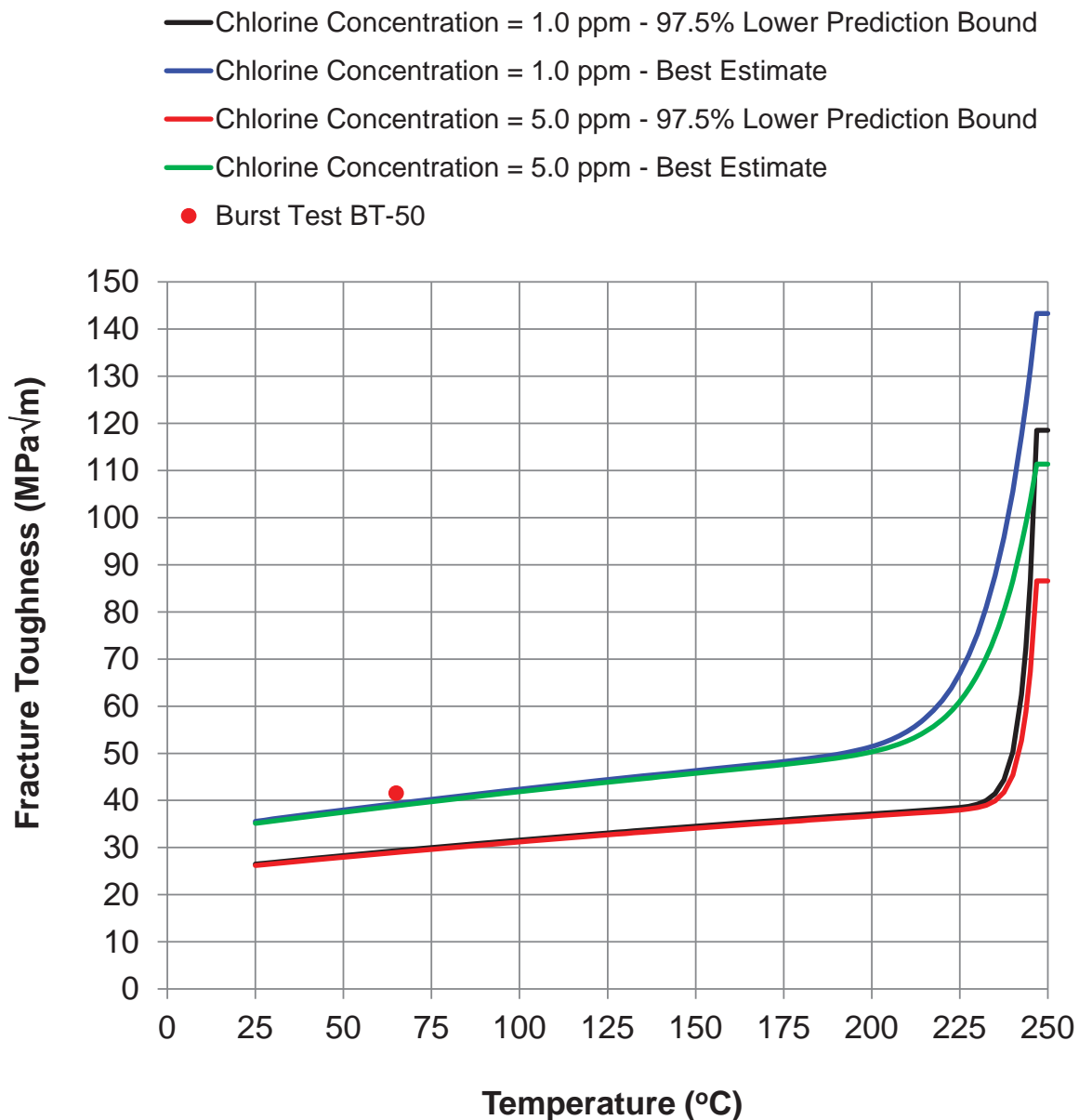
Figure 3-2: Comparison of Revision 2 Engineering Fracture Toughness Model Against Result from Rising Pressure Burst Test BT-50 Front-End Inlet Specimen B6N07-2 with an H_{eq} of 178 ppm

RISK-INFORMED DETERMINISTIC EVALUATION OF FRACTURE PROTECTION FOR THE REGION OF INTEREST IN OUTLET ROLLED JOINTS IN BRUCE UNIT 3

Kinectrics Report No. B2038/RP/0009 R00

4. FRACTURE TOUGHNESS OF IRRADIATED Zr-2.5Nb PRESSURE TUBE MATERIAL, ZIRCALOY-2 AND ZIRCALOY-4 MATERIALS, WITH MEDIUM TO HIGH LEVELS OF HYDROGEN EQUIVALENT CONCENTRATION

The effect of the geometry of small Curved Compact Tension Specimens on measured fracture toughness relative to fracture toughness measured from rising pressure burst tests for hydrided irradiated Zr-2.5Nb pressure tube material is described in Section 4.1 of this report.

Measured fracture toughness from small test specimens comprised of irradiated Zircaloy-2 and Zircaloy-4 materials with ranges of levels of H_{eq} that in some cases exceed 250 ppm were obtained from the literature and used in the context of surrogate materials to gain insights into the fracture toughness of zirconium alloys at these high levels of H_{eq}. Fracture toughness tests and levels of fracture toughness of irradiated Zr-2.5Nb pressure tube material, Zircaloy-2 and Zircaloy-4 materials, with medium to high levels of H_{eq}, are described in Section 4.2. Tabular values of the fracture toughness of irradiated Zr-2.5Nb pressure tube material, Zircaloy-2 and Zircaloy-4 materials, with medium to high levels of hydrogen equivalent concentration are provided in Appendix A of this report.

The fracture toughness of irradiated Zircaloy-2 and Zircaloy-4 materials are compared in Section 4.3 of this report with fracture toughness from small specimens from hydrided irradiated rising pressure burst test specimens from Zr-2.5Nb pressure tubes.

4.1 Effect of Geometry of Curved Compact Tension Specimens on Measured Fracture Toughness Relative to Fracture Toughness Measured from Rising Pressure Burst Tests

Due to the effect of specimen geometry, the value of fracture toughness measured from a small test specimen, such as the Curved Compact Tension Specimen (CCTS), is typically lower than the fracture toughness measured from a rising pressure burst test under otherwise the same conditions. Sets of fracture toughness from a CCTS removed from a hydrided irradiated rising pressure burst test specimen, and the fracture toughness from the same burst test specimen, at the same temperature are compared in Figure 4-1. The values of fracture toughness were taken from Reference [10]. The fracture toughness values in this figure are from burst tests that exhibited transition temperature regime fracture behaviour. The fracture toughness values from the CCTS are lower than the fracture toughness from the corresponding burst test at the same temperature. Use of fracture toughness from small specimens to represent the fracture toughness from rising pressure burst test specimens is considered to be conservative.

4.2 Review of Fracture Toughness of Irradiated Zr-2.5Nb Pressure Tube Material, Zircaloy-2 and Zircaloy-4 Materials, with Medium to High Levels of Hydrogen Equivalent Concentration

Fracture toughness from all of the irradiated Zr-2.5Nb pressure tube material, as well as all of the Zircaloy-2 and Zircaloy-4 materials, with medium to high levels of H_{eq}, which are described in this report are shown in Figure 4-2. In all figures in this report, the fracture toughness from the

RISK-INFORMED DETERMINISTIC EVALUATION OF FRACTURE PROTECTION FOR THE REGION OF INTEREST IN OUTLET ROLLED JOINTS IN BRUCE UNIT 3

Kinectrics Report No.
B2038/RP/0009 R00

irradiated Zr-2.5Nb pressure tube material with high levels of H_{eq} are shown in the figures with the Zircaloy-2 and Zircaloy-4 materials for reference.

4.2.1 Fracture Toughness of Irradiated Zr-2.5Nb Pressure Tube Material with High Levels of Hydrogen Equivalent Concentration

Results from fracture toughness tests that were performed on hydrided, cold-worked Zr-2.5Nb pressure tube material that was irradiated in the NRU test reactor at Canadian Nuclear Laboratories are given by Davies *et al* in the report COG-95-176 [11]. The irradiation temperature was 255°C and the fluence levels were either 2.3×10^{24} or 5.2×10^{24} n/m^2. The fracture toughness tests were performed using CCTS with a wall thickness of 4.0 mm. The test specimens were in the C-L orientation that corresponded to an axial through-wall crack in the pressure tube under an applied hoop stress. The chlorine concentration of the material was 4 ppm. Fracture toughness from test specimens with levels of H_{eq} of 173 through 230 ppm were selected from Reference [11] to be included in the current report. A measurement of the bulk hydride orientation is the Hydride Continuity Coefficient (*HCC*) [12], where an *HCC* that is close to zero corresponds to circumferential bulk hydrides and an *HCC* close to 1.0 corresponds to radial bulk hydrides. Values of *HCC* were measured for a limited number of test specimens. For the selected test specimens used in this report, the *HCC* varied between 0.06 and 0.31. The test temperatures of the selected test specimens ranged between 30 and 240°C. The values of fracture toughness corresponded to the maximum load in the test.

4.2.2 Fracture Toughness of Irradiated Zircaloy-2 Materials with Medium and High Levels of Hydrogen Equivalent Concentration

Results from fracture toughness tests that were performed on rolled and annealed Zircaloy-2 plate material that was irradiated in a test reactor are given by Hoagland and Rowe [13]. The irradiation temperature was 280°C and the fluence level was 2.5×10^{24} n/m^2. The fracture toughness tests were performed using Double Cantilever Beam test specimens with a wall thickness of 6.35 mm. The test specimens were in the RD orientation where the applied load is in the plate width direction perpendicular to the plate rolling direction and crack growth is in the plate rolling direction. Fracture toughness from test specimens with an H_{eq} of 100 ppm were selected from Reference [13] to be included in the current report. The bulk hydride morphology was mixed with a range of bulk hydride orientation angles. The test temperatures of the selected test specimens ranged between 19 and 140°C. Tabular values for fracture toughness data were not provided in Reference [13], and the fracture toughness data were digitized from a plot. The associated uncertainty from using digitized test data is not significant in the context of the results of the risk-informed deterministic evaluation of fracture protection. The values of fracture toughness corresponded to the onset of fracture initiation in the test.

Results from fracture toughness tests that were performed on cold-worked Zircaloy-2 pressure tube material that was removed from fuel channel G16 in Pickering Unit 2 are given by Chow and Simpson [14]. The irradiation temperature was 280°C. The fracture toughness tests were performed using CCTS with a wall thickness of 5.0 mm. The test specimens were in the C-L orientation that corresponded to an axial through-wall crack in the pressure tube under an applied

RISK-INFORMED DETERMINISTIC EVALUATION OF FRACTURE PROTECTION FOR THE REGION OF INTEREST IN OUTLET ROLLED JOINTS IN BRUCE UNIT 3

Kinectrics Report No.
B2038/RP/0009 R00

hoop stress. Fracture toughness from test specimens with levels of H_{eq} of 58 through 146 ppm were selected from Reference [14] to be included in the current report. The bulk hydride morphology was described as containing a large fraction of radial bulk hydrides. The test temperatures of the selected test specimens were 230 or 280°C. The values of fracture toughness corresponded to the onset of fracture initiation in the test.

Results from fracture toughness tests that were performed on cold-worked Zircaloy-2 pressure tube material that was removed from fuel channel F08 in the NPD demonstration reactor are given by Coleman *et al* [15]. The irradiation temperature was in the range of 260 through 270°C. One fracture toughness test was performed at nominally 30°C using a rising pressure burst test specimen, and the remaining fracture toughness tests were performed using CCTS test specimens. The wall thickness of both types of test specimens was 4.2 mm. The CCTS test specimens were in the C-L orientation that corresponded to an axial through-wall crack in the pressure tube under an applied hoop stress. The level of H_{eq} or deuterium concentration for an individual test specimen were not provided in Reference [15]. From Reference [15], the deuterium concentrations in the test specimens ranged between 160 and 235 ppm in terms of hydrogen equivalent concentration. The initial hydrogen concentrations were not provided in Reference [15]. For the analysis in this report, a lower estimate of the initial hydrogen concentration is more conservative. An initial hydrogen concentration of 10 ppm is considered to be a representative lower estimate and was assumed. The levels of H_{eq} were therefore taken to range between 170 and 245 ppm and were used in the analysis in the current report. The bulk hydride morphology was mixed with a range of bulk hydride orientation angles. The test temperatures of the selected test specimens were 30 through 300°C. Tabular values for fracture toughness data were not provided in Reference [15], and the fracture toughness data were digitized from a plot. The associated uncertainty from using digitized test data is not significant in the context of the results of the risk-informed deterministic evaluation of fracture protection. The values of fracture toughness corresponded to the maximum load in the test.

Results from fracture toughness tests that were performed on cold-worked Zircaloy-2 pressure tubes that were removed from the Hanford Site N reactor are given by Huang [16]. The irradiation temperatures ranged between 210 and 280°C, and the fluence levels ranged between 45×10^{24} and 61×10^{24} n/m². The fracture toughness tests were performed using Compact Tension Specimens with a wall thickness of 5.0 mm. The test specimens were in the C-L orientation that corresponded to an axial through-wall crack in the pressure tube under an applied hoop stress. Fracture toughness from test specimens with levels of H_{eq} of 52 through 220 ppm were selected from Reference [16] to be included in the current report. The bulk hydride morphology was described as mainly circumferential. The test temperatures of the selected test specimens ranged between 32 and 260°C. The values of fracture toughness corresponded to the onset of fracture initiation in the test.

Results from fracture toughness tests that were performed on cold-worked Zircaloy-2 pressure tubes that were removed from the Hanford Site N reactor are given by Huang and Mills [17]. The irradiation temperatures are not reported in Reference [17]. The fluence levels were either 46×10^{24} or 50×10^{24} n/m². The fracture toughness tests were performed using Compact Tension Specimens with a wall thickness of 5.0 mm. The test specimens were in the C-L orientation that

RISK-INFORMED DETERMINISTIC EVALUATION OF
FRACTURE PROTECTION FOR THE REGION OF
INTEREST IN OUTLET ROLLED JOINTS IN BRUCE UNIT 3

Kinectrics Report No.
B2038/RP/0009 R00

corresponded to an axial through-wall crack in the pressure tube under an applied hoop stress. Fracture toughness from test specimens with levels of H_{eq} of 52 through 259 ppm were selected from Reference [17] to be included in the current report. The bulk hydride morphology was described as mainly circumferential. The test temperatures of the selected test specimens ranged between 32 and 260°C. The values of fracture toughness corresponded to the onset of fracture initiation in the test.

4.2.3 Fracture Toughness of Irradiated Zircaloy-4 Materials with High Levels of Hydrogen Equivalent Concentration

Results from fracture toughness tests that were performed on rolled and alpha-annealed Zircaloy-4 plate material that was irradiated in a test reactor are given by Walker and Kass [18]. The irradiation temperature is not reported in Reference [18]. The fluence levels ranged between 5.1×10^{24} and 20.8×10^{24} n/m². The fracture toughness tests were performed using Compact Tension Specimens with a wall thickness of 10.2 mm. Values of fracture toughness for two test specimen orientations were included in the current report. The first was the T-W orientation where the applied load is in the plate thickness direction and crack growth is in the plate width direction perpendicular to the rolling direction. The second is the W-T orientation where the applied load is in the plate width direction perpendicular to the rolling direction and crack growth is in plate thickness direction. Fracture toughness from test specimens with an H_{eq} of 238 ppm were selected from Reference [18] to be included in the current report. The bulk hydride morphology was described as parallel to the plane of the plate. This means that the bulk hydrides in the test specimens with the T-W orientation were in the plane of the crack similar to radial bulk hydrides in a pressure tube. The test temperatures of the selected test specimens ranged between 22 and 316°C. The values of fracture toughness corresponded to the maximum load in the test.

Results from fracture toughness tests that were performed on beta-quenched Zircaloy-4 plate material that was irradiated in a test reactor are also given by Walker and Kass [18]. The irradiation temperature is not reported in Reference [18]. The fluence levels ranged between 10.35×10^{24} and 20.4×10^{24} n/m². The fracture toughness tests were performed using Compact Tension Specimens with a wall thickness of 10.2 mm. The test specimens were in the W-T orientation where the applied load is in the plate width direction perpendicular to the rolling direction and crack growth is in plate thickness direction. Fracture toughness from test specimens with an H_{eq} of 238 ppm were selected from Reference [18] to be included in the current report. The bulk hydride morphology was described as parallel to the plane of the plate. The test temperatures of the selected test specimens ranged between 22 and 260°C. The values of fracture toughness corresponded to the maximum load in the test.

Results from fracture toughness tests that were performed on beta-quenched Zircaloy-4 plate material and Zircaloy-4 weld-metal that were irradiated in a test reactor are given by Kreyns *et al* [19]. The irradiation temperature was 260°C, and the fluence levels ranged between 10.1×10^{24} and 47×10^{24} n/m². The fracture toughness tests were performed using Compact Tension Specimens with a wall thickness of between 2.0 and 10.0 mm. The test specimen orientation was not provided in Reference [19]. Fracture toughness from test specimens with levels of H_{eq}

RISK-INFORMED DETERMINISTIC EVALUATION OF
FRACTURE PROTECTION FOR THE REGION OF
INTEREST IN OUTLET ROLLED JOINTS IN BRUCE UNIT 3

Kinectrics Report No.
B2038/RP/0009 R00

of 240 through 262 ppm were selected from Reference [19] to be included in the current report. The bulk hydride morphology was mixed with a range of bulk hydride orientation angles. The test temperature of the selected test specimens was 24°C. The values of fracture toughness corresponded to the maximum load in the test.

Additional results from fracture toughness tests that were performed on beta-quenched Zircaloy-4 plate material that was irradiated in a test reactor are given by Kreyns *et al* [19]. The irradiation temperature was 260°C, and the fluence levels ranged between 10.3×10^{24} and 53×10^{24} n/m^2. The fracture toughness tests were performed using Compact Tension Specimens with a wall thickness of 10.0 mm. The test specimen orientation was not provided in Reference [19]. Fracture toughness from test specimens with levels of H_{eq} of 240 and 253 ppm were selected from Reference [19] to be included in the current report. The bulk hydride morphology was mixed with a range of bulk hydride orientation angles. The test temperature of the selected test specimens was 149°C. The values of fracture toughness corresponded to the maximum load in the test.

4.3   Comparison of Fracture Toughness of Hydrided Irradiated Zircaloy-2 and Zircaloy-4 Materials with Hydrided Irradiated Zr-2.5Nb Pressure Tube Material

Due to the wide range of material conditions and test conditions, as well as the lack of details on some material conditions and test conditions, it was not possible to perform a detailed statistical analysis or other quantitative analysis of the fracture toughness from the irradiated Zircaloy-2 and Zircaloy-4 materials to compare with the fracture toughness from the hydrided irradiated Zr-2.5Nb pressure tube material. However, significant insights were obtained by comparing the plots of fracture toughness from the different materials.

A conservative value of fracture toughness from the set of fracture toughness values for irradiated Zircaloy-2 and Zircaloy-4 materials was used to develop an adjustment factor that is less than 1.0 and is intended to account for uncertainty in the application of the Revision 2 engineering fracture toughness model to these postulated high levels of H_{eq} in the region of interest. As described in Section 5 of this report, the adjustment factor on the fracture toughness was based on the 97.5% lower prediction bound. For this reason, comparison of the fracture toughness from the CCTS from the hydrided irradiated Zr-2.5Nb rising pressure burst test specimens with the fracture toughness from irradiated Zircaloy-2 and Zircaloy-4 materials was made by comparing the lowest measured values of fracture toughness.

Fracture toughness from irradiated Zr-2.5Nb pressure tube material with high levels of H_{eq}, and from irradiated Zircaloy-2 and Zircaloy-4 materials with medium levels of H_{eq}, are shown in Figure 4-3. Fracture toughness from CCTS removed from hydrided irradiated rising pressure burst test specimens BT-6 through BT-14 with medium levels of H_{eq} are shown in Figure 4-4. Fracture toughness from CCTS removed from hydrided irradiated rising pressure burst test specimens BT-16 through BT-30 with medium levels of H_{eq} are shown in Figure 4-5. Fracture toughness from CCTS removed from hydrided irradiated rising pressure burst test specimens BT-31 through BT-42 with medium levels of H_{eq} are shown in Figure 4-6. The lower values of

RISK-INFORMED DETERMINISTIC EVALUATION OF FRACTURE PROTECTION FOR THE REGION OF INTEREST IN OUTLET ROLLED JOINTS IN BRUCE UNIT 3

Kinectrics Report No. B2038/RP/0009 R00

fracture toughness from the irradiated Zircaloy-2 and Zircaloy-4 materials in Figure 4-3 are lower than the lower values of fracture toughness from the CCTS from the hydrided irradiated rising pressure burst test specimens in Figures 4-4 through 4-6. These results indicate that the use of the fracture toughness from the irradiated Zircaloy-2 and Zircaloy-4 materials as a surrogate for irradiated Zr-2.5Nb pressure tube material with high levels of H_{eq} is representative or conservative.

RISK-INFORMED DETERMINISTIC EVALUATION OF FRACTURE PROTECTION FOR THE REGION OF INTEREST IN OUTLET ROLLED JOINTS IN BRUCE UNIT 3

Kinectrics Report No.
B2038/RP/0009 R00
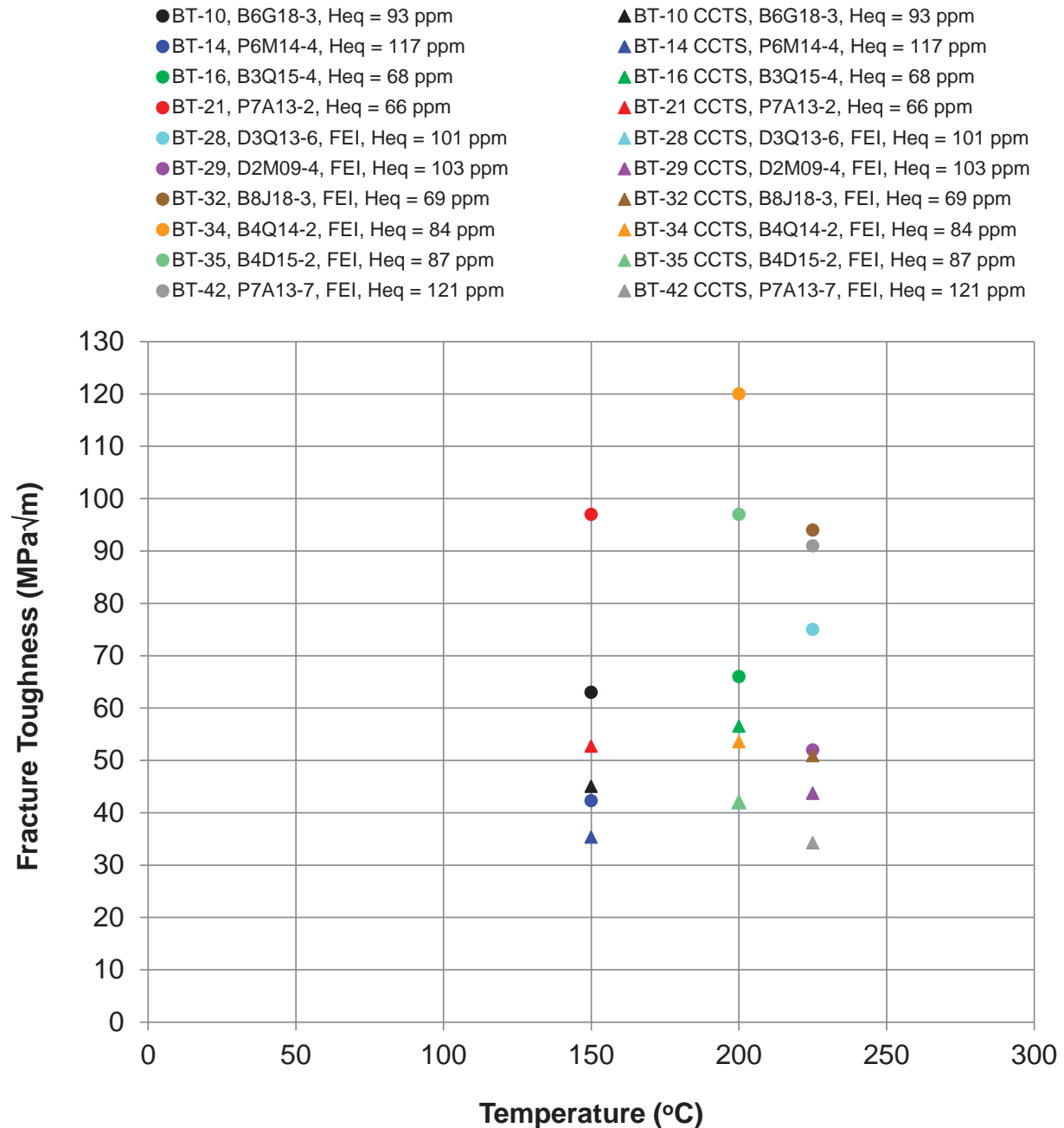
Figure 4-1: Comparison of Sets of Fracture Toughness from a Curved Compact Tension Specimen Removed from a Hydrided Irradiated Rising Pressure Burst Test Specimen with the Burst Test Result at the Same Temperature

RISK-INFORMED DETERMINISTIC EVALUATION OF FRACTURE PROTECTION FOR THE REGION OF INTEREST IN OUTLET ROLLED JOINTS IN BRUCE UNIT 3

Legend:
- COG-95-176, Zr-2.5Nb, C-L, Heq = 173 - 192 ppm
- COG-95-176, Zr-2.5Nb, C-L, Heq = 203 - 230 ppm
- Hoagland and Rowe, Zr-2, RD, Heq = 100 ppm
- Chow and Simpson, Zr-2, C-L, Heq = 58 - 95 ppm
- Chow and Simpson, Zr-2, C-L, Heq = 109 - 146 ppm
- Coleman et al, Zr-2, C-L, Heq = 170 - 245 ppm
- Huang, Zr-2, C-L, Heq = 52 - 89 ppm
- Huang, Zr-2, C-L, Heq = 150, 220 ppm
- Huang and Mills, Zr-2, C-L, Heq = 52 - 138 ppm
- Huang and Mills, Zr-2, C-L, Heq = 205, 259 ppm
- Walker and Kass, alpha-annealed Zr-4, Heq = 238 ppm, T-W
- Walker and Kass, alpha-annealed Zr-4, Heq = 238 ppm, W-T
- Walker and Kass, beta-quenched Zr-4, Heq = 238 ppm, W-T
- Kreyns et al, beta-quench and WM Zr-4, Heq = 240 - 262 ppm
- Kreyns et al, beta-quenched Zr-4, Heq = 240 - 253 ppm

Figure 4-2: Fracture Toughness from Irradiated Zr-2.5Nb Pressure Tube Material, Zircaloy-2 and Zircaloy-4 Materials, with Medium to High Levels of H_{eq}

KINECTRICS INC.

RISK-INFORMED DETERMINISTIC EVALUATION OF FRACTURE PROTECTION FOR THE REGION OF INTEREST IN OUTLET ROLLED JOINTS IN BRUCE UNIT 3

**Kinectrics Report No.
B2038/RP/0009 R00**
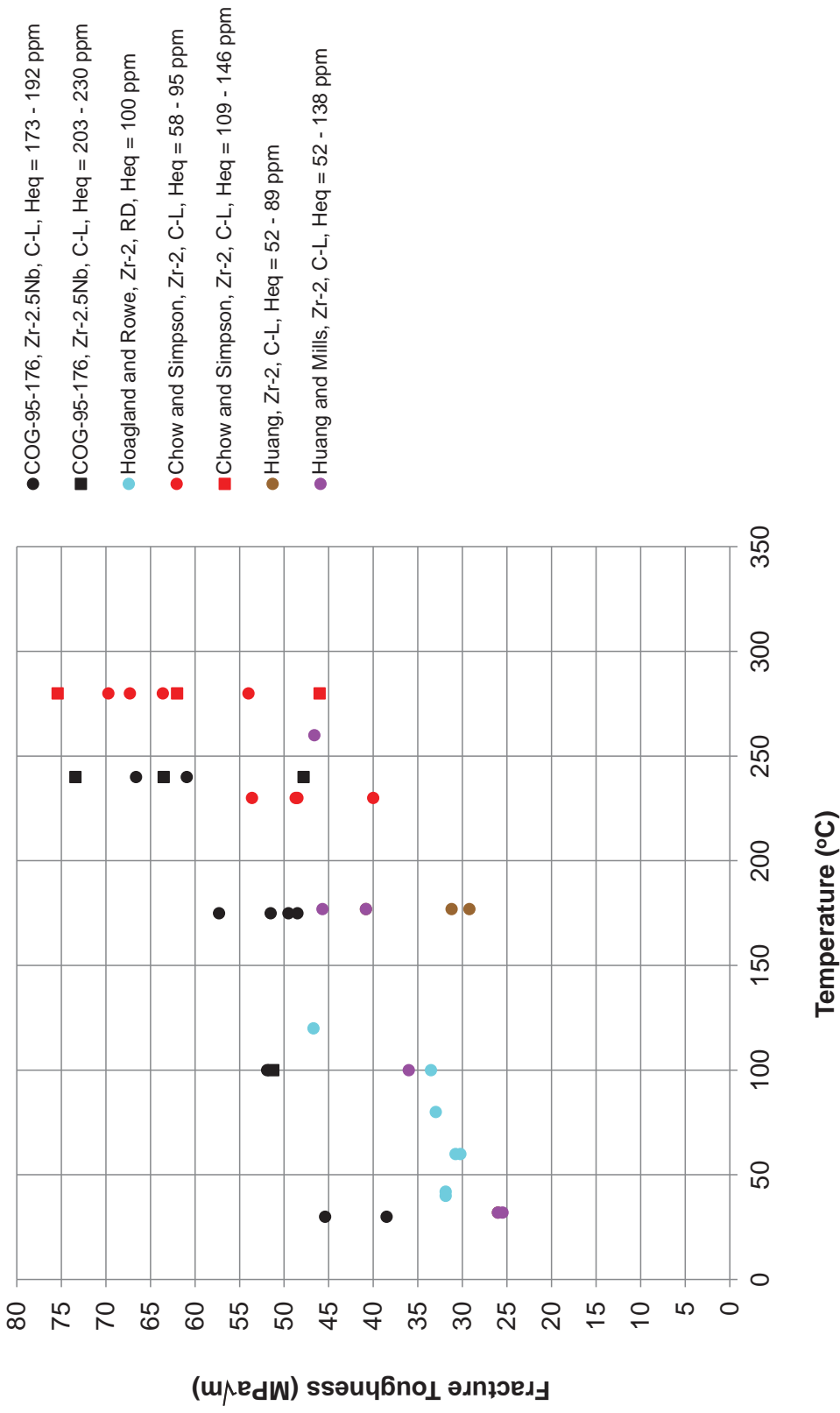
Figure 4-3: Fracture Toughness from Irradiated Zr-2.5Nb Pressure Tube Material with High Levels of H_{eq}, and from Zircaloy-2 and Zircaloy-4 Materials with Medium Levels of H_{eq}

RISK-INFORMED DETERMINISTIC EVALUATION OF FRACTURE PROTECTION FOR THE REGION OF INTEREST IN OUTLET ROLLED JOINTS IN BRUCE UNIT 3

Kinectrics Report No.
B2038/RP/0009 R00

○ BT-6, L1P12-2, Heq = 97 ppm □ BT-7, L1P12-3, Heq = 75 ppm △ BT-8, D2O18-2, Heq = 63 ppm

○ BT-9, B6G18-2, Heq = 87 ppm □ BT-10, B6G18-3, Heq = 93 ppm △ BT-11, P6M14-2, Heq = 109 ppm

○ BT-12, D3Q13-2, Heq = 106 ppm □ BT-14, P6M14-4, Heq = 117 ppm

Figure 4-4: Fracture Toughness from Curved Compact Tension Specimens Removed from Hydrided Irradiated Rising Pressure Burst Test Specimens for BT-6 Through BT-14 from Ex-Service Zr-2.5Nb Pressure Tubes

RISK-INFORMED DETERMINISTIC EVALUATION OF FRACTURE PROTECTION FOR THE REGION OF INTEREST IN OUTLET ROLLED JOINTS IN BRUCE UNIT 3

Kinectrics Report No.
B2038/RP/0009 R00

△ BT-16, B3Q15-4, Heq = 68 ppm   ○ BT-17, D3Q13-3, Heq = 63 ppm   □ BT-21, P7A13-2, Heq = 66 ppm

△ BT-26, D2M09-2, Heq = 95 ppm   ○ BT-27, D2M09-3, Heq = 144 ppm   □ BT-28, D3Q13-6, FEI, Heq = 101 ppm

△ BT-29, D2M09-4, FEI, Heq = 103 ppm   ○ BT-30, B8J18-2, Heq = 204 ppm
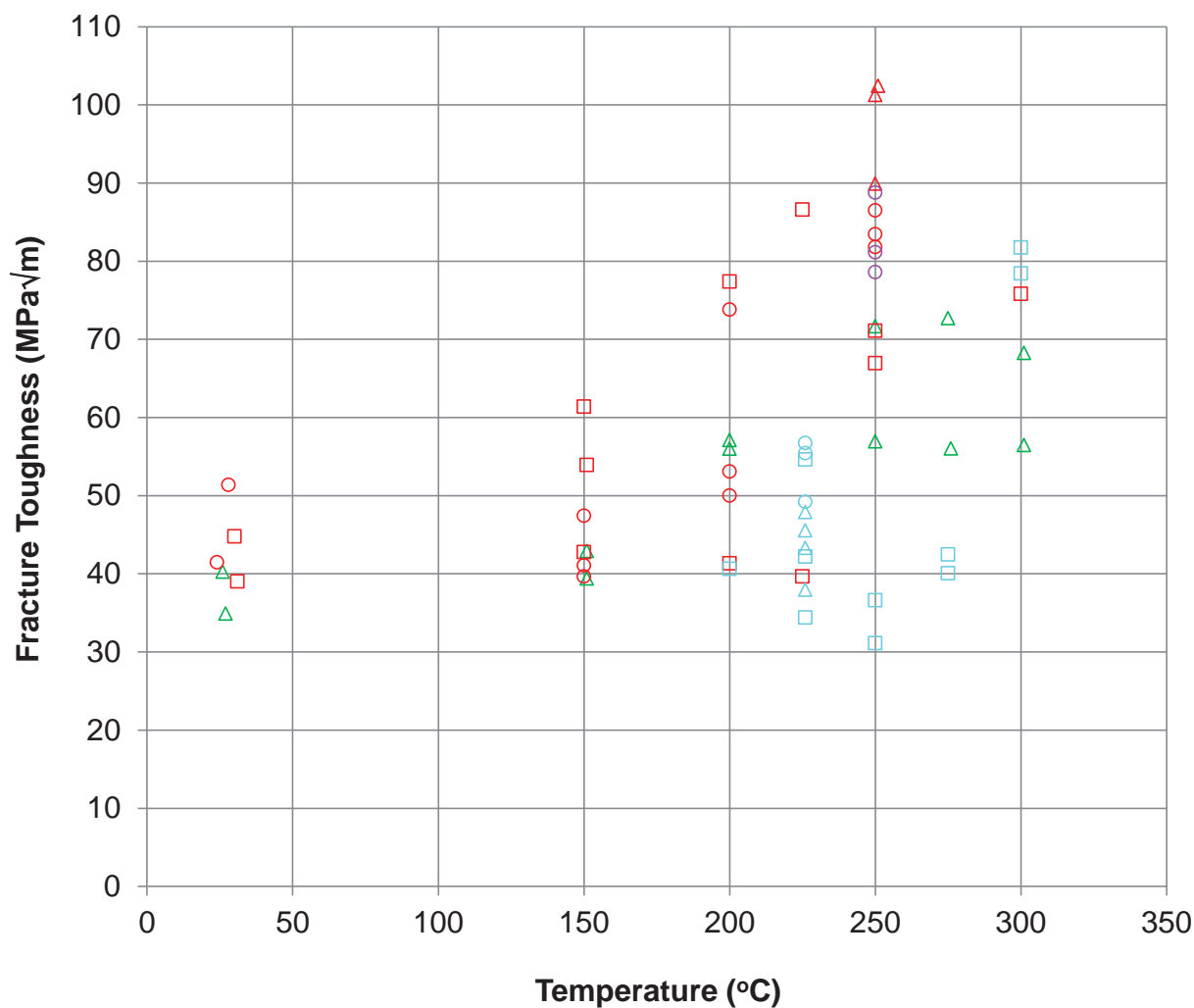
Figure 4-5: Fracture Toughness from Curved Compact Tension Specimens Removed from Hydrided Irradiated Rising Pressure Burst Test Specimens for BT-16 Through BT-30 from Ex-Service Zr-2.5Nb Pressure Tubes

RISK-INFORMED DETERMINISTIC EVALUATION OF FRACTURE PROTECTION FOR THE REGION OF INTEREST IN OUTLET ROLLED JOINTS IN BRUCE UNIT 3

Kinectrics Report No. B2038/RP/0009 R00

□ BT-31, P7O07-2, FEI, Heq = 70 ppm   △ BT-32, B8J18-3, FEI, Heq = 69 ppm   ○ BT-33, D1U09-2, FEI, Heq = 86 ppm

□ BT-34, B4Q14-2, FEI, Heq = 84 ppm   △ BT-35, B4D15-2, FEI, Heq = 87 ppm   ○ BT-37, B3K20-2, FEO, Heq = 115 ppm

□ BT-42, P7A13-7, FEI, Heq = 121 ppm

Figure 4-6: Fracture Toughness from Curved Compact Tension Specimens Removed from Hydrided Irradiated Rising Pressure Burst Test Specimens for B-31 Through BT-42 from Ex-Service Zr-2.5Nb Pressure Tubes

RISK-INFORMED DETERMINISTIC EVALUATION OF FRACTURE PROTECTION FOR THE REGION OF INTEREST IN OUTLET ROLLED JOINTS IN BRUCE UNIT 3

Kinectrics Report No. B2038/RP/0009 R00

5. ADJUSTMENT FACTOR ON FRACTURE TOUGHNESS FROM REVISION 2 ENGINEERING MODEL FOR HIGH LEVELS OF HYDROGEN EQUIVALENT CONCENTRATION

5.1 Method of Adjustment of Fracture Toughness from Revision 2 Engineering Model for High Levels of Hydrogen Equivalent Concentration

As stated in Section 3 of this report, the Revision 2 engineering fracture toughness model predicts fracture toughness as a function of the distance from the front end of the pressure tube, H_{eq}, chlorine concentration, temperature under evaluation, and irradiation temperature. From Section 9 of Reference [2], the fracture toughness from the Revision 2 engineering fracture toughness model is also dependent on the single-tailed statistical confidence level, ζ.

$$K_c = K_c\left(\zeta, D_{fr}, H_{eq}, Cl, T, T_{irr}\right) \qquad (5\text{-}1)$$

where

D_{fr}	=	distance from the front end of the pressure tube, m
Cl	=	chlorine concentration, ppm
H_{eq}	=	hydrogen equivalent concentration, ppm
T	=	temperature under evaluation, °C
T_{irr}	=	irradiation temperature, °C
ζ	=	single-tailed statistical confidence level (such as 0.975), dimensionless

A conservative value of fracture toughness from the set of fracture toughness values for irradiated Zircaloy-2 and Zircaloy-4 materials described in Section 4 and provided in Appendix A of this report was used to develop an adjustment factor that is intended to account for uncertainty in the application of the Revision 2 engineering fracture toughness model to postulated high levels of H_{eq} of up to 250 ppm in the region of interest. The adjustment factor was developed based on the 97.5% lower prediction bound on fracture toughness from the Revision 2 engineering fracture toughness model. The adjustment factor was developed by equating a reference value of measured fracture toughness from the set of test data to an adjusted 97.5% lower prediction bound on fracture toughness from the Revision 2 engineering fracture toughness model. In addition, in accordance with Clause D.13.2.1 of the CSA Standard N285.8 [20], the calculated values of fracture toughness that are used in an evaluation are divided by a correction factor to account for the potential effect of reinforcement of the sealing patch on the results from rising pressure burst tests. The resultant equation is given by

$$K_{\exp} = \beta_H \frac{K_{c,ref}\left(0.975, D_{fr}, H_{eq}, Cl, T, T_{irr}\right)}{F_{sp}} \qquad (5\text{-}2)$$

where

RISK-INFORMED DETERMINISTIC EVALUATION OF FRACTURE PROTECTION FOR THE REGION OF INTEREST IN OUTLET ROLLED JOINTS IN BRUCE UNIT 3

Kinectrics Report No.
B2038/RP/0009 R00

F_{sp} =   correction factor to account for the potential effect of reinforcement of the sealing patch on the results from rising pressure burst tests, = 1.04

$K_{c,ref}$ =   fracture toughness from the Revision 2 engineering fracture toughness model at a reference set of conditions, MPa$\sqrt{m}$

K_{exp} =   reference value of measured fracture toughness, MPa$\sqrt{m}$

β_H =   adjustment factor on fracture toughness to account for uncertainty in the application of the Revision 2 engineering fracture toughness model to high levels of H_{eq} of up to 250 ppm, dimensionless

From Eq. (5-2),

$$\beta_H = \frac{F_{sp}K_{exp}}{K_{c,ref}\left(0.975, D_{fr}, H_{eq}, Cl, T, T_{irr}\right)} \tag{5-3}$$

The adjusted fracture toughness that was used in the risk-informed deterministic evaluation of fracture protection, without the correction factor for the potential effect of reinforcement of the sealing patch (that is applied later in the evaluation) is then given by

$$K_{c,adj} = \beta_H K_c\left(\zeta, D_{fr}, H_{eq}, Cl, T, T_{irr}\right) \tag{5-4}$$

where

$K_{c,adj}$ =   adjusted fracture toughness to account for uncertainty in the application of the Revision 2 engineering fracture toughness model to high levels of H_{eq} of up to 250 ppm, MPa$\sqrt{m}$

5.2 Determination of Adjustment Factor on Fracture Toughness from Revision 2 Engineering Model for High Levels of Hydrogen Equivalent Concentration

The temperature range of interest for development of the adjustment factor on fracture toughness is less than 200°C. From Figure 4-2, at temperatures less than 200°C the most conservative values of fracture toughness are from the fracture toughness tests that were performed on cold-worked Zircaloy-2 pressure tube material that was removed from fuel channel F08 in the NPD demonstration reactor as given by Coleman *et al* [15]. The irradiation temperature was in the range of 260 through 270°C. The levels of H_{eq} were taken to range between 170 and 245 ppm. The bulk hydride morphology was mixed with a range of bulk hydride orientation angles. From Section 9 of this report, the most limiting temperature for demonstrating fracture protection based on the revised ROH pressure-temperature operating limits for reactor Heatup is 130°C, and for reactor Cooldown is 175°C. From Appendix A of this report, the value of fracture toughness of 27.7 MPa$\sqrt{m}$ at a test temperature of 150°C was used as the reference value, K_{exp}, to determine the adjustment factor.

RISK-INFORMED DETERMINISTIC EVALUATION OF FRACTURE PROTECTION FOR THE REGION OF INTEREST IN OUTLET ROLLED JOINTS IN BRUCE UNIT 3

Kinectrics Report No.
B2038/RP/0009 R00

The reference set of conditions that were used to calculate the 97.5% lower prediction bound on fracture toughness from the Revision 2 engineering fracture toughness model were determined as given below.

(1) The location of the individual test specimens was not provided in Reference [15]. The reference distance from the front end of the pressure tube, D_{fr} was the value of 0.069 m that is used in the fracture protection evaluations of the front-end outlet rolled joints in Bruce Unit 3.

(2) The chlorine concentration of the test specimens was not provided in Reference [15]. The reference value of chlorine concentration, Cl, of 5.5 ppm that is provided in Reference [21], and is used in deterministic fracture protection evaluations of Bruce Unit 3, was used.

(3) A reference level of H_{eq} of 210 ppm was used. This reference level of H_{eq} is the nominal average of the range of 170 through 245 ppm for the fracture toughness tests in Reference [15].

(4) A reference temperature, T, that is equal to the test temperature of 150°C was used.

(5) The irradiation temperatures, T_{irr}, of the test specimens in Reference [15] were in the range of 260 through 270°C. A reference irradiation temperature of 290°C at the outlet rolled joints in Bruce Unit 3 [8] was used. In general, use of a reference irradiation temperature that is higher than the irradiation temperature of the test specimens is conservative. However, at the reference temperature of 150°C the irradiation temperature has essentially no effect on the predicted fracture toughness.

A comparison of the unadjusted 97.5% lower prediction bound on fracture toughness from the Revision 2 engineering fracture toughness model for levels of H_{eq} of 200 through 250 ppm with fracture toughness from Zircaloy-2 and Zircaloy-4 materials with high levels of H_{eq} is shown in Figure 5-1. The fracture toughness was calculated using the above conditions except the H_{eq} was varied between 200 and 250 ppm. The same comparison is shown in Figure 5-2 using an expanded scale for fracture toughness. The 97.5% lower prediction bounds on fracture toughness for H_{eq} between 200 and 250 ppm are greater than a number of measured values of fracture toughness. The Revision 2 engineering fracture toughness model predicts fracture toughness for an axial through-wall flaw in a pressure tube and was calibrated to the results from rising pressure burst tests that were performed on hydrided irradiated specimens. The transition temperature to the upper-shelf fracture regime from the rising pressure burst tests has been found to be not greater than 250°C, and this is reflected in the temperature dependence of the curves of the unadjusted 97.5% lower prediction bound on fracture toughness from the Revision 2 engineering fracture toughness model. It is not unusual for small test specimens to exhibit a transition temperature to the upper-shelf fracture regime that is greater than 250°C, and this is reflected by the values of measured fracture toughness from the small specimens at temperatures greater than 250°C in Figures 5-1 and 5-2.

The reference 97.5% lower prediction bound on fracture toughness from the Revision 2 engineering fracture toughness model, $K_{c,ref}$, for the above reference conditions is 31.68 MPa√m.

RISK-INFORMED DETERMINISTIC EVALUATION OF FRACTURE PROTECTION FOR THE REGION OF INTEREST IN OUTLET ROLLED JOINTS IN BRUCE UNIT 3

Kinectrics Report No.
B2038/RP/0009 R00

Substitution of K_{exp} equal to 27.7 MPa√m, $K_{c,ref}$ equal to 31.68 MPa√m, and F_{sp} equal to 1.04, into Eq. (5-3) gives β_H equal to 0.909.

A comparison of the unadjusted and adjusted 97.5% lower prediction bounds on fracture toughness from the Revision 2 engineering fracture toughness model for an H_{eq} of 210 ppm with fracture toughness from Zircaloy-2 and Zircaloy-4 materials with high levels of H_{eq} is shown in Figure 5-3. The same comparison is shown in Figure 5-4 using an expanded scale for fracture toughness. The adjusted 97.5% lower prediction bound on fracture toughness at an H_{eq} of 210 ppm is a conservative representation of the test results.

A comparison of the adjusted 97.5% lower prediction bounds on fracture toughness from the Revision 2 engineering fracture toughness model for levels of H_{eq} of 200 through 250 ppm with fracture toughness from Zircaloy-2 and Zircaloy-4 materials with high levels of H_{eq} is shown in Figure 5-5. The same comparison is shown in Figure 5-6 using an expanded scale for fracture toughness. The adjusted 97.5% lower prediction bound on fracture toughness at the higher levels of H_{eq} is a more conservative representation of the test results.

RISK-INFORMED DETERMINISTIC EVALUATION OF FRACTURE PROTECTION FOR THE REGION OF INTEREST IN OUTLET ROLLED JOINTS IN BRUCE UNIT 3

Kinectrics Report No.
B2038/RP/0009 R00
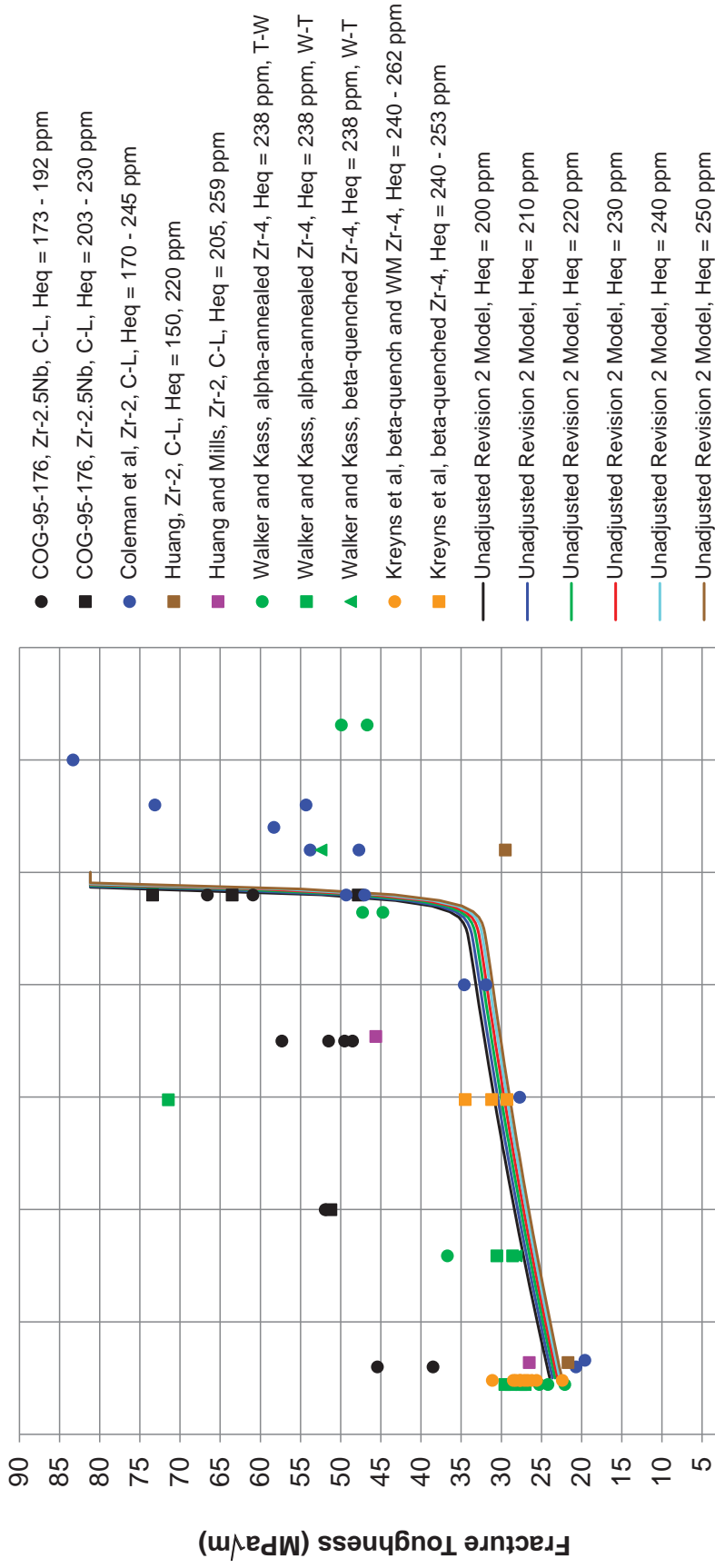
Figure 5-1: Comparison of the Unadjusted 97.5% Lower Prediction Bound on Fracture Toughness from the Revision 2 Engineering Fracture Toughness Model with Fracture Toughness from Zircaloy-2 and Zircaloy-4 Materials with High Levels of H_{eq}

RISK-INFORMED DETERMINISTIC EVALUATION OF FRACTURE PROTECTION FOR THE REGION OF INTEREST IN OUTLET ROLLED JOINTS IN BRUCE UNIT 3

Kinectrics Report No.
B2038/RP/0009 R00

- COG-95-176, Zr-2.5Nb, C-L, Heq = 173 - 192 ppm
- COG-95-176, Zr-2.5Nb, C-L, Heq = 203 - 230 ppm
- Coleman et al, Zr-2, C-L, Heq = 170 - 245 ppm
- Huang, Zr-2, C-L, Heq = 150, 220 ppm
- Huang and Mills, Zr-2, C-L, Heq = 205, 259 ppm
- Walker and Kass, alpha-annealed Zr-4, Heq = 238 ppm, T-W
- Walker and Kass, alpha-annealed Zr-4, Heq = 238 ppm, W-T
- Walker and Kass, beta-quenched Zr-4, Heq = 238 ppm, W-T
- Kreyns et al, beta-quench and WM Zr-4, Heq = 240 - 262 ppm
- Kreyns et al, beta-quenched Zr-4, Heq = 240 - 253 ppm
- Unadjusted Revision 2 Model, Heq = 200 ppm
- Unadjusted Revision 2 Model, Heq = 210 ppm
- Unadjusted Revision 2 Model, Heq = 220 ppm
- Unadjusted Revision 2 Model, Heq = 230 ppm
- Unadjusted Revision 2 Model, Heq = 240 ppm
- Unadjusted Revision 2 Model, Heq = 250 ppm

Figure 5-2: Comparison of the Unadjusted 97.5% Lower Prediction Bound on Fracture Toughness from the Revision 2 Engineering Fracture Toughness Model with Fracture Toughness from Zircaloy-2 and Zircaloy-4 Materials with High Levels of H_{eq} (expanded scale for fracture toughness)

RISK-INFORMED DETERMINISTIC EVALUATION OF FRACTURE PROTECTION FOR THE REGION OF INTEREST IN OUTLET ROLLED JOINTS IN BRUCE UNIT 3

Legend:
- ● COG-95-176, Zr-2.5Nb, C-L, Heq = 173 - 192 ppm
- ■ COG-95-176, Zr-2.5Nb, C-L, Heq = 203 - 230 ppm
- ● Coleman et al, Zr-2, C-L, Heq = 170 - 245 ppm
- ■ Huang, Zr-2, C-L, Heq = 150, 220 ppm
- ■ Huang and Mills, Zr-2, C-L, Heq = 205, 259 ppm
- ● Walker and Kass, alpha-annealed Zr-4, Heq = 238 ppm, T-W
- ■ Walker and Kass, alpha-annealed Zr-4, Heq = 238 ppm, W-T
- ▲ Walker and Kass, beta-quenched Zr-4, Heq = 238 ppm, W-T
- ● Kreyns et al, beta-quench and WM Zr-4, Heq = 240 - 262 ppm
- ■ Kreyns et al, beta-quenched Zr-4, Heq = 240 - 253 ppm
- — Unadjusted Revision 2 Model, Heq = 210 ppm
- — Adjusted Revision 2 Model, Heq = 210 ppm

Figure 5-3: Comparison of the Unadjusted and Adjusted 97.5% Lower Prediction Bound on Fracture Toughness from the Revision 2 Engineering Fracture Toughness Model for an H_{eq} of 210 ppm with Fracture Toughness from Zircaloy-2 and Zircaloy-4 Materials with High Levels of H_{eq}

KINECTRICS INC.

RISK-INFORMED DETERMINISTIC EVALUATION OF
FRACTURE PROTECTION FOR THE REGION OF
INTEREST IN OUTLET ROLLED JOINTS IN BRUCE UNIT 3

Kinectrics Report No.
B2038/RP/0009 R00
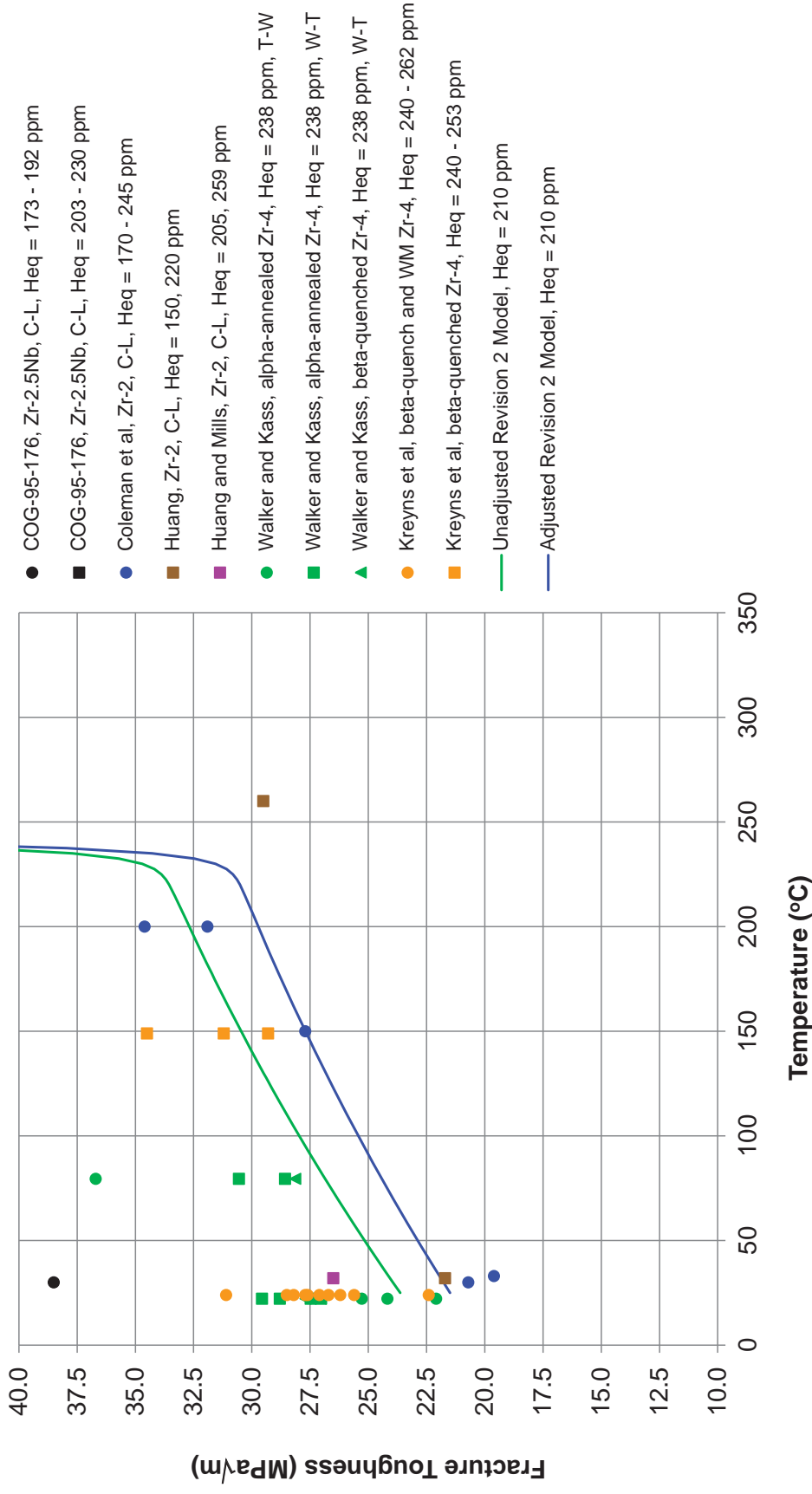
Figure 5-4: Comparison of the Unadjusted and Adjusted 97.5% Lower Prediction Bound on Fracture Toughness from the Revision 2 Engineering Fracture Toughness Model for an H_{eq} of 210 ppm with Fracture Toughness from Zircaloy-2 and Zircaloy-4 Materials with High Levels of H_{eq} (expanded scale for fracture toughness)

RISK-INFORMED DETERMINISTIC EVALUATION OF FRACTURE PROTECTION FOR THE REGION OF INTEREST IN OUTLET ROLLED JOINTS IN BRUCE UNIT 3

**Kinectrics Report No.
B2038/RP/0009 R00**
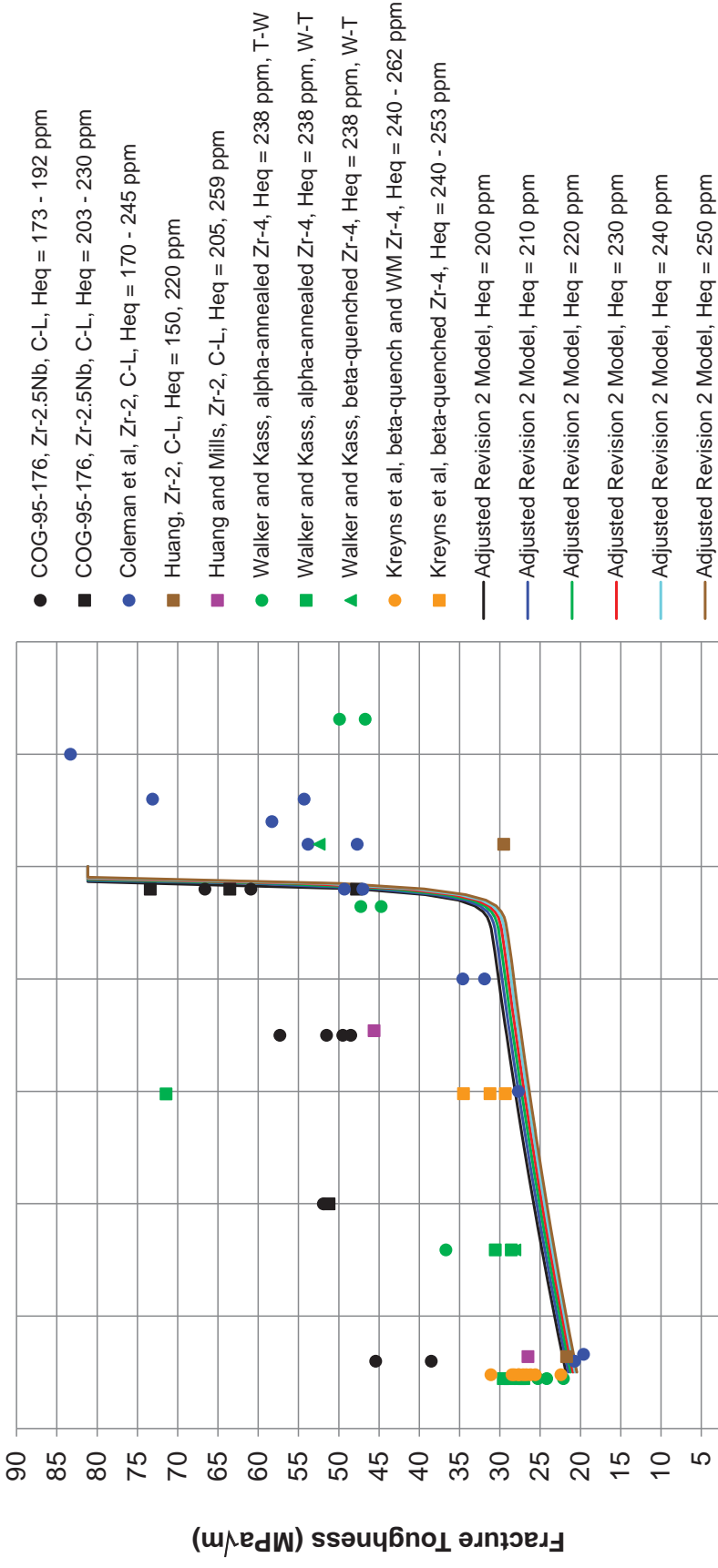
Figure 5-5: Comparison of the Adjusted 97.5% Lower Prediction Bound on Fracture Toughness from the Revision 2 Engineering Fracture Toughness Model with Fracture Toughness from Zircaloy-2 and Zircaloy-4 Materials with High Levels of H_{eq}

RISK-INFORMED DETERMINISTIC EVALUATION OF FRACTURE PROTECTION FOR THE REGION OF INTEREST IN OUTLET ROLLED JOINTS IN BRUCE UNIT 3

Kinectrics Report No.
B2038/RP/0009 R00
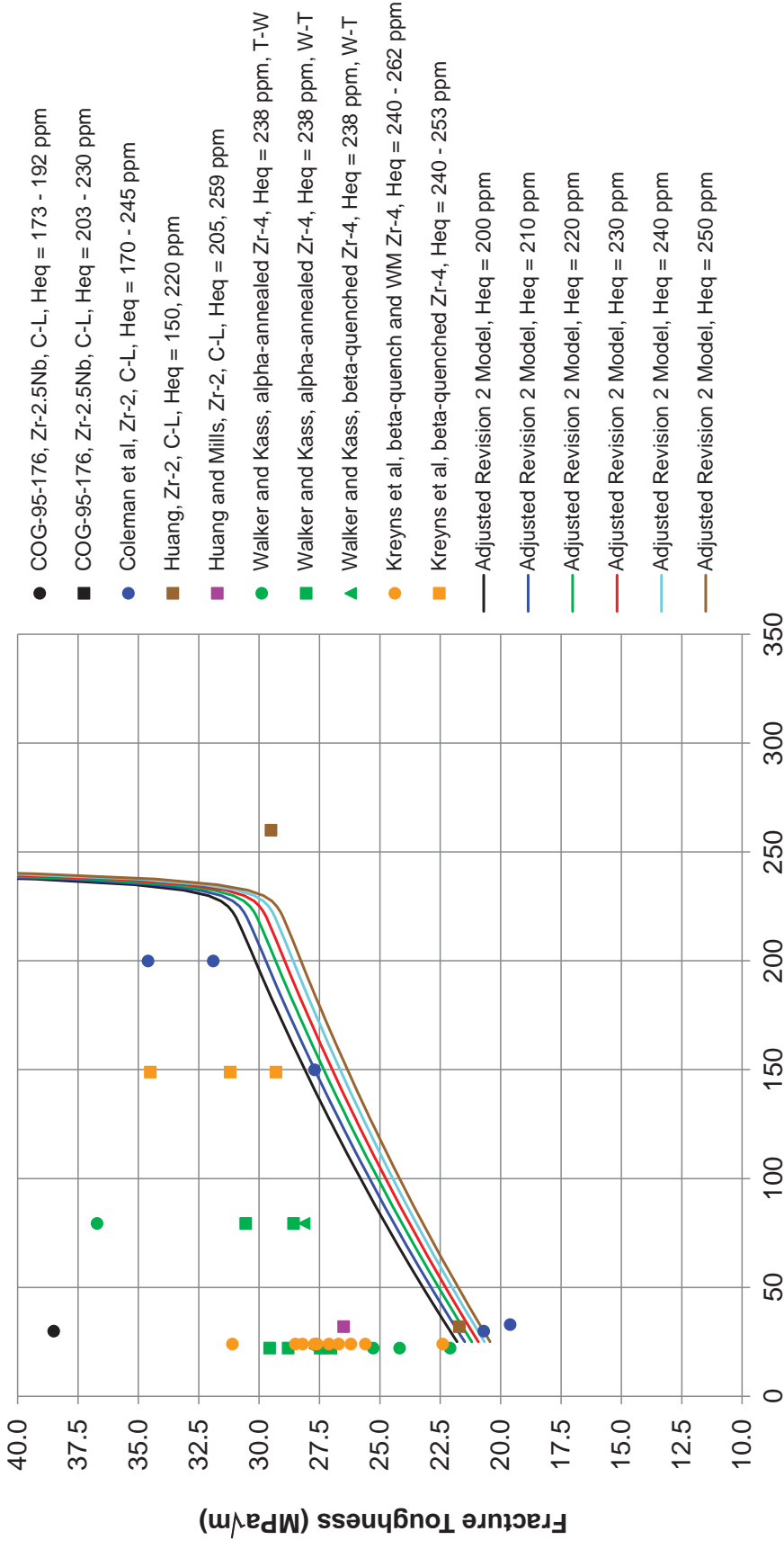
Figure 5-6: Comparison of the Adjusted 97.5% Lower Prediction Bound on Fracture Toughness from the Revision 2 Engineering Fracture Toughness Model with Fracture Toughness from Zircaloy-2 and Zircaloy-4 Materials with High Levels of H_{eq} (expanded scale for fracture toughness)

RISK-INFORMED DETERMINISTIC EVALUATION OF FRACTURE PROTECTION FOR THE REGION OF INTEREST IN OUTLET ROLLED JOINTS IN BRUCE UNIT 3

Kinectrics Report No.
B2038/RP/0009 R00

6. DETERMINISTIC FRACTURE PROTECTION EVALUATION PROCEDURE FOR REACTOR HEATUP AND COOLDOWN

The deterministic fracture protection evaluation procedure based on an axial through-wall flaw postulated in the region of interest in the front-end outlet rolled joints in Bruce Unit 3 for the Service Level A reactor Heatup and Cooldown transients is described in this Section. The calculation procedure is in accordance with the CSA Standard N285.8, except that the Revision 2 engineering fracture toughness model in Reference [2] was used instead of the Revision 1 engineering fracture toughness model that is provided in Clause D.13.2.2 in the CSA Standard N285.8. The steps involved in the calculation are given below.

(a) The lower-bound fracture toughness was calculated as described in Section 6.1.

(b) The critical internal pressure at the location of the postulated axial through-wall flaw was calculated as a function of temperature as described in Section 6.2.

(c) The safety factor on internal pressure at the location of the postulated axial through-wall flaw was calculated as described in Section 6.3. The critical Reactor Outlet Header (ROH) internal pressure was calculated as described in Section 6.3.

6.1 Method of Calculation of Lower-Bound Fracture Toughness

The lower-bound fracture toughness for levels of H_{eq} less than or equal to 30 ppm was calculated using Clause D.13.2.2.1 of the CSA Standard N285.8 [20] and as given in Section 6.1.1 of this report. The 97.5% lower prediction bound on fracture toughness using the Revision 2 engineering fracture toughness model that is provided in Reference [2] was calculated as described in Section 6.1.2. In accordance with Clause D.13.2.1 of the CSA Standard N285.8, the lower of the values of fracture toughness from Clause D.13.2.2.1 and the Revision 2 engineering fracture toughness model was used.

6.1.1 Lower-Bound Fracture Toughness for Levels of H_{eq} of 30 ppm or Less from Clause D.13.2.2.1 of CSA Standard N285.8

For H_{eq} less than 30 ppm, and temperatures less than or equal to 150°C, the lower-bound fracture toughness, K_c, from Clause D.13.2.2.1 of the CSA Standard N285.8 is given by [20]

$$K_c = 27 + 0.30T \qquad (6\text{-}1)$$

where

K_c = fracture toughness at through-wall flaw instability, MPa√m
T = temperature, °C

RISK-INFORMED DETERMINISTIC EVALUATION OF FRACTURE PROTECTION FOR THE REGION OF INTEREST IN OUTLET ROLLED JOINTS IN BRUCE UNIT 3

Kinectrics Report No. B2038/RP/0009 R00

For temperatures greater than 150°C, the lower-bound fracture toughness is given by

$$K_c = 72 \tag{6-2}$$

6.1.2 97.5% Lower Prediction Bound on Fracture Toughness from Revision 2 Engineering Fracture Toughness Model

As stated in Section 3 of this report, the Revision 2 engineering fracture toughness model predicts fracture toughness as a function of the distance from the front end of the pressure tube, H_{eq}, chlorine concentration, temperature under evaluation, and irradiation temperature. From Section 9 of Reference [2], the fracture toughness from the Revision 2 engineering fracture toughness model is also dependent on the single-tailed statistical confidence level, ζ.

$$K_c = K_c\left(\zeta, D_{fr}, H_{eq}, Cl, T, T_{irr}\right) \tag{6-3}$$

where

D_{fr}	=	distance from the front end of the pressure tube, m
Cl	=	chlorine concentration, ppm
H_{eq}	=	hydrogen equivalent concentration, ppm
T	=	temperature under evaluation, °C
T_{irr}	=	irradiation temperature, °C
ζ	=	single-tailed statistical confidence level (such as 0.975), dimensionless

The 97.5% lower prediction bound on fracture toughness was calculated using the Revision 2 engineering fracture toughness model that is provided in Section 9 of Reference [2] using ζ equal to 0.975.

From Eq. (5-4), the corresponding adjusted fracture toughness is given by

$$K_{c,adj} = \beta_H K_c\left(0.975, D_{fr}, H_{eq}, Cl, T, T_{irr}\right) \tag{6-4}$$

where

$K_{c,adj}$	=	adjusted fracture toughness to account for uncertainty in the application of the Revision 2 engineering fracture toughness model to high levels of H_{eq} of up to 250 ppm, MPa√m
β_H	=	adjustment factor on fracture toughness to account for uncertainty in the application of the Revision 2 engineering fracture toughness model to high levels of H_{eq} of up to 250 ppm, dimensionless

RISK-INFORMED DETERMINISTIC EVALUATION OF FRACTURE PROTECTION FOR THE REGION OF INTEREST IN OUTLET ROLLED JOINTS IN BRUCE UNIT 3

Kinectrics Report No.
B2038/RP/0009 R00

6.2 Critical Internal Pressure at Location of Postulated Axial Through-Wall Flaw

The critical internal pressure at instability of a postulated axial through-wall flaw was calculated in accordance with Clause C.2.2.3.2.3 of the CSA Standard N285.8 [20]. In accordance with Clause D.13.2.1 of the CSA Standard N285.8, the calculated values of fracture toughness are divided by a correction factor to account for the potential effect of reinforcement of the sealing patch on the results from rising pressure burst tests.

$$p_{cr} = \left(\frac{w}{R_i + w} \right) \left(\frac{2\,\sigma_f}{\pi\,M_b} \right) \cos^{-1} \left[\exp \left(\frac{-\pi}{8} \frac{K_{c,adj}^{\,2}}{F_{sp}c\,\sigma_f^{\,2}} \right) \right] \tag{6-5}$$

where

$$M_b = \left[1 + 1.255 \left(\frac{c^2}{R_m w} \right) - 0.0135 \left(\frac{c^2}{R_m w} \right)^2 \right]^{1/2} \tag{6-6}$$

and

c	=	half-length of the postulated axial through-wall flaw, m
F_{sp}	=	correction factor to account for the potential effect of reinforcement of the sealing patch on the results from rising pressure burst tests, = 1.04
$K_{c,adj}$	=	adjusted fracture toughness for axial through-wall flaw instability, MPa√m
M_b	=	bulging factor for an axial through-wall flaw, dimensionless
p_{cr}	=	critical internal pressure at instability of a postulated axial through-wall flaw, MPa
R_i	=	pressure tube inner radius, m
R_m	=	pressure tube mean radius, m
w	=	pressure tube wall thickness, m
σ_f	=	flow stress of the material, MPa

The flow stress of the material, σ_f, is defined as the average of the yield strength and ultimate tensile strength. The lower-bound transverse flow stress is given by

$$\sigma_f = \frac{\sigma_{ys} + \sigma_u}{2} \tag{6-7}$$

where

σ_u	=	lower-bound transverse ultimate tensile strength, MPa
σ_{ys}	=	lower-bound transverse yield strength, MPa

RISK-INFORMED DETERMINISTIC EVALUATION OF FRACTURE PROTECTION FOR THE REGION OF INTEREST IN OUTLET ROLLED JOINTS IN BRUCE UNIT 3

Kinectrics Report No.
B2038/RP/0009 R00

From Clause D.3.4.3 of the CSA Standard N285.8, for fully irradiated material, the lower-bound transverse yield strength is given by

$$\sigma_{ys} = 988 - 1.154T \tag{6-8}$$

and the lower-bound transverse ultimate tensile strength is given by

$$\sigma_u = 1,021 - 1.245T \tag{6-9}$$

where

T = temperature, °C

6.3 Safety Factor on Internal Pressure and Critical Reactor Outlet Header Internal Pressure

The safety factor on internal pressure is the ratio of the calculated critical internal pressure at flaw instability divided by the internal pressure at the location of the postulated flaw.

$$SF = \frac{p_{cr}}{p_{FL}} \tag{6-10}$$

where

p_{FL} = internal pressure at the location of the postulated axial through-wall flaw, MPa
SF = safety factor on internal pressure, dimensionless

The pressure-temperature evaluation is given in terms of ROH internal pressure. The critical ROH internal pressure, $(p_{FLcr})_{ROH}$, is given by

$$\left(p_{FLcr}\right)_{ROH} = p_{cr} - \Delta p_{ROH} \tag{6-11}$$

where

$(p_{Flcr})_{ROH}$ = critical internal pressure at the ROH at instability of a postulated axial through-wall flaw, MPa

Δp_{ROH} = pressure differential between the axial location of the postulated axial through-wall flaw and the ROH, MPa

RISK-INFORMED DETERMINISTIC EVALUATION OF FRACTURE PROTECTION FOR THE REGION OF INTEREST IN OUTLET ROLLED JOINTS IN BRUCE UNIT 3

Kinectrics Report No.
B2038/RP/0009 R00

7. DETERMINISTIC FRACTURE PROTECTION EVALUATION PROCEDURE FOR REACTOR OVERPRESSURE EXCURSION

The deterministic fracture protection evaluation procedure based on an axial through-wall flaw postulated in the region of interest in the front-end outlet rolled joints in Bruce Unit 3 for the reactor overpressure excursion that is treated as Service Level C is described in this Section. The calculation procedure is in accordance with the CSA Standard N285.8, except that the Revision 2 engineering fracture toughness model in Reference [2] was used instead of the Revision 1 engineering fracture toughness model that is provided in Clause D.13.2.2 of the CSA Standard N285.8. The steps involved in the calculation are given below.

(a) A statistical lower prediction bound on fracture toughness was calculated as described in Section 7.1.

(b) The critical internal pressure at the location of the postulated axial through-wall flaw was calculated in accordance with Section 7.2.

(c) The safety factor on internal pressure at the location of the postulated axial through-wall flaw was calculated as described in Section 7.3. The critical Reactor Outlet Header (ROH) internal pressure was calculated as described in Section 7.3.

7.1 Method of Calculation of Statistical Lower Prediction Bounds on Fracture Toughness

The 90% lower prediction bound on fracture toughness for levels of H_{eq} less than or equal to 30 ppm was calculated using Clause D.13.2.2.2 of the CSA Standard N285.8 and as given in Section 7.1.1 of this report. The 90% lower prediction bound on fracture toughness using the Revision 2 engineering fracture toughness model that is provided in Reference [2] was calculated as described in Section 7.1.2. In accordance with Clause D.13.2.1 of the CSA Standard N285.8, the lower of the values of fracture toughness from Clause D.13.2.2.2 and the Revision 2 engineering fracture toughness model was used.

7.1.1 Statistical Lower Prediction Bound on Fracture Toughness for Levels of H_{eq} of 30 ppm or Less from Clause D.13.2.2.2 of CSA Standard N285.8

For H_{eq} less than 30 ppm, and for temperatures less than or equal to 150°C, the statistical lower prediction bound on fracture toughness, K_c, from Clause D.13.2.2.2 of the CSA Standard N285.8 is given by

$$K_c = \exp(3.762 + 0.0058849\,T - \varepsilon_{Kc1})$$ (7-1)

where

RISK-INFORMED DETERMINISTIC EVALUATION OF FRACTURE PROTECTION FOR THE REGION OF INTEREST IN OUTLET ROLLED JOINTS IN BRUCE UNIT 3

Kinectrics Report No. B2038/RP/0009 R00

$$\varepsilon_{Kc1} \;=\; 0.174 U\left(\zeta, 29\right)\left[1 + \frac{1}{31} + \frac{(T - 87.742)^2}{103,653.9}\right]^{1/2} \tag{7-2}$$

and

K_c	=	statistical lower prediction bound on fracture toughness at flaw instability, MPa√m
T	=	temperature, °C
$U(\zeta, 29)$	=	ζ-quantile of Student's t-distribution with 29 degrees of freedom, dimensionless
ε_{Kc1}	=	error term for fracture toughness for levels of H_{eq} of 30 ppm or less and for temperatures less than or equal to 150°C from Clause D.13.2.2.2 of the CSA Standard N285.8, dimensionless
ζ	=	single-tailed statistical confidence level (such as 0.90), dimensionless

For temperatures greater than 150°C, the statistical lower prediction bound on fracture toughness, K_c, from Clause D.13.2.2.2 of the CSA Standard N285.8 is given by

$$K_c \;=\; \exp\left(4.6495 - \varepsilon_{Kc2}\right) \tag{7-3}$$

where

$$\varepsilon_{Kc2} \;=\; 0.1809 U\left(\zeta, 34\right)\left[1 + \frac{1}{35}\right]^{1/2} \tag{7-4}$$

and

$U(\zeta, 34)$	=	ζ-quantile of Student's t-distribution with 34 degrees of freedom, dimensionless
ε_{Kc2}	=	error term for fracture toughness for levels of H_{eq} of 30 ppm or less and for temperatures greater than 150°C from Clause D.13.2.2.2 of the CSA Standard N285.8, dimensionless

The 90% lower prediction bound on fracture toughness was calculated using ζ equal to 0.90. The industry practice is to use the 90% lower prediction bound on the fracture toughness for deterministic fracture protection evaluations of a Service Level C loading, which is consistent with Clause D.13.2.3.4 of the CSA Standard N285.8.

RISK-INFORMED DETERMINISTIC EVALUATION OF FRACTURE PROTECTION FOR THE REGION OF INTEREST IN OUTLET ROLLED JOINTS IN BRUCE UNIT 3

Kinectrics Report No. B2038/RP/0009 R00

7.1.2 Lower Prediction Bound on Fracture Toughness from Revision 2 Engineering Fracture Toughness Model

As stated in Section 3 of this report, the Revision 2 engineering fracture toughness model predicts fracture toughness as a function of the distance from the front end of the pressure tube, H_{eq}, chlorine concentration, temperature under evaluation, irradiation temperature, and the single-tailed statistical confidence level, ζ.

$$K_c \;=\; K_c\left(\zeta, D_{fr}, H_{eq}, Cl, T, T_{irr}\right) \tag{7-5}$$

where

D_{fr}	=	distance from the front end of the pressure tube, m
Cl	=	chlorine concentration, ppm
H_{eq}	=	hydrogen equivalent concentration, ppm
T	=	temperature under evaluation, °C
T_{irr}	=	irradiation temperature, °C
ζ	=	single-tailed statistical confidence level (such as 0.90), dimensionless

The 90% lower prediction bound on fracture toughness was calculated using the Revision 2 engineering fracture toughness model that is provided in Section 9 of Reference [2] using ζ equal to 0.90.

From Eq. (5-4), the corresponding adjusted fracture toughness is given by

$$K_{c,adj} \;=\; \beta_H K_c\left(0.90, D_{fr}, H_{eq}, Cl, T, T_{irr}\right) \tag{7-6}$$

where

$K_{c,adj}$	=	adjusted fracture toughness to account for uncertainty in the application of the Revision 2 engineering fracture toughness model to high levels of H_{eq} of up to 250 ppm, MPa√m
β_H	=	adjustment factor on fracture toughness to account for uncertainty in the application of the Revision 2 engineering fracture toughness model to high levels of H_{eq} of up to 250 ppm, dimensionless

7.2 Critical Internal Pressure at Location of Postulated Axial Through-Wall Flaw

The critical internal pressure at instability of a postulated axial through-wall flaw, p_{cr}, was calculated as described in Section 6.2 of this report.

RISK-INFORMED DETERMINISTIC EVALUATION OF FRACTURE PROTECTION FOR THE REGION OF INTEREST IN OUTLET ROLLED JOINTS IN BRUCE UNIT 3

Kinectrics Report No.
B2038/RP/0009 R00

7.3 Safety Factor on Internal Pressure and Critical Reactor Outlet Header Internal Pressure

The safety factor on internal pressure is the ratio of the calculated critical internal pressure at flaw instability divided by the internal pressure at the location of the postulated flaw as given by Eq. (6-10) that is also given below.

$$SF = \frac{p_{cr}}{p_{FL}} \tag{7-7}$$

where

p_{cr}	=	critical internal pressure at instability of a postulated axial through-wall flaw, MPa
p_{FL}	=	internal pressure at the location of the postulated axial through-wall flaw, MPa
SF	=	safety factor on internal pressure, dimensionless

The pressure-temperature evaluation is given in terms of ROH internal pressure. The critical ROH internal pressure, $(p_{FLcr})_{ROH}$, is given by Eq. (6-11) that is also given below.

$$\left(p_{FLcr} \right)_{ROH} = p_{cr} - \Delta p_{ROH} \tag{7-8}$$

where

$(p_{Flcr})_{ROH}$	=	critical internal pressure at the ROH at instability of a postulated axial through-wall flaw, MPa
Δp_{ROH}	=	pressure differential between the axial location of the postulated axial through-wall flaw and the ROH, MPa

RISK-INFORMED DETERMINISTIC EVALUATION OF
FRACTURE PROTECTION FOR THE REGION OF
INTEREST IN OUTLET ROLLED JOINTS IN BRUCE UNIT 3

Kinectrics Report No.
B2038/RP/0009 R00

8. INPUTS FOR FRACTURE PROTECTION EVALUATION

8.1 Location and Length of Postulated Axial Through-Wall Flaw

The outboard tip of the axial through-wall flaw was postulated to reside at the burnish mark of the front-end outlet rolled joint.

The provisions for fracture protection in Clause 7.2 of the CSA Standard N285.8 require that the length of the postulated axial through-wall flaw be justified, and do not specify the flaw length. Calculations were performed for a postulated axial through-wall flaw length of 20 mm that is typically used. Calculations were also performed for a postulated axial through-wall flaw length of 18 mm. A postulated axial through-wall flaw length of 18 mm was used in the technical basis for the safety factor of 1.20 that is proposed in Reference [22] for the companion deterministic fracture protection evaluation that is performed with a probabilistic fracture protection evaluation. The technical basis for a postulated axial through-wall flaw length of 18 mm for use in the risk-informed deterministic evaluation of fracture protection of the front-end outlet rolled joints in Bruce Unit 3 is summarized in Appendix B of this report. From Appendix B, and based on the volumetric inspection results, a small, localized region at the top of the pressure tube just inboard of the outlet burnish mark that is postulated to have a higher than expected level of H_{eq} is very unlikely to contain flaws that are of a severity that would be a site for crack initiation and growth. From Appendix B, a postulated axial through-wall flaw length of 18 mm corresponds to a cumulative probability of 78% of a DHC crack at initial wall penetration being less than 18 mm. A 10% reduction in the postulated axial through-wall flaw length from 20 to 18 mm is considered reasonable.

As stated in Section 3.1 of this report, the fracture toughness from the Revision 2 engineering fracture toughness model depends on the distance from the front end of the pressure tube [2]. The predicted fracture toughness decreases with a decrease in the distance from the front end. Calculation of the fracture toughness using the distance from the outlet rolled joint burnish mark to the front end of 0.069 m instead of the distance from the inboard tip of the postulated 20 mm long axial through-wall flaw to the front end of 0.089 m results in an insignificant decrease in the fracture toughness of 0.1% over the temperature range of interest. For simplicity, the fracture toughness was calculated using the distance from the outlet rolled joint burnish mark to the front end as a bounding distance for both postulated flaw lengths.

8.2 Pressure Tube Dimensions

Pressure tube dimensions that are bounding for the end of the evaluation period and that are given in Reference [23] were used. A pressure tube inner radius, R_i, of 52.53 mm, and a wall thickness, w, of 3.99 mm, were used.

RISK-INFORMED DETERMINISTIC EVALUATION OF
FRACTURE PROTECTION FOR THE REGION OF
INTEREST IN OUTLET ROLLED JOINTS IN BRUCE UNIT 3

Kinectrics Report No.
B2038/RP/0009 R00

8.3   Hydrogen Equivalent Concentrations and Chlorine Concentration

As described above, the axial and radial extents of the higher than expected levels of H_{eq} inboard of the outlet rolled joint burnish mark have been found to be confined to a localized region with a central tendency about the top of the pressure tube [1]. As also described above, this localized region inboard of the outlet rolled joint burnish mark with a central tendency about the top of the pressure tube that has higher than expected levels of H_{eq} is defined as the region of interest. The focus of the calculations was at the inboard tip of the postulated axial through-wall flaw with a length of 18 or 20 mm in the region of interest, which corresponds to a distance of 18 or 20 mm inboard of the burnish mark, respectively.

For the region of interest in fuelled channels, the estimate of H_{eq} at a distance of 20 mm inboard of the outlet rolled joint burnish mark at the end of the evaluation period, which is the date of the Major Component Replacement (MCR), which is recommended to be used in the deterministic fracture protection evaluation is 200 ppm [1]. In addition, it is recommended in Reference [1] to also use an H_{eq} of 220 ppm as a sensitivity case to address uncertainties in assumptions and inputs used in the calculations for future projections of H_{eq}. The risk-informed deterministic evaluation of fracture protection was performed for postulated levels of H_{eq} of 200 through 250 ppm in the region of interest to address any unanticipated levels of H_{eq} that are great than 220 ppm. These postulated levels of H_{eq} were used for the postulated axial through-wall flaw lengths of 18 and 20 mm.

The levels of H_{eq} in the outlet rolled joints of the three fuel channels B3J14, B3K10 and B3U11 that will operate defuelled following the current outage have been measured by scrape sampling [24]. The estimate of H_{eq} at a distance of 20 mm inboard of the outlet rolled joint burnish mark at the end of the evaluation period that is recommended to be used in the deterministic fracture protection evaluation is 100 ppm [1]. The risk-informed deterministic evaluation of fracture protection was therefore not performed for the three channels that will operate defuelled following the current outage.

The reference value of chlorine concentration, Cl, of 5.5 ppm that is provided in Reference [21], and is used in deterministic fracture protection evaluations of Bruce Unit 3, was used in the calculations.

8.4   Pressure Differential Between Location of Postulated Flaw at Outlet Rolled Joint of Fuelled Channel and Reactor Outlet Header

The procedure to calculate the pressure differential between the location of the postulated axial through-wall flaw at outlet rolled joint burnish mark in a fuelled channel and the ROH was taken from Reference [25]. The pressure differential between the location of the flaw and the ROH depends on the temperature.

The pressure differential between the thermalhydraulic inlet of the fuel channel and the ROH is given by [25]

RISK-INFORMED DETERMINISTIC EVALUATION OF FRACTURE PROTECTION FOR THE REGION OF INTEREST IN OUTLET ROLLED JOINTS IN BRUCE UNIT 3

Kinectrics Report No.
B2038/RP/0009 R00

$$\Delta p_{ROH}{}^{in} \;=\; 1.68285 \;-\; 2.80919 \times 10^{-3}\, T \tag{8-1}$$

and the pressure differential between the thermalhydraulic outlet of the fuel channel and the ROH is given by [25]

$$\Delta p_{ROH}{}^{out} \;=\; 0.47729 \;-\; 6.40345 \times 10^{-4}\, T \tag{8-2}$$

where

$\Delta p_{ROH}{}^{in}$ =   pressure differential between the thermalhydraulic inlet of the fuel channel and the ROH, MPa

$\Delta p_{ROH}{}^{out}$ =   pressure differential between the thermalhydraulic outlet of the fuel channel and the ROH, MPa

T =   temperature, °C

The pressure differential between the axial location of the postulated axial through-wall flaw at the outlet rolled joint burnish mark, which is inboard of the thermalhydraulic outlet of the fuel channel, and the ROH was calculated by linear interpolation along the pressure tube [25].

$$\Delta p_{ROH} \;=\; \Delta p_{ROH}{}^{in} \;-\; \frac{d_{FL}}{L_{PT}}\left(\Delta p_{ROH}{}^{in} \;-\; \Delta p_{ROH}{}^{out}\right) \tag{8-3}$$

where

d_{FL} =   distance between the axial location of the postulated axial through-wall flaw at the outlet rolled joint burnish mark and the inlet end of the pressure tube, = 6.243 m

L_{PT} =   length of the pressure tube, = 6.312 m

Δp_{ROH} =   pressure differential between the axial location of the postulated axial through-wall flaw at the outlet rolled joint burnish mark and the ROH, MPa

8.5 Revised Reactor Outlet Header Pressure-Temperature Operating Limits for Heatup and Cooldown

The revised ROH pressure-temperature operating limits for reactor Heatup and Cooldown are provided in Reference [3], and are given in Table 8-1.

8.6 Revised Reactor Outlet Header Pressure-Temperature Limits for Overpressure Excursion

As described above, revised pressure-temperature limits for a Service Level C overpressure excursion were used in the development of a revised procedure for the DCC Feedpump trip to mitigate a Cold Over-Pressurization Transient and increase fracture protection margins [3]. The variation of the critical ROH internal pressure, $(p_{Flcr})_{ROH}$, with temperature for an overpressure

RISK-INFORMED DETERMINISTIC EVALUATION OF FRACTURE PROTECTION FOR THE REGION OF INTEREST IN OUTLET ROLLED JOINTS IN BRUCE UNIT 3

Kinectrics Report No.
B2038/RP/0009 R00

excursion for a fuelled channel with a postulated axial through-wall flaw length of 20 mm, and an H_{eq} of 200 ppm, is shown in Figure 8-1. This curve was developed in Reference [26] using the 90% lower prediction bound on fracture toughness using the Revision 2 engineering fracture toughness model that is provided in Reference [2] without the application of the adjustment factor for high levels of H_{eq}. The revised ROH pressure-temperature limits for an overpressure excursion are based on application of a 15% margin on the critical ROH internal pressure [3] and are also shown in Figure 8-1.

Tabular values of the variation of the critical ROH internal pressure with temperature for an overpressure excursion for a fuelled channel are given in Appendix C of this report. The revised ROH pressure-temperature limits for the overpressure excursion based on a 15% margin on the critical pressures are also given in Appendix C.

RISK-INFORMED DETERMINISTIC EVALUATION OF
FRACTURE PROTECTION FOR THE REGION OF
INTEREST IN OUTLET ROLLED JOINTS IN BRUCE UNIT 3

Kinectrics Report No.
B2038/RP/0009 R00

TABLE 8-1
**REVISED REACTOR OUTLET HEADER PRESSURE-TEMPERATURE
OPERATING LIMITS FOR REACTOR HEATUP AND COOLDOWN [3]**

Reactor Heatup ROH Temperature (°C)	Reactor Heatup ROH Internal Pressure (MPa)	Reactor Cooldown ROH Temperature (°C)	Reactor Cooldown ROH Internal Pressure (MPa)
40	0.00	300	7.30
40	4.00	175	7.30
68	4.00	175	6.30
68	5.80	100	6.30
78	5.80	100	6.20
78	6.00	90	6.20
100	6.20	90	5.50
130	6.20	68	5.50
130	6.80	68	4.00
250	6.80	27	4.00
250	9.08	27	0.00
300	9.08		

RISK-INFORMED DETERMINISTIC EVALUATION OF FRACTURE PROTECTION FOR THE REGION OF INTEREST IN OUTLET ROLLED JOINTS IN BRUCE UNIT 3

Kinectrics Report No. B2038/RP/0009 R00
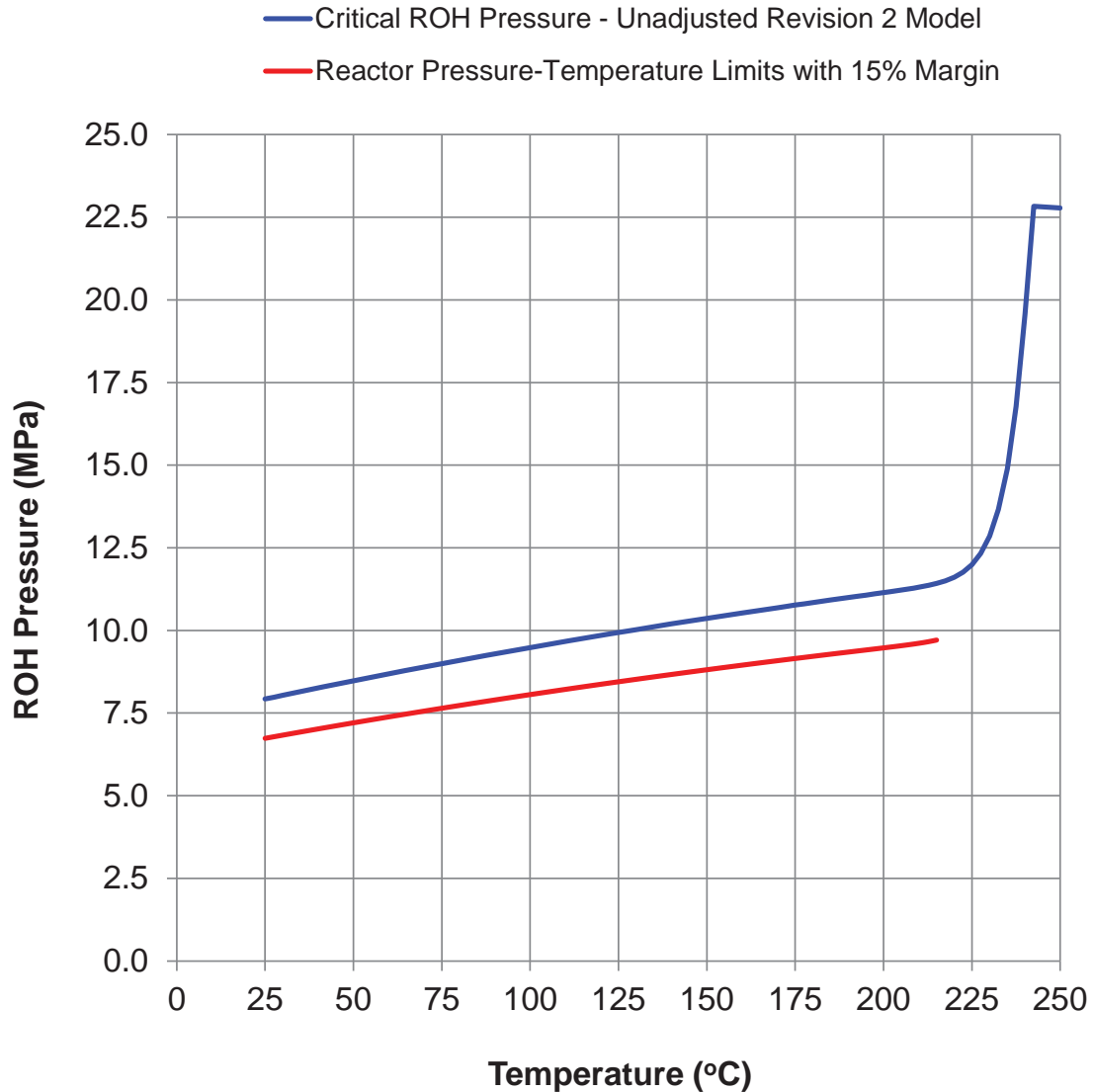
Figure 8-1: Variation of Critical ROH Internal Pressure with Temperature for a Fuelled Channel with a Postulated Flaw Length of 20 mm and an H_{eq} of 200 ppm, and Revised ROH Pressure-Temperature Limits for an Overpressure Excursion

RISK-INFORMED DETERMINISTIC EVALUATION OF FRACTURE PROTECTION FOR THE REGION OF INTEREST IN OUTLET ROLLED JOINTS IN BRUCE UNIT 3

Kinectrics Report No.
B2038/RP/0009 R00

9. RISK-INFORMED FRACTURE PROTECTION EVALUATION RESULTS FOR REACTOR HEATUP AND COOLDOWN

Deterministic fracture protection evaluation results for reactor Heatup and Cooldown for the region of interest that is the localized region inboard of the outlet rolled joint burnish mark with a central tendency about the top of the pressure tube that has higher than expected levels of H_{eq} are provided in this Section. For temperatures below the transition to the upper-shelf fracture regime, the 97.5% lower prediction bound on fracture toughness using the Revision 2 engineering fracture toughness model that is provided in Reference [2] was less than the lower-bound fracture toughness in Clause D.13.2.2.1 of the CSA Standard N285.8. The 97.5% lower prediction bound on fracture toughness from the Revision 2 engineering fracture toughness model for front-end outlet rolled joints was therefore selected to be used for temperatures below the transition to the upper-shelf fracture regime.

9.1 Comparison of Critical Pressure-Temperature Curves Based on Adjusted Fracture Toughness with Revised Pressure-Temperature Operating Limits for Reactor Heatup and Cooldown

The critical internal pressure at the ROH at instability of a postulated axial through-wall flaw, $(p_{Flcr})_{ROH}$, was calculated over a range of temperatures using the procedure described in Section 6 of this report. The adjustment factor on fracture toughness to account for uncertainty in the application of the Revision 2 engineering fracture toughness model to postulated high levels of H_{eq} of up to 250 ppm in the region of interest, β_H, which is equal to 0.909, was applied to the 97.5% lower prediction bound on fracture toughness from the Revision 2 model.

Calculated critical internal pressures based on a postulated axial flaw length of 18 mm, levels of H_{eq} of 200 and 250 ppm, and the adjusted fracture toughness from the Revision 2 engineering fracture toughness model, are compared in Figure 9-1 with the revised ROH pressure-temperature operating limits for reactor Heatup. Calculated critical internal pressures based on a postulated axial flaw length of 18 mm, levels of H_{eq} of 200 and 250 ppm, and the adjusted fracture toughness from the Revision 2 engineering fracture toughness model, are compared in Figure 9-2 with the revised ROH pressure-temperature operating limits for reactor Cooldown. At a given temperature there are substantial margins between the critical internal pressures and the revised operating internal pressure limit for reactor Heatup and Cooldown.

Calculated critical internal pressures based on a postulated axial flaw length of 20 mm, levels of H_{eq} of 200 and 250 ppm, and the adjusted fracture toughness from the Revision 2 engineering fracture toughness model, are compared in Figure 9-3 with the revised ROH pressure-temperature operating limits for reactor Heatup. Calculated critical internal pressures based on a postulated axial flaw length of 20 mm, levels of H_{eq} of 200 and 250 ppm, and the adjusted fracture toughness from the Revision 2 engineering fracture toughness model are compared in Figure 9-4 with the revised ROH pressure-temperature operating limits for reactor Cooldown. At a given temperature there are margins between the critical internal pressures and the revised operating internal pressure limit for reactor Heatup and Cooldown.

RISK-INFORMED DETERMINISTIC EVALUATION OF FRACTURE PROTECTION FOR THE REGION OF INTEREST IN OUTLET ROLLED JOINTS IN BRUCE UNIT 3

Kinectrics Report No. B2038/RP/0009 R00

9.2 Safety Factors on Internal Pressure Based on Adjusted Fracture Toughness

As stated above, the safety factor on internal pressure is the ratio of the calculated critical internal pressure at flaw instability divided by the actual internal pressure at the location of the postulated axial through-wall flaw. The safety factors on internal pressure for the revised pressure-temperature operating limits for reactor Heatup and Cooldown were calculated using the procedure described in Section 6 of this report using the 97.5% lower prediction bound on fracture toughness from the Revision 2 engineering fracture toughness model with the adjustment factor, β_H.

The minimum safety factors on internal pressure for reactor Heatup at temperatures less than 250°C for postulated axial through-wall flaw lengths of 18 and 20 mm, and postulated levels of H_{eq} of 200 through 250 ppm, are given in Table 9-1. The internal pressure at the location of the postulated flaw at the fuel channel outlet, the internal pressure at the ROH, and the temperature at the fuel channel outlet, at which the safety factor on internal pressure is the lowest, are given in Table 9-1. In all cases the internal pressure at the location of the postulated flaw corresponding to the lowest safety factor is 7.20 MPa, the ROH internal pressure is 6.80 MPa, and the temperature is 130°C. The adjusted fracture toughness, $K_{c,adj}$, at 130°C is also given in Table 9-1.

The minimum safety factors on internal pressure for reactor Cooldown at temperatures less than 250°C for postulated axial through-wall flaw lengths of 18 and 20 mm, and postulated levels of H_{eq} of 200 through 250 ppm, are given in Table 9-2. The internal pressure at the location of the postulated flaw at the fuel channel outlet, the internal pressure at the ROH, and the temperature at the fuel channel outlet, at which the safety factor on internal pressure is the lowest, are given in Table 9-2. In all cases the internal pressure at the location of the postulated flaw corresponding to the lowest safety factor is 7.67 MPa, the ROH internal pressure is 7.30 MPa, and the temperature is 175°C. The adjusted fracture toughness, $K_{c,adj}$, at 175°C is also given in Table 9-2.

The safety factors on internal pressure in Tables 9-1 and 9-2 decrease with an increase in the length of the postulated axial through-wall flaw, or an increase in the level of H_{eq}, as expected. For a postulated axial through-wall flaw length of 18 mm and an H_{eq} of 200 ppm, the safety factor on internal pressure for reactor Heatup is 1.30 and for reactor Cooldown is 1.31. These safety factors meet the required safety factor of 1.30 in the acceptance criteria for fracture protection during a reactor Heatup or Cooldown shutdown state in the CSA Standard N285.8. For a postulated axial through-wall flaw length of 18 mm and postulated levels of H_{eq} of 200 through 250 ppm, the safety factors on internal pressure for reactor Heatup and Cooldown are greater than 1.20. The lowest safety factor is 1.12, and is for a postulated axial through-wall flaw length of 20 mm and an H_{eq} of 250 ppm.

The effect of the adjustment factor, β_H, of 0.909 on the safety factors on internal pressure for the revised pressure-temperature operating limits for reactor Heatup and Cooldown for an H_{eq} of 200 ppm was determined. The safety factors on internal pressure for the revised pressure-

RISK-INFORMED DETERMINISTIC EVALUATION OF FRACTURE PROTECTION FOR THE REGION OF INTEREST IN OUTLET ROLLED JOINTS IN BRUCE UNIT 3

Kinectrics Report No.
B2038/RP/0009 R00

temperature operating limits for reactor Heatup and Cooldown were calculated for postulated axial through-wall flaw lengths of 18 and 20 mm, an H_{eq} of 200 ppm, the 97.5% lower prediction bound on fracture toughness from the Revision 2 engineering fracture toughness model, and the adjustment factor, β_H, equal to 1.0. The minimum safety factors on internal pressure are given in Table 9-3. The internal pressure at the location of the postulated flaw at the fuel channel outlet, the internal pressure at the ROH, and the temperature at the fuel channel outlet, at which the safety factor on internal pressure is the lowest, are given in Table 9-3 and are the same as for the corresponding cases with β_H equal to 0.909 in Tables 9-1 and 9-2. The corresponding values of unadjusted fracture toughness, K_c, are also given in Table 9-3. The minimum safety factors for reactor Heatup and Cooldown for the postulated axial through-wall flaw length of 18 mm are 1.43. The minimum safety factors for reactor Heatup and Cooldown for the postulated axial through-wall flaw length of 20 mm are 1.31. These safety factors are greater than the required safety factor of 1.30 in the acceptance criteria for fracture protection during a reactor Heatup or Cooldown shutdown state in the CSA Standard N285.8.

In the event of the unanticipated existence of an axial through-wall flaw in the region of interest in a front-end outlet rolled joint in Bruce Unit 3, and given the conservatisms in the deterministic evaluation of fracture protection, these results demonstrate there would be a very low risk of instability of a flaw with a length up to 20 mm in the region of interest during reactor Heatup or Cooldown.

RISK-INFORMED DETERMINISTIC EVALUATION OF FRACTURE PROTECTION FOR THE REGION OF INTEREST IN OUTLET ROLLED JOINTS IN BRUCE UNIT 3

Kinectrics Report No.
B2038/RP/0009 R00

TABLE 9-1

SAFETY FACTORS ON INTERNAL PRESSURE FROM DETERMINISTIC EVALUATION OF FRACTURE PROTECTION OF REACTOR HEATUP AT TEMPERATURES LESS THAN 250°C USING 97.5% LOWER PREDICTION BOUND ON ADJUSTED FRACTURE TOUGHNESS

Length of Postulated Axial Through-Wall Flaw (mm)	H_{eq} (ppm)	Internal Pressure at Location of Postulated Flaw at Outlet at Minimum Safety Factor (MPa)	Internal Pressure at ROH at Minimum Safety Factor (MPa)	Temperature at Fuel Channel Outlet at Minimum Safety Factor (°C)	Adjusted Fracture Toughness at Minimum Safety Factor Temperature, $K_{c,adj}$ (MPa√m)	Safety Factors Based on a 97.5% Lower Prediction Bound on Adjusted Fracture Toughness
18	200	7.20	6.80	130	28.3	1.30
18	210	7.20	6.80	130	27.9	1.28
18	220	7.20	6.80	130	27.5	1.26
18	230	7.20	6.80	130	27.2	1.25
18	240	7.20	6.80	130	26.8	1.23
18	250	7.20	6.80	130	26.5	1.22
20	200	7.20	6.80	130	28.3	1.19
20	210	7.20	6.80	130	27.9	1.17
20	220	7.20	6.80	130	27.5	1.16
20	230	7.20	6.80	130	27.2	1.14
20	240	7.20	6.80	130	26.8	1.13
20	250	7.20	6.80	130	26.5	1.12

KINECTRICS INC.

RISK-INFORMED DETERMINISTIC EVALUATION OF FRACTURE PROTECTION FOR THE REGION OF INTEREST IN OUTLET ROLLED JOINTS IN BRUCE UNIT 3

Kinectrics Report No.
B2038/RP/0009 R00

TABLE 9-2

SAFETY FACTORS ON INTERNAL PRESSURE FROM DETERMINISTIC EVALUATION OF FRACTURE PROTECTION OF REACTOR COOLDOWN AT TEMPERATURES LESS THAN 250°C USING 97.5% LOWER PREDICTION BOUND ON ADJUSTED FRACTURE TOUGHNESS

Length of Postulated Axial Through-Wall Flaw (mm)	H_{eq} (ppm)	Internal Pressure at Location of Postulated Flaw at Outlet at Minimum Safety Factor (MPa)	Internal Pressure at ROH at Minimum Safety Factor (MPa)	Temperature at Fuel Channel Outlet at Minimum Safety Factor (°C)	Adjusted Fracture Toughness at Minimum Safety Factor Temperature, $K_{c,adj}$ (MPa√m)	Safety Factors Based on a 97.5% Lower Prediction Bound on Adjusted Fracture Toughness
18	200	7.67	7.30	175	30.3	1.31
18	210	7.67	7.30	175	29.9	1.29
18	220	7.67	7.30	175	29.5	1.27
18	230	7.67	7.30	175	29.1	1.25
18	240	7.67	7.30	175	28.8	1.24
18	250	7.67	7.30	175	28.4	1.22
20	200	7.67	7.30	175	30.3	1.20
20	210	7.67	7.30	175	29.9	1.18
20	220	7.67	7.30	175	29.5	1.16
20	230	7.67	7.30	175	29.1	1.15
20	240	7.67	7.30	175	28.8	1.13
20	250	7.67	7.30	175	28.4	1.12

RISK-INFORMED DETERMINISTIC EVALUATION OF
FRACTURE PROTECTION FOR THE REGION OF
INTEREST IN OUTLET ROLLED JOINTS IN BRUCE UNIT 3

Kinectrics Report No.
B2038/RP/0009 R00

TABLE 9-3

SAFETY FACTORS ON INTERNAL PRESSURE FROM DETERMINISTIC EVALUATION OF FRACTURE PROTECTION OF REACTOR HEATUP AND COOLDOWN AT TEMPERATURES LESS THAN 250°C USING 97.5% LOWER PREDICTION BOUND ON UNADJUSTED FRACTURE TOUGHNESS FOR H_{eq} of 200 ppm

Reactor Transient	Length of Postulated Axial Through-Wall Flaw (mm)	H_{eq} (ppm)	Internal Pressure at Location of Postulated Flaw at Outlet at Minimum Safety Factor (MPa)	Internal Pressure at ROH at Minimum Safety Factor (MPa)	Temperature at Fuel Channel Outlet at Minimum Safety Factor (°C)	Unadjusted Fracture Toughness at Minimum Safety Factor Temperature, K_c (MPa√m)	Safety Factors Based on a 97.5% Lower Prediction Bound on Unadjusted Fracture Toughness
Heatup	18	200	7.20	6.80	130	31.1	1.43
Heatup	20	200	7.20	6.80	130	31.1	1.31
Cooldown	18	200	7.67	7.30	175	33.4	1.43
Cooldown	20	200	7.67	7.30	175	33.4	1.31

RISK-INFORMED DETERMINISTIC EVALUATION OF FRACTURE PROTECTION FOR THE REGION OF INTEREST IN OUTLET ROLLED JOINTS IN BRUCE UNIT 3

Kinectrics Report No. B2038/RP/0009 R00

Figure 9-1: Comparison of Critical Internal Pressures for a Fuelled Channel with a Postulated Flaw Length of 18 mm Based on Adjusted Fracture Toughness from the Revision 2 Engineering Model with Revised ROH Pressure-Temperature Operating Limits for Reactor Heatup

RISK-INFORMED DETERMINISTIC EVALUATION OF FRACTURE PROTECTION FOR THE REGION OF INTEREST IN OUTLET ROLLED JOINTS IN BRUCE UNIT 3

Kinectrics Report No. B2038/RP/0009 R00

Figure 9-2: Comparison of Critical Internal Pressures for a Fuelled Channel with a Postulated Flaw Length of 18 mm Based on Adjusted Fracture Toughness from the Revision 2 Engineering Model with Revised ROH Pressure-Temperature Operating Limits for Reactor Cooldown

RISK-INFORMED DETERMINISTIC EVALUATION OF FRACTURE PROTECTION FOR THE REGION OF INTEREST IN OUTLET ROLLED JOINTS IN BRUCE UNIT 3

Kinectrics Report No.
B2038/RP/0009 R00

Figure 9-3: Comparison of Critical Internal Pressures for a Fuelled Channel with a Postulated Flaw Length of 20 mm Based on Adjusted Fracture Toughness from the Revision 2 Engineering Model with Revised ROH Pressure-Temperature Operating Limits for Reactor Heatup

RISK-INFORMED DETERMINISTIC EVALUATION OF FRACTURE PROTECTION FOR THE REGION OF INTEREST IN OUTLET ROLLED JOINTS IN BRUCE UNIT 3

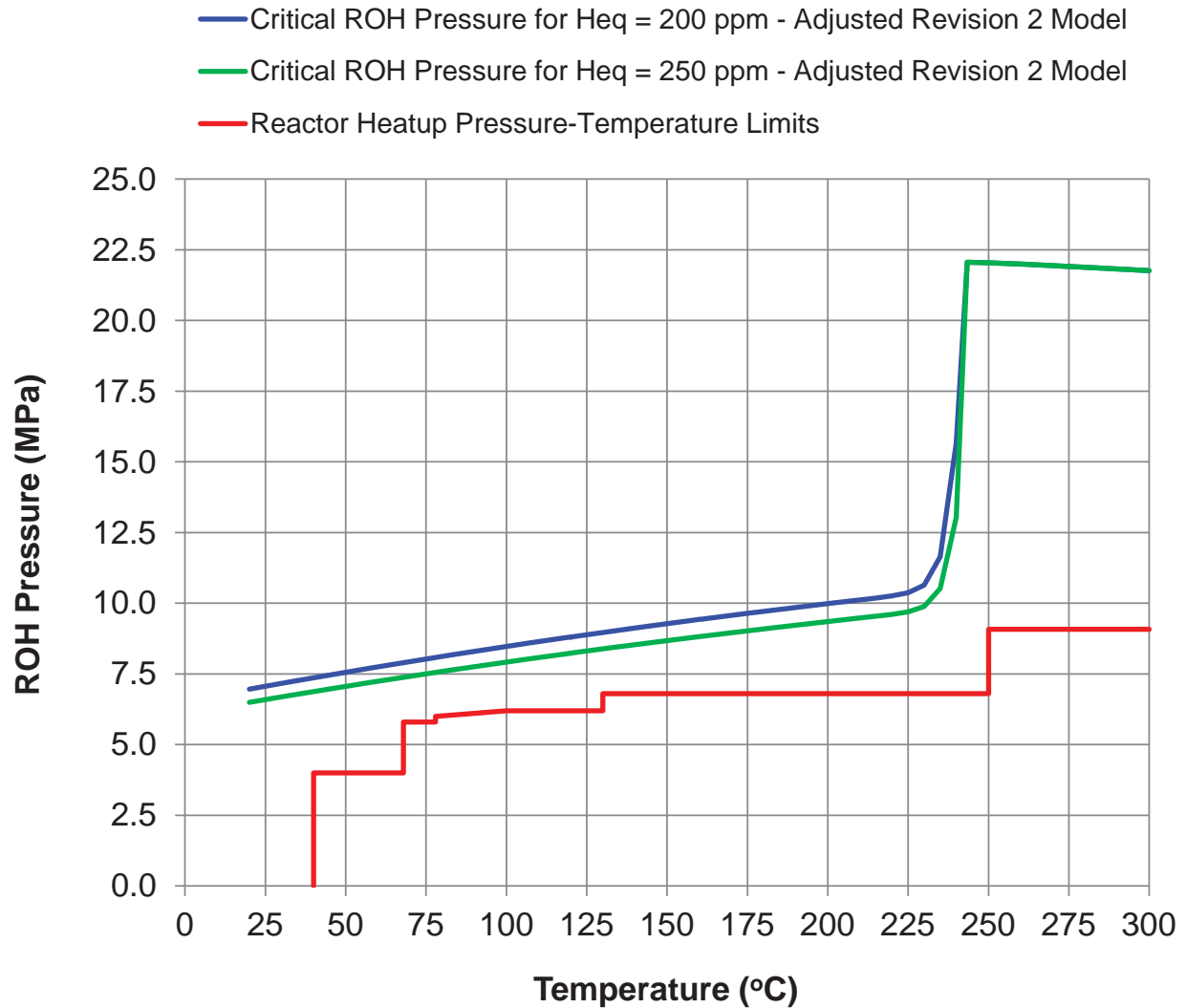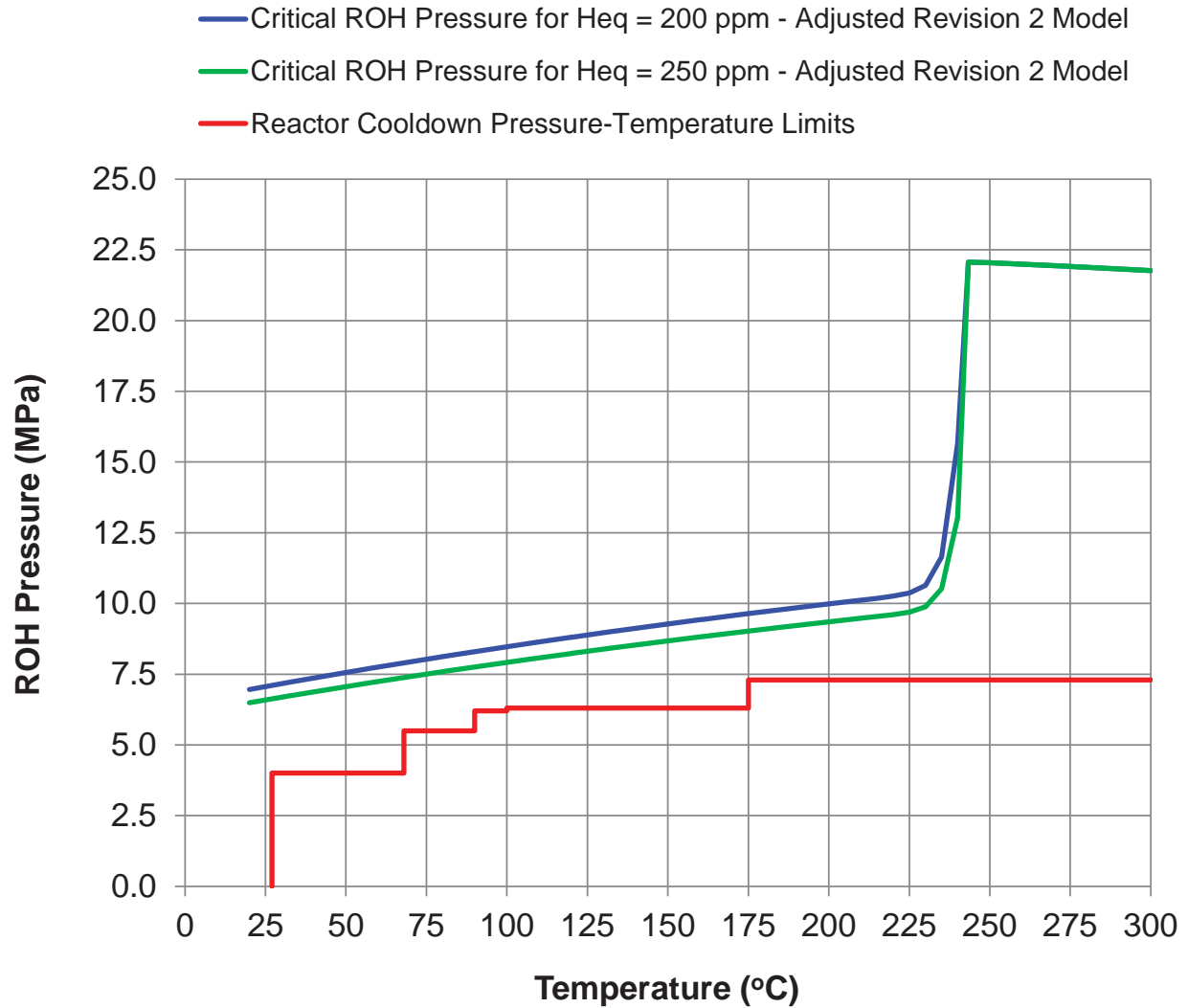**Kinectrics Report No. B2038/RP/0009 R00**
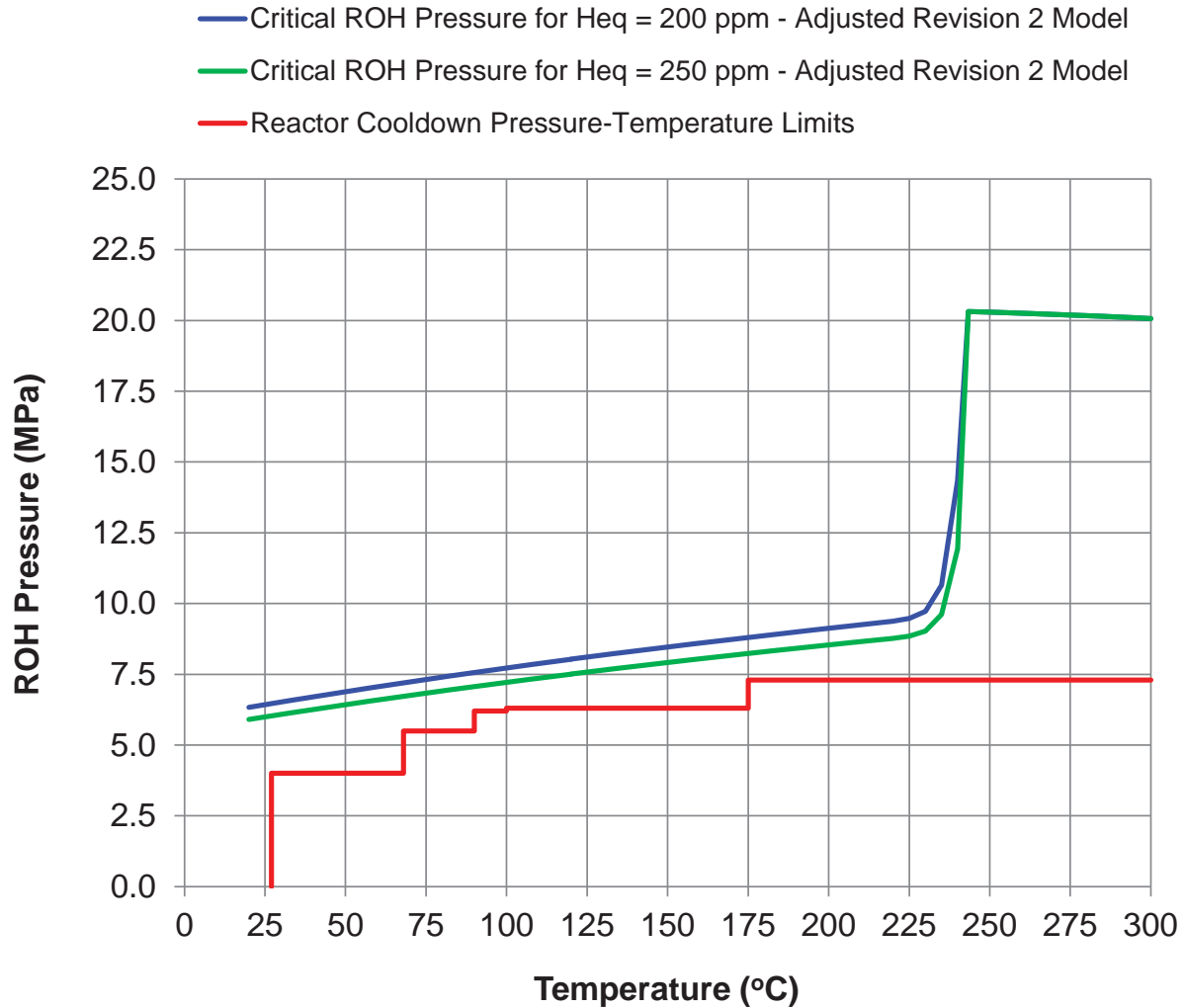
Figure 9-4: Comparison of Critical Internal Pressures for a Fuelled Channel with a Postulated Flaw Length of 20 mm Based on Adjusted Fracture Toughness from the Revision 2 Engineering Model with Revised ROH Pressure-Temperature Operating Limits for Reactor Cooldown
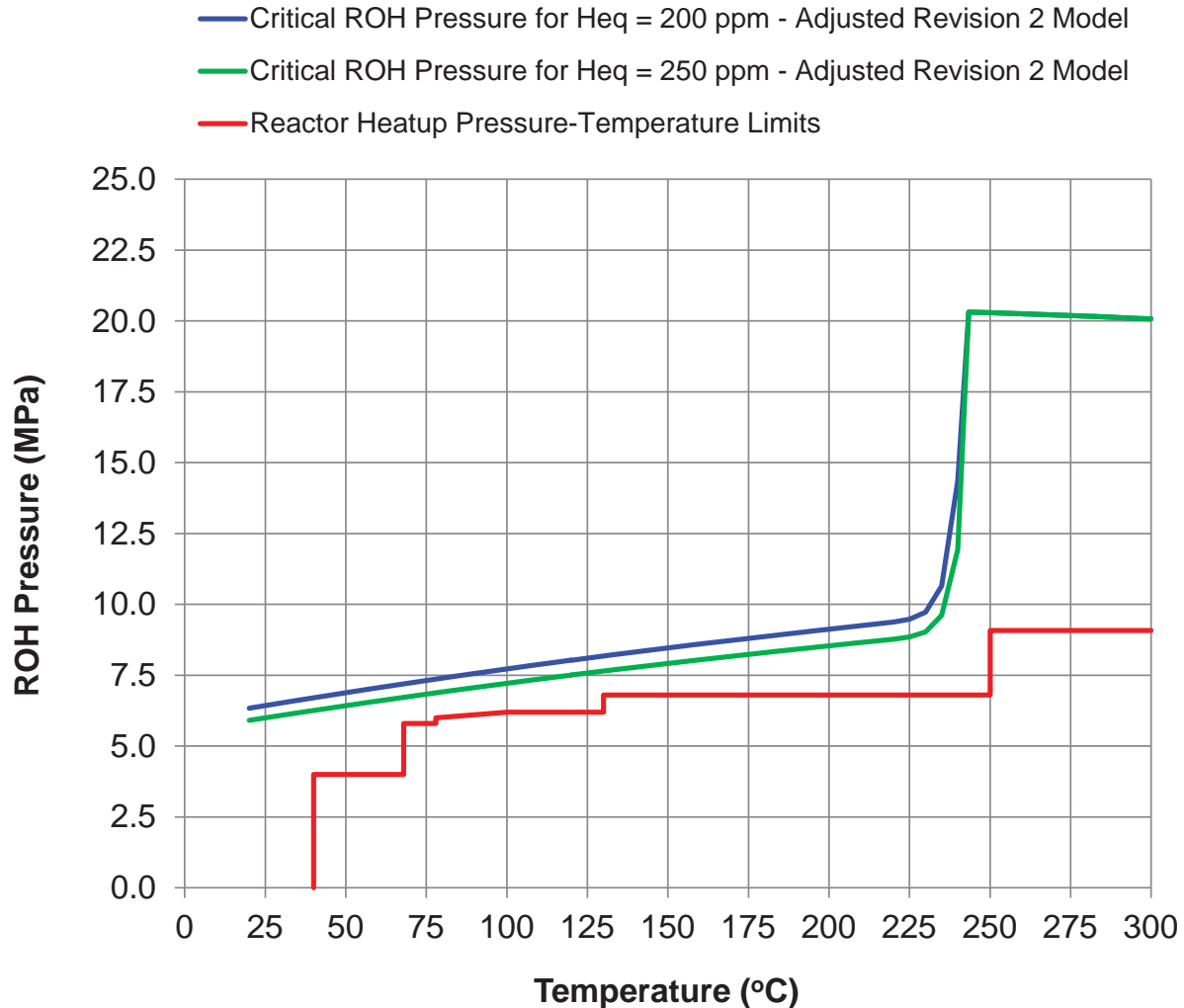
RISK-INFORMED DETERMINISTIC EVALUATION OF FRACTURE PROTECTION FOR THE REGION OF INTEREST IN OUTLET ROLLED JOINTS IN BRUCE UNIT 3

Kinectrics Report No. B2038/RP/0009 R00

10. RISK-INFORMED FRACTURE PROTECTION EVALUATION RESULTS FOR REACTOR OVERPRESSURE EXCURSION TRANSIENT

Deterministic fracture protection evaluation results for the Service Level C overpressure excursion for the region of interest that is the localized region inboard of the outlet rolled joint burnish mark with a central tendency about the top of the pressure tube that has higher than expected levels of H_{eq} are provided in this Section. For temperatures below the transition to the upper-shelf fracture regime, the 90% lower prediction bound on fracture toughness using the Revision 2 engineering fracture toughness model that is provided in Reference [2] was less than the lower-bound fracture toughness in Clause D.13.2.2.2 of the CSA Standard N285.8. The 90% lower prediction bound on fracture toughness from the Revision 2 engineering fracture toughness model for front-end outlet rolled joints was therefore selected to be used for temperatures below the transition to the upper-shelf fracture regime.

10.1 Comparison of Critical Pressure-Temperature Curves Based on Adjusted Fracture Toughness with Revised Pressure-Temperature Limits for Overpressure Excursion

The critical internal pressure at the ROH at instability of a postulated axial through-wall flaw, $(p_{Flcr})_{ROH}$, was calculated over a range of temperatures using the procedure described in Section 7 of this report. The adjustment factor on fracture toughness to account for uncertainty in the application of the Revision 2 engineering fracture toughness model to postulated high levels of H_{eq} of up to 250 ppm in the region of interest, β_H, which is equal to 0.909, was applied to the 90% lower prediction bound on fracture toughness from the Revision 2 model.

Calculated critical internal pressures based on a postulated axial flaw length of 18 mm, levels of H_{eq} of 200 and 250 ppm, and the adjusted fracture toughness from the Revision 2 engineering fracture toughness model are compared in Figure 10-1 with the revised ROH pressure-temperature limits for the overpressure excursion. At a given temperature there are substantial margins between the critical internal pressures and the revised internal pressure limit for the overpressure excursion.

Calculated critical internal pressures based on a postulated axial flaw length of 20 mm, levels of H_{eq} of 200 and 250 ppm, and the adjusted fracture toughness from the Revision 2 engineering fracture toughness model are compared in Figure 10-2 with the revised ROH pressure-temperature limits for the overpressure excursion. For an H_{eq} of 250 ppm, the critical internal pressures based on a postulated axial flaw length of 20 mm are essentially equal to the revised ROH pressure-temperature limits for the overpressure excursion, and the curves lie on top of one another in Figure 10-2.

RISK-INFORMED DETERMINISTIC EVALUATION OF FRACTURE PROTECTION FOR THE REGION OF INTEREST IN OUTLET ROLLED JOINTS IN BRUCE UNIT 3

Kinectrics Report No.
B2038/RP/0009 R00

10.2   Safety Factors on Internal Pressure Based on Adjusted Fracture Toughness

The safety factors on internal pressure for the revised pressure-temperature limits for the overpressure excursion were calculated using the procedure described in Section 7 of this report using the 90% lower prediction bound on fracture toughness from the Revision 2 engineering fracture toughness model with the adjustment factor, β_H. As described in Section 8.6 of this report, the revised pressure-temperature limits for a Service Level C overpressure excursion are based on application of a 15% margin on the critical ROH internal pressure that was calculated using a postulated axial through-wall flaw length of 20 mm, an H_{eq} of 200 ppm, and the 90% lower prediction bound on fracture toughness using the Revision 2 engineering fracture toughness model without the application of the adjustment factor for high levels of H_{eq}. The result of the application of a margin of 15% is that the safety factors on internal pressure that are calculated using the Revision 2 engineering fracture toughness model with the adjustment factor, β_H, are nearly constant over the temperature range. This is seen by comparing the curves of the calculated critical internal pressure with the revised ROH pressure-temperature limits in Figures 10-1 and 10-2. The safety factors on internal pressure that cover the temperature range of 25 through 215°C for postulated axial through-wall flaw lengths of 18 and 20 mm, and postulated levels of H_{eq} of 200 through 250 ppm, are given in Table 10-1. The safety factor for a given postulated axial through-wall flaw length and level of H_{eq} varies by no more than nominally 0.01 over the temperature range of 25 through 215°C. The adjusted fracture toughness, $K_{c,adj}$, at 100°C is also given in Table 10-1 to show an example of the dependency of the fracture toughness on H_{eq}.

The safety factors on internal pressure in Table 10-1 decrease with an increase in the length of the postulated axial through-wall flaw, or an increase in the level of H_{eq}, as expected. For the postulated axial through-wall flaw length of 18 mm and postulated levels of H_{eq} of 200 through 250 ppm, and for the postulated axial through-wall flaw length of 20 mm and levels of H_{eq} of 200 through 240 ppm, the safety factors on internal pressure are greater than 1.0. The lowest safety factor is 0.99, and is for a postulated axial through-wall flaw length of 20 mm and an H_{eq} of 250 ppm. These safety factors essentially meet the required safety factor of 1.0 in the acceptance criteria for fracture protection during a Service Level C event in the CSA Standard N285.8.

In the event of the unanticipated existence of an axial through-wall flaw in the region of interest in a front-end outlet rolled joint in Bruce Unit 3, and given the conservatisms in the deterministic evaluation of fracture protection, these results demonstrate there would be a low risk of instability of a flaw with a length up to 20 mm in the region of interest during an overpressure excursion.

RISK-INFORMED DETERMINISTIC EVALUATION OF
FRACTURE PROTECTION FOR THE REGION OF
INTEREST IN OUTLET ROLLED JOINTS IN BRUCE UNIT 3

Kinectrics Report No.
B2038/RP/0009 R00

TABLE 10-1
**SAFETY FACTORS ON INTERNAL PRESSURE FROM DETERMINISTIC
EVALUATION OF FRACTURE PROTECTION OF OVERPRESSURE
EXCURSION AT TEMPERATURES LESS THAN 215°C USING
90% LOWER PREDICTION BOUND ON ADJUSTED FRACTURE TOUGHNESS**

Length of Postulated Axial Through-Wall Flaw (mm)	H_{eq} (ppm)	Adjusted Fracture Toughness at 100°C, $K_{c,adj}$ (MPa√m)	Safety Factors Over Range of Temperatures of Evaluation Based on a 90% Lower Prediction Bound on Adjusted Fracture Toughness
18	200	29.8	1.16
18	210	29.3	1.14 – 1.15
18	220	28.9	1.13
18	230	28.6	1.11 – 1.12
18	240	28.2	1.10
18	250	27.9	1.09
20	200	29.8	1.06 – 1.07
20	210	29.3	1.04 – 1.05
20	220	28.9	1.03 – 1.04
20	230	28.6	1.02
20	240	28.2	1.01
20	250	27.9	0.99 – 1.00
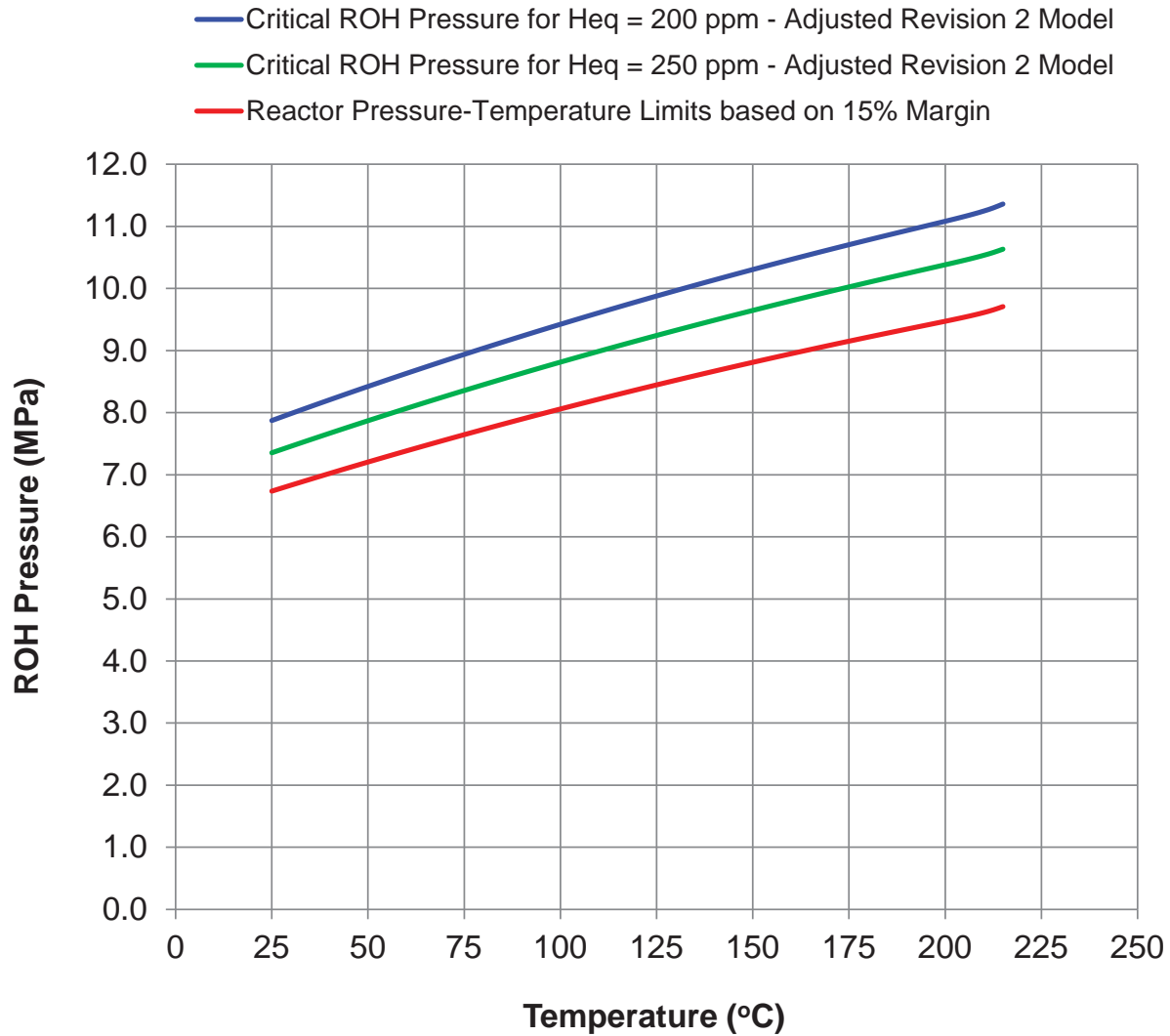
Proprietary and Confidential

RISK-INFORMED DETERMINISTIC EVALUATION OF FRACTURE PROTECTION FOR THE REGION OF INTEREST IN OUTLET ROLLED JOINTS IN BRUCE UNIT 3

Kinectrics Report No.
B2038/RP/0009 R00

Figure 10-1: Comparison of Critical Internal Pressures for a Fuelled Channel with a Postulated Flaw Length of 18 mm Based on Adjusted Fracture Toughness from the Revision 2 Engineering Model with Revised ROH Pressure-Temperature Limits for an Overpressure Excursion

RISK-INFORMED DETERMINISTIC EVALUATION OF FRACTURE PROTECTION FOR THE REGION OF INTEREST IN OUTLET ROLLED JOINTS IN BRUCE UNIT 3

Kinectrics Report No. B2038/RP/0009 R00
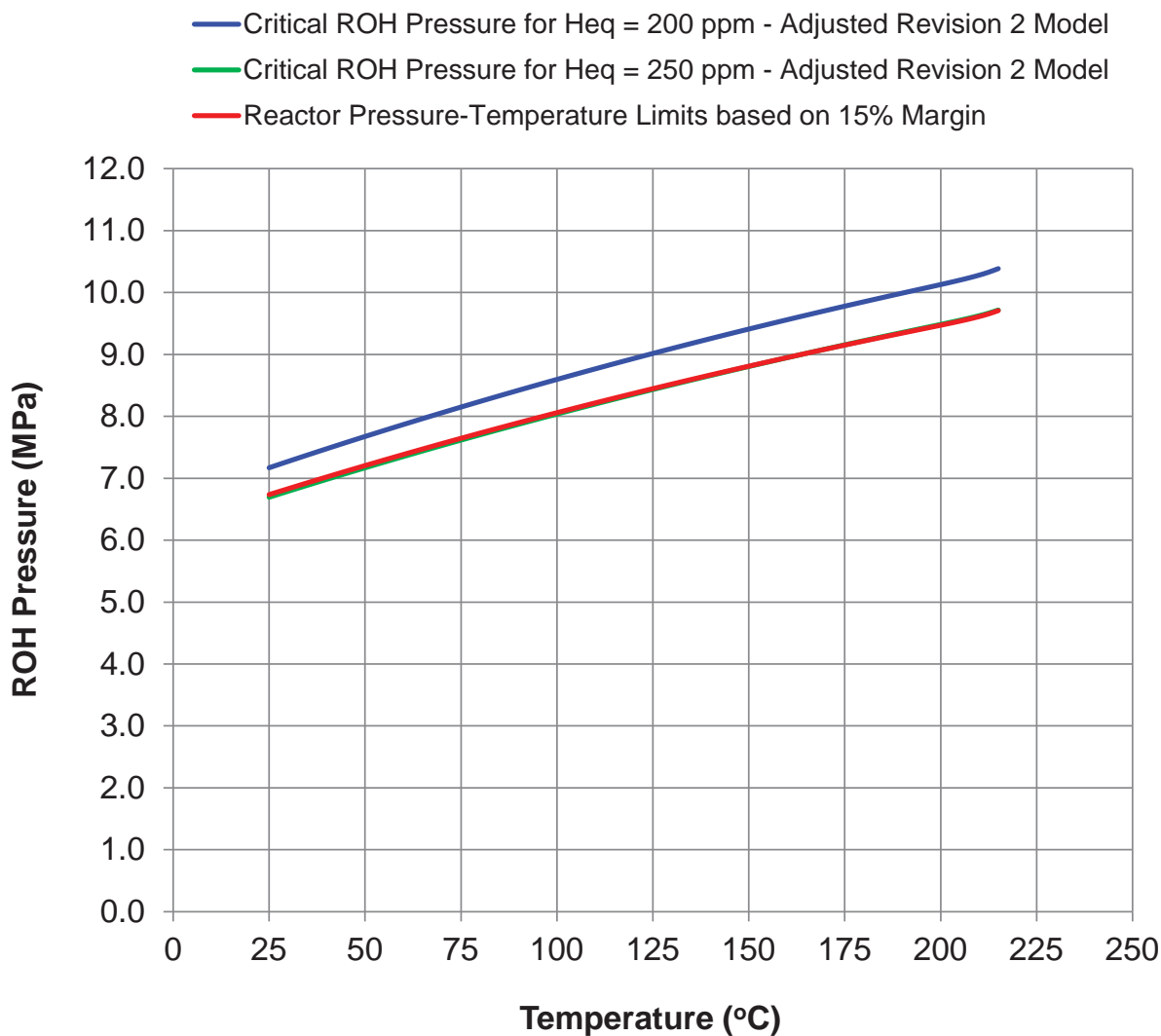
Figure 10-2: Comparison of Critical Internal Pressures for a Fuelled Channel with a Postulated Flaw Length of 20 mm Based on Adjusted Fracture Toughness from the Revision 2 Engineering Model with Revised ROH Pressure-Temperature Limits for an Overpressure Excursion
(For an H_{eq} of 250 ppm, the curve of critical internal pressure is nearly coincident with the revised ROH pressure-temperature limits.)

RISK-INFORMED DETERMINISTIC EVALUATION OF FRACTURE PROTECTION FOR THE REGION OF INTEREST IN OUTLET ROLLED JOINTS IN BRUCE UNIT 3

Kinectrics Report No.
B2038/RP/0009 R00

11. CONSERVATISMS IN RISK-INFORMED DETERMINISTIC EVALUATION OF FRACTURE PROTECTION OF FRONT-END OUTLET ROLLED JOINTS IN BRUCE UNIT 3

The risk-informed deterministic evaluation of fracture protection of the region of interest in front-end outlet rolled joints in Bruce Unit 3 involves a number of conservatisms as described below.

(a) For a through-wall flaw to exist there needs to be a pre-existing service-induced flaw, such as due to fretting, and which would need to be a site for crack initiation and growth. From Appendix B of this report, and based on the volumetric inspection results, the small, localized region just inboard of the outlet burnish mark with a central tendency about the top of the pressure tube that is postulated to have a higher than expected level of H_{eq} is very unlikely to contain flaws that are of a severity that would be a site for crack initiation and growth.

(b) The postulated through-wall flaw is assumed to be not leaking and not detected.

(c) The lower temperature portions of the fracture toughness curves that are most limiting in fracture protection evaluations of front-end outlet rolled joints in Bruce Unit 3 do not take into account the benefit of the higher irradiation temperatures at the outlets that result in an increase in the fracture toughness.

RISK-INFORMED DETERMINISTIC EVALUATION OF FRACTURE PROTECTION FOR THE REGION OF INTEREST IN OUTLET ROLLED JOINTS IN BRUCE UNIT 3

Kinectrics Report No. B2038/RP/0009 R00

12.   SUMMARY AND CONCLUSIONS

(a) A risk-informed deterministic evaluation of fracture protection based on a postulated axial through-wall flaw in the region of interest in the front-end outlet rolled joints in fuelled channels in Bruce Unit 3 has been performed for postulated high levels of H_{eq} of 200 through 250 ppm as described in this report. The region of interest is defined as the localized region inboard of the outlet rolled joint burnish mark with a central tendency about the top of the pressure tube that has higher than expected levels of H_{eq}. The scope of the risk-informed deterministic evaluation of fracture protection is limited to the region of interest. For the same set of conditions such as H_{eq}, the results of the risk-informed deterministic evaluation of fracture protection for the region of interest in the front-end outlet rolled joints in this report can be used as a conservative bound on the results from a risk-informed deterministic evaluation of fracture protection of the region of interest in back-end outlet rolled joints in Bruce Unit 3. Although the results of the evaluation in this report are specific to the region of interest in the front-end outlet rolled joints in Bruce Unit 3, the framework of the risk-informed deterministic evaluation of fracture protection is applicable to a region of interest in any Bruce reactor. The risk-informed deterministic evaluation of fracture protection of the region of interest was performed over an evaluation period of operation of Bruce Unit 3 up to the MCR that is estimated to be bounded by 246,000 EFPH.

(b) Measured fracture toughness from small test specimens comprised of irradiated Zircaloy-2 and Zircaloy-4 materials for a range of levels of H_{eq} that in some cases exceed 250 ppm were obtained from the literature and used in the context of surrogate materials to gain insights into the fracture toughness of zirconium alloys at these high levels of H_{eq}. A conservative value of fracture toughness from the set of fracture toughness values for irradiated Zircaloy-2 and Zircaloy-4 materials was used to develop an adjustment factor that is less than 1.0 and is intended to account for uncertainty in the application of the Revision 2 engineering fracture toughness model to these postulated high levels of H_{eq} in the region of interest. The values of fracture toughness that were used in the evaluation were predicted by the Revision 2 engineering fracture toughness model and then reduced by multiplying by the adjustment factor.

(c) A risk-informed deterministic evaluation of fracture protection for the Service Level A reactor Heatup and Cooldown transients was performed for the region of interest based on revised Heatup and Cooldown pressure-temperature operating limits for Bruce Unit 3 that are intended to increase fracture protection margins. The safety factors on internal pressure for the revised pressure-temperature operating limits for reactor Heatup and Cooldown were calculated using postulated axial through-wall flaw lengths of 18 and 20 mm, and postulated levels of H_{eq} of 200 through 250 ppm. For a postulated axial through-wall flaw length of 18 mm and postulated levels of H_{eq} of 200 through 250 ppm, the safety factors on internal pressure for reactor Heatup and Cooldown are greater than 1.20. The lowest safety factor is 1.12, and is for a postulated axial through-wall flaw length of 20 mm and an H_{eq} of 250 ppm.

(d) A risk-informed deterministic evaluation of fracture protection was performed for the region of interest based on revised pressure-temperature limits for a Service Level C overpressure excursion that were used in the development of a revised procedure for the DCC Feedpump trip

RISK-INFORMED DETERMINISTIC EVALUATION OF FRACTURE PROTECTION FOR THE REGION OF INTEREST IN OUTLET ROLLED JOINTS IN BRUCE UNIT 3

Kinectrics Report No.
B2038/RP/0009 R00

to mitigate a Cold Over-Pressurization Transient and increase fracture protection margins. The safety factors on internal pressure were calculated for the overpressure excursion using postulated axial through-wall flaw lengths of 18 and 20 mm, and postulated levels of H_{eq} of 200 through 250 ppm. For the postulated axial through-wall flaw length of 18 mm and postulated levels of H_{eq} of 200 through 250 ppm, and for the postulated axial through-wall flaw length of 20 mm and levels of H_{eq} of 200 through 240 ppm, the safety factors on internal pressure are greater than 1.0. The lowest safety factor is 0.99, and is for a postulated axial through-wall flaw length of 20 mm and an H_{eq} of 250 ppm. These safety factors essentially meet the required safety factor of 1.0 in the acceptance criteria for fracture protection during a Service Level C event in the CSA Standard N285.8.

(e) The risk-informed deterministic evaluation of fracture protection for the region of interest in front-end outlet rolled joints in Bruce Unit 3 involves a number of conservatisms. Based on the volumetric inspection results, a small, localized region just inboard of the outlet burnish mark with a central tendency about the top of the pressure tube that is postulated to have a higher than expected level of H_{eq} is very unlikely to contain flaws that are of a severity that would be a site for crack initiation and growth. In addition, the postulated through-wall flaw is assumed to be not leaking and not detected. The lower temperature portions of the fracture toughness curves that are most limiting in fracture protection evaluations of front-end outlet rolled joints in Bruce Unit 3 do not take into account the benefit of the higher irradiation temperatures at the outlets that result in an increase in the fracture toughness.

(f) In the event of the unanticipated existence of an axial through-wall flaw in the region of interest in a front-end outlet rolled joint in Bruce Unit 3, and given the conservatisms in the deterministic evaluation of fracture protection, these results demonstrate there would be a low risk of instability of a flaw with a length up to 20 mm in the region of interest during reactor Heatup or Cooldown, or during an overpressure excursion.

13.   ACKNOWLEDGMENTS

REFERENCES

1. Letter, C. Nam and K. Harrison, "Postulated Bounding $[H]_{eq}$ Levels for Bruce Unit 3 Fracture Protection Evaluation," Kinectrics File No. B2038/LET/0009 R00, August 24, 2021.

2. Scarth, D.A. and Gutkin, L. "Revision 2 of Engineering Fracture Toughness Model Based on Cohesive-Zone Model for Zr-2.5Nb Pressure Tubes," COG Report No. COG-JP-4583-V094, May 2021.

3. Email from A. Glover, "Risk Informed Approach for Fracture Protection," Bruce Power, September 1, 2021.

4. Scarth, D.A., Gutkin, L. and Liu, C., "Development of Revision 2 of Analytical Cohesive-Zone Fracture Toughness Model for Zr-2.5Nb Pressure Tubes," COG Report No. COG-JP-4583-V012-R01, May 2021.

5. Scarth, D.A., "Technical Basis for Validity Limit on Equivalent Hydrogen Concentration of 120 ppm for Application of Revision 2 Fracture Toughness Model Within 1.5 m from Front End Outlets in Bruce Unit 3," Kinectrics File No. B2038/RP/0004 R00, Bruce Power Document No. B-REP-31100-00030, July 21, 2021.

6. Email from S. St Lawrence, "Results from BT-50," Canadian Nuclear Laboratories, Kinectrics File No. K-026818, August 16, 2021.

7. Email from S. St Lawrence, "[Heq] for BT-50 (B6N07-2)," Canadian Nuclear Laboratories, Kinectrics File No. K-026818, August 23, 2021.

8. Email from A. Sahoo, "Information on irradiation temperature is needed urgently," Kinectrics, Kinectrics File No. K-024045, May 23, 2020.

9. Ding, Y. and St Lawrence, S., "A Statistical Analysis of Pressure Tube Fracture Toughness Data," COG Report No. COG-JP-4583-V021, August 2020.

10. "Revision 8 of Fracture Toughness Database," COG Other Product OP-JP-4583-V019 R3, 2020, with updates in "Revision 11 of Fracture Toughness Database," COG Other Product OP-JP-4583-V019 R6, February 4, 2021, Canadian Nuclear Laboratories, Kinectrics File No. K-024045.

11. Davies, P.H, Smeltzer, J.M. and Longhurst, G.C., "Fracture Toughness of Hydrided Zr-2.5Nb Pressure Tube Material Irradiated in the NRU Test Reactor," COG Report COG-95-176, September 1995.

12. Bell, L.G. and Duncan, R.G., "Hydride Orientation in Zr-2.5%Nb; How it is Affected by Stress, Temperature and Heat Treatment," AECL Report No. AECL-5110, June 1975.

RISK-INFORMED DETERMINISTIC EVALUATION OF FRACTURE PROTECTION FOR THE REGION OF INTEREST IN OUTLET ROLLED JOINTS IN BRUCE UNIT 3

Kinectrics Report No.
B2038/RP/0009 R00

13. Hoagland, R.G. and Rowe, R.G., "Fracture of Irradiated Zircaloy-2," *Journal of Nuclear Materials*, Volume 30, 1969, pp. 179-195.

14. Chow, C.K. and Simpson, L.A., "Analysis of the Unstable Fracture of a Reactor Pressure Tube Using Fracture Toughness Mapping," *Case Histories Involving Fatigue and Fracture Mechanics*, ASTM STP 918, C.M. Hudson and T.P. Rich, Eds., American Society for Testing and Materials, 1986, pp. 78-101.

15. Coleman, C.E., Cheadle, B.A., Causey, A.R., Chow, P.C.K., Davies, P.H., McManus, M.D., Rodgers, D.K., Sagat, S. and van Drunen, G., "Evaluation of Zircaloy-2 Pressure Tubes from NPD," *Zirconium in the Nuclear Industry: Eighth International Symposium*, ASTM STP 1023, L.F.P. Van Swam and C.M. Eucken, Eds., American Society for Testing and Materials, Philadelphia, 1989, pp. 35-49.

16. Huang, F.H., "Brittle-Fracture Potential of Irradiated Zircaloy-2 Pressure Tubes," *Journal of Nuclear Materials*, Volume 207, 1993, pp. 103-115.

17. Huang, F.H. and Mills, W.J., "Fracture and Tensile Properties of Irradiated Zircaloy-2 Pressure Tubes," *Nuclear Technology*, Volume 102, No. 3, 1993, pp. 367-375.

18. Walker, T.J. and Kass, J.N., "Variation of Zircaloy Fracture Toughness with Irradiation," *Zirconium in Nuclear Applications*, ASTM STP 551, American Society for Testing and Materials, 1974, pp. 328-354.

19. Kreyns, P.H., Bourgeois, W.F., White, C.J., Charpentier, P.L., Kammenzind, B.F., and Franklin, D.G., "Embrittlement of Reactor Core Materials," *Zirconium in the Nuclear Industry: Eleventh International Symposium*, ASTM STP 1295, E. R. Bradley and G. P. Sabol, Eds., American Society for Testing and Materials, 1996, pp. 758-782.

20. "Technical Requirements for In-Service Evaluation of Zirconium Alloy Pressure Tubes in CANDU Reactors," *Canadian Standards Association*, CSA Standard N285.8-15, with Update No. 1.

21. Sahoo, A., "Evaluation of Reference Chlorine Concentration for Calculation of Lower-Bound Fracture Toughness Using the New Fracture Toughness Models," COG Report No. COG-JP-4452-V038-R00, March 2014.

22. Scarth, D.A., Doddihal, P. and Gutkin, L., "Technical Basis for Safety Factors on Pressure for use with Design-Intent Reactor Core-Based Acceptance Criteria for Probabilistic Evaluations of Fracture Protection," COG Report No. COG-JP-4583-V031-R00, October 10, 2018.

23. Manu, C., "PT Dimensions and COPT Conditions for B3, 4, 5, 7, 8 for 2021 Fracture Protection Evaluations," Kinectrics File No. B2210/RE/0019 R02, July 21, 2021.

RISK-INFORMED DETERMINISTIC EVALUATION OF FRACTURE PROTECTION FOR THE REGION OF INTEREST IN OUTLET ROLLED JOINTS IN BRUCE UNIT 3

Kinectrics Report No.
B2038/RP/0009 R00

24. Letter, H. Zhou to L. Micuda, "Hydrogen Equivalent Concentration Measurements Taken Near the Outlet Burnish Mark in the Bruce Unit 3 2021 Outage (A2131)," Kinectrics File No. B2038/LET/0013 R00, September 13, 2021.

25. Doddihal, P. and Scarth, D.A., "Implicit Safety Factors on Pressure for Heatup and Cooldown in Ontario Power Generation and Bruce Power Reactors," COG Report No. COG-JP-4583-V032-R00, November 2018.

26. Scarth, D.A., "Deterministic Sensitivity Evaluation of Fracture Protection for Outlet Rolled Joints in Bruce Unit 3," Kinectrics Report No. B2038/RP/0005 R00, August 26, 2021.

27. Robertson, J., "B3-B8 Database of Pressure Tube Flaws Just Inboard of the Outlet Burnish Mark," Kinectrics File No. B2266/RP/0002 R00, September 15, 2021.

28. "Technical Basis for the Fitness for Service Guidelines for Zirconium Alloy Pressure Tubes in Operating CANDU Reactors," COG Report No. COG-96-651, Revision 0, December 1996.

29. NIST/Sematech "e-Handbook of Statistical Methods," http://www.itl.nist.gov/div898/handbook/, 2017.

30. Letter, M. Burton to L. Sigouin, "Response to CNSC's Remaining Comments on Technical Basis for Safety Factors on Pressure for Use with the Design-Intent Reactor Core Based Acceptance Criteria for Probabilistic Evaluation of Fracture Protection," Bruce Power File No. BP-CORR-00531-01382, February 11, 2021.

31. Ip, M., "Fuel Channel Condition Assessment," Bruce Power File No. B-REP-31100-00003 Rev 004, Kinectrics File No. B1714/IC/016 R00, February 2016.

32. Leemans, D., "Estimation of Encountering Reportable & Dispositionable Pressure Tube Flaws in Various Regions of Interest in Bruce Power Units 3-8," Kinectrics File No. B2266/RP/0001 R00, September 17, 2021.

RISK-INFORMED DETERMINISTIC EVALUATION OF FRACTURE PROTECTION FOR THE REGION OF INTEREST IN OUTLET ROLLED JOINTS IN BRUCE UNIT 3

Kinectrics Report No.
B2038/RP/0009 R00

APPENDIX A

VALUES OF FRACTURE TOUGHNESS OF IRRADIATED Zr-2.5Nb PRESSURE TUBE MATERIAL, ZIRCALOY-2 AND ZIRCALOY-4 MATERIALS, WITH MEDIUM TO HIGH LEVELS OF HYDROGEN EQUIVALENT CONCENTRATION

Tabular values of fracture toughness of hydrided irradiated Zr-2.5Nb pressure tube material, Zircaloy-2 and Zircaloy-4 materials, with medium to high levels of hydrogen equivalent concentration are provided in this Appendix. Tabular values of fracture toughness of hydrided irradiated Zr-2.5Nb pressure tube material are provided in Table A-1. Tabular values of fracture toughness of hydrided irradiated Zircaloy-2 materials are provided in Table A-2. Tabular values of fracture toughness of hydrided irradiated Zircaloy-4 materials are provided in Table A-3.

RISK-INFORMED DETERMINISTIC EVALUATION OF FRACTURE PROTECTION FOR THE REGION OF INTEREST IN OUTLET ROLLED JOINTS IN BRUCE UNIT 3

Kinectrics Report No.
B2038/RP/0009 R00

TABLE A-1
FRACTURE TOUGHNESS OF HYDRIDED IRRADIATED Zr-2.5Nb PRESSURE TUBE MATERIAL

Specimen Identification	Material	Specimen Orientation	Irradiation Temperature (°C)	Irradiation Fluence ×10²⁴ n/m²	H_{eq} (ppm)\	Test Temperature (°C)	Fracture Toughness (MPa√m)	Reference
M3-4-4	Cold-worked Zr-2.5Nb	C-L	255	2.3	173	240	66.6	[11]
M3-4-3	Cold-worked Zr-2.5Nb	C-L	255	5.2	176	240	60.9	[11]
M3-1-2	Cold-worked Zr-2.5Nb	C-L	255	2.3	177	30	45.4	[11]
M3-1-1	Cold-worked Zr-2.5Nb	C-L	255	5.2	178	30	38.5	[11]
M3-4-7	Cold-worked Zr-2.5Nb	C-L	255	5.2	185	175	48.5	[11]
M3-1-7	Cold-worked Zr-2.5Nb	C-L	255	5.2	189	100	51.9	[11]
M3-2-7	Cold-worked Zr-2.5Nb	C-L	255	5.2	191	175	51.5	[11]
M3-2-4	Cold-worked Zr-2.5Nb	C-L	255	2.3	191	175	57.3	[11]
M3-2-3	Cold-worked Zr-2.5Nb	C-L	255	5.2	192	175	49.5	[11]
M3-3-7	Cold-worked Zr-2.5Nb	C-L	255	5.2	203	240	63.5	[11]
M3-2-8	Cold-worked Zr-2.5Nb	C-L	255	2.3	209	100	51.2	[11]
M3-4-2	Cold-worked Zr-2.5Nb	C-L	255	2.3	220	240	47.8	[11]
M3-2-2	Cold-worked Zr-2.5Nb	C-L	255	2.3	230	240	73.4	[11]

RISK-INFORMED DETERMINISTIC EVALUATION OF FRACTURE PROTECTION FOR THE REGION OF INTEREST IN OUTLET ROLLED JOINTS IN BRUCE UNIT 3

Kinectrics Report No. B2038/RP/0009 R00

TABLE A-2
FRACTURE TOUGHNESS OF HYDRIDED IRRADIATED ZIRCALOY-2 MATERIALS

Specimen Identification	Material	Specimen Orientation	Irradiation Temperature (°C)	Irradiation Fluence ×10²⁴ n/m²	H_{eq} (ppm)\	Test Temperature(1) (°C)	Fracture Toughness(1) (MPa√m)	Reference
na	Annealed before irradiation Zircaloy-2	R-D	280	2.5	100	40	31.9	[13]
na	Annealed before irradiation Zircaloy-2	R-D	280	2.5	100	42	31.9	[13]
na	Annealed before irradiation Zircaloy-2	R-D	280	2.5	100	60	30.2	[13]
na	Annealed before irradiation Zircaloy-2	R-D	280	2.5	100	60	30.8	[13]
na	Annealed before irradiation Zircaloy-2	R-D	280	2.5	100	80	33.0	[13]
na	Annealed before irradiation Zircaloy-2	R-D	280	2.5	100	100	33.5	[13]
na	Annealed before irradiation Zircaloy-2	R-D	280	2.5	100	120	46.7	[13]
na	Annealed before irradiation Zircaloy-2	R-D	280	2.5	400	19	26.4	[13]
na	Annealed before irradiation Zircaloy-2	R-D	280	2.5	400	20	26.4	[13]
na	Annealed before irradiation Zircaloy-2	R-D	280	2.5	400	21	25.8	[13]
na	Annealed before irradiation Zircaloy-2	R-D	280	2.5	400	38	26.9	[13]
na	Annealed before irradiation Zircaloy-2	R-D	280	2.5	400	40	25.8	[13]
na	Annealed before irradiation Zircaloy-2	R-D	280	2.5	400	60	28.0	[13]
na	Annealed before irradiation Zircaloy-2	R-D	280	2.5	400	60	26.9	[13]
na	Annealed before irradiation Zircaloy-2	R-D	280	2.5	400	80	27.5	[13]
na	Annealed before irradiation Zircaloy-2	R-D	280	2.5	400	100	26.4	[13]
na	Annealed before irradiation Zircaloy-2	R-D	280	2.5	400	100	28.0	[13]
na	Annealed before irradiation Zircaloy-2	R-D	280	2.5	400	120	26.4	[13]
na	Annealed before irradiation Zircaloy-2	R-D	280	2.5	400	120	28.0	[13]
na	Annealed before irradiation Zircaloy-2	R-D	280	2.5	400	140	24.7	[13]

General Note:
na – not available.
Note:
(1) Tabular values for fracture toughness data were not provided in Reference [13], and the fracture toughness data were digitized from a plot. The associated uncertainty from using digitized test data is not significant in the context of the results of the risk-informed deterministic evaluation of fracture protection.

RISK-INFORMED DETERMINISTIC EVALUATION OF FRACTURE PROTECTION FOR THE REGION OF INTEREST IN OUTLET ROLLED JOINTS IN BRUCE UNIT 3

Kinectrics Report No.
B2038/RP/0009 R00

TABLE A-2 (continued)
FRACTURE TOUGHNESS OF HYDRIDED IRRADIATED ZIRCALOY-2 MATERIALS

Specimen Identification	Material	Specimen Orientation	Irradiation Temperature (°C)	Irradiation Fluence ×10²⁴ n/m²	H_{eq} (ppm)	Test Temperature[1] (°C)	Fracture Toughness[1] (MPa√m)	Reference
C31	Cold-worked Zircaloy-2	C-L	280	na	58	280	67.3	[14]
C7	Cold-worked Zircaloy-2	C-L	280	na	59	280	63.6	[14]
C5	Cold-worked Zircaloy-2	C-L	280	na	61	280	54.0	[14]
C6	Cold-worked Zircaloy-2	C-L	280	na	63	230	53.6	[14]
C37	Cold-worked Zircaloy-2	C-L	280	na	66	230	48.5	[14]
C1	Cold-worked Zircaloy-2	C-L	280	na	72	230	48.7	[14]
C36	Cold-worked Zircaloy-2	C-L	280	na	81	230	40.0	[14]
C13	Cold-worked Zircaloy-2	C-L	280	na	95	280	69.7	[14]
C20	Cold-worked Zircaloy-2	C-L	280	na	109	280	46.0	[14]
C11	Cold-worked Zircaloy-2	C-L	280	na	110	280	75.4	[14]
C24	Cold-worked Zircaloy-2	C-L	280	na	146	280	62.0	[14]
na	Cold-worked Zircaloy-2	Burst test	260 - 270	na	170 - 245	30	20.7	[15]
na	Cold-worked Zircaloy-2	C-L	260 - 270	na	170 - 245	33	19.6	[15]
na	Cold-worked Zircaloy-2	C-L	260 - 270	na	170 - 245	150	27.7	[15]
na	Cold-worked Zircaloy-2	C-L	260 - 270	na	170 - 245	200	34.6	[15]
na	Cold-worked Zircaloy-2	C-L	260 - 270	na	170 - 245	200	31.9	[15]
na	Cold-worked Zircaloy-2	C-L	260 - 270	na	170 - 245	240	47.0	[15]
na	Cold-worked Zircaloy-2	C-L	260 - 270	na	170 - 245	240	49.3	[15]
na	Cold-worked Zircaloy-2	C-L	260 - 270	na	170 - 245	260	47.7	[15]
na	Cold-worked Zircaloy-2	C-L	260 - 270	na	170 - 245	260	53.8	[15]
na	Cold-worked Zircaloy-2	C-L	260 - 270	na	170 - 245	270	58.3	[15]
na	Cold-worked Zircaloy-2	C-L	260 - 270	na	170 - 245	280	54.3	[15]
na	Cold-worked Zircaloy-2	C-L	260 - 270	na	170 - 245	280	73.1	[15]
na	Cold-worked Zircaloy-2	C-L	260 - 270	na	170 - 245	300	83.3	[15]

Note:
(1) Tabular values for fracture toughness data were not provided in Reference [15], and the fracture toughness data were digitized from a plot. The associated uncertainty from using digitized test data is not significant in the context of the results of the risk-informed deterministic evaluation of fracture protection.

RISK-INFORMED DETERMINISTIC EVALUATION OF FRACTURE PROTECTION FOR THE REGION OF INTEREST IN OUTLET ROLLED JOINTS IN BRUCE UNIT 3

Kinectrics Report No.
B2038/RP/0009 R00

TABLE A-2 (continued)
FRACTURE TOUGHNESS OF HYDRIDED IRRADIATED ZIRCALOY-2 MATERIALS

Specimen Identification	Material	Specimen Orientation	Irradiation Temperature (°C)	Irradiation Fluence ×10²⁴ n/m²	H_{eq} (ppm)	Test Temperature (°C)	Fracture Toughness (MPa√m)	Reference
ZZ4C3E	Cold-worked Zircaloy-2	C-L	210 - 280	50.0	52	177	40.8	[16]
3G2A1	Cold-worked Zircaloy-2	C-L	210 - 280	61.0	64	177	31.2	[16]
J3A2	Cold-worked Zircaloy-2	C-L	210 - 280	56.0	72	177	29.2	[16]
ZZ4C3F	Cold-worked Zircaloy-2	C-L	210 - 280	50.0	89	32	26.0	[16]
J4A2A1	Cold-worked Zircaloy-2	C-L	210 - 280	56.0	150	260	29.5	[16]
14B5B	Cold-worked Zircaloy-2	C-L	210 - 280	45.0	220	32	21.7	[16]
na	Cold-worked Zircaloy-2	C-L	na	50.0	52	177	40.8	[17]
na	Cold-worked Zircaloy-2	C-L	na	46.0	84	177	45.7	[17]
na	Cold-worked Zircaloy-2	C-L	na	50.0	89	32	26.0	[17]
na	Cold-worked Zircaloy-2	C-L	na	50.0	90	100	36.0	[17]
na	Cold-worked Zircaloy-2	C-L	na	50.0	111	260	46.6	[17]
na	Cold-worked Zircaloy-2	C-L	na	46.0	138	32	25.5	[17]
na	Cold-worked Zircaloy-2	C-L	na	50.0	205	32	26.5	[17]
na	Cold-worked Zircaloy-2	C-L	na	46.0	259	177	45.6	[17]

General Note:
na – not available.

RISK-INFORMED DETERMINISTIC EVALUATION OF FRACTURE PROTECTION FOR THE REGION OF INTEREST IN OUTLET ROLLED JOINTS IN BRUCE UNIT 3

Kinectrics Report No.
B2038/RP/0009 R00

TABLE A-3
FRACTURE TOUGHNESS OF HYDRIDED IRRADIATED ZIRCALOY-4 MATERIALS

Specimen Identification	Material	Specimen Orientation	Irradiation Temperature (°C)	Irradiation Fluence ×10²⁴ n/m²	H_{eq} (ppm)\	Test Temperature (°C)	Fracture Toughness (MPa√m)	Reference
82-5613	alpha-annealed Zircaloy-4	T-W	na	5.1	238	22	22.1	[18]
82-5758	alpha-annealed Zircaloy-4	T-W	na	10.35	238	22	25.3	[18]
82-5617	alpha-annealed Zircaloy-4	T-W	na	13.5	238	22	24.2	[18]
82-5615	alpha-annealed Zircaloy-4	T-W	na	5.1	238	79	36.7	[18]
82-5763	alpha-annealed Zircaloy-4	T-W	na	20.8	238	232	44.7	[18]
82-5628	alpha-annealed Zircaloy-4	T-W	na	20.8	238	232	47.3	[18]
82-5764	alpha-annealed Zircaloy-4	T-W	na	20.8	238	316	46.7	[18]
82-5716	alpha-annealed Zircaloy-4	T-W	na	20.8	238	316	49.9	[18]
82-5737	alpha-annealed Zircaloy-4	W-T	na	4.9	238	22	28.8	[18]
82-5746	alpha-annealed Zircaloy-4	W-T	na	10.0	238	22	27.5	[18]
82-5739	alpha-annealed Zircaloy-4	W-T	na	12.8	238	22	29.6	[18]
82-5744	alpha-annealed Zircaloy-4	W-T	na	20.5	238	22	27.0	[18]
82-5738	alpha-annealed Zircaloy-4	W-T	na	4.9	238	79	28.6	[18]
82-5767	alpha-annealed Zircaloy-4	W-T	na	9.4	238	79	30.5	[18]
82-5740	alpha-annealed Zircaloy-4	W-T	na	12.8	238	149	71.4	[18]
82-5777	beta-quenched Zircaloy-4	W-T	na	10.35	238	22	27.7	[18]
82-5780	beta-quenched Zircaloy-4	W-T	na	20.4	238	22	27.0	[18]
82-5779	beta-quenched Zircaloy-4	W-T	na	10.75	238	79	28.1	[18]
82-5781	beta-quenched Zircaloy-4	W-T	na	20.4	238	260	52.4	[18]

General Note:
na – not available.

RISK-INFORMED DETERMINISTIC EVALUATION OF FRACTURE PROTECTION FOR THE REGION OF INTEREST IN OUTLET ROLLED JOINTS IN BRUCE UNIT 3

Kinectrics Report No.
B2038/RP/0009 R00

TABLE A-3 (continued)
FRACTURE TOUGHNESS OF HYDRIDED IRRADIATED ZIRCALOY-4 MATERIALS

Specimen Identification	Material	Specimen Orientation	Irradiation Temperature (°C)	Irradiation Fluence $\times 10^{24}$ n/m^2	H_{eq} (ppm)\	Test Temperature (°C)	Fracture Toughness (MPa√m)	Reference
na	Beta-quenched and weld-metal Zircaloy-4	na	260	47.0	240	24	27.6	[19]
na	Beta-quenched and weld-metal Zircaloy-4	na	260	47.0	240	24	28.5	[19]
na	Beta-quenched and weld-metal Zircaloy-4	na	260	47.0	240	24	28.2	[19]
na	Beta-quenched and weld-metal Zircaloy-4	na	260	47.0	240	24	31.1	[19]
na	Beta-quenched and weld-metal Zircaloy-4	na	260	47.0	240	24	25.6	[19]
na	Beta-quenched and weld-metal Zircaloy-4	na	260	47.0	240	24	27.7	[19]
na	Beta-quenched and weld-metal Zircaloy-4	na	260	28.8	247	24	22.4	[19]
na	Beta-quenched and weld-metal Zircaloy-4	na	260	10.1	250	24	26.7	[19]
na	Beta-quenched and weld-metal Zircaloy-4	na	260	20.4	250	24	27.1	[19]
na	Beta-quenched and weld-metal Zircaloy-4	na	260	10.3	262	24	26.2	[19]
na	Beta-quenched and weld-metal Zircaloy-4	na	260	29.9	405	24	21.1	[19]
na	Beta-quenched Zircaloy-4	na	260	53.0	240	149	34.5	[19]
na	Beta-quenched Zircaloy-4	na	260	10.3	253	149	31.2	[19]
na	Beta-quenched Zircaloy-4	na	260	29.3	253	149	29.3	[19]
na	Beta-quenched Zircaloy-4	na	260	14.0	441	260	33.9	[19]

General Note:
na – not available.

RISK-INFORMED DETERMINISTIC EVALUATION OF FRACTURE PROTECTION FOR THE REGION OF INTEREST IN OUTLET ROLLED JOINTS IN BRUCE UNIT 3

Kinectrics Report No. B2038/RP/0009 R00

APPENDIX B

TECHNICAL BASIS FOR LENGTH OF A POSTULATED AXIAL THROUGH-WALL FLAW OF 18 mm FOR USE IN RISK-INFORMED DETERMINISTIC EVALUATION OF FRACTURE PROTECTION OF FRONT-END OUTLET ROLLED JOINTS IN BRUCE UNIT 3

B-1. INTRODUCTION

The technical basis for a postulated axial through-wall flaw length of 18 mm for use in the risk-informed deterministic evaluation of fracture protection of the front-end outlet rolled joints in Bruce Unit 3 is provided in this Appendix. A postulated axial through-wall flaw length of 18 mm was used in the technical basis for the safety factor of 1.20 that is proposed in Reference [22] for the companion deterministic fracture protection evaluation that is performed with a probabilistic fracture protection evaluation. A summary of the developments in Reference [22], as well as an additional statistical analysis, are provided in this Appendix. A summary of an investigation of the number of flaws in the outlet rolled joint regions of pressure tubes in Bruce reactors in Reference [27] is also provided in this Appendix.

B-2. TECHNICAL BASIS FOR THE REFERENCE 20 mm LENGTH OF THE POSTULATED AXIAL THROUGH-WALL FLAW

B-2.1 Background

The technical basis for the reference 20 mm length of the postulated axial through-wall flaw that is used in the deterministic evaluations of fracture protection is provided in the technical basis document for the *Fitness-for-Service Guidelines*, report COG-96-651 [28]. The ratios of the axial lengths divided by pressure tube wall thickness of twelve delayed hydride cracking (DHC) cracks at initial wall penetration that were measured in ex-service over-extended rolled joints are provided in Reference [28], and are given below in Table B-1. From Reference [28], a nominal pressure tube wall thickness of 4.1 mm was used to convert the normalized lengths of the DHC cracks to dimensions of mm. From Table B-1, the maximum length of a DHC crack at initial wall penetration is 19.43 mm and corresponds to DHC crack number 3 from the pressure tube removed from fuel channel P4G08. The reference 20 mm length of the postulated axial through-wall flaw is therefore an engineering upper bound on the lengths of DHC cracks at initial wall penetration that were detected in over-extended rolled joints. The axial through-wall flaw length of 20 mm is not based on a statistical analysis of the DHC crack lengths at initial wall penetration.

B-2.2 Statistical Distribution of Crack Length at Initial Penetration of the Pressure Tube Wall

A statistical distribution of the crack length at initial wall penetration was developed to enable calculation of the cumulative probability of the penetration length of a DHC crack being less than the postulated axial through-wall flaw length [22]. To maintain consistency with the technical basis for the reference 20 mm length of the postulated axial through-wall flaw, the lengths at initial wall penetration of the twelve DHC cracks that were measured in ex-service over-extended rolled joints, and are given in Table B-1, were parameterized statistically in Reference [22] in terms of a normal distribution. The mean crack length at initial wall penetration, L_{pm}, was estimated to be 16.68 mm, and the standard deviation of the sample, sd_{Lp}, was estimated to be 1.711 mm. The length of a DHC crack at initial wall penetration is given by

$$L_p(Pr) = N\left(L_{pm}, sd_{Lp}\right) \tag{B-1}$$

where

$L_p(Pr)$	=	crack length at initial wall penetration for a specific cumulative probability, Pr, mm
L_{pm}	=	mean value of the crack length at initial wall penetration, mm
$N(L_{Pm}, sd_{Lp})$ =		normal distribution of crack length at initial wall penetration with a mean, L_{pm}, and standard deviation, sd_{Lp}, mm
Pr	=	cumulative probability of the crack length at initial penetration being less than L_p, dimensionless
sd_{Lp}	=	standard deviation of crack length at initial wall penetration, mm

The empirical distribution of measured lengths of the DHC cracks at initial wall penetration is compared with the normal distribution of penetration length at the same cumulative probabilities in Table B-2 and Figure B-1. The cumulative probability inferred from empirical distribution of the measured lengths of the DHC cracks at initial wall penetration is compared with the cumulative probability of the normally distributed penetration length in Figure B-2. From Table B-2, and Figures B-1 and B-2, there is some deviation of the distribution of the measured crack lengths from a normal distribution. The P-value of Kolmogorov-Smirnov test for normality [29] is 0.43, and there is insufficient evidence to reject the null hypothesis that the underlying distribution of penetration length is normal.

The possibility of other parametric distributions providing an acceptable representation of the empirical distribution was investigated [30]. Ten different parametric probability distributions were fitted to the empirical distribution of the measured lengths of the DHC cracks at initial wall penetration, L_p. The P-value of Kolmogorov-Smirnov goodness-of-fit test, and the cumulative probability of the crack length at initial wall penetration being less than or equal to a postulated flaw length of 17.2 or 18.2 mm, are given for each parametric distribution in Table B-3. The ten different parametric probability distributions are sorted in the descending order of the P-value of the Kolmogorov-Smirnov goodness-of-fit test. The P-values of all of these distributions are in the tens of percent range, and all of these distributions would provide an acceptable

RISK-INFORMED DETERMINISTIC EVALUATION OF
FRACTURE PROTECTION FOR THE REGION OF
INTEREST IN OUTLET ROLLED JOINTS IN BRUCE UNIT 3

Kinectrics Report No.
B2038/RP/0009 R00

representation of the empirical distribution. Considering the distributions with the P-value higher than that of the normal distribution, the cumulative probability of L_p being less than or equal to the postulated flaw length of either 17.2 mm or 18.2 mm exceeds this cumulative probability for the normal distribution. For the distributions with the P-value lower than that of the normal distribution, the cumulative probability of L_p being less than or equal to the postulated flaw length typically also exceeds that for the normal distribution, except for the Weibull distribution. It is therefore concluded that the normal distribution is acceptable, and typically slightly conservative, for parameterization of the empirical distribution of flaw penetration lengths.

The variation of the cumulative probability of the normally distributed length of DHC cracks at initial wall penetration is shown using expanded scales in Figure B-3. The crack length at initial wall penetration inferred from the normal distribution shown in Figure B-3 at a cumulative probability of 97.5% is 20.04 mm, which is essentially the same as the reference 20 mm length of the postulated axial through-wall flaw that is an engineering upper bound on the lengths of DHC cracks at initial penetration.

B-3. INVESTIGATION OF NUMBER OF FLAWS IN THE OUTLET ROLLED JOINT REGIONS OF PRESSURE TUBES IN BRUCE REACTORS

As described in Section 8.3 of this report, the axial and radial extents of the higher than expected levels of H_{eq} inboard of the outlet rolled joint burnish mark have been found to be confined to a localized region with a central tendency about the top of the pressure tube. Based on full length volumetric in-service inspections of this region in collectively 16% of the pressure tubes in Bruce Units 3 through 8, only two reportable flaws whose entire axial extent is within the first 100 mm inboard of the outlet burnish mark have been detected [27]. These flaws were caused by fretting of trapped debris, had non-dispositionable depths of 0.13 and 0.11 mm, and were located at 41 and 30 mm from the outlet burnish mark in the lower hemisphere of the pressure tube [27]. No flaws were detected in the small, localized regions just inboard of the outlet burnish mark with a central tendency about the top of the pressure tube that are postulated to have a higher than expected level of H_{eq} [27]. This finding for the axial range of 0 through 100 mm inboard of the outlet burnish mark is consistent with the pressure tube flaw axial distribution figures from Section 6 of the Bruce Power Fuel Channel Condition Assessment [31]. There is no reason to expect that the flaw distributions in this region of the inspected population of pressure tubes would be different from the uninspected population of pressure tubes. The probability of encountering at least one dispositionable flaw in the region of interest that is within 50 mm inboard of the outlet rolled joint burnish mark and within a circumferential extent of 120 degrees centred at the top of the pressure tube in the uninspected population of pressure tubes in Bruce Unit 3 has been determined in Reference [32] to be 3.95×10^{-3}. A small, localized region at the top of the pressure tube just inboard of the outlet burnish mark that is postulated to have a higher than expected level of H_{eq} is very unlikely to contain flaws that are of a severity that would be a site for crack initiation and growth.. This is considered particularly the case since flaws caused by fretting are not observed at the top of the pressure tube where the elevated levels of H_{eq} were detected.

RISK-INFORMED DETERMINISTIC EVALUATION OF FRACTURE PROTECTION FOR THE REGION OF INTEREST IN OUTLET ROLLED JOINTS IN BRUCE UNIT 3

Kinectrics Report No.
B2038/RP/0009 R00

A large number of flaws have been detected by in-service inspection of pressure tubes in Bruce Power reactors over decades of operation. The flaws have a wide range of length, depth and root radius. Based on service experience of successful dispositioning of essentially all of the detected flaws regardless of the flaw length and depth, it would be rare if a flaw existed that did not meet the acceptance criteria for prevention of crack initiation in the CSA Standard N285.8 [20]. Any flaw that is smaller than the detection threshold of the ultrasonic examination technique would therefore not be a risk of being a site for crack initiation and growth. For this reason, the flaw detection limits of the ultrasonic examination technique are considered to not be related to the length of the postulated axial through-wall flaw.

B-4. TECHNICAL BASIS FOR LENGTH OF A POSTULATED AXIAL THROUGH-WALL FLAW OF 18 mm

From Section B-2.2 of this Appendix, the crack length at initial wall penetration inferred from the normal distribution shown in Figure B-3 at a cumulative probability of 97.5% is 20.04 mm. The reference 20 mm length of the postulated axial through-wall flaw is therefore an engineering upper bound on the lengths of DHC cracks at initial wall penetration. From Section B-3, based on service experience of successful dispositioning of essentially all of the detected flaws regardless of the flaw length and depth, it would be rare if a flaw existed that did not meet the acceptance criteria for prevention of crack initiation in the CSA Standard N285.8. From Figure B-3, a postulated axial through-wall flaw length of 18 mm corresponds to a cumulative probability of 78% of a DHC crack at initial wall penetration being less than 18 mm. A 10% reduction in the postulated axial through-wall flaw length from 20 to 18 mm is considered reasonable.

RISK-INFORMED DETERMINISTIC EVALUATION OF FRACTURE PROTECTION FOR THE REGION OF INTEREST IN OUTLET ROLLED JOINTS IN BRUCE UNIT 3

Kinectrics Report No.
B2038/RP/0009 R00

TABLE B-1
LENGTHS OF DHC CRACKS AT INITIAL WALL PENETRATION THAT WERE MEASURED IN EX-SERVICE OVER-EXTENDED ROLLED JOINTS

Fuel Channel and Crack Number	DHC Crack Length Divided by Wall Thickness, L_p/w	DHC Crack Length, L_p (mm)
P4C10 - 4	4.552	18.66
P4C10 - 5	4.552	18.66
P4C10 - 6	3.656	14.99
P4G08 - 1	4.298	17.62
P4G08 - 3	4.738	19.43
P4K04 - 3	4.142	16.98
P4R06 - B1	3.758	15.41
P4R06 - B9	3.572	14.65
P3J08 - 2	3.782	15.51
P3U09 - 1	3.676	15.07
B2A14 - 1	4.360	17.88
B2X14 - 1	3.742	15.34

RISK-INFORMED DETERMINISTIC EVALUATION OF FRACTURE PROTECTION FOR THE REGION OF INTEREST IN OUTLET ROLLED JOINTS IN BRUCE UNIT 3

Kinectrics Report No. B2038/RP/0009 R00

TABLE B-2
COMPARISON OF EMPIRICAL DISTRIBUTION OF MEASURED LENGTHS OF DHC CRACKS AT INITIAL WALL PENETRATION WITH NORMAL DISTRIBUTION OF PENETRATION LENGTH AT THE SAME CUMULATIVE PROBABILITIES

Cumulative Probability of Measured Penetration Length L_p, Pr	Measured Penetration Length, L_p (mm)	Penetration Length Inferred from Normal Distribution at Cumulative Probability Pr, $L_p(Pr)$ (mm)
0.042	14.65	13.72
0.125	14.99	14.72
0.208	15.07	15.29
0.292	15.34	15.74
0.375	15.41	16.14
0.458	15.51	16.50
0.542	16.98	16.86
0.625	17.62	17.23
0.708	17.88	17.62
0.792	18.66	18.07
0.875	18.66	18.65
0.958	19.43	19.64

RISK-INFORMED DETERMINISTIC EVALUATION OF FRACTURE PROTECTION FOR THE REGION OF INTEREST IN OUTLET ROLLED JOINTS IN BRUCE UNIT 3

Kinectrics Report No.
B2038/RP/0009 R00

TABLE B-3
EFFECT OF PARAMETRIC PROBABILITY DISTRIBUTION ON THE CUMULATIVE PROBABILITY OF THE CRACK LENGTH AT INITIAL WALL PENETRATION BEING LESS THAN OR EQUAL TO A POSTULATED FLAW LENGTH OF 17.2 OR 18.2 mm

Parametric distribution	P-value of Kolmogorov-Smirnov goodness-of-fit test	Cumulative probability of $L_p \leq 17.2$ mm	Cumulative probability of $L_p \leq 18.2$ mm
Laplace	0.64	0.733	0.862
Gumbel	0.51	0.690	0.841
Log-logistic	0.49	0.655	0.828
Logistic	0.47	0.642	0.827
Lognormal	0.45	0.636	0.817
Normal	0.43	0.619	0.812
Inverse Gaussian	0.40	0.641	0.827
Birnbaum-Saunders	0.40	0.641	0.827
Gamma	0.39	0.636	0.826
Weibull	0.38	0.575	0.798

RISK-INFORMED DETERMINISTIC EVALUATION OF FRACTURE PROTECTION FOR THE REGION OF INTEREST IN OUTLET ROLLED JOINTS IN BRUCE UNIT 3
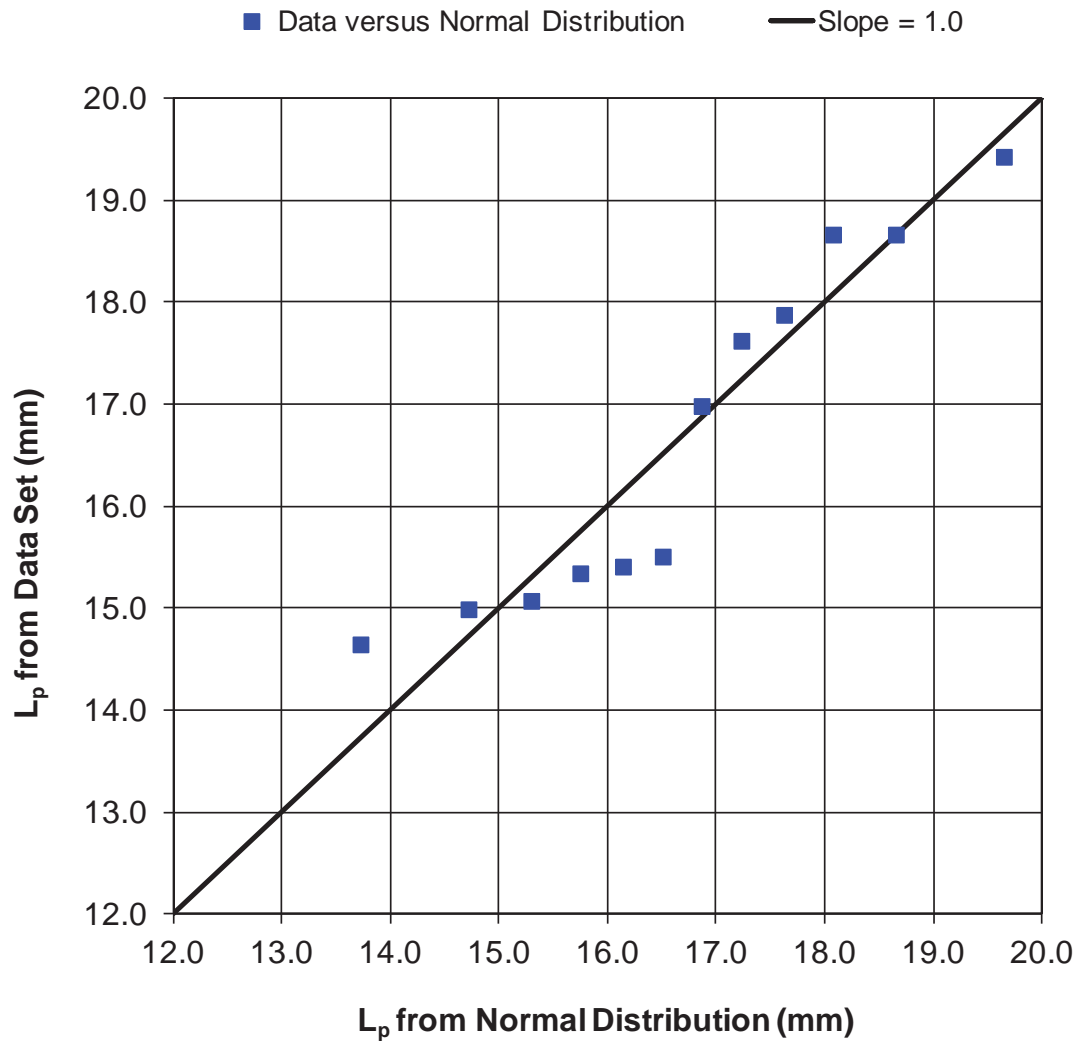
Kinectrics Report No.
B2038/RP/0009 R00

Figure B-1: Comparison of Empirical Distribution of Measured Lengths of DHC Cracks at Initial Wall Penetration with Normal Distribution of Penetration Length at the Same Cumulative Probabilities
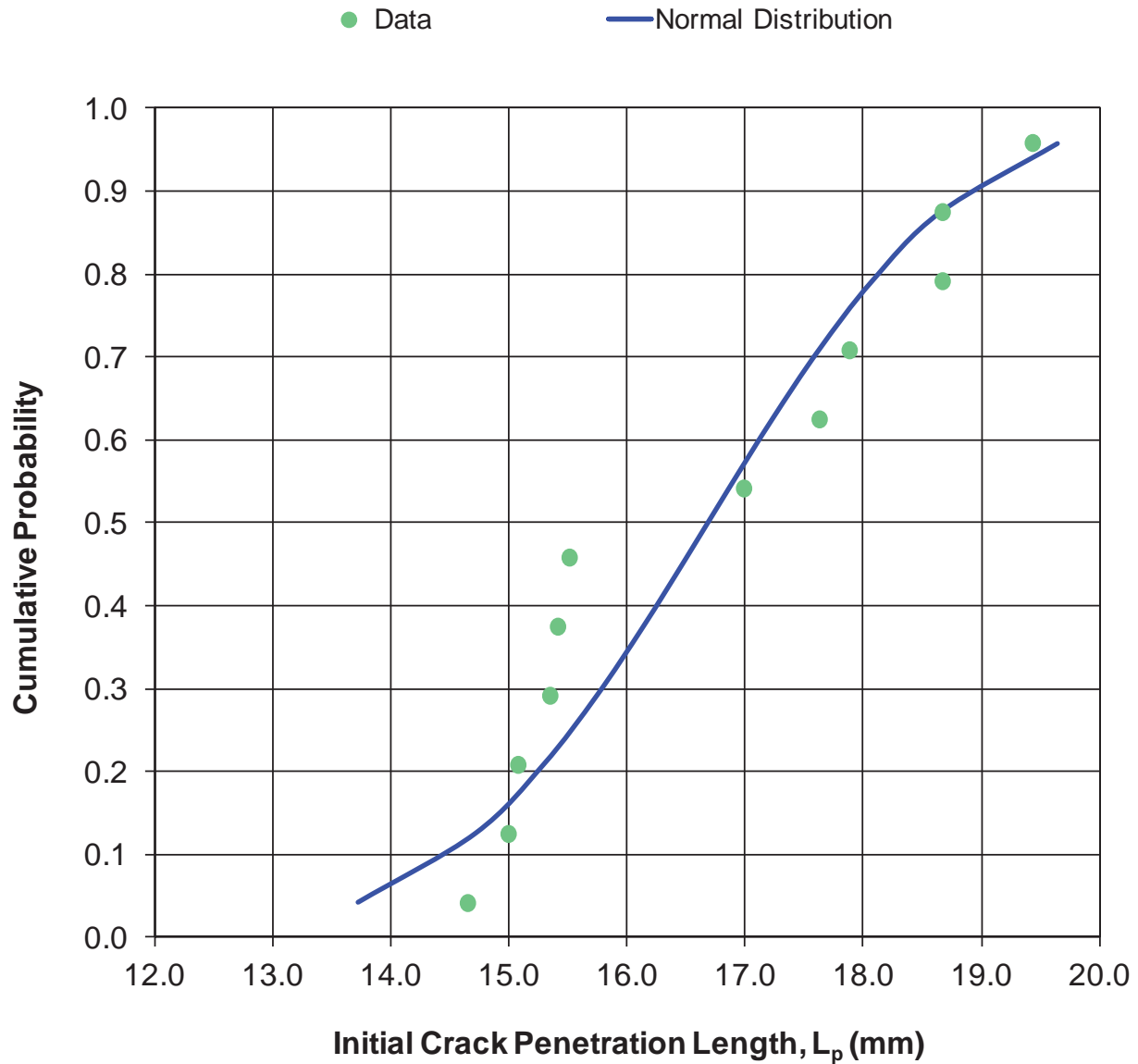
RISK-INFORMED DETERMINISTIC EVALUATION OF FRACTURE PROTECTION FOR THE REGION OF INTEREST IN OUTLET ROLLED JOINTS IN BRUCE UNIT 3

Kinectrics Report No. B2038/RP/0009 R00

Figure B-2: Comparison of Cumulative Probability Inferred from Empirical Distribution of Measured Lengths of DHC Cracks at Initial Wall Penetration with Cumulative Probability of Normally Distributed Penetration Length
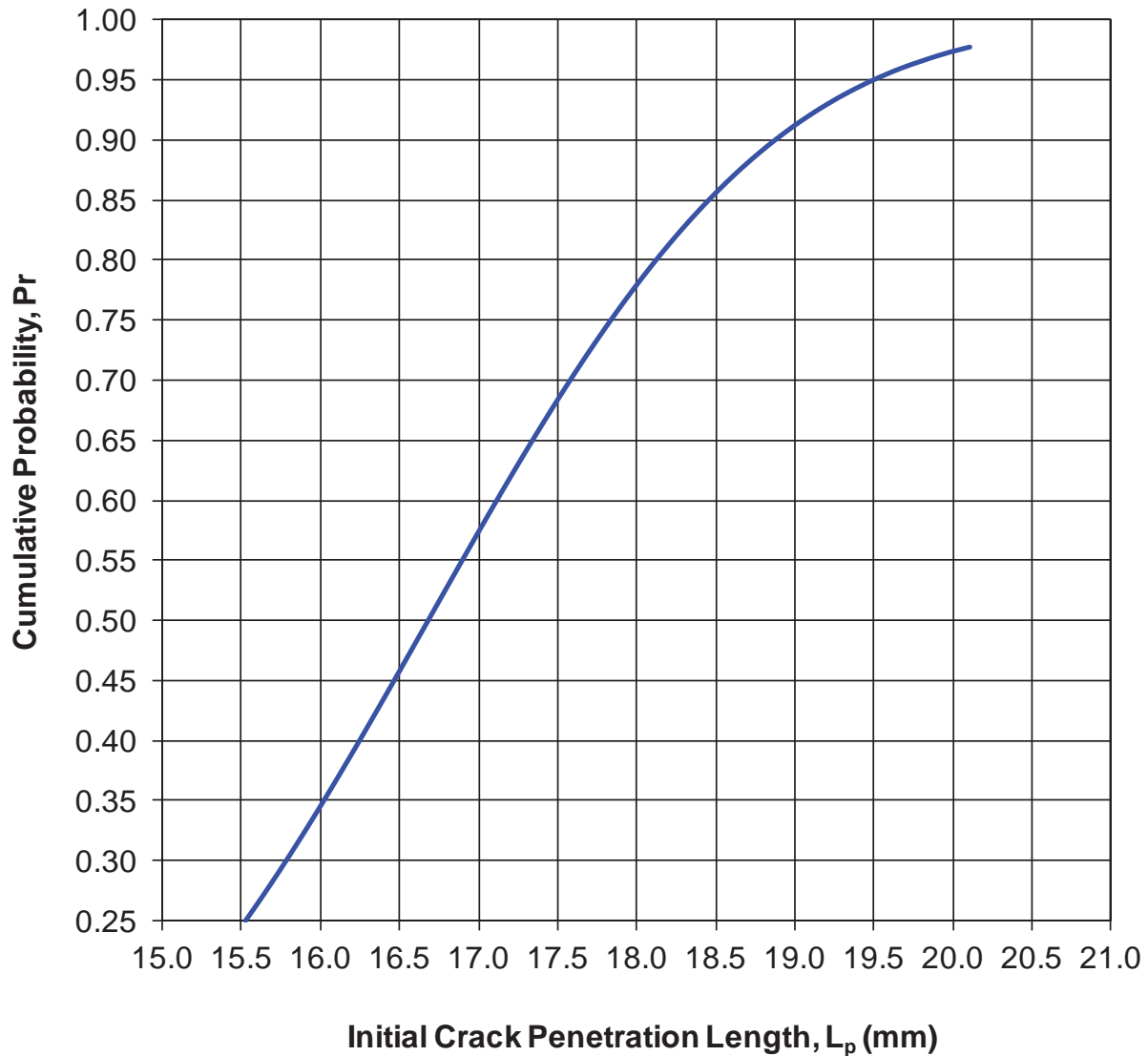
RISK-INFORMED DETERMINISTIC EVALUATION OF FRACTURE PROTECTION FOR THE REGION OF INTEREST IN OUTLET ROLLED JOINTS IN BRUCE UNIT 3

Kinectrics Report No.
B2038/RP/0009 R00

Figure B-3: Variation of Cumulative Probability of Normally Distributed Length of DHC Cracks at Initial Wall Penetration

RISK-INFORMED DETERMINISTIC EVALUATION OF FRACTURE PROTECTION FOR THE REGION OF INTEREST IN OUTLET ROLLED JOINTS IN BRUCE UNIT 3

Kinectrics Report No. B2038/RP/0009 R00

APPENDIX C

TABULAR VALUES OF REACTOR OUTLET HEADER CRITICAL INTERNAL PRESSURES AND REVISED PRESSURE-TEMPERATURE LIMITS FOR OVERPRESSURE EXCURSION

With reference to Section 8.6 of this report, tabular values of the variation of the critical ROH internal pressure, $(p_{Flcr})_{ROH}$, with temperature for an overpressure excursion for a fuelled channel with a postulated axial through-wall flaw length of 20 mm, and an H_{eq} of 200 ppm, are given in Table C-1. The critical pressures are based on the Revision 2 engineering fracture toughness model with no adjustment factor for high levels of H_{eq}. The revised ROH pressure-temperature limits for the overpressure excursion based on a 15% margin on the critical pressures are also given in Table C-1 [3].

RISK-INFORMED DETERMINISTIC EVALUATION OF FRACTURE PROTECTION FOR THE REGION OF INTEREST IN OUTLET ROLLED JOINTS IN BRUCE UNIT 3

Kinectrics Report No. B2038/RP/0009 R00

TABLE C-1
TABULAR VALUES OF REACTOR OUTLET HEADER
CRITICAL INTERNAL PRESSURES AND REVISED
PRESSURE-TEMPERATURE LIMITS FOR OVERPRESSURE EXCURSION

Temperature (°C)	Critical Internal Pressure at ROH (MPa)	Revised ROH Pressure-Temperature Limit for Overpressure Excursion (MPa)
25.0	7.92	6.74
27.5	7.98	6.78
30.0	8.04	6.83
32.5	8.09	6.88
35.0	8.15	6.93
38.0	8.22	6.98
40.0	8.26	7.02
42.5	8.31	7.07
45.0	8.37	7.11
47.5	8.42	7.16
50.0	8.48	7.20
52.5	8.53	7.25
55.0	8.58	7.29
57.5	8.63	7.34
60.0	8.69	7.38
62.5	8.74	7.43
65.0	8.79	7.47
67.5	8.84	7.52
70.0	8.89	7.56
72.5	8.94	7.60
75.0	8.99	7.65
77.5	9.04	7.69
80.0	9.09	7.73
82.5	9.14	7.77
85.0	9.19	7.81
87.5	9.24	7.86
90.0	9.29	7.90
92.5	9.34	7.94
95.0	9.39	7.98
97.5	9.43	8.02
100.0	9.48	8.06

Proprietary and Confidential

RISK-INFORMED DETERMINISTIC EVALUATION OF FRACTURE PROTECTION FOR THE REGION OF INTEREST IN OUTLET ROLLED JOINTS IN BRUCE UNIT 3

Kinectrics Report No.
B2038/RP/0009 R00

TABLE C-1 (continued)
TABULAR VALUES OF REACTOR OUTLET HEADER
CRITICAL INTERNAL PRESSURES AND REVISED
PRESSURE-TEMPERATURE LIMITS FOR OVERPRESSURE EXCURSION

Temperature (°C)	Critical Internal Pressure at ROH (MPa)	Revised ROH Pressure-Temperature Limit for Overpressure Excursion (MPa)
102.5	9.53	8.10
105.0	9.57	8.14
107.5	9.62	8.18
110.0	9.67	8.22
112.5	9.71	8.26
115.0	9.76	8.29
117.5	9.80	8.33
120.0	9.85	8.37
122.5	9.89	8.41
125.0	9.94	8.45
127.5	9.98	8.48
130.0	10.03	8.52
132.5	10.07	8.56
135.0	10.11	8.60
137.5	10.15	8.63
140.0	10.20	8.67
142.5	10.24	8.70
145.0	10.28	8.74
147.5	10.32	8.78
150.0	10.37	8.81
152.5	10.41	8.85
155.0	10.45	8.88
157.5	10.49	8.91
160.0	10.53	8.95
162.5	10.57	8.98
165.0	10.61	9.02
167.5	10.65	9.05
170.0	10.69	9.08
172.5	10.73	9.12
175.0	10.77	9.15
177.5	10.80	9.18

RISK-INFORMED DETERMINISTIC EVALUATION OF
FRACTURE PROTECTION FOR THE REGION OF
INTEREST IN OUTLET ROLLED JOINTS IN BRUCE UNIT 3

Kinectrics Report No.
B2038/RP/0009 R00

TABLE C-1 (continued)
TABULAR VALUES OF REACTOR OUTLET HEADER
CRITICAL INTERNAL PRESSURES AND REVISED
PRESSURE-TEMPERATURE LIMITS FOR OVERPRESSURE EXCURSION

Temperature (°C)	Critical Internal Pressure at ROH (MPa)	Revised ROH Pressure-Temperature Limit for Overpressure Excursion (MPa)
180.0	10.84	9.22
182.5	10.88	9.25
185.0	10.92	9.28
187.5	10.96	9.31
190.0	10.99	9.34
192.5	11.03	9.38
195.0	11.07	9.41
197.5	11.11	9.44
200.0	11.14	9.47
202.5	11.18	9.50
205.0	11.22	9.54
207.5	11.26	9.57
210.0	11.31	9.61
212.5	11.36	9.66
215.0	11.42	9.71

Enclosure 4

B-03644.4 LOF NSAS, Revision 000

**Concentrating Hydrogen Isotopes at the Top of Tube
at the Outlet End Rolled Joint Region**

CANADIAN NUCLEAR LABORATORIES

CONCENTRATING HYDROGEN ISOTOPES AT THE TOP OF THE TUBE AT THE OUTLET END ROLLED JOINT REGION

B-03644.4 LOF NSAS

REV. 000

☒ Accepted ☐ Accepted As Noted – Revision Required

☐ Rejected ☐ Accepted As Noted – No Revision Required

FOR USE AT BRUCE POWER

ACCEPTED: **MONIQUE IP**

(Print Name) (Signature)

TITLE: **SENIOR TECHNICAL OFFICER**

(Print Title)

DATE: **17SEP2021**

(DDMMMYYYY)

ACCEPTANCE OF THIS DOCUMENT DOES NOT RELIEVE THE

CONTRACTOR OF RESPONSIBILITY FOR ANY ERRORS OR OMISSIONS.

File No.:	153	31113	401	000
	Doc. Collection ID	Subject Index	Doc. Code	Serial No.

Non-Standard ID: **RCC-21-018**
Date: 2021/09/17

To: L. Micuda

From: I.J. Muir

Cc: D. Cho, A. Glover, M. Ip, D. Metzger, A.C. Wallace, H. Chaput, E. Phillion, B. Payne

Subject: Concentrating Hydrogen Isotopes at the Top of Tube at the Outlet End Rolled Joint Region

1.   BACKGROUND

The intent of this communication is to provide a technical basis for the observed segregation of hydrogen isotope concentrations towards the top region at the very outlet end of the B6S13 pressure tube and its implication in defining a region of interest with respect to hydrogen isotope concentrations in excess of 120 ppm which is the validity limit of Rev. 1 of the Cohesive-Zone Fracture Toughness model for the backend of the pressure tube [1]. Tube G0291 was removed from lattice site S13 of the Bruce Unit 6 reactor after 271,729 hot hours (243,773 EFPH) as part of the Unit 6 Major Component Replacement project. The pressure tube, end fittings and garter springs were shipped to Chalk River Laboratories for surveillance analysis under COG Joint Project 4680.

While in service, hydrogen isotope concentration measurements were acquired from the outlet rolled joint region of channel B6S13 during both the B1561 (233,970 HH) and B1761 (253,093 HH) outages. The B1561 outage sampled close to the top of the tube (16° scrape sample centered at +12°) on the 3 o'clock side[1] where deuterium concentrations in excess of 300 ppm were observed outboard of the burnish mark. In contrast, when sampling marginally further from the top of tube (16° scrape sample centered at -28°) on the 9 o'clock side during B1761, much lower concentrations between 100 and 150 ppm D were reported. In hindsight, this large difference in hydrogen isotope concentrations around the top of tube is indicative of hydrogen segregation to the top of tube and one of the motivators for selecting the B6S13 tube for surveillance. It is noteworthy that the higher concentration measured closer to the top of tube was measured in 2015 and the lower concentration measured in 2017 after a further operating interval of approximately 20,000 hot hours.

---

[1] Circumferential locations reported as clock position are as viewed from the outlet end of the tube.

The segregation of hydrogen isotopes to the top of tube is attributed to hydrogen isotope migration to the cooler portion of the tube owing to the effect of flow bypass resulting from diametral creep of the pressure tube. Diametral creep and flow bypass are known phenomenon toward the outlet end of the tube; while peak diametral creep occurs inboard of the outlet rolled joint, the thermal gradient between top and bottom continue into the outlet rolled joint. Hydrogen isotope segregation to the top of tube on the order of 20 ppm (difference in [Heq] between top and bottom of the tube) attributed to thermal gradients between top and bottom of the tube have been observed at the outlet rolled joint region in previous surveillance tubes [2].

2.   OBSERVATIONS FROM RECENT SURVEILLANCE TUBE EXAMINATIONS

Hydrogen isotopes in the rolled joint region of the pressure tube originate from three sources: hydrogen initially present in the tube from fabrication, deuterium (including minor amounts of hydrogen) entering the tube during operation from corrosion reactions between the tube and coolant, and deuterium (including minor amounts of hydrogen) entering the tube from the stainless steel end fitting during operation from corrosion reactions between the end fitting and coolant. The operational sources are evaluated during surveillance examinations and ingress through the end fitting has been observed to be the greater contributor to hydrogen isotope concentrations in this region. For the case of B6S13, the ingress through the inside surface of the pressure tube is in line with other surveillance tubes and scrape campaigns, while the ingress through the rolled joint is marginally greater but well within prior experience projected forward. There is no need, or obvious evidence, for an additional and unknown source of hydrogen to account for the current observations.

Many of the recent surveillance tubes prior to B6S13 were found to experience low levels of ingress through the outlet rolled joint and as a result, hydrogen segregation to the top of the tube was observed to be on the order of 20 ppm on total concentrations of 60 to 70 ppm hydrogen equivalent. On the other hand, the B6S13 tube exhibited a higher amount of ingress through the rolled joint but within projections based on prior surveillance experience. The higher ingress coupled with longer service life has resulted in substantially greater segregation of hydrogen isotopes towards the top of the tube (Figure 1).

In Figure 1, it is observed that while the hydrogen isotope concentrations at the top of the tube are quite high throughout the axial length of the profile, the concentrations in the lower portion of the tube are on the order of 60 – 70 ppm hydrogen equivalent much like prior experience. That is, high hydrogen isotope concentrations are only observed in the upper few clock positions: 12:00, 1:00, and to some extent 11:00. Also evident from Figure 1 is the beginning of the convergence of the profiles for each circumferential position for sampling locations inboard of the roll transition (i.e., burnish mark) of the joint.
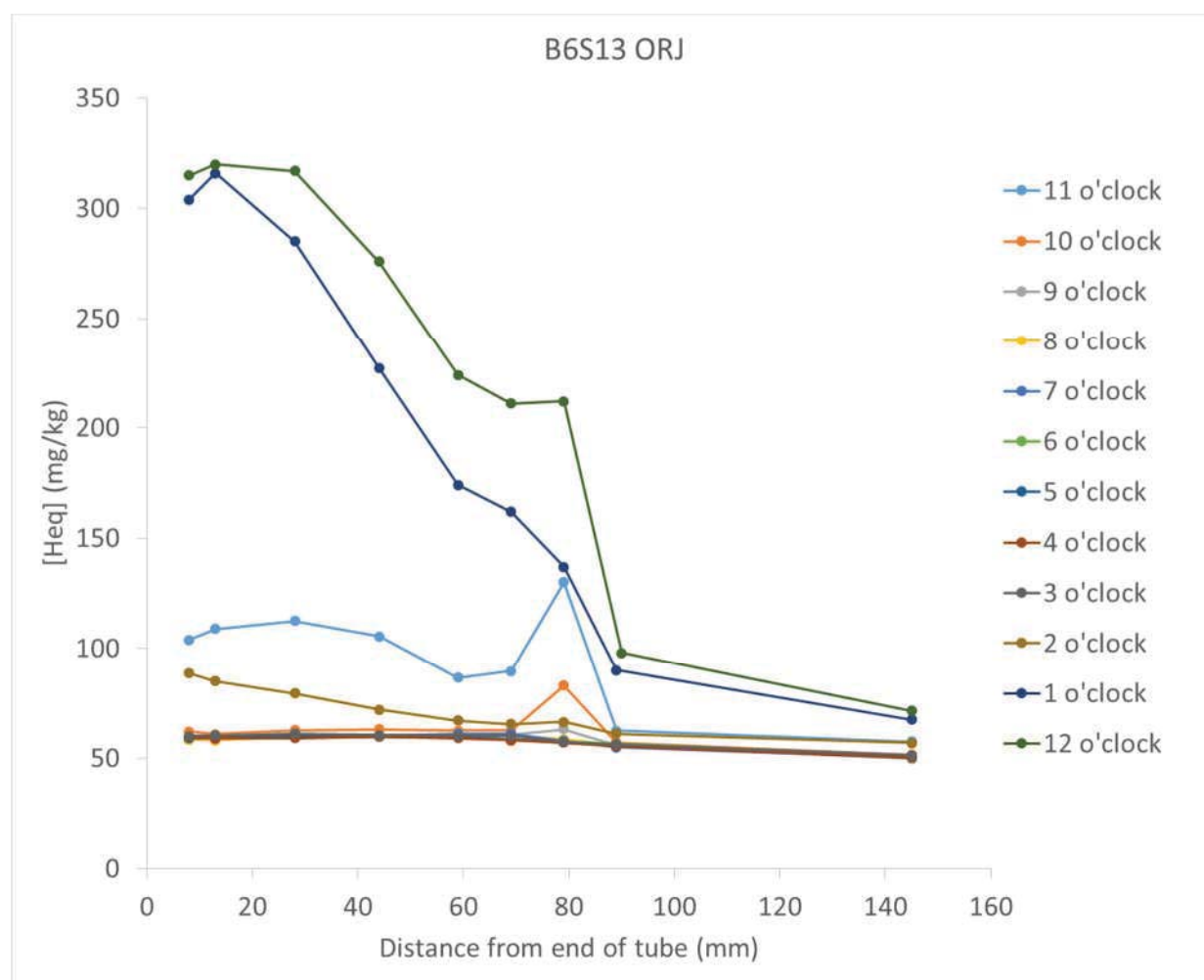
Figure 1: Hydrogen equivalent concentration measurements (obtained to date) from the outlet end of the B6S13 surveillance tube plotted as a function of axial location for the various clock positions.

3.   IMPACT OF THERMAL GRADIENTS ON HYDROGEN ISOTOPE MIGRATION

For the rolled joint region at the outlet end of the pressure tube, the main factors for high hydrogen isotope concentrations at the top of the tube compared to regions lower down are ingress over a long-service life coupled with diametral creep resulting in flow bypass. Diametral creep and flow bypass towards the outlet end of the tube can result in thermal gradients on the order of 20 °C (or slightly more) between the top and bottom of the tube.

Hydrogen isotopes will migrate to the cooler regions, in this case the top of the tube. Furthermore, the saturation concentration for hydrogen is a function of temperature with lower temperatures resulting in lower saturation concentrations. The migration of hydrogen isotopes to the top of the tube where the saturation concentration is lower is followed by precipitation of solid hydride/deuteride phases at the top of the tube. Precipitation of solid hydrides is a key part of the mechanism as it serves to remove hydrogen from solution thereby preventing an opposing top to bottom concentration gradient that would limit the migration

due to the thermal gradient. The end result is a concentrating effect of solid hydride phases at the top of the tube while the hydrogen isotope concentration in the rest of the circumference remain near the saturation concentration.

4.   IMPLICATIONS ON THE REGION OF INTEREST OF HIGH HYDROGEN EQUIVALENT CONCENTRATIONS

Bruce Power has defined the region of interest for high hydrogen isotope concentrations as the top 120° of the tube, which is substantiated by data obtained to date from the B6S13 surveillance program along with recent scrape samples from the Bruce Unit 3 2021 outage. The concentrating mechanism described above is based on thermodynamics for which it would be improbable for the system to reverse and redistribute the hydrogen isotopes elsewhere within the tube.

Any expansion of the region of interest is expected to be slow and will rely upon further ingress of hydrogen isotopes when returning the unit to operation. Continued operation of the unit, implies continued ingress into the tube with the outlet rolled joint region being of concern. Even with additional ingress, the ingress rates observed to date are not expected to expand the region of interest beyond the 120° over the next planned operating interval.

5.   SUMMARY

The high hydrogen isotope concentrations recently observed in scrape samples obtained from Bruce Unit 3 and the B6S13 surveillance tube are confined to the very top of the tube. These observations are consistent with thermodynamics such that the region of interest is not likely to expand beyond the current top 120° of the tube. Ingress of hydrogen isotopes over the coming operating intervals is not expected to expand the region of interest currently suggested to be confined to the top 120° of the tube. These claims are consistent with previous results from repeat scraped channels where high deuterium concentrations were observed close to the top of the tube only to be followed in subsequent outages by lower deuterium concentrations slightly down the tube from top of center.

6.   REFERENCES

[1]   D. Scarth, C. Liu, S. Xu, and L. Gutkin, "Cohesive-Zone Based Fracture Toughness Model for Zr-2.5Nb Pressure Tubes," Revision 1, COG Report No. COG-JP-4363- V256/COG-12-1007-R01, May 2013.

[2]   B. Payne, "Examination of Circumferential Variation of Hydrogen Isotope Concentrations In The Rolled Joint Regions Of Ex-Service Pressure Tubes By Hot Vacuum Extraction Mass Spectrometry", COG Report No. COG-19-1034, March 2021.

Ian Muir
Technical Manager,
Reactor Components & Systems
Reactor Fleet Sustainability Directorate

Enclosure 5

NK21-03644.4 LOF NSAS, Revision 000

**Re: Hydrogen Equivalent Concentration Measurements Taken Near the Outlet
Burnish Mark in the Bruce Unit 3 2021 Outage (A2131)**

Supplier Document Acceptance Form

Bruce *Power*™

KINECTRICS

RE: HYDROGEN EQUIVALENT CONCENTRATION MEASUREMENTS TAKEN NEAR THE OUTLET BURNISH MARK IN THE BRUCE UNIT 3 OUTAGE (A2131)

NK21-03644.4 LOF NSAS

REV. 000

☒ Accepted ☐ Accepted As Noted – Revision Required
☐ Rejected ☐ Accepted As Noted – No Revision Required

FOR USE AT BRUCE POWER

ACCEPTED: **MONIQUE IP**

_____ _____
(Print Name) (Signature)

TITLE: **SENIOR TECHNICAL OFFICER**

_____
(Print Title)

DATE: **17SEP2021**

_____
(DDMMMYYYY)

ACCEPTANCE OF THIS DOCUMENT DOES NOT RELIEVE THE

CONTRACTOR OF RESPONSIBILITY FOR ANY ERRORS OR OMISSIONS.

Kinectrics Inc.
4th Floor, 393 University Avenue
Toronto, Ontario, Canada M5G 1E6
Tel: (416) 592-7000
www.kinectrics.com

September 17, 2021

L. Micuda
Bruce Power
123 Front St., 4th Floor
Toronto, ON, M5J 2M2

Re: Hydrogen Equivalent Concentration Measurements Taken Near the Outlet Burnish Mark in the Bruce Unit 3 2021 Outage (A2131)

Dear Mr. Micuda,

1.0   INTRODUCTION

The purpose of this letter is to provide a graphical summary of [H]eq derived from measurements taken during the Bruce Unit 3 2021 outage (A2131). The purpose of this revision is to add additional plots with fixed scales on the [H]eq axis for comparison purposes.

2.0   METHODOLOGY

The relevant measurements were taken from axial locations corresponding to ~10 mm outboard, ~20 mm inboard and ~43 mm inboard of the outlet burnish mark (BM) of Bruce Unit 3 pressure tubes (PT). The applicable measurements [1] [2] [3] [4] were converted using the following equation:

$$[H]_{eq} = \frac{[D]_{measured}}{2} + [H]_{initial}$$

Where,

$[H]_{eq}$ = Hydrogen equivalent concentration

$[D]_{measured}$ = Measured deuterium concentration

$[H]_{initial}$ = Initial hydrogen concentration at pressure tube installation time (estimated based on offcut measurements)

This method assumes that measured [H] beyond the initial [H] is due solely to sample contamination. However, elevated [H] measurements have been observed in the region of interest (just inboard of the outlet rolled joint (RJ) at the top of the tube) which cannot be attributed entirely to contamination during scrape sampling and/or analysis, consistent with OPEX from removed tubes. Development of an approach for appropriately accounting for elevated [H] measurements in RJ scrape samples is ongoing[1].

For comparison, measurements of punch samples from Bruce Unit 6 ex-service tubes B6N07 [6] and B6S13 [7] have been included where applicable (at 10 mm outboard and 20 mm inboard

---

[1] Note that the postulated bounding [H]eq level at MCR time for the risk-informed deterministic evaluation of fracture protection in the region of interest of Bruce Unit 3 has accounted for elevated observed [H] [5].

of the outlet BM). For these samples, all measured [H] is accounted for as no contamination is expected during punch sampling.

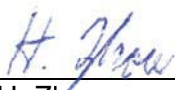The PTs were grouped based on which end of the PT was installed at the outlet; the front end or the back end.

3.0   RESULTS

The measurements separated by axial location and pressure tube orientation are plotted in Figures 1 to 6. There are no elevated $[H]_{eq}$ measurements outside of the 10 o'clock to 2 o'clock (-60° and +60° from top-dead-center) region of interest (this region is indicated in each plot). In addition, the magnitude of the circumferential variation in $[H]_{eq}$ measurements decreases with increasing distance inboard of the outlet BM. This is especially visible in Figures 7 to 12, which are the same plots as in Figures 1 to 6 but with a fixed scale for the $[H]_{eq}$ axis.

A comparison of measured $[H]_{eq}$ acquired from outlet RJ locations outside the region of interest against the current Bruce Unit 3 outlet RJ generic deterministic $[H]_{eq}$ predictions [8] is shown in Figure 13. As shown, all the data are well bounded by the current generic deterministic predictions that are used in fitness for service assessments.

Prepared by:

H. Zhou
Analyst
Fuel Channel Integrity & Services
Materials & Major Components

Prepared by:

L. Popescu
Technical Expert
Fuel Channel Integrity & Projects
Materials & Major Components

Verified by:

A. Sahoo
Senior Research Analyst
Fuel Channel Integrity & Methods
Materials & Major Components

Reviewed by:

G. Allen, P.Eng
Section Manager
Fuel Channel Integrity & Services
Materials & Major Components

Approved by:

J. Robertson, P.Eng
Service Line Director
Fuel Channel Integrity & Operations
Materials & Major Components

4.0   REFERENCES

[1] H. Chaput, E-mail to L. Micuda, "Verified A2131 Results - Shipments up to July 2021", Kinectrics File: B2266/CT/0002 R00, September 7, 2020.

[2] M. McDonald, E-mail to J. Goldberg et al., "Kinectrics TDMS Final Report", Kinectrics File: B2210/RP/0006 R00, August 6, 2021.

[3] F. Baig, E-mail to L. Micuda, "Verified A2131 Results - August shipment", Kinectrics File: B2266/CT/0003 R00, September 9, 2021.

[4] M. McDonald, E-mail to L. Popescu, "TDMS A2131 Results - 8SEP2021", Kinectrics File: B2266/RE/0004 R00, September 8, 2021.

[5] C. Nam and K. Harrison, Letter to D. Scarth, "Postulated Bounding [H]eq Levels for Bruce Unit 3 Fracture Protection Evaluation", Kinectrics File: B2038/LET/0009 R00, August 24, 2021.

[6] E. Phillion, E-mail to L.Micuda. et al., "B6N07 IRJ and ORJ Results Sampled to Date", Kinectrics File: B2266/CT/0005 R00, September 9, 2021.

[7] E. Phillion, E-mail to L. Micuda et al., "B6S13 IRJ and ORJ Results Sampled to Date", Kinectrics File: B2266/CT/0004 R00, September 9, 2021..

[8] C. Nam, "2014 Revised Estimates of Generic Hydrogen Equivalent Concentration for Inlet and Outlet Rolled Joint Regions of Bruce 3 Pressure Tubes", Kinectrics File: B1450/RP/012 R00, Bruce Power File: NK21-REP-03644.4-00032 R00, December 5, 2014.
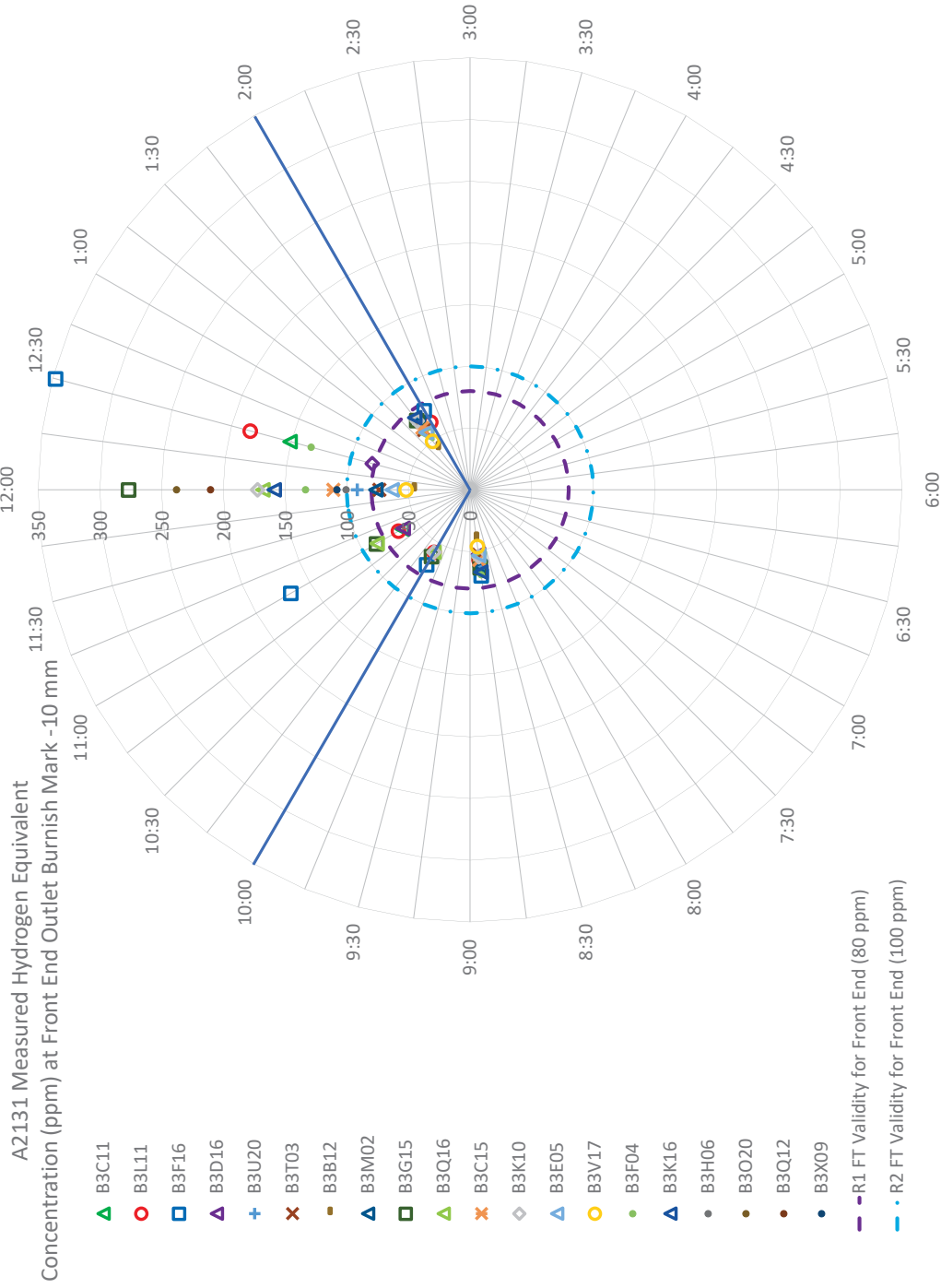
Figure 1: A2131 Measured $[H]_{eq}$ (ppm) at Front End Outlet Burnish Mark -10 mm

Note for Figure 1:

R1 FT and R2 FT refer to the fracture protection validity limits for the Rev1 and Rev2 fracture toughness models, respectively. They do not apply outboard of the BM but they are shown here for illustrative purposes.
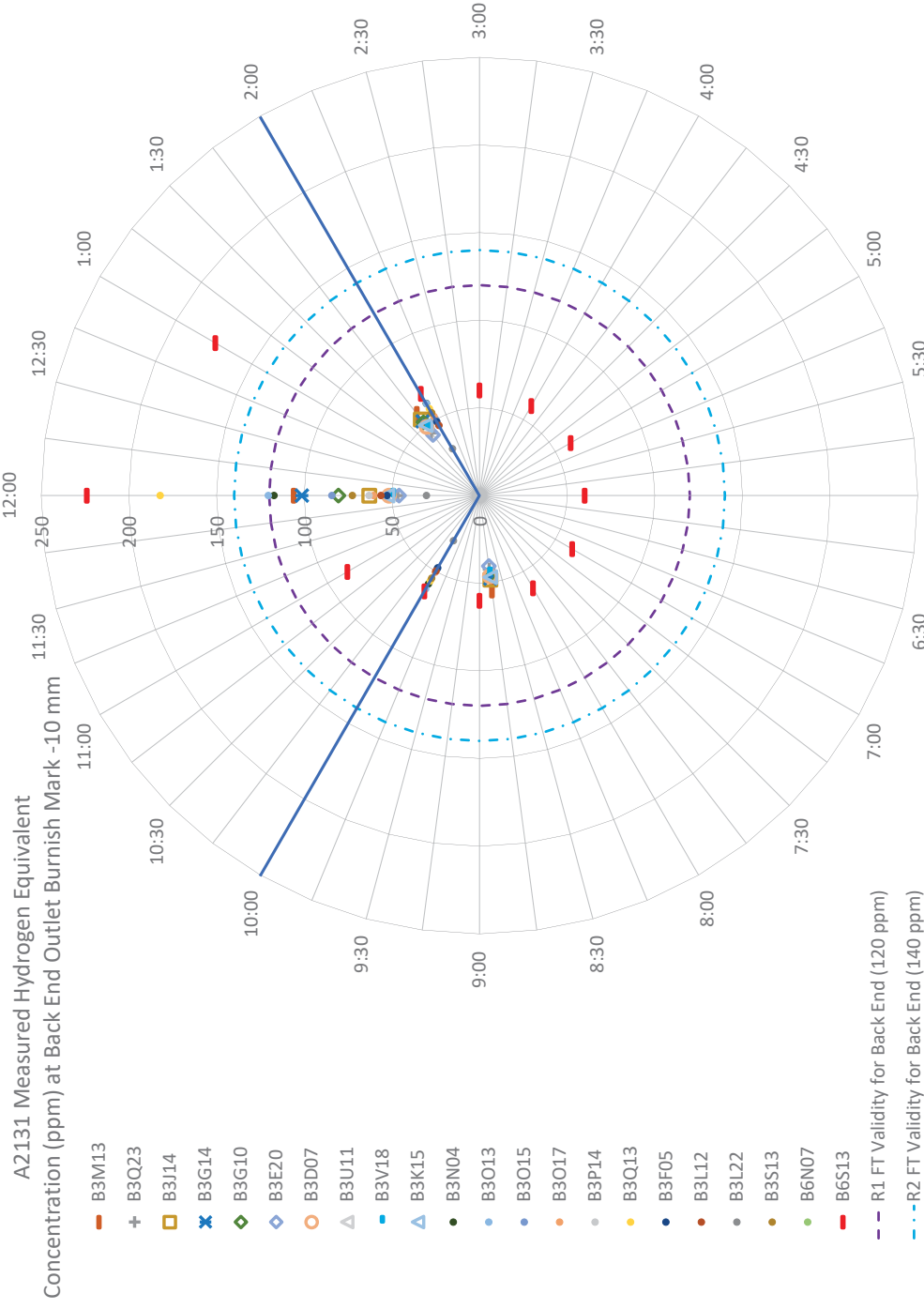
A2131 Measured Hydrogen Equivalent
Concentration (ppm) at Back End Outlet Burnish Mark -10 mm

Legend: B3M13, B3Q23, B3J14, B3G14, B3G10, B3E20, B3D07, B3U11, B3V18, B3K15, B3N04, B3O13, B3O15, B3O17, B3P14, B3Q13, B3F05, B3L12, B3L22, B3S13, B6N07, B6S13, R1 FT Validity for Back End (120 ppm), R2 FT Validity for Back End (140 ppm)

Figure 2: A2131 [H]eq (ppm) at Back End Outlet Burnish Mark -10 mm

Note for Figure 2:

R1 FT and R2 FT refer to the fracture protection validity limits for the Rev1 and Rev2 fracture toughness models, respectively. They do not apply outboard of the BM but they are shown here for illustrative purposes.
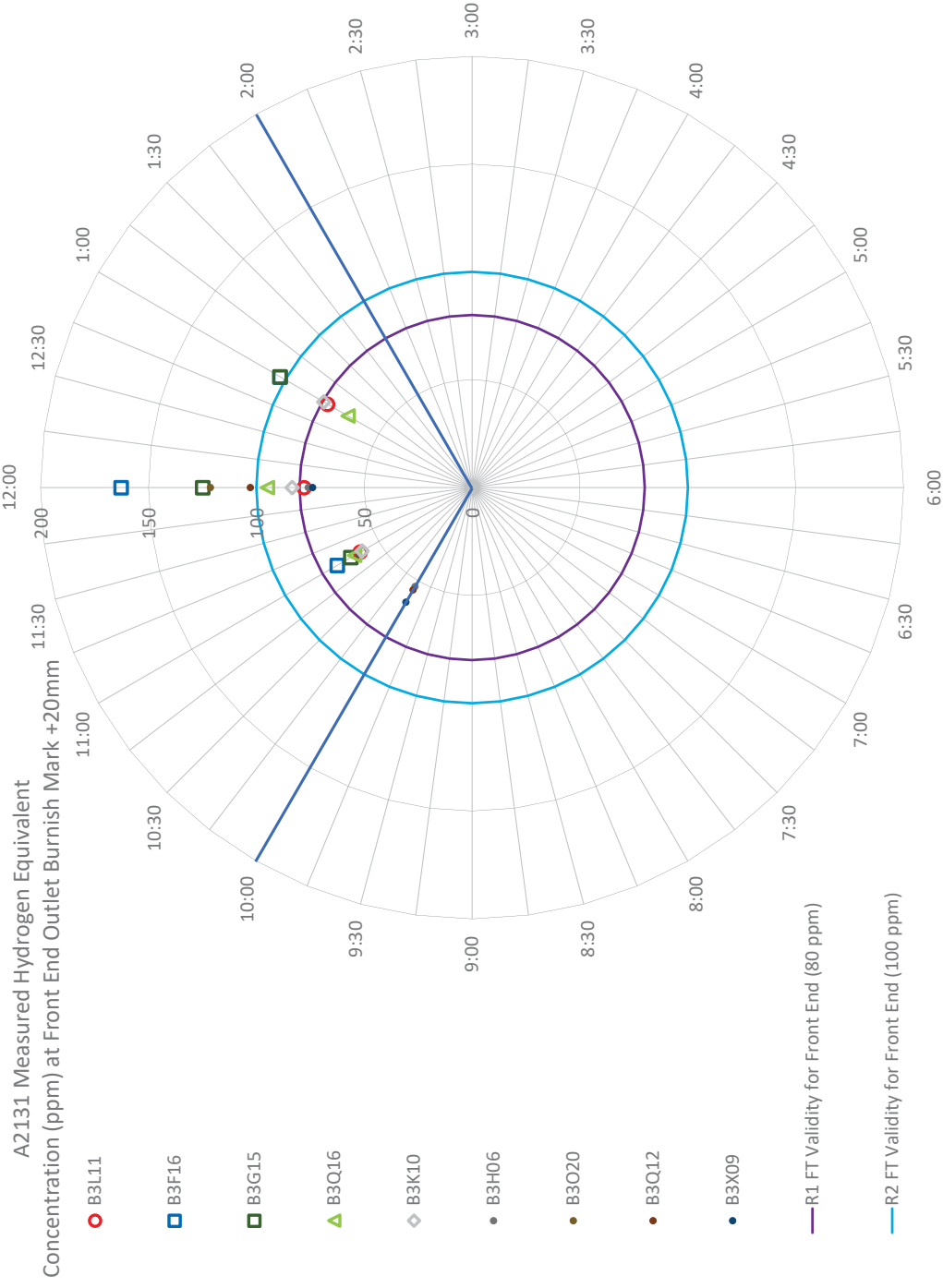
A2131 Measured Hydrogen Equivalent
Concentration (ppm) at Front End Outlet Burnish Mark +20mm

○ B3L11
□ B3F16
□ B3G15
◁ B3Q16
◇ B3K10
• B3H06
• B3O20
• B3Q12
• B3X09
—— R1 FT Validity for Front End (80 ppm)
—— R2 FT Validity for Front End (100 ppm)

Figure 3: A2131 Measured [H]$_{eq}$ (ppm) at Front End Outlet Burnish Mark +20 mm

Note for Figure 3:

R1 FT and R2 FT refer to the fracture protection validity limits for the Rev1 and Rev2 fracture toughness models, respectively.

A2131 Measured Hydrogen Equivalent
Concentration (ppm) at Back End Outlet Burnish Mark +20mm

Legend:
- B3N04
- B3O13
- B3O15
- B3O17
- B3P14
- B3Q13
- B3F05
- B3L12
- B3L22
- B3S13
- B6N07
- B6S13
- R1 FT Validity for Back End (120 ppm)
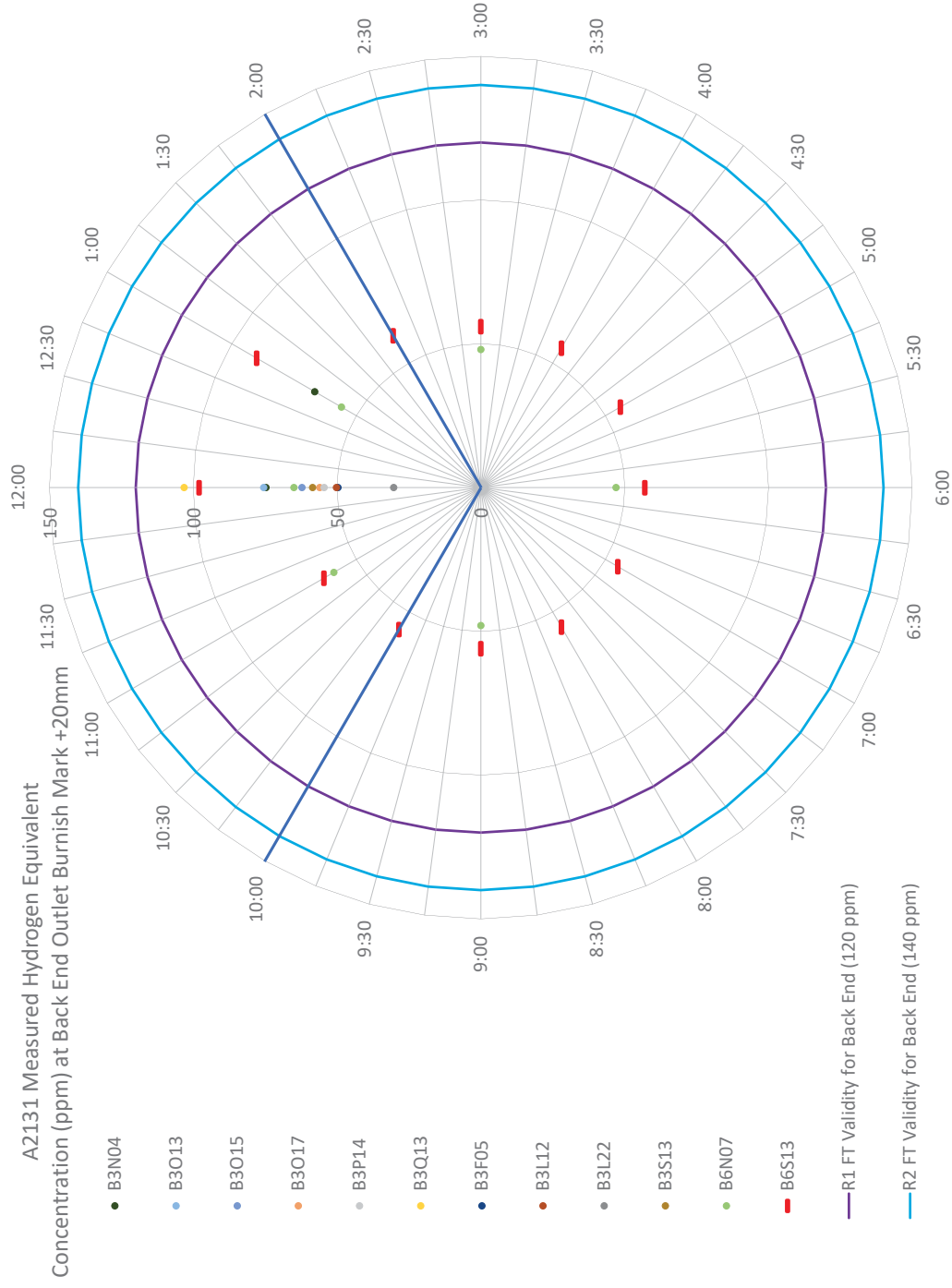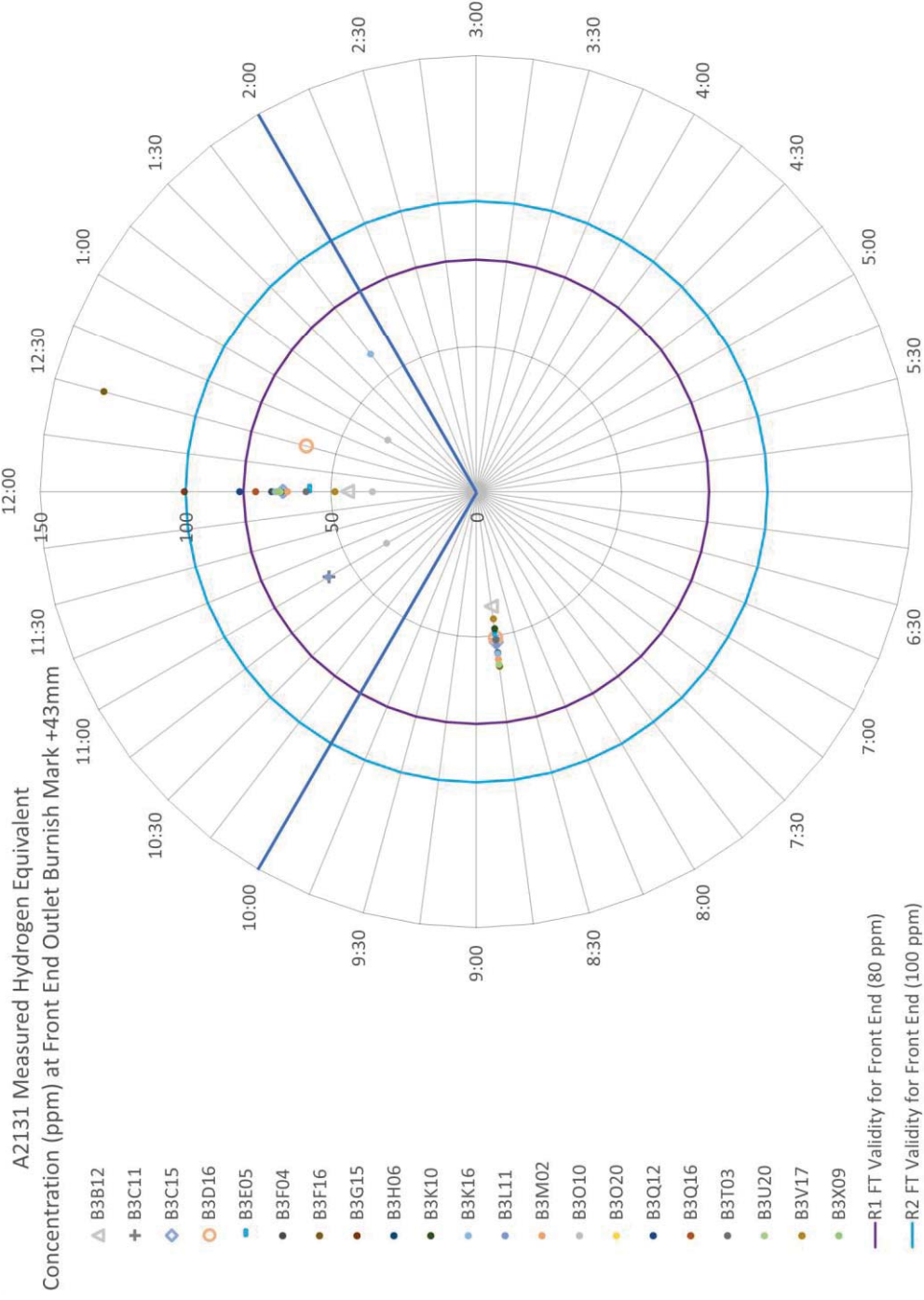- R2 FT Validity for Back End (140 ppm)

Figure 4: A2131 Measured $[H]_{eq}$ (ppm) at Back End Outlet Burnish Mark +20 mm

Note for Figure 4:

R1 FT and R2 FT refer to the fracture protection validity limits for the Rev1 and Rev2 fracture toughness models, respectively.

A2131 Measured Hydrogen Equivalent
Concentration (ppm) at Front End Outlet Burnish Mark +43mm

Legend:
△ B3B12
+ B3C11
◇ B3C15
○ B3D16
▪ B3E05
• B3F04
• B3F16
• B3G15
• B3H06
• B3K10
• B3K16
• B3L11
• B3M02
• B3O10
• B3O20
• B3Q12
• B3Q16
• B3T03
• B3U20
• B3V17
• B3X09
—— R1 FT Validity for Front End (80 ppm)
—— R2 FT Validity for Front End (100 ppm)

Figure 5: A2131 Measured [H]$_{eq}$ (ppm) at Front End Outlet Burnish Mark +43 mm

Note for Figure 5:

R1 FT and R2 FT refer to the fracture protection validity limits for the Rev1 and Rev2 fracture toughness models, respectively.
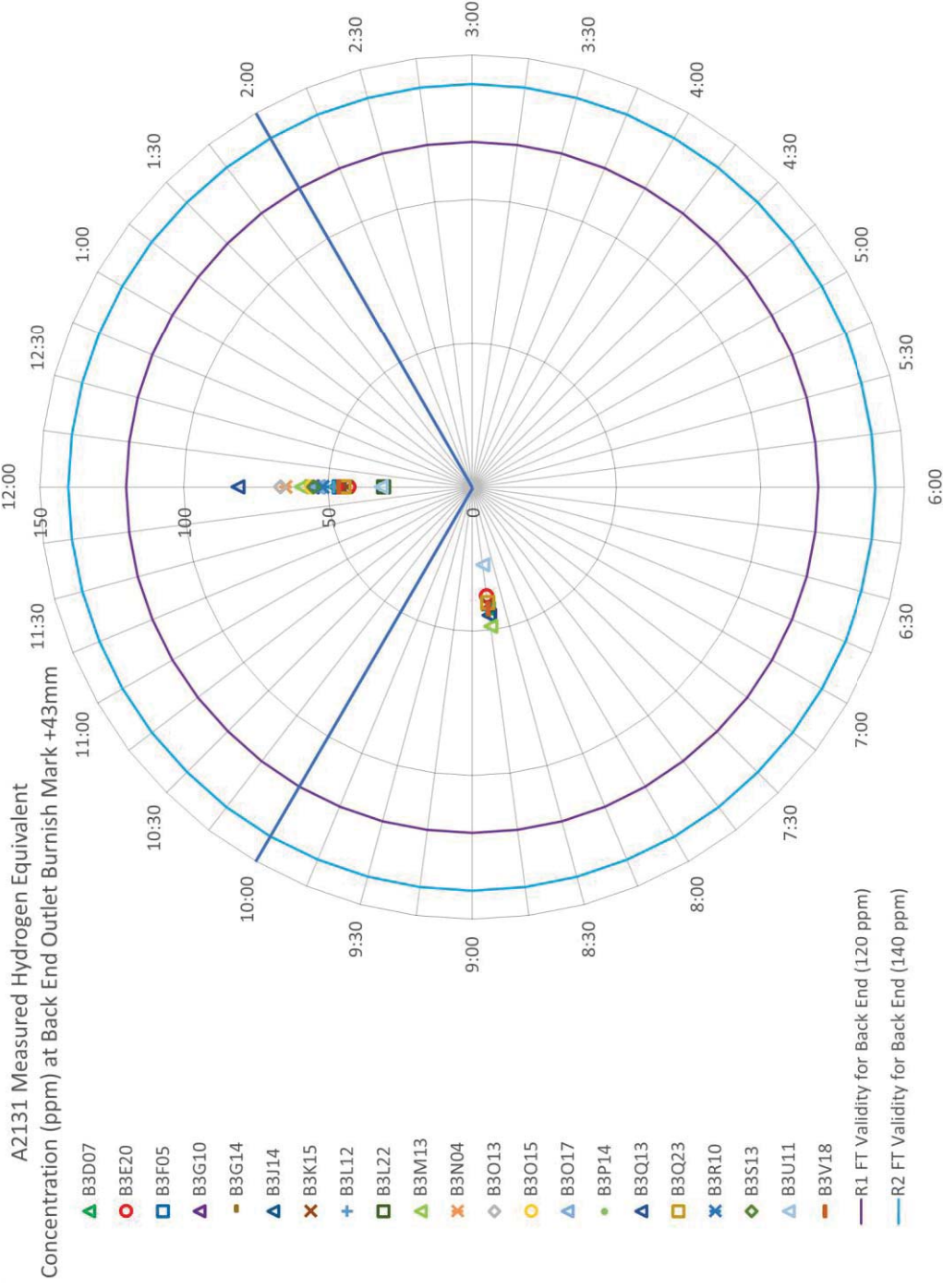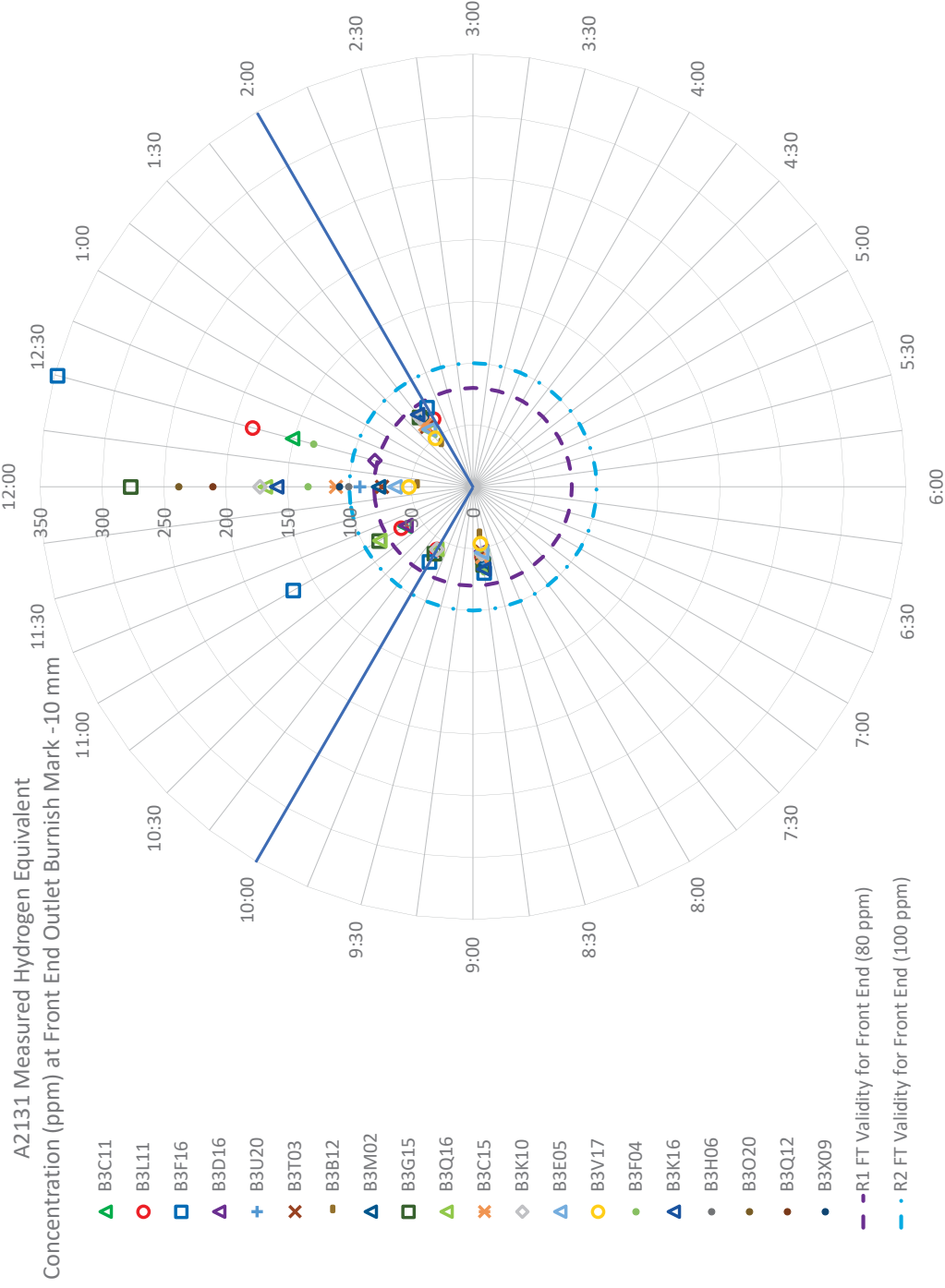
Figure 6: A2131 Measured [H]$_{eq}$ (ppm) at Back End Outlet Burnish Mark +43 mm

Note for Figure 6:

R1 FT and R2 FT refer to the fracture protection validity limits for the Rev1 and Rev2 fracture toughness models, respectively.

Figure 7: A2131 Measured [H]eq (ppm) at Front End Outlet Burnish Mark -10 mm with [H]eq axis scale fixed from 0 to 350 ppm.

Note for Figure 7:

R1 FT and R2 FT refer to the fracture protection validity limits for the Rev1 and Rev2 fracture toughness models, respectively. They do not apply outboard of the BM but they are shown here for illustrative purposes.
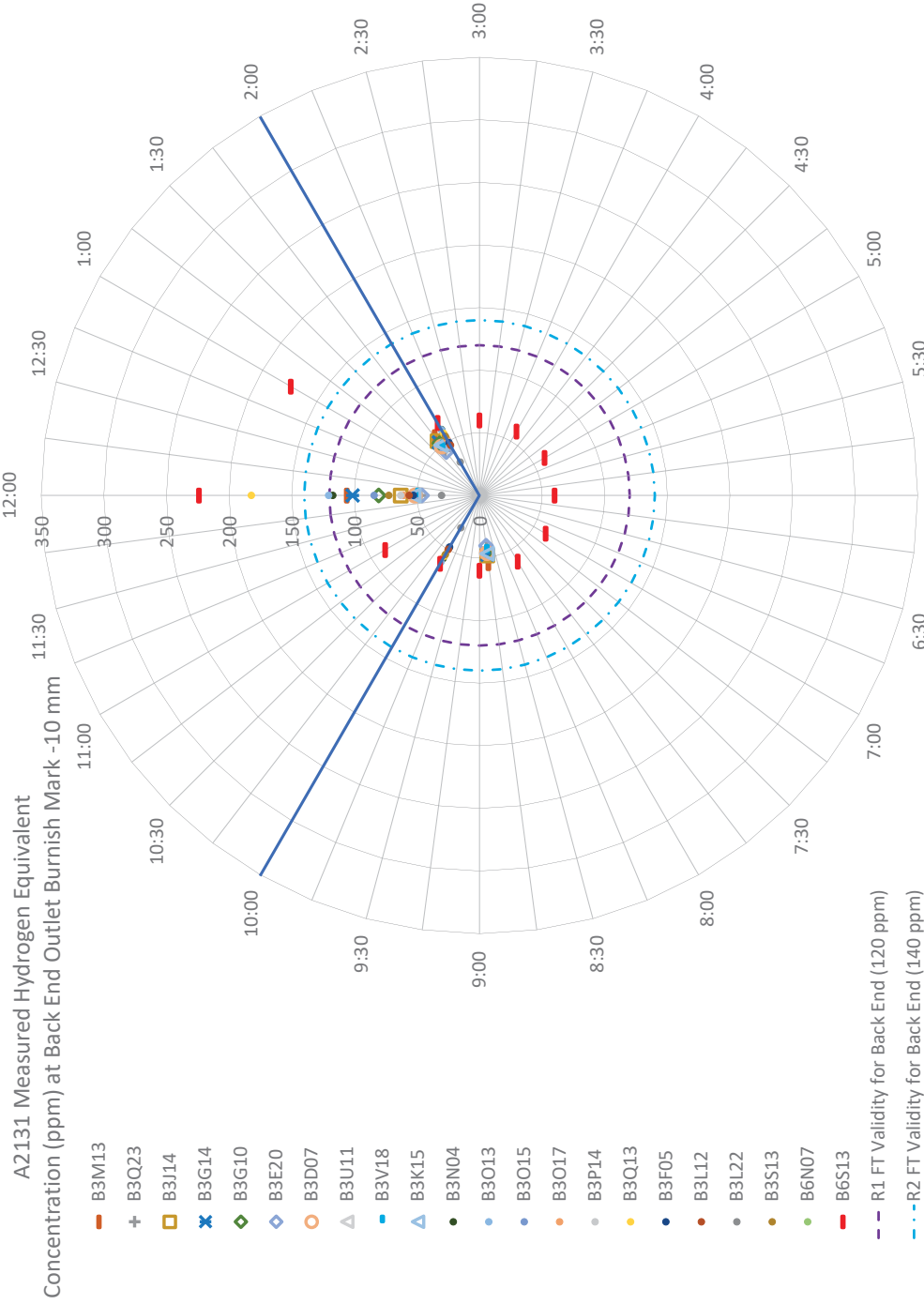
Figure 8: A2131 Measured [H]eq (ppm) at Back End Outlet Burnish Mark -10 mm with [H]eq axis scale fixed from 0 to 350 ppm

Note for Figure 8:

R1 FT and R2 FT refer to the fracture protection validity limits for the Rev1 and Rev2 fracture toughness models, respectively. They do not apply outboard of the BM but they are shown here for illustrative purposes.
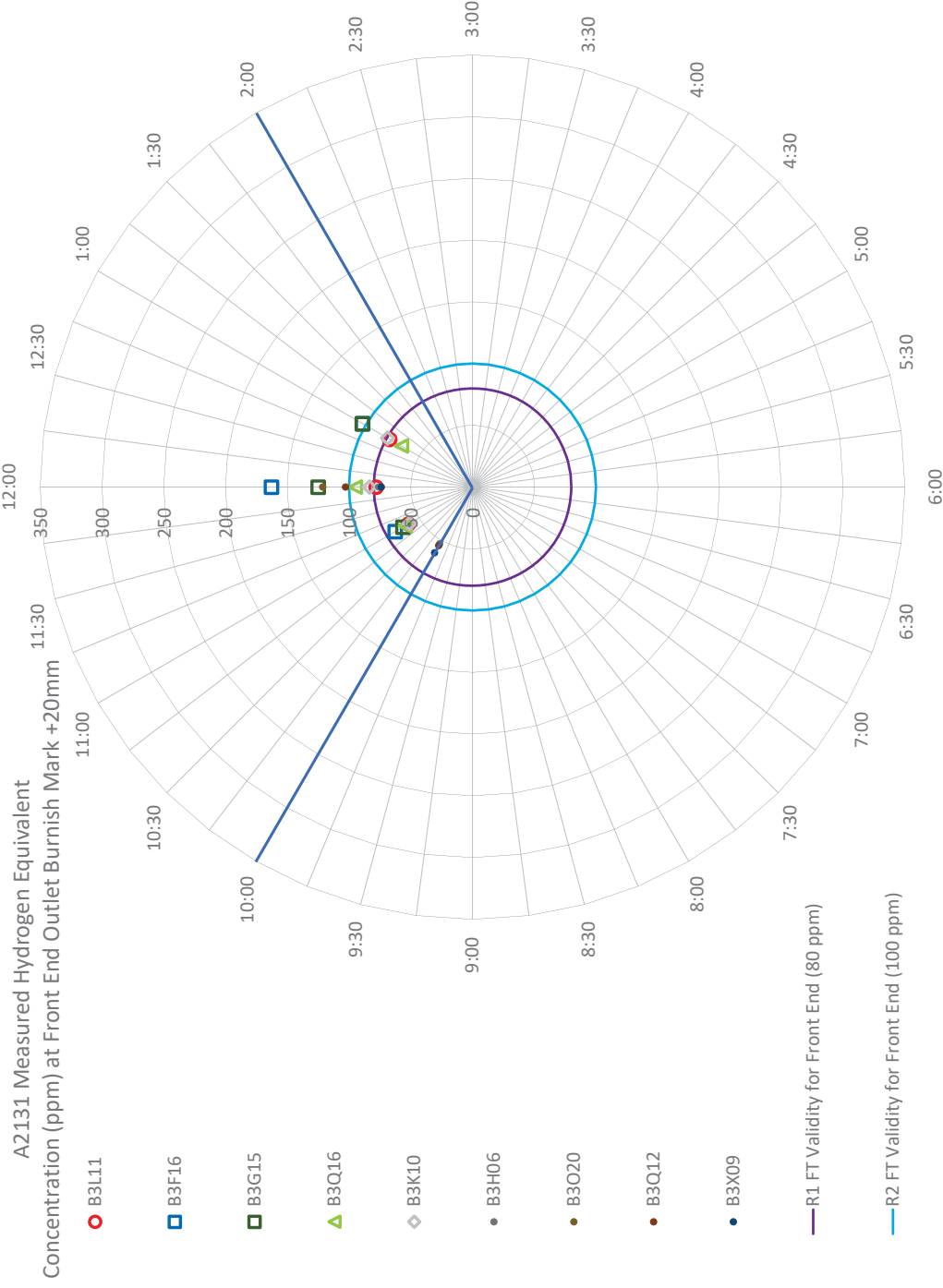
A2131 Measured Hydrogen Equivalent
Concentration (ppm) at Front End Outlet Burnish Mark +20mm

Legend:
- ○ B3L11
- □ B3F16
- □ B3G15
- △ B3Q16
- ◇ B3K10
- • B3H06
- • B3O20
- • B3Q12
- • B3X09
- —— R1 FT Validity for Front End (80 ppm)
- —— R2 FT Validity for Front End (100 ppm)

Figure 9: A2131 Measured [H]$_{eq}$ (ppm) at Front End Outlet Burnish Mark +20 mm with [H]$_{eq}$ axis scale fixed from 0 to 350 ppm

Note for Figure 9:

R1 FT and R2 FT refer to the fracture protection validity limits for the Rev1 and Rev2 fracture toughness models, respectively.
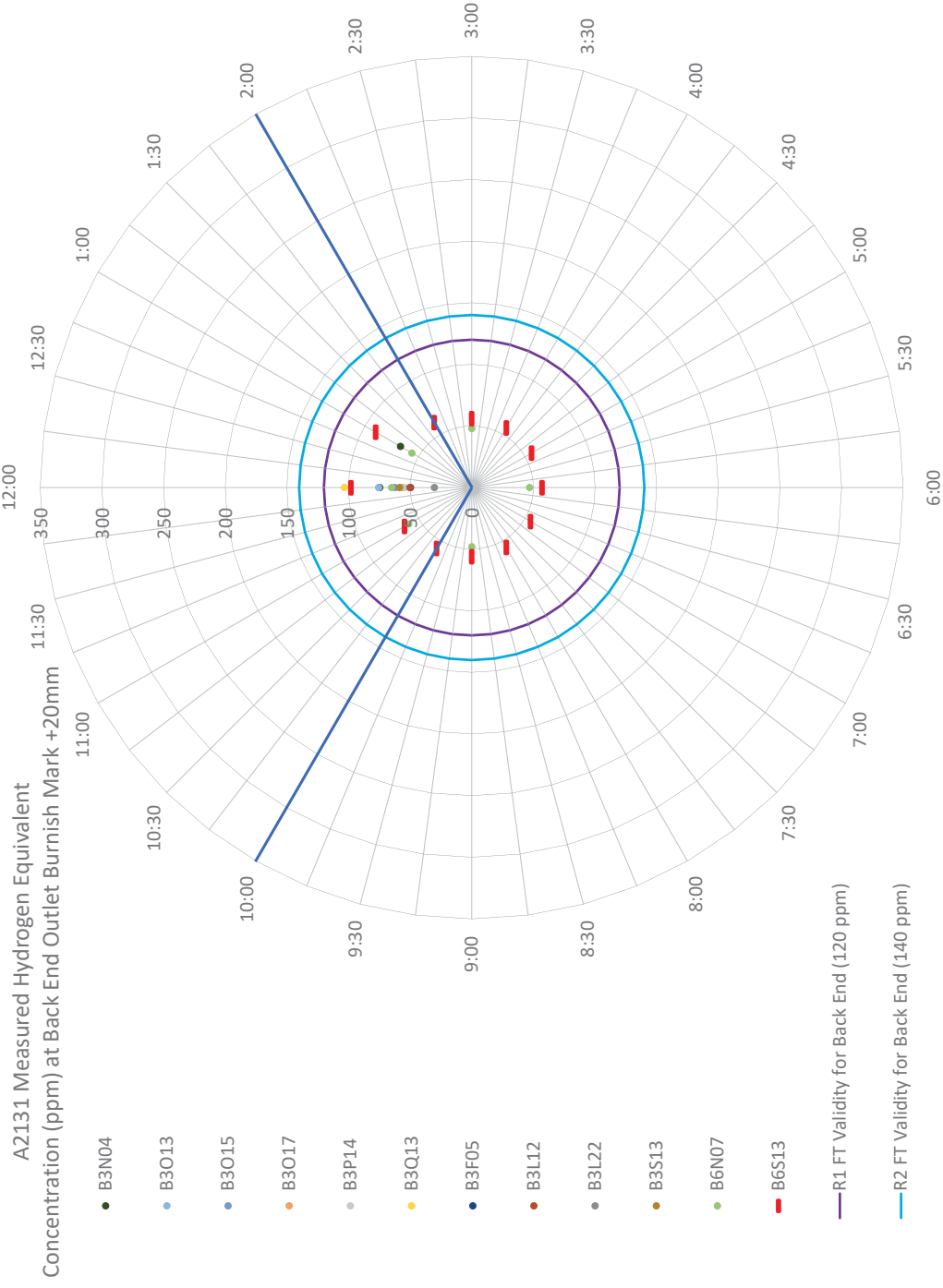
A2131 Measured Hydrogen Equivalent
Concentration (ppm) at Back End Outlet Burnish Mark +20mm

Legend:
- B3N04
- B3O13
- B3O15
- B3O17
- B3P14
- B3Q13
- B3F05
- B3L12
- B3L22
- B3S13
- B6N07
- B6S13
- R1 FT Validity for Back End (120 ppm)
- R2 FT Validity for Back End (140 ppm)

Figure 10: A2131 Measured [H]$_{eq}$ (ppm) at Back End Outlet Burnish Mark +20 mm with [H]$_{eq}$ axis scale fixed from 0 to 350 ppm

Note for Figure 10:

R1 FT and R2 FT refer to the fracture protection validity limits for the Rev1 and Rev2 fracture toughness models, respectively.
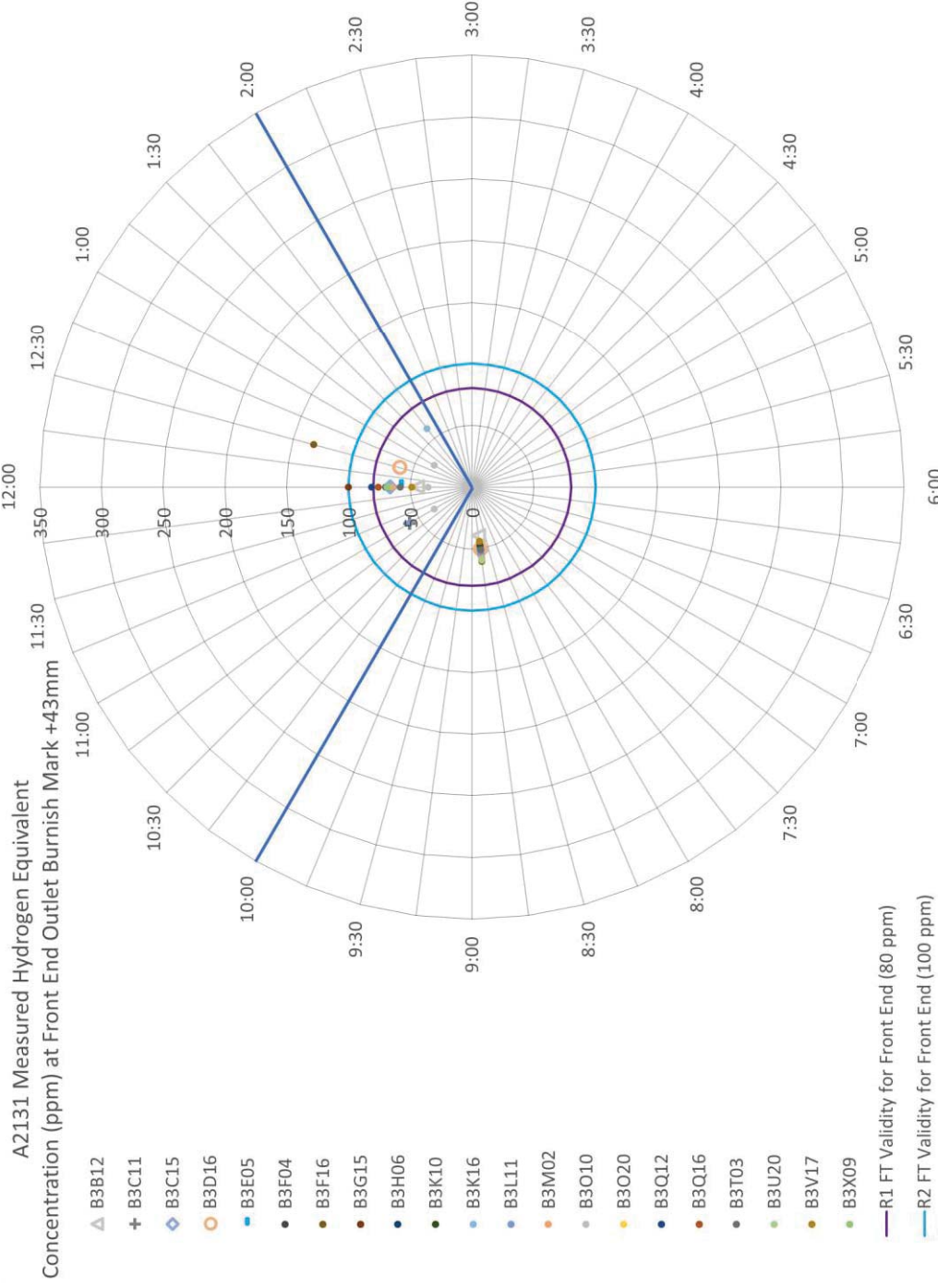
A2131 Measured Hydrogen Equivalent
Concentration (ppm) at Front End Outlet Burnish Mark +43mm

Legend:
△ B3B12
+ B3C11
◇ B3C15
○ B3D16
▬ B3E05
● B3F04
● B3F16
● B3G15
● B3H06
● B3K10
● B3K16
● B3L11
● B3M02
● B3O10
● B3O20
● B3Q12
● B3Q16
● B3T03
● B3U20
● B3V17
● B3X09
── R1 FT Validity for Front End (80 ppm)
── R2 FT Validity for Front End (100 ppm)

Figure 11: A2131 Measured [H]$_{eq}$ (ppm) at Front End Outlet Burnish Mark +43 mm with [H]$_{eq}$ axis scale fixed from 0 to 350 ppm

Note for Figure 11:

R1 FT and R2 FT refer to the fracture protection validity limits for the Rev1 and Rev2 fracture toughness models, respectively.
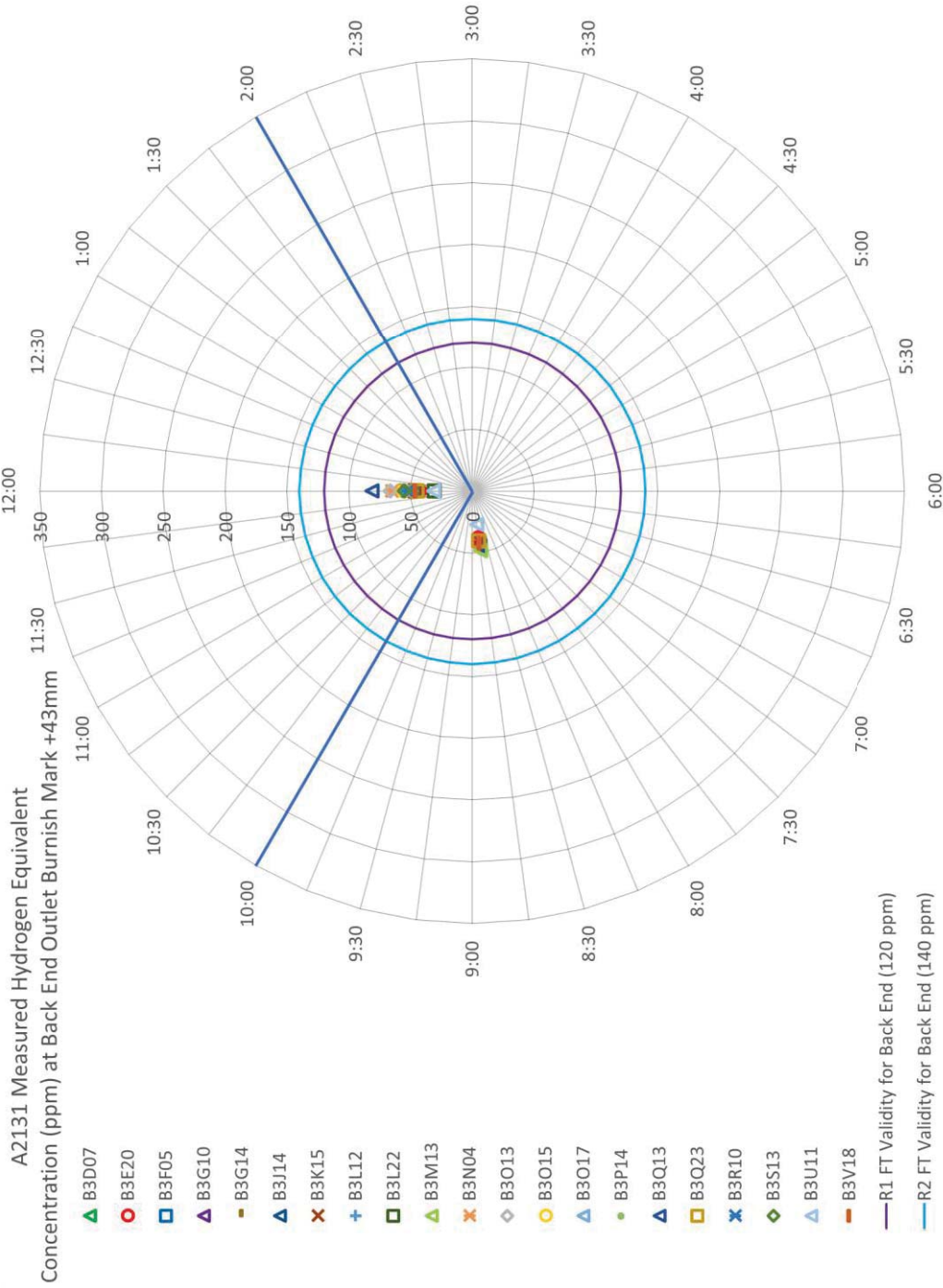
Figure 12: A2131 Measured [H]$_{eq}$ (ppm) at Back End Outlet Burnish Mark +43 mm with [H]$_{eq}$ axis scale fixed from 0 to 350 ppm

Note for Figure 12:

R1 FT and R2 FT refer to the fracture protection validity limits for the Rev1 and Rev2 fracture toughness models, respectively.
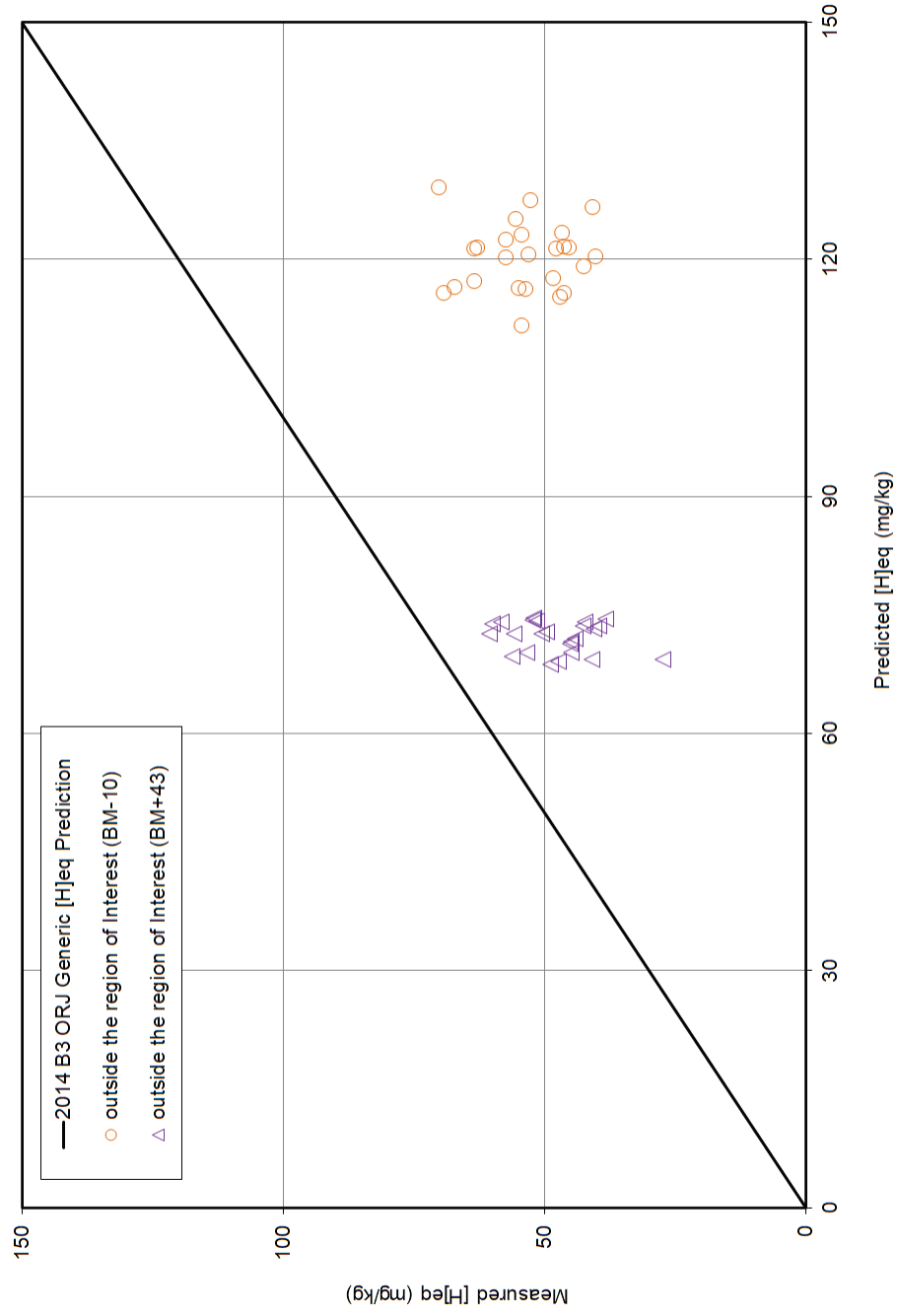
Figure 13: Comparison of Measured $[H]_{eq}$ and the Generic Deterministic Outlet RJ $[H]_{eq}$ Predictions for Locations Outside the Region of Interest